2020

Design and synthesis of photoactivated BODIPY dyes for photocaging and superresolution imaging with visible light

Julie Ann Peterson
Iowa State University

Design and synthesis of photoactivated BODIPY dyes for photocaging and super-resolution imaging with visible light

by

Julie Ann Peterson

A dissertation submitted to the graduate faculty

in partial fulfillment of the requirements for the degree of

DOCTOR OF PHILOSOPHY

Major: Organic Chemistry

Program of Study Committee:
Arthur H. Winter, Major Professor
Emily Smith
William Jenks
Theresa Windus
Brett VanVeller

The student author, whose presentation of the scholarship herein was approved by the program of study committee, is solely responsible for the content of this dissertation. The Graduate College will ensure this dissertation is globally accessible and will not permit alterations after a degree is conferred.

Iowa State University

Ames, Iowa

2020

TABLE OF CONTENTS

Page

ACKNOWLEDGMENTS

I would like to thank my advisor Dr. Arthur Winter who is the best PhD advisor a graduate student could ask for. When we feel like we are at a dead end, we can always walk into his office and leave with fresh motivation. I also want to thank the graduate students in the group that I have shared an office with. We have been together for many highs and a few lows, all of which have helped form me into the human I am now. I am particularly grateful for Katie, Pratik, and Mark, who were formative in making this lab a great place to work. I am also grateful for my current labmates who have made my time at Iowa State great and will continue on with the tradition of the Winter lab. Of my current labmates I want to specifically mention Frank, Logan, Josh, Liz, and Ding. Frank has been a good friend since we joined the lab together. Logan is the nicest, most patient, and in general best person I know and he is going to go on to be a great professor. Josh and Liz have helped make the office quite an adventurous and fun place to work. Ding has helped me with some of my latest projects and she is truly a great person.

I also want to thank Dr. Richard Givens and Dr. Tom Field who I worked with as an undergraduate at University of Kansas. They inspired me to be a chemist and they sparked my love for photochemistry. I would also like to thank Jess, who was the first strong woman scientist I knew. Lastly, I would also like to thank my friends and family who have helped keep me sane(ish) through my chemistry obsession, reminding me that there is a life outside of graduate school.

ABSTRACT

The research herein describes design of BODIPY derived photoremovable protecting groups. Chapter 1 describes the design and synthesis of red-shifted BODIPY photoremovable protecting groups. The initial boron-fluorinated BODIPY derivatives have low quantum yields of photorelease. Boron-methylation of these red-shifted BODIPY photoremovable protecting groups effectively increases quantum yields of release. The boron methyl bond is thermally stable; however, upon irradiation it is cleaved and replaced with solvent, resulting in a chromophore with a higher quantum yield of fluorescence. Chapter 2 describes the application of this photoproduct for single molecule localization microscopy. Chapter 3 discusses the ability for the boron-methylated BODIPY derivatives to release alcohols directly from the *meso* position without use of a carbonate linkage. Chapter 4 describes selective photorelease of red and green BODIPY photoremovable protecting groups along with a UV-absorbing coumarin photoremovable protecting group.

CHAPTER 1. GENERAL INTRODUCTION

Studies of biological species are important for elucidating the mechanisms in the complex biological system. In order to get accurate cause and effect relationships in such a complex environment, molecules of interest must be introduced with spatial and temporal control. Light is an ideal stimulus to activate or deliver a molecule in a spatially and controlled manner. Photoremovable protecting groups (photocages) are molecules that can be covalently linked to the active site of a molecule, hindering its activity. Upon irradiation, the covalent bond is cleaved and the biologically active molecule regains its function. To be used in biological systems, they must be biologically compatible. This includes solubility, stability in biological pH, and the photocage and its photoproduct must ideally be nontoxic to the system. Additionally, irradiation within the "biological window" (650-1000 nm) is preferred for optimal tissue penetration.

O-nitrobenzyl derived photoremovable protecting groups remain the go-to derivatives for initial photorelease studies despite the need for activation with short wavelength light and the potentially toxic nitrosoarene byproducts.[1-4] Much work has been done developing new visible-light absorbing photoremovable protecting groups,[5-9] as well as methods such as two photon absorption that can be used to activate natively UV-absorbing chromophores with two photons of visible to IR light.[10-17] However, more work needs to be done in developing photocages with narrow red-shifted absorbance bands that can be activated with low intensity light within the biological window.

Our group discovered that *meso* substituted BODIPY derivatives can undergo photoheterolysis upon excitation with green light (**Figure 1.1**).[18] Roy Weinstain's group discovered this reactivity independently from us in overlapping timeframes.[19, 20] Our groups collaborated with Klan's group on a structure-reactivity study in an attempt to find modifications that might increase the quantum yields of release of these new photoremovable protecting groups. One of our most surprising findings was that

substituting the boron with alkyl groups leads to a drastic increase in quantum yields of photoheterolysis.

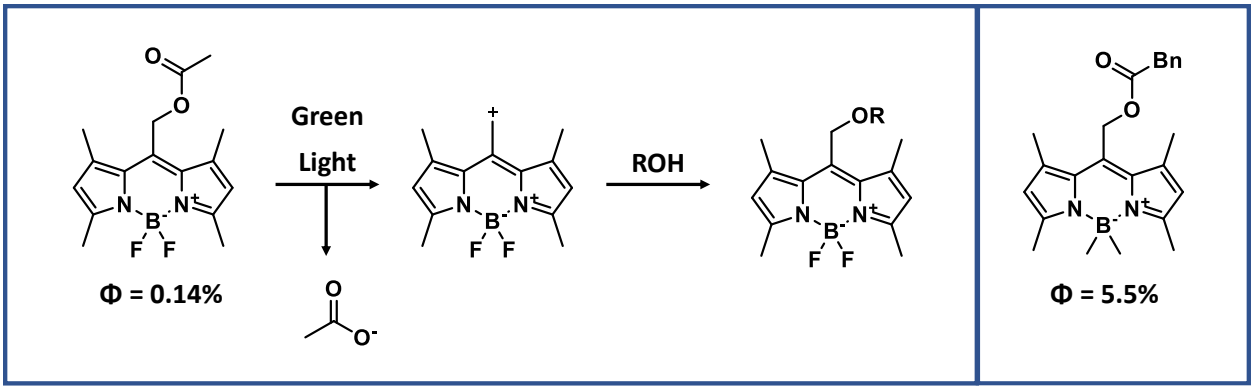

Figure I.1. Photoheterolysis of *meso* substituted BODIPY derivatives

My work in Dr. Arthur Winter's group has been on investigating the photoreactivity of these boron-alkylated BODIPY derivatives and finding potential applications.

Organization of the dissertation

Chapter one focuses on extending the conjugation of BODIPY chromophores so that they can undergo photoheterolysis upon activation with red light. In this chapter, we describe boron-fluorinated derivatives that have low quantum yields of photoheterolysis. Methylating the boron of these derivatives effectively increases the quantum yields of photoheterolysis. We were successfully able to synthesize a derivative to demonstrate utility of these photoremovable protecting groups in cell studies.

Chapter two describes the discovery of a photoactivatable BODIPY probe for single molecule localization microscopy. The boron-alkyl bond can be used as a protecting group of the $-BF_2$ in chemical transformations.[21] However, as we were working with boron-alkylated compounds we discovered that they were photolabile and can be exchanged for solvent, resulting in a photoproduct with an enhanced

quantum yield of fluorescence. In chapter two we describe the synthesis and use of boron-ethylated derivatives for single molecule localization microscopy.

Chapter three describes direct release of phenolic and aliphatic alcohols from alkylated BODIPY derivatives without the use of a carbonate linkage. Many biologically relevant substrates have alcohol functional groups (e.g. dopamine, cholesterol, taxol, carbohydrates). Carbonate linkages can in principle be cleaved either by hydrolysis or by cellular esterases which allows for background thermal release. Ether linkages are more stable. In chapter three we show that methylated BODIPY ethers are able to achieve direct release of alcohols. We show viability in cell studies by using 7-hydroxycoumarin as a fluorescent reporter of photorelease.

Chapter four describes wavelength-selective activation of red and green BODIPY derivatives as well as a coumarin derivative. These photoremovable protecting groups have well-separated absorbance bands and the quantum yield of the BODIPY derivatives can be tuned based on the substitution on the boron. Mixtures irradiated in solution have fair to excellent selectivity, while the low-wavelength selectivity of chromophores attached to a single substrate suffers. We were able to show that a mixture of the three chromophores is able to undergo sequential selectivity with irradiation of red, green, then UV LEDs.

References

1. Sarode, B. R.; Kover, K.; Tong, P. Y.; Zhang, C.; Friedman, S. H., Light Control of Insulin Release and Blood Glucose Using an Injectable Photoactivated Depot. *Molecular Pharmaceutics* **2016,** *13* (11), 3835-3841.

2. Smaga, L. P.; Pino, N. W.; Ibarra, G. E.; Krishnamurthy, V.; Chan, J., A Photoactivatable Formaldehyde Donor with Fluorescence Monitoring Reveals Threshold To Arrest Cell Migration. *Journal of the American Chemical Society* **2020,** *142* (2), 680-684.

3. Kong, L.; Dawkins, E.; Campbell, F.; Winkler, E.; Derks, R. J. E.; Giera, M.; Kamp, F.; Steiner, H.; Kros, A., Photo-controlled delivery of very long chain fatty acids to cell membranes and modulation of membrane protein function. *Biochimica et Biophysica Acta (BBA) - Biomembranes* **2020,** *1862* (5), 183200.

4. Sun, F.; Zhang, P.; Liu, Y.; Lu, C.; Qiu, Y.; Mu, H.; Duan, J., A photo-controlled hyaluronan-based drug delivery nanosystem for cancer therapy. *Carbohydrate Polymers* **2019,** *206*, 309-318.

5. Gandioso, A.; Palau, M.; Nin-Hill, A.; Melnyk, I.; Rovira, C.; Nonell, S.; Velasco, D.; García-Amorós, J.; Marchán, V., Sequential Uncaging with Green Light can be Achieved by Fine-Tuning the Structure of a Dicyanocoumarin Chromophore. *ChemistryOpen* **2017,** *6* (3), 375-384.

6. Gorka, A. P.; Nani, R. R.; Zhu, J.; Mackem, S.; Schnermann, M. J., A near-IR uncaging strategy based on cyanine photochemistry. *Journal of the American Chemical Society* **2014,** *136* (40), 14153-14159.

7. Lovely Angel Panamparambil Antony, T. S., Peter Sebej, Tomas Solomek, Petr Klan, Fluorescein Analogue Xanthene-9-Carboxylic Acid: A Transition-Metal-Free CO Releasing Molecule Activated by Green Light. *Organic Letters* **2013,** *15* (17), 4552-4555.

8. Marturano, V.; Marcille, H.; Cerruti, P.; Bandeira, N. A. G.; Giamberini, M.; Trojanowska, A.; Tylkowski, B.; Carfagna, C.; Ausanio, G.; Ambrogi, V., Visible-Light Responsive Nanocapsules for Wavelength-Selective Release of Natural Active Agents. *ACS Applied Nano Materials* **2019,** *2* (7), 4499-4506.

9. Wang, X.; Kalow, J. A., Rapid Aqueous Photouncaging by Red Light. *Organic Letters* **2018,** *20* (7), 1716-1719.

10. Bader, T. K.; Xu, F.; Hodny, M. H.; Blank, D. A.; Distefano, M. D., Methoxy-Substituted Nitrodibenzofuran-Based Protecting Group with an Improved Two-Photon Action Cross-Section for Thiol Protection in Solid Phase Peptide Synthesis. *The Journal of Organic Chemistry* **2020,** *85* (3), 1614-1625.

11. Becker, Y.; Unger, E.; Fichte, M. A. H.; Gacek, D. A.; Dreuw, A.; Wachtveitl, J.; Walla, P. J.; Heckel, A., A red-shifted two-photon-only caging group for three-dimensional photorelease. *Chemical Science* **2018,** *9* (10), 2797-2802.

12. Christine Tran, T. G., Morgane Petit, Riadh Slimi, Hamid Dhimane, Mireille Blanchard-Desce, Francine C. Acher, David Ogden, Peter I. Dalko, Two-photon caging groups: effect of position isomery on the photorelease properties of aminoquinoline-derived photolabile protecting groups. *Organic Letters* **2015,** *17* (3), 402-405.

13. Edward B. Brown, J. B. S., Stephen R. Adams, Roger Y. Tsien, Watt W. Webb, Photolysis of caged calcium in femtoliter volumes using two-photon excitation. *Biophysical journal* **1999,** *76*, 199.

14. Ellis-Davies, G. C. R., Two-Photon Uncaging of Glutamate. *Frontiers in Synaptic Neuroscience* **2019,** *10*, 48.

15. Fichte, M. A. H.; Weyel, X. M. M.; Junek, S.; Schäfer, F.; Herbivo, C.; Goeldner, M.; Specht, A.; Wachtveitl, J.; Heckel, A., Three-Dimensional Control of DNA Hybridization by Orthogonal Two-Color Two-Photon Uncaging. *Angewandte Chemie* **2016,** *128* (31), 9094-9098.

16. Mitosz Pawlicki, H. A. C., Robert G. Denning, Harry L. Anderson, Two-photon absorption and the design of two-photon dyes. *Angew. Chem. Int. Ed.* **2009,** *48*, 3244-3266.

17. Qiuning Lin, Q. H., Chunyan Li, Chunyan Bao, Zhenzhen Liu, Fuyou Li, Linyoung Zhu, Anticancer Drug Release from a Mesoporous Silica Based Nanophotocage Regulated by either a one- or two-photon process. *J. Am. Chem. Soc* **2010,** *132* (31), 10645-10647.

18. Goswami, P.; Syed, A.; Beck, C. L.; Albright, T. R.; Mahoney, K. M.; Unash, R.; Smith, E. A.; Winter, A. H., BODIPY-Derived Photoremovable Protecting Groups Unmasked with Green Light. *J. Am. Chem. Soc* **2015,** *137*, 3783-3786.

19. Palao, E.; Salanina, T.; Muchova, L.; Solomek, T.; Vitek, L.; Klan, P., Transition-Metal-Free CO-Releasing BODIPY Derivatives Activatable by Visible to NIR Light as Promising Bioactive Molecules. *J. Am. Chem. Soc* **2015,** *138* (1), 126–133.

20. Rubinstein, N.; Liu, P.; Miller, E. W.; Weinstain, R., meso-Methylhydroxy BODIPY: a scaffold for photo-labile protecting groups. *Chem. Commun.* **2015,** *51*, 6369-6372.

21. More, A. B.; Mula, S.; Thakare, S.; Sekar, N.; Ray, A. K.; Chattopadhyay, S., Masking and Demasking Strategies for the BF2–BODIPYs as a Tool for BODIPY Fluorophores. *The Journal of Organic Chemistry* **2014,** *79* (22), 10981-10987.

CHAPTER 2. FAMILY OF BODIPY PHOTOCAGES CLEAVED BY SINGLE PHOTONS OF VISIBLE/NEAR-INFRARED LIGHT

Julie A. Peterson, Chamari Wijesooriya, Elizabeth J. Gehrmann, Kaitlyn M. Mahoney, Pratik P. Goswami, Toshia R. Albright, Aleem Syed, Andrew S. Dutton, Emily A. Smith, Arthur H. Winter

Modified from a manuscript published in *Journal of the American Chemical Society*

Abstract

Photocages are light-sensitive chemical protecting groups that provide external control over when, where, and how much of a biological substrate is activated in cells using targeted light irradiation. Regrettably, most popular photocages (e.g., *o*-nitrobenzyl groups) absorb cell-damaging ultraviolet wavelengths. A challenge with achieving longer wavelength bond-breaking photochemistry is that long-wavelength-absorbing chromophores have shorter excited-state lifetimes and diminished excited-state energies. However, here we report the synthesis of a family of BODIPY-derived photocages with tunable absorptions across the visible/near-infrared that release chemical cargo under irradiation. Derivatives with appended styryl groups feature absorptions above 700 nm, yielding photocages cleaved with the highest known wavelengths of light via a direct single photon release mechanism. Photorelease with red light is demonstrated in living HeLa cells, Drosophila S2 cells, and bovine GM07373 cells upon ~5 min irradiation. No cytotoxicity is observed at 20 μM photocage concentration using the trypan blue exclusion assay. Improved B-alkylated derivatives feature improved quantum efficiencies of photorelease ~20-fold larger, on par with the popular *o*-nitrobenzyl photocages ($\varepsilon\Phi$ = 50–100 M^{-1} cm^{-1}), but absorbing red/near-IR light in the biological window instead of UV light.

Introduction

Photocages are light-sensitive moieties that are prized for giving investigators spatial and temporal control over the release of covalently linked substrates.[1–4] When a photocage blocks a critical functional group on the substrate (e.g., a carboxylic acid), the substrate is rendered biologically inert. Light-induced cleavage of the photocage−substrate bond restores the reactivity or function of the

substrate. Photocages have been used to activate proteins,[5,6] nucleotides,[7,8] ions,[9–11] neurotransmitters,[12,13] pharmaceuticals,[14,15] and fluorescent dyes using light.[16–18] The vast majority of photocaging compounds used in biological studies exploit the o-nitrobenzyl photocages[19,20] and their derivatives, but others include those based on the phenacyl,[21,22] acridinyl,[23] benzoinyl,[24,25] coumarinyl,[26] and o-hydroxynaphthyl[27] structures. A major limitation of these popular photocages is that their chromophores absorb mostly in the ultraviolet region of the optical spectrum. Ultraviolet light has limited tissue penetration, restricting photocaging studies to cells and tissue slices. In addition, exposure of cells or tissues to intense UV light results in phototoxic cell damage or death. The ideal wavelength range to be used in animal tissues, known as the biological window, is ~600−1000 nm, where tissues have maximal light transmittance. At these far red/near-infrared wavelengths, light achieves maximal tissue penetration while minimizing phototoxicity.[28] Photorelease using these wavelengths holds promise for studies in living animals or as targeted photoactivated therapeutics. The drawbacks of using UV light as a biological initiator have led to a number of different approaches to permit photorelease of biologically active substrates using visible light. The de facto method for releasing target molecules with visible light is to exploit multiphoton absorption methods, wherein a UVabsorbing photocage is excited with two or more visible light photons.[29–31] Other methods to achieve photorelease using visible light include photorelease initiated via photoinduced electron transfer,[32–34] via metal−ligand photocleavage,[35] or by using photosensitizers that generate reactive singlet oxygen that can initiate reaction cascades, leading to substrate release.[36–38] However, it is advantageous to achieve photorelease with simple, biologically benign organic structures that directly release substrates with single photons of visible light. Recently, a new class of photoremovable protecting groups derived from meso-substituted BODIPY dyes was reported by us and Weinstain.[39,41] For these photocages (**1** and **2 Figure 1**), cleavage occurs using green wavelengths ~520 nm. In related recent work, Klan and co-workers have also demonstrated the photorelease of carbon monoxide from irradiation of BODIPY[42] and xanthene-substituted[43] carboxylic acids. Also of relevance, aminoquinones are reported to undergo neighboring H

atom abstraction with long-wavelength light that can lead to hydroquinones that release appended leaving groups via a self-immolative release pathway.[44] A recent structure−activity relationship varying substituents and leaving groups on BODIPY photocages was conducted in collaborative work between us, Weinstain, and Klan.[40] Sitkowska, Feringa, and Szymanski have recently demonstrated amine-releasing BODIPY derivatives by irradiation of BODIPY carbamates.

Results and Discussion

We synthesized compounds 3−9 that have extended conjugation and a red-shifted λmax values between 580 and 690 nm (λ_{em} between 600 and 750 nm) (**Figure 1.2**). Compounds **3−9** are thermally stable, showing no change by NMR when refluxed in the dark for 1 h (**Figure S11**), yet release carboxylates when irradiated with visible light (**Figure S1**). The quantum yields of the release of the leaving groups (ϕ) of **3−9** were determined by ferrioxalate actinometry (see Supporting Information (**SI**)) and are reported as the average value of three trials. The extinction coefficient (ε) at the λ_{max} was determined by UV−vis spectroscopy (**Table 1**).

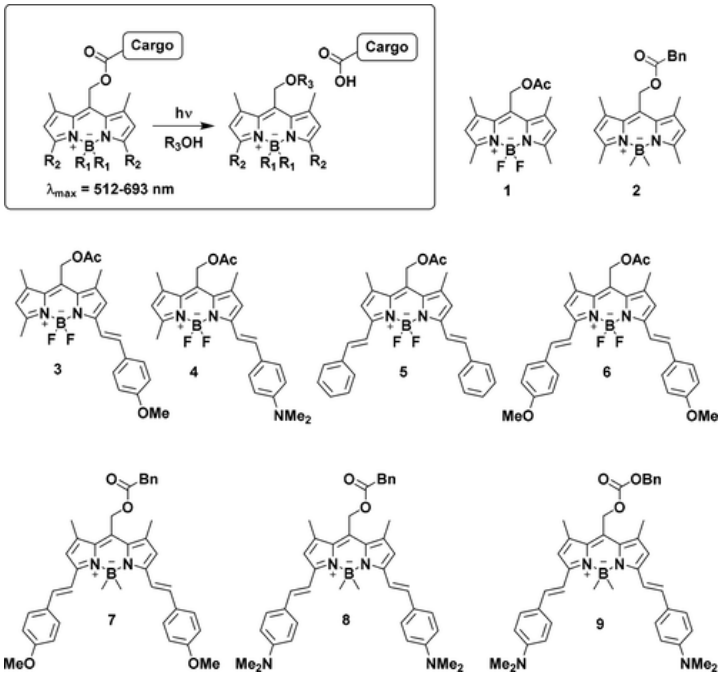

Figure 2.1. Substrates described in this study. Substrates **1** and **2** are from our prior work,[39,40] while **3-9** are from this work.

These photocages feature high extinction coefficients typical of BODIPY dyes (~50 000−120 000 M−1 cm−1 at λ_{max}). In general, the quantum yields (ϕ) for photorelease of acetic acid for the longest-wavelength-absorbing photocages 3−6 are an order of magnitude lower than those of the unconjugated substrates (**1** or **2**). However, boron alkylation leads to a large increase in the quantum yield of release, while not significantly perturbing the λmax of the chromophore. For example, the boron-alkylated **7** has a quantum yield ~20-fold larger than that of **6**, which is boron-fluorinated. Because many biologically interesting compounds have alcohols, we also synthesized compound **9** to demonstrate release of benzyl alcohol. This compound releases benzyl alcohol with a quantum yield similar to that of the carboxylates via a decarboxylation mechanism that liberates CO_2 as a byproduct. For comparison, the most popular photocages, the o-nitrobenzyl photocages, have $\varepsilon\Phi \approx 100$ M−1 cm−1 at $\lambda_{irr} = 350$ nm, and much less at $\lambda_{irr} > 400$ nm. Thus, the quantum efficiencies of **8** and **9** are on the same order of magnitude as nitrobenzyl photocages, but absorb light in the biological window ~700 nm instead of UV light. An interesting observation is that while the mono styryl **4** bearing a dimethylamino group has a smaller quantum yield than **3** bearing a methoxy, bis(styryl) compound 8 bearing the two dimethylamino groups has a larger quantum yield than **7** bearing the two methoxy groups. This change cannot be explained in a simple way, as a calculation of the LUMO p orbital coefficients at the meso carbon of these compounds did not reveal a trend that explained the difference in quantum yields (**Scheme S2**). Probably, more subtle effects such as the rates of competitive pathways are needed to explain this difference.

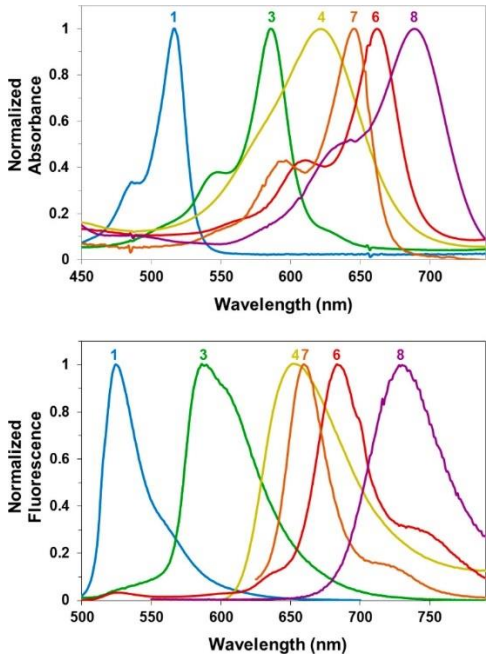

Figure 2.2. Absorbance (top) and emission (bottom) spectra of selected BODIPY photocages. Data for all photocages can be found in Appendix A.

Table 2.1. Optical and Photochemical Properties of **1-9**

	λ_{max} (nm)	λ_{em} (nm)	ε ($\times 10^4$ M^{-1} cm^{-1})	Φ (%)[a]	εΦ (M^{-1} cm^{-1})
1[b]	515	526	7.1	.099	70
2[b]	512	550	6.9	5.5	3800
3	586	607	6.1	0.0098	6.0
4	633	650	6.0	0.0069	4.1
5	640	656	6.5	0.0045	2.9
6	661	684	6.5	0.0041	2.7
7	647	660	4.9	0.084	41
8	689	728	7.8	0.11	86
9	693	745	5.2	0.14	73

[a]Quantum yields (Φ) determined by ferrioxalate actinometry in MeOH with a 532 nm Nd:YAG laser source and release followed using quantitative LC-UV (average of three runs).[b]Values from refs.[39,40]

Compound **10** was synthesized to test the usefulness of these photocages in live-cell imaging. 4-Nitrobenzoic acid was used as the leaving group, since nitrobenzoic acids are known fluorescence quenchers of BODIPY dyes. A short ethylene glycol chain was appended to the styryl groups to aid with water solubility. Compound **10** does not exhibit detectable fluorescence when kept in the dark at room temperature. We anticipated that, upon irradiation and release of 4-nitrobenzoic acid, a fluorescent photoproduct would be formed with a $\lambda_{em} \approx 685$ nm. However, we found that, when **10** was irradiated in MeOH or cell culture buffer under air, we instead observed an increase in fluorescence at 610 nm. Similarly, when **6** was irradiated in methanol, we saw a peak grow in at 610 nm as the peak at 685 nm decreased (see **Figures 3** and **S6**). This new blue-shifted fluorescent peak is similar to the emission wavelength of 3. ^{1}H NMR studies of the photolysis of **10** confirm that the quencher is released upon irradiation (Figure S10). Photoproduct studies of **6** and **10** under air show that, in addition to acetic acid, p-anisaldehyde is a minor photoproduct for **6**, and the tri(ethylene glycol)-substituted anisaldehyde is a minor photoproduct for 10 (**Figures S2** and **S3**). Formation of the benzaldehyde and a λ_{em} at a wavelength similar to that of **3** indicate that photocage byproducts have either cleaved or broken the conjugation of a styryl group (further information on product studies of **6** can be found in the SI), explaining the wavelength shift. We considered two possible mechanisms for this cleavage and aldehyde formation. First, the photocage could sensitize singlet oxygen, which could then oxidatively cleave the olefin. This process would be independent of photorelease. Alternatively, oxidative cleavage could arise from oxygen trapping a cation intermediate (possibly in its triplet state), a mechanism that is correlated with the photorelease process. The simplest release mechanism to consider is a photoheterolysis mechanism, either from the singlet or triplet excited state. The putative carbocation formed by heterolysis of 6 is computed to be a triplet ground state carbocation by ca. 3 kcal/mol using density functional theory (UB3LYP/6-31G(d), including correction for singlet spin contamination; see SI). Photolysis occurring through the triplet excited state would be expected to yield the triplet carbocation to conserve spin. Indeed, we selected meso-substituted BODIPY dyes as potential

photocages based on these ions having low-lying diradical states, which we had previously suggested might be critical for providing a surface crossing (conical intersection) between the excited-state surface and the ground-state ion pair surface.[46] Inspection of the computed SOMOs of the triplet carbocation indicates that the radicals are located on the styryl groups. Little is known about triplet carbocation reactivity,[47] but triplet diradicals are known to react with oxygen, which could lead to a pathway involving oxidative cleavage at one of the styryl groups. A similar styryl BODIPY compound has been demonstrated to be reactive to radicals in the ground state, breaking the conjugation of the olefin and causing a wavelength shift similar to what we observe.[48] To corroborate that this fluorescence blue-shift was correlated with release of the carboxylic acid, a derivative of compound **6** with no leaving group was synthesized as a control and showed no fluorescence blue-shift upon photolysis (**Scheme S1** and **Figure S7**). Irradiation of this compound simply led to a slow fluorescence bleaching at long irradiation times. If oxidative cleavage were independent of the photorelease process, this compound, which is identical except for the absence of the leaving group, would be expected to have a similar fluorescence blue-shift. That it does not supports the mechanism involving trapping of a reactive intermediate following the photorelease. This blue-shifted fluorescence provides a convenient assay by which to follow the photorelease process using fluorescence microscopy, since the photocaged acid **6** does not absorb at 605 nm, the wavelength at which the blue-shifted byproduct absorbs. NMR studies showed that there is mass balance between compound **6** and acetic acid over 3 h of irradiation (**Figure S5**).

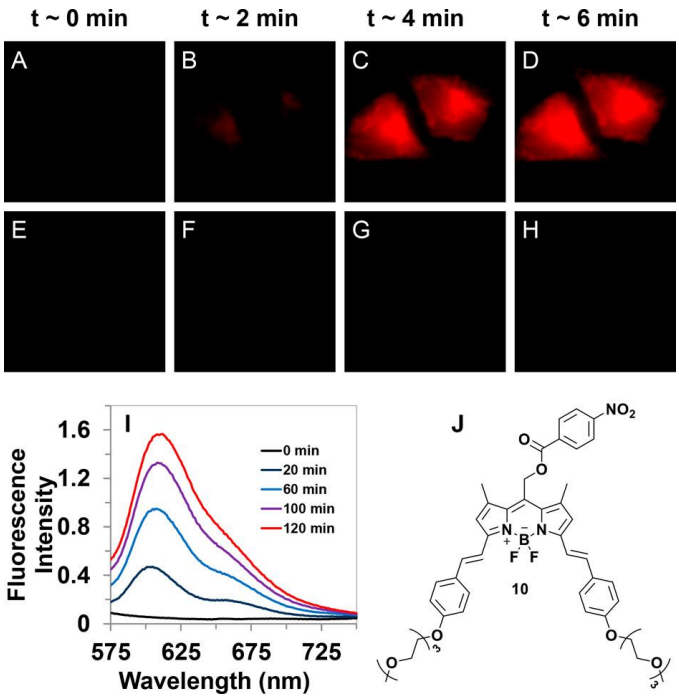

Figure 2.3. Fluorescence images of (A–D) HeLa cells incubated with 20 μM compound **10** irradiated with 635 nm light and (E–H) cells incubated with compound **10** with no irradiation as a function of time. (I) Increase in fluorescence of compound **10** in H_2O with 5% BSA when irradiated.

As a proof-of-principle demonstration that photorelease could be performed in cells, 20 μM compound 10 was incubated with HeLa cells at 36 ± 2 °C. The cells were irradiated with 635 ± 15 nm light. Fluorescence emission was measured at 605 nm. Control experiments were performed without irradiation. An increase in fluorescence was observed at 605 nm when irradiated (**Figure 3A−D**). In control studies, no increase in fluorescence was observed in the dark (**Figure 3E− H**). Similar imaging studies were performed in bovine GM07373 cells and Drosophila S2 cells (**Figures S13** and **S14**), yielding similar results. Cytotoxicity studies (Trypan blue exclusion assay) showed no decrease in cell viability with treatment of 10 (90 ± 3% for HeLa cells with no treatment, 92 ± 5% for HeLa cells with 10, 95 ± 2% for S2 cells without treatment, 93 ± 2% for S2 cells with 10, 90 ± 1% for GM07373 cells without treatment, and 92 ± 5% for GM07373 cells with 10).

Conclusion

A family of BODIPY-derived photocages have been synthesized that release chemical cargos at a range of wavelengths in the visible from ~450−700 nm. The longest-wavelength-absorbing

derivatives (8, 9) represent photocages that can release substrates with the highest known wavelengths of light via a single-photon direct photorelease pathway. The wide range of wavelengths of absorbance allows photorelease to be achievedusing essentially any color of visible light. This work opens up the possibility of the targeted and controlled release of pharmaceuticals or other biomolecules using irradiation with red light in the biological window. It is remarkable that a net photoheterolysis reaction can be achieved using red light given the much diminished photon energies associated with these wavelengths (~40 kcal/mol for 700 nm vs ~100 kcal/mol for a UV photon), and it will be interesting to test the maximum wavelengths of photorelease possible, as increasing wavelengths correspond to increasingly diminished photon energies.

References

1. Klan, P.; Solomek, T.; Bochet, C. G.; Blanc, A.; Givens, R.; Rubina, M.; Popik, V.; Kostikov, A.; Wirz, J. Chem. Rev. 2013, 113, 119−191.
2. Ellis-Davies, G. C. R. Nat. Methods 2007, 4 (8), 619−628.
3. Adams, S. R.; Tsien, R. Y. Annu. Rev. Physiol. 1993, 55, 755−784.
4. Specht, A.; Bolze, F.; Omran, Z.; Nicoud, J.-F.; Goeldner, M. HFSP J. 2009, 3 (4), 255−264.
5. Zhao, J.; Lin, S.; Huang, Y.; Zhao, J.; Chen, P. R. J. Am. Chem. Soc. 2013, 135 (20), 7410−7413.
6. Lawrence, D. S. Curr. Opin. Chem. Biol. 2005, 9, 570−575.
7. Kretschy, N.; Holik, A.-K.; Somoza, V.; Stengele, G.-P.; Somoza, M. M. Angew. Chem., Int. Ed. 2015, 54, 8555−8559.
8. Pirrung, M. C. Chem. Rev. 1997, 97, 473−488.
9. Priestman, M. A.; Lawrence, D. S. Biochim. Biophys. Acta, Proteins Proteomics 2010, 1804 (3), 547.
10. Mbatia, H. W.; Bandara, H. M. D.; Burdette, S. C. Chem. Commun. 2012, 48, 5331−5333.
11. Gomez, T. M.; Spitzer, N. C. Nature 1999, 397 (28), 350−355.
12. Sjulson, L.; Miesenbock, G. Chem. Rev. 2008, 108 (5), 1588− 1602.
13. Kramer, R. H.; Chambers, J. J.; Trauner, D. Nat. Chem. Biol. 2005, 1 (7), 360−365.

14. Katz, J. S.; Burdick, J. A. Macromol. Biosci. 2010, 10, 339−348.

15. Blake, J. A.; Bareiss, B.; Jimenez, L.; Griffith, M.; Scaiano, J. C. Photochem. Photobiol. Sci. 2012, 11 (3), 539−547.

16. Puliti, D.; Warther, D.; Orange, C.; Specht, A.; Goeldner, M. Bioorg. Med. Chem. 2011, 19 (3), 1023−1029.

17. Li, W.-h.; Zheng, G. Photochem. Photobiol. Sci. 2012, 11, 460.

18. Yu, H.; Li, J.; Wu, D.; Qiu, Z.; Zhang, Y. Chem. Soc. Rev. 2010, 39, 464−473.

19. Kaplan, J. H.; Ellis-Davies, G. C. R. Proc. Natl. Acad. Sci. U. S. A. 1988, 85, 6571−6575.

20. Engels, J.; Schlaeger, E. J. J. Med. Chem. 1977, 20, 907−911.

21. Anderson, J. C.; Reese, C. B. Tetrahedron Lett. 1962, 3, 1−4.

22. Park, C.-H.; Givens, R. S. J. Am. Chem. Soc. 1997, 119 (10), 2453−2463.

23. Ackmann, A. J.; Frechet, M. J. Chem. Commun. 1996, 5, 605− 606.

24. Sheehan, J. C.; Wilson, R. M. J. Am. Chem. Soc. 1964, 86, 5277− 5281.

25. Sheehan, J. C.; Wilson, R. M.; Oxford, A. W. J. Am. Chem. Soc. 1971, 93, 7222−7228.

26. Givens, R. S.; Matuszewski, B. J. Am. Chem. Soc. 1984, 106, 6860−6861.

27. Arumugam, S.; Popik, V. V. J. Am. Chem. Soc. 2009, 131 (33), 11892−11899.

28. Smith, A. M.; Mancini, M. C.; Nie, S. Nat. Nanotechnol. 2009, 4, 710−711.

29. Tran, C.; Gallavardin, T.; Petit, M.; Slimi, R.; Dhimane, H.; Blanchard-Desce, M.; Acher, F. C.; Ogden, D.; Dalko, P. I. Org. Lett. 2015, 17 (3), 402−405.

30. Brown, E. B.; Shear, J. B.; Adams, S. R.; Tsien, R. Y.; Webb, W. W. Biophys. J. 1999, 76, 489−499.

31. Lin, Q.; Huang, Q.; Li, C.; Bao, C.; Liu, Z.; Li, F.; Zhu, L. J. Am. Chem. Soc. 2010, 132 (31), 10645−10647.

32. Denning, D. M.; Pedowitz, N. J.; Thum, M. D.; Falvey, D. E. Org. Lett. 2015, 17 (24), 5986−5989.

33. Sundararajan, C.; Falvey, D. E. J. Am. Chem. Soc. 2005, 127 (22), 8000−8001.

34. Falvey, D. E.; Sundararajan, C. Photochem. Photobiol. Sci. 2004, 3, 831−838.

35. Shell, T. A.; Shell, J. R.; Rodgers, Z. L.; Lawrence, D. S. Angew. Chem., Int. Ed. 2014, 53 (3), 875−878.

36. Saravanakumar, G.; Lee, J.; Kim, J.; Kim, W. J. Chem. Commun. 2015, 51 (49), 9995−9998.

37. Atilgan, A.; Eaik, E. T.; Guliyev, R.; Uyar, T. B.; Erbas-Cakmak, S.; Akkaya, E. U. Angew. Chem., Int. Ed. 2014, 53 (40), 10678−10681.

38. Nani, R. R.; Gorka, A. P.; Nagaya, T.; Kobayashi, H.; Schnermann, M. J. Angew. Chem. 2015, 127 (46), 13839−13842.

39. Goswami, P.; Syed, A.; Beck, C. L.; Albright, T. R.; Mahoney, K. M.; Unash, R.; Smith, E. A.; Winter, A. H. J. Am. Chem. Soc. 2015, 137, 3783−3786.

40. Slanina, T.; Shrestha, P.; Palao, E.; Kand, D.; Peterson, J. A.; Dutton, A. S.; Rubinstein, N.; Weinstain, R.; Winter, A. H.; Klan, P.́ J. Am. Chem. Soc. 2017, 139 (42), 15168−15175.

41. Rubinstein, N.; Liu, P.; Miller, E. W.; Weinstain, R. Chem. Commun. 2015, 51, 6369−6372.

42. Palao, E.; Slanina, T.; Muchova, L.; Solomek, T.; Vitek, L.; Klan, P. J. Am. Chem. Soc. 2016, 138 (1), 126−133.

43. Antony, L. A. P.; Slanina, T.; Sebej, P.; Solomek, T.; Klan, P. Org. Lett. 2013, 15 (17), 4552−4555.

44. Wang, X.; Kalow, J. A. Org. Lett. 2018, 20 (7), 1716−1719.

45. Sitkowska, K.; Feringa, B. L.; Szymański, W. J. Org. Chem. 2018, 83 (4), 1819−1827.

46. Buck, A. T.; Beck, C. L.; Winter, A. H. J. Am. Chem. Soc. 2014, 136 (25), 8933−8940.

47. Albright, T. R.; Winter, A. H. J. Am. Chem. Soc. 2015, 137 (9), 3402−3410.

48. Haidasz, E. A.; Van Kessel, A. T. M.; Pratt, D. A. J. Org. Chem. 2016, 81 (3), 737−744.

CHAPTER 3. A PHOTOACTIVATABLE BODIPY PROBE FOR LOCALIZATION-BASED SUPER-RESOLUTION CELLULAR IMAGING

Chamari S. Wijesooriya, Julie A. Peterson, Pradeep Shrestha, Elizabeth J. Gehrmann, Arthur H. Winter, Emily A. Smith

Modified from a manuscript published in *Angewandte Chemie International Edition*

Abstract

The synthesis and application of a photoactivatable boron-alkylated BODIPY probe for localization-based super-resolution microscopy is reported. Photoactivation and excitation of the probe is achieved by a previously unknown boron-photodealkylation reaction with a single low-power visible laser and without requiring the addition of reducing agents or oxygen scavengers in the imaging buffer. These features lead to a versatile probe for localization-based microscopy of biological systems. The probe can be easily linked to nucleophile-containing molecules to target specific cellular organelles. By attaching paclitaxel to the photoactivatable BODIPY, in vitro and in vivo super-resolution imaging of microtubules is demonstrated. This is the first example of single-molecule localization-based super-resolution microscopy using a visible-light-activated BODIPY compound as a fluorescent probe.

Introduction

Fluorescence microscopy is a useful tool for imaging cellular components in their native environments. The spatial resolution of conventional optical microscopy is limited by the diffraction limit of light, which depends on the wavelength of light and the numerical aperture of the objective. Over the past two decades, optical imaging techniques with sub-diffraction spatial resolution, or super-resolution, have been developed.[1] Among these techniques, single-molecule localization microscopies (SMLM) such as stochastic optical reconstruction microscopy (STORM)[1d, 2] and photoactivated localization microscopy (PALM)[1b, 3] sequentially activate sparse subsets of fluorophores, localize their positions with high precision, and generate an image by summing the positions of the localized molecules in each frame.

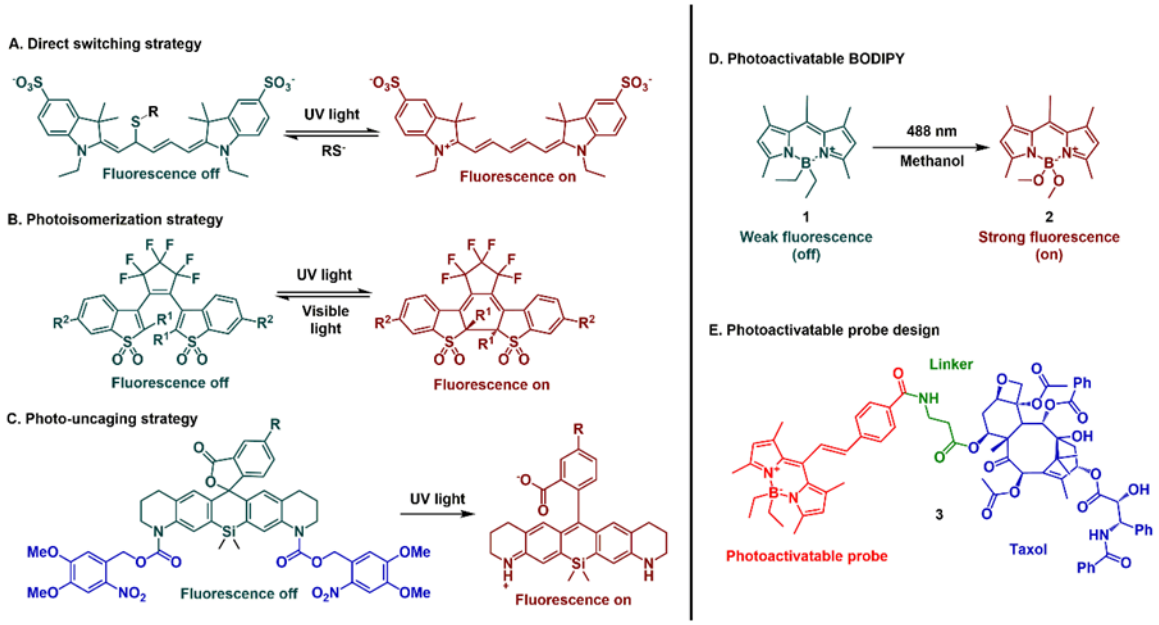

Figure 3.1. Examples of SMLM probes based on (A) direct switching[4a, 4b], (B) photoisomerization[4c], and (C) photo-uncaging[5b]. (D) photoactivation of B-dialkylated BODIPY with visible light generates a fluorescent signal. (E) Photoactivatable BODIPY probe for SMLM imaging of microtubules.

Fluorescent probes play an important role in SMLM. Ideal probes should have low fluorescence in the "off" state and high photon release in the "on" state. Only a sparse subset of fluorophores should be on in any frame to ensure high localization precision. Photoswitchable probes[4] (**Figure 2.1 A,B**) have no fluorescence in the off state. Common photoswitchable probes require a UV laser to convert the molecules into the on state from the off state and a second laser to excite the active fluorophore. While the use of two lasers decouples the switching rate and the signal intensity, a high-power UV laser affects cell health and may increase the autofluorescence in the cells. Typical laser irradiances used with common SMLM probes are listed in the Supporting Information, **Table S1**. These probes also often necessitate the use of additives in the imaging media to ensure switching to the off state.

Photocages[5] (**Figure 2.1 C**) releasing fluorescent compounds have been used as fluorescent probes, including probes for SMLM.[6] Photoactivated fluorescent probes are most commonly derived from the *o*-nitrobenzyl photocage.[5b, 6] This photocage has high quantum yields of release but requires UV light activation and has potentially toxic nitrosoarene photoproducts. In addition, a second high-

power laser is necessary to excite the activated fluorophore. It would be beneficial to have a SMLM probe that only necessitates a single low-power visible-light laser. The use of a single laser is beneficial because it simplifies the instrumentation, but it also couples the mechanism to achieve photoactivation and the signal intensity.

Previously, *meso*-substituted BODIPY fluorophores have been introduced as photocages.[7] We recently discovered that BODIPY compounds with alkyl groups on the boron have higher quantum yields of photorelease than their fluoro analogues.[8] Serendipitously, we found that these dyes have a significant increase in fluorescence after irradiation with green light, independent of substitution at the *meso*-position. Herein, we describe a BODIPY fluorescent probe with photoactivation using circa-500 nm light and its application for SMLM. We show the laser flux can be optimized to achieve a sufficient single molecule density and signal intensities that permit accurate localization of a sufficient number of fluorophores with a short analysis time.

Results and Discussion

The photophysics of the parent boron-alkylated BODIPY compound and its photoproduct were measured in methanol, a solvent in which both compounds are well dissolved. Product studies showed that upon irradiation, the alkyl groups on the boron are cleaved and replaced with the solvent adduct (**Figure 2.1 D** and the Supporting Information, **Figure S1**). The photophysical properties of compound **1** and **2** are typical of BODIPY dyes (**Table 2.1**), though it is notable that compound **2** has a circa 6-fold higher fluorescence quantum yield than compound **1** in methanol. The photoactivation quantum yield measured in methanol using a 532 nm Nd:YAG laser with a ferrioxalate actinometer was 0.79±0.02 %. This photoactivation quantum yield is lower than those of typical *o*-nitro benzyl derivatives,[9] however the much higher extinction coefficient of BODIPY leads to a similar photoactivation quantum efficiency (that is, the photoactivation quantum yield times the extinction coefficient), and the use of visible light and lack of the nitrosoarene byproduct makes the BODIPY probe more compatible with biological samples.

The photoreaction of compound **1** occurs in aqueous media, which is a requirement for biological imaging. The photoactivation quantum yield in 90:10 acetonitrile/water was 0.8±0.1 %, similar to the activation quantum yield in methanol. The fluorescence quantum yields of **1** and its photoproduct were measured in 90:10 acetonitrile/water to be 0.06 and 0.35, respectively. While the quantum yield was diminished in aqueous solution compared to methanol, the 6-fold increase in quantum yield when comparing **1** and its photoproduct was consistent with both media. The fluorescence intensity increased circa 3-fold upon irradiation in PBS buffer compared to the initial fluorescence intensity of compound **1** (Supporting Information, **Figure S3**), which was similar to the reaction in methanol. Competitive photoactivation and photobleaching during the irradiation likely explains the discrepancy between the circa 3-fold increase in fluorescence measured after 5 min of irradiation in an aqueous medium (**Figure S3**) and the circa 6-fold increase in the fluorescence quantum yield (**Table 2.1**). Mass spectrometry analysis indicates that the photoproduct in aqueous media is the expected dihydroxy species (Supporting Information, **Scheme S3** and **Figure S2**).

A 4-(*N*-hydroxysuccinamidylcarbonyl)styryl group was added to **1** to facilitate the attachment of nucleophile-containing compounds that could be used to target the photoactivatable BODIPY probe to specific cellular structures. In order to show that the B-alkylated BODIPY compounds could be used for SMLM imaging we chose to target microtubules as a proof of principle. Microtubules are rigid structures with an approximately 25 nm diameter.[10] They are a good target for testing super-resolution imaging approaches since their size is below the diffraction limit of light. Paclitaxel was chosen as an inexpensive and readily available microtubule probe. Compound **3** was synthesized with paclitaxel attached in a manner that preserves the binding sites to microtubules (**Figure 2.1 E**).

Compound **3** initially has a lower fluorescence than **1** owing to the styryl group on the *meso* position.[11] To verify that the molecule still undergoes photoactivation, it was irradiated in a cuvette in PBS buffer. Similar to the irradiation of **1**, the fluorescence intensity was enhanced three-fold over the initial fluorescence intensity at the start of the illumination (**Figure 2.2 A**). After

photoactivation, the excitation maximum was 498 nm and the emission maximum was 517 nm (Supporting Information, **Figure S5**).

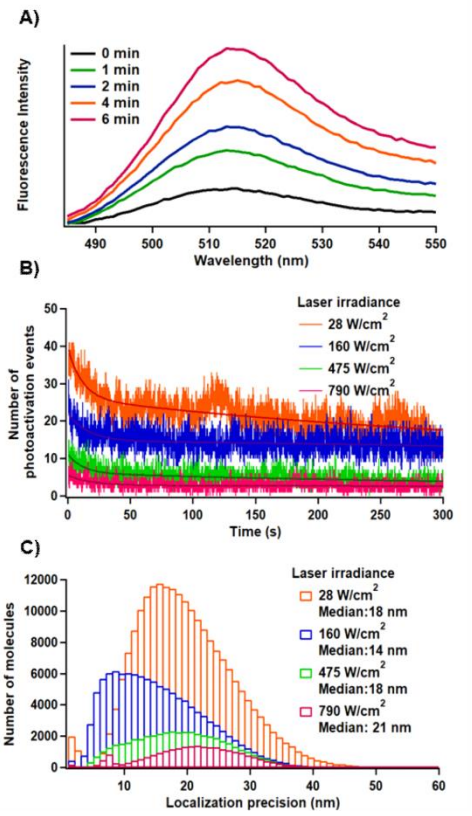

Figure 3.2. (A) Fluorescence increase of compound **3** irradiated with a 500 W halogen arc lamp in a quartz cuvette. The start of illumination is 0 min. The fluorescence was measured using a 475 nm excitation wavelength. (B) Plots of the number of photoactivated BODIPY over time (measured in each frame starting after 3 s) using a 488 nm laser with the indicated irradiance. There is an exponential decay in photoactivation events with illumination time after 3 s. (C) Histogram of the localization precision of the photoactivated molecules.

In addition, the photoactivation quantum yield of an analogue of **3** without paclitaxel attached in 90:10 acetonitrile/water was 0.12±0.02 %. The photoactivation quantum yield is likely lower than that of **1** (0.80 %) owing to the additional vibrational relaxation introduced with the styryl group in the *meso* position.

In order to optimize the laser irradiance for SMLM, compound **3** was drop cast onto a clean glass coverslip and imaged using a home-built SMLM microscope. The laser irradiance affects the number and density of photoactivation events recorded in each frame of the movie. Highly inclined and laminated optical sheet (HILO) illumination was used to reduce background while generating signal from up to a 3 micron depth from the glass slide (that is, the same illumination used for the cell studies). The fluorescence was detected using an electron multiplying charge coupled device (EMCCD) detector. No photoactivation of compound **3** was observed with laser irradiances lower than 28 W cm^{-2}. Graphs of the number of photoactivation events in each frame of the movie were constructed for laser irradiances between 28 to 790 W cm^{-2} (**Figure 2 B**). All irradiances generated numerous photoactivation events and conditions not suitable for localization within the first 3 s but sparse photoactivation events at subsequent times (Supporting Information, **Figure S6**). Laser irradiances of 28, 160, 475, and 790 W cm^{-2} were suitable to activate an average of 21, 12, 5 and 3 molecules sparsely distributed throughout the frame over the 5 min movie. The number of localizable events in each frame decreased with increasing laser irradiance because the number of photoactivation events that occur in the first three seconds increases with increasing laser irradiance, leaving a smaller subset of molecules at later times to undergo photoactivation. For all irradiances between 28 to 790 W cm^{-2} most molecules were on for less than 30 ms before photobleaching (Supporting Information, **Figure S7**).

The localization precision for each localizable photoactivation event was determined using the ThunderSTORM plug-in for ImageJ.[12] A histogram of the localization precision was generated for each laser irradiance (**Figure 2.2 C**). The smallest median localization precision (14 nm) was obtained with an irradiance of 160 W cm^{-2}.

Combining the results for the number of localization events in each frame and their precision, a laser irradiance of 160 W cm^{-2} was used in subsequent imaging experiments. Importantly, this irradiance is significantly lower than those used for many conventional SMLM experiments, which are

generally greater than 1 kW cm^{-2} (Supporting Information, **Tables S1** and **S2**).[13] The lower irradiance used in these experiments means photodamage to biological cells and tissues should be minimized.

The ability of compound **3** to bind to microtubules and retain the optical properties required for

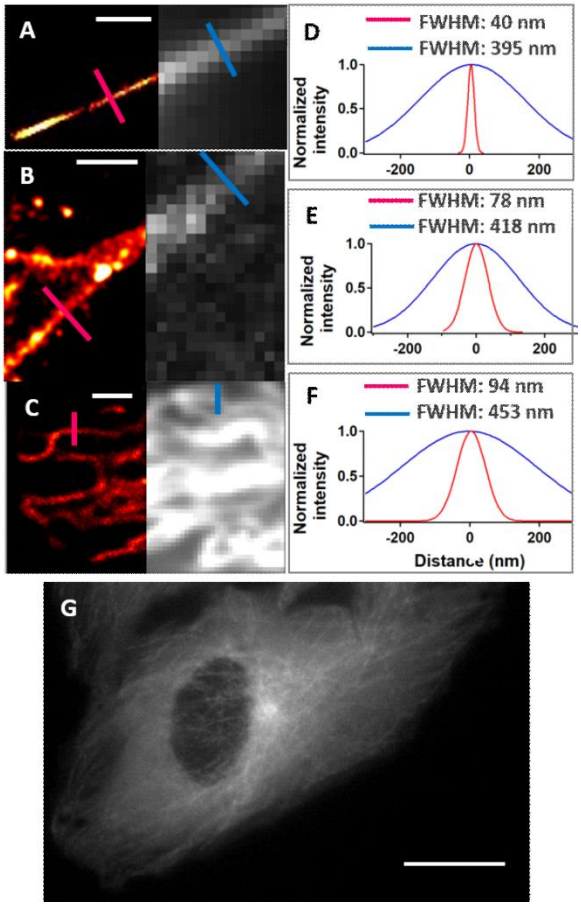

Figure 3.3. (A) In vitro, (B) fixed HeLa cell, and (C) live HeLa cell SMLM images of compound **3**-labeled microtubules (color scale images). Gray scale images are the diffraction-limited images generated by summing all the frames in the movie without localizing the fluorophores. HEPES buffer was used as the imaging medium for live cells and PBS buffer was used for in vitro and fixed cell images. A single 160 W/cm^{-2} 488 nm laser was used for activation and excitation. (D), (E) and (F) are the Gaussian fits of line-scan intensities across the indicated areas in the SMLM images (red line) and corresponding diffraction limited images (blue line) of (A), (B) and (C), respectively. Images (B) and (C) show only a small area of the cell; (G) is the diffraction-limited image of microtubules showing the entire cell. Scale bar: (A) and (B) 500 nm, (C) 1 μm, (G) 20 μm.

SMLM was tested using in vitro assembled microtubules spread on a glass slide (**Figure 2.3 A,D**). Total internal reflection (TIR) illumination was used to reduce background and achieve a median signal-to-noise ratio of 48 upon photoactivation (Supporting Information, **Figure S8**). Fifty thousand frames were collected at which point no additional molecules could be detected. Localization data were used to

reconstruct the super-resolution images. The microtubules were imaged with an average full-width-at-half maximum (FWHM) diameter of 45±10 nm. This is smaller than the diffraction limit of light but larger than the reported microtubule diameter (25 nm). The additional distance that separates the microtubule and the fluorescent label is minimal using compound **3** when compared to antibody-coupled fluorescent probes.[14] The microtubule was not immobilized on the glass slide, and the larger measured FWHM may be the result of the movement of the microtubule as a result of the presence of imaging buffer. SMLM was performed using HeLa cells fixed with 0.5 % glutaraldehyde and subsequently incubated with 1 μm compound **3** for 1 h. The fluorescence signal was observed in the nucleus and was highly concentrated in the nucleoli (Supporting Information, **Figure S9**). This result was consistent with previous reports[15] stating formaldehyde and glutaraldehyde fixation agents destroy the paclitaxel binding site on microtubules. Using ethylene glycol bis(succinimidyl succinate) (EGS) to fix the cells, however, the paclitaxel binding site on microtubules was retained (**Figure 2.3 B,E**).[15b]

To determine the utility of compound **3** for SMLM of microtubules in live cells, HeLa cells were incubated with 1 μm compound **3** in complete growth medium. Paclitaxel is a known substrate of the P-glycoprotein efflux transporter, therefore the P-glycoprotein inhibitor verapamil was used to enhance the concentration of compound **3** in the intracellular environment.[15b, 16] The diffraction-limited image showed the intracellular concentration was suitable for imaging the microtubules (**Figure 2.3 G**). Super-resolution images of microtubules were generated using the localization data (**Figure 2.3 C,F**). The data demonstrate that the photoactivatable BODIPY probe enables live-cell SMLM. This will facilitate measuring cellular structures that are altered by fixation procedures, although the dynamics of the imaged features should be slow relative to the data collection time.

Alexa Fluor 488 and ATTO 488 SMLM probes have similar excitation and emission profiles as the BODIPY probe used in this study. Alexa Fluor 488 and ATTO 488, however, require higher laser irradiances (1.2 to 3 kW cm^{-2})[13a, 17] to achieve the switching properties preferable for SMLM compared to the BODIPY photoactivatable probe (0.16 kW cm^{-2}). In addition, Alexa Fluor 488 and ATTO 488

require two lasers for SMLM. A UV laser is used to achieve the switching between on and off states, which is not preferable for cell imaging. Photoactivatable probes used for SMLM, such as coumarin oxazine[18] and rhodamine-based photocages[4e, 5b, 19] also require UV irradiation (355 nm to 405 nm) and two lasers for the activation and excitation of the probe (**Table S2**). The photoactivatable BODIPY can be activated and excited with a single laser in the visible range, which overcomes the drawbacks of UV activation. Moreover, the BODIPY probe does not require reducing agents or oxygen scavengers as required for the photoswitchable class of SMLM probes.

Conclusion

In summary, the photoactivatable BODIPY probe is versatile and can be easily attached to nucleophile-containing molecules, thus it can be used to image various biological targets. We have demonstrated the utility of a B-alkylated BODIPY probe for SMLM by attaching paclitaxel for super-resolution imaging of microtubules. When the dynamics of the structure being imaged are sufficiently slow on the timescale of the imaging experiment, the photoactivatable BODIPY can be used to image live cells with a range of imaging buffers that do not contain reducing agents or oxygen scavengers. In addition, activation and excitation of the photoactivatable BODIPY probe is achieved with a single visible laser at comparably lower irradiances than alternative SMLM approaches, so it is suitable for a variety of biological samples that might otherwise be damaged by the high power or UV lasers used with many current SMLM probes. The photophysical properties of BODIPY are easily tuned, which opens opportunities for making probes with various wavelengths of visible light activation. To further enhance the applicability of this probe, structural modifications to the BODIPY structure could be made to enhance water solubility, increase the brightness of the activated fluorophore in order to increase the localization precision, and introduce a palette of photoactivatable BODIPY with varying emission maxima for multicolor SMLM imaging.

References

1. (a) S. W. Hell, Nat. Biotechnol. 2003, 21, 1347– 1355; (b) E. Betzig, G. H. Patterson, R. Sougrat, O. W. Lindwasser, S. Olenych, J. S. Bonifacino, M. W. Davidson, J. Lippincott-Schwartz, H. F. Hess, Science 2006, 313, 1642– 1645; (c) S. R. Pavani, M. A. Thompson, J. S. Biteen, S. J. Lord, N. Liu, R. J. Twieg, R. Piestun, W. E. Moerner, Proc. Natl. Acad. Sci. USA 2009, 106, 2995– 2999; (d) M. J. Rust, M. Bates, X. Zhuang, Nat. Methods 2006, 3, 793– 795.

2. M. Heilemann, S. van de Linde, M. Schuttpelz, R. Kasper, B. Seefeldt, A. Mukherjee, P. Tinnefeld, M. Sauer, Angew. Chem. Int. Ed. 2008, 47, 6172– 6176; Angew. Chem. 2008, 120, 6266– 6271.

3. (a) S. T. Hess, T. P. Girirajan, M. D. Mason, Biophys. J. 2006, 91, 4258– 4272; (b) H. Deschout, T. Lukes, A. Sharipov, D. Szlag, L. Feletti, W. Vandenberg, P. Dedecker, J. Hofkens, M. Leutenegger, T. Lasser, A. Radenovic, Nat. Commun. 2016, 7, 13693.

4. (a) G. T. Dempsey, M. Bates, W. E. Kowtoniuk, D. R. Liu, R. Y. Tsien, X. Zhuang, J. Am. Chem. Soc. 2009, 131, 18192– 18193; (b) J. C. Vaughan, G. T. Dempsey, E. Sun, X. Zhuang, J. Am. Chem. Soc. 2013, 135, 1197– 1200; (c) B. Roubinet, M. Weber, H. Shojaei, M. Bates, M. L. Bossi, V. N. Belov, M. Irie, S. W. Hell, J. Am. Chem. Soc. 2017, 139, 6611– 6620; (d) M. K. Lee, P. Rai, J. Williams, R. J. Twieg, W. E. Moerner, J. Am. Chem. Soc. 2014, 136, 14003– 14006; (e) J. Fölling, V. Belov, R. Kunetsky, R. Medda, A. Schonle, A. Egner, C. Eggeling, M. Bossi, S. W. Hell, Angew. Chem. Int. Ed. 2007, 46, 6266– 6270; Angew. Chem. 2007, 119, 6382– 6386.

5. (a) S. Banala, D. Maurel, S. Manley, K. Johnsson, ACS Chem. Biol. 2012, 7, 289– 293; (b) J. B. Grimm, T. Klein, B. G. Kopek, G. Shtengel, H. F. Hess, M. Sauer, L. D. Lavis, Angew. Chem. Int. Ed. 2016, 55, 1723– 1727; Angew. Chem. 2016, 128, 1755– 1759; (c) S. Hauke, A. von Appen, T. Quidwai, J. Ries, R. Wombacher, Chem. Sci. 2017, 8, 559– 566; (d) T. Kobayashi, T. Komatsu, M. Kamiya, C. Campos, M. Gonzalez-Gaitan, T. Terai, K. Hanaoka, T. Nagano, Y. Urano, J. Am. Chem. Soc. 2012, 134, 11153– 11160; (e) V. N. Belov, G. Y. Mitronova, M. L. Bossi, V. P. Boyarskiy, E. Hebisch, C. Geisler, K. Kolmakov, C. A. Wurm, K. I. Willig, S. W. Hell, Chem. Eur. J. 2014, 20, 13162– 13173; (f) D. P. Klötzner, K. Klehs, M. Heilemann, A. Heckel, Chem. Commun. 2017, 53, 9874– 9877.

6. W. H. Li, G. Zheng, Photochem. Photobiol. Sci. 2012, 11, 460– 471.

7. (a) P. Goswami, A. Syed, C. L. Beck, T. R. Albright, K. M. Mahoney, R. Unash, E. A. Smith, A. H. Winter, J. Am. Chem. Soc. 2015, 137, 3783– 3786; (b) E. Palao, T. Slanina, L. Muchova, T. Solomek, L. Vitek, P. Klan, J. Am. Chem. Soc. 2016, 138, 126– 133; (c) N. Rubinstein, P. Liu, E. W. Miller, R. Weinstain, Chem. Commun. 2015, 51, 6369– 6372.

8. T. Slanina, P. Shrestha, E. Palao, D. Kand, J. A. Peterson, A. S. Dutton, N. Rubinstein, R. Weinstain, A. H. Winter, P. Klan, J. Am. Chem. Soc. 2017, 139, 15168– 15175.

9. P. Klán, T. Solomek, C. G. Bochet, A. Blanc, R. Givens, M. Rubina, V. Popik, A. Kostikov, J. Wirz, Chem. Rev. 2013, 113, 119– 191.

10. C. M. Waterman-Storer, Mol. Biol. Cell 1998, 9, 3263– 3271.

11. R. Lincoln, L. E. Greene, C. Bain, J. O. Flores-Rizo, D. S. Bohle, G. Cosa, J. Phys. Chem. B 2015, 119, 4758– 4765.

12. M. Ovesný, P. Krizek, J. Borkovec, Z. Svindrych, G. M. Hagen, Bioinformatics 2014, 30, 2389–2390.

13. (a) G. T. Dempsey, J. C. Vaughan, K. H. Chen, M. Bates, X. Zhuang, Nat. Methods 2011, 8, 1027– 1036; (b) S. van de Linde, A. Loschberger, T. Klein, M. Heidbreder, S. Wolter, M. Heilemann, M. Sauer, Nat. Protoc. 2011, 6, 991– 1009.

14. (a) Z. Chen, V. W. Cornish, W. Min, Curr. Opin. Chem. Biol. 2013, 17, 637– 643; (b) T. J. Chozinski, L. A. Gagnon, J. C. Vaughan, FEBS Lett. 2014, 588, 3603– 3612.

15. (a) R. Guy, Z. Scott, R. Sloboda, K. Nicolaou, Chem. Biol. 1996, 3, 1021– 1031; (b) G. Lukinavičius, L. Reymond, E. D'Este, A. Masharina, F. Gottfert, H. Ta, A. Guther, M. Fournier, S. Rizzo, H. Waldmann, C. Blaukopf, C. Sommer, D. W. Gerlich, H. D. Arndt, S. W. Hell, K. Johnsson, Nat. Methods 2014, 11, 731– 733.

16. M. M. Lee, Z. Gao, B. R. Peterson, Angew. Chem. Int. Ed. 2017, 56, 6927– 6931; Angew. Chem. 2017, 129, 7031– 7035.

17. M. Heilemann, S. van de Linde, A. Mukherjee, M. Sauer, Angew. Chem. Int. Ed. 2009, 48, 6903– 6908; Angew. Chem. 2009, 121, 7036– 7041.

18. E. Deniz, M. Tomasulo, J. Cusido, I. Yildiz, M. Petriella, M. L. Bossi, S. Sortino, F. M. Raymo, J. Phys. Chem. C 2012, 116, 6058– 6068.

19. (a) H. He, Z. Ye, Y. Zheng, X. Xu, C. Guo, Y. Xiao, W. Yang, X. Qian, Y. Yang, Chem. Commun. 2018, 54, 2842– 2845; (b) D. Pan, Z. Hu, F. Qiu, Z. L. Huang, Y. Ma, Y. Wang, L. Qin, Z. Zhang, S. Zeng, Y. H. Zhang, Nat. Commun. 2014, 5, 5573; (c) B. Roubinet, M. Bischoff, S. Nizamov, S. Yan, C. Geisler, S. Stoldt, G. Y. Mitronova, V. N. Belov, M. L. Bossi, S. W. Hell, J. Org. Chem. 2018, 83, 6466– 6476.

CHAPTER 4. DIRECT PHOTORELEASE OF ALCOHOLS FROM BORON-ALKYLATED BODIPY PHOTOCAGES

Julie A. Peterson, Logan J. Fischer, Elizabeth J. Gehrmann, Pradeep Shrestha, Ding Yuan, Chamari S. Wijesooriya, Emily A. Smith, Arthur H. Winter

Modified from a manuscript under revisions for *Journal of Organic Chemistry*

Abstract

BODIPY photocages are a recently-developed class of light-sensitive protecting groups that allow photorelease of substrates using biologically-benign visible light irradiation, but they have the drawback of requiring reasonably good leaving groups with relatively low conjugate acid pKa values. Consequently, photorelease of alcohols is generally accomplished by attachment with carbonate linkages, which upon photorelease liberate CO_2 gas to generate the alcohol. Here, we show that boron-alkylated BODIPY photocages are capable of directly photoreleasing both aliphatic alcohols and phenols upon irradiation via photocleavage of ether linkages. Quantum yields for direct photorelease of alcohols are lower than those for the indirect photorelease of alcohols via the better carbonate leaving group, but the overall quantum efficiencies of the photorelease reactions are on par with direct photorelease of alcohols from the popular nitrobenzyl photocages, while absorbing visible light instead of UV light. Direct photorelease of alcohols has the advantage of the higher thermal stability, ease of synthesis, and stability to cellular esterases that ether linkages provide relative to carbonate linkages. To demonstrate biological relevance, direct photorelease of a hydroxycoumarin dye was demonstrated in living HeLa cells.

Introduction

Photocages are light-sensitive chemical protecting groups that can be covalently linked to a substrate of interest, rendering it inactive. Upon irradiation, the bond is cleaved and the substrate is released, restoring its activity. Photocages are useful in studies that require the spatial and temporal control

that can be provided by pulsed light irradiation. These include biological investigations of short-lived species, small molecules, and signaling agents;[1, 2] targeted phototherapeutics;[3, 4] and microarray synthesis.[5-8] Visible light absorbing photocages have been an exciting new development as they allow for less toxic visible light irradiation in biological studies.[1, 4, 9-11] In particular, our group along with others have developed BODIPY photocages which can release leaving groups from the *meso* position after activation with single photons of green to near IR light.[12-18] Many biological targets (e.g. paclitaxel, dopamine) have phenolic or aliphatic alcohol functional groups which remain challenging targets for current photocages.

Previously, *meso*-substituted BODIPY compounds have been used to release alcohols and amines via carbonate or carbamate linkages (**Figure 1**).[13, 15-17] While carbonate linkages permit photorelease of alcohols, they have several potential drawbacks. First, while they are easy to make in theory, carbonates can be less synthetically tractable compared to ether linkages. Moreover, they can in principle be cleaved by cellular esterases which would yield undesirable background thermal deprotection, and in some cases may be less hydrolytically stable than ethers. In addition, there is required thermal decarboxylation step after photolysis which interferes with the temporal control that photoactivation allows. Direct photorelease of alcohols from the corresponding BODIPY ethers would address these disadvantages.

Recently, Weinstain and coworkers demonstrated direct release of 2,4-dinitrophenol, which has a pKa on par with acetic acid, from a BODIPY photocage.[13] Our group along with Klan's and Weinstain's groups recently conducted a structure-reactivity investigation of BODIPY photocages and discovered that boron-alkylation leads to a large increase in quantum yields of photorelease for carboxylic acids (see **2-PAA** in **Scheme 1** and **Table 1**).[18] We thus considered the possibility that these improved structures might be able to achieve direct photorelease of alcohols.

Results and Discussion

We synthesized BODIPY photocages (**Scheme 1**) with benzyl and phenyl ethers in the meso position in order to investigate their ability to release aliphatic alcohols and phenols, respectively, upon excitation with visible light.

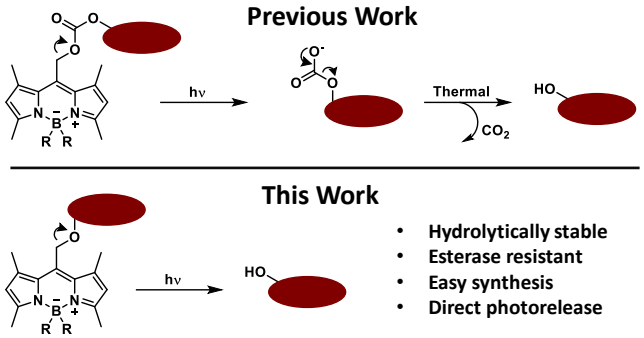

Figure 4.1. Photochemical reaction followed by thermal decarboxylation to release alcohols via a carbonate linker (top). Direct photochemical release of an alcohol via an ether linkage (bottom).

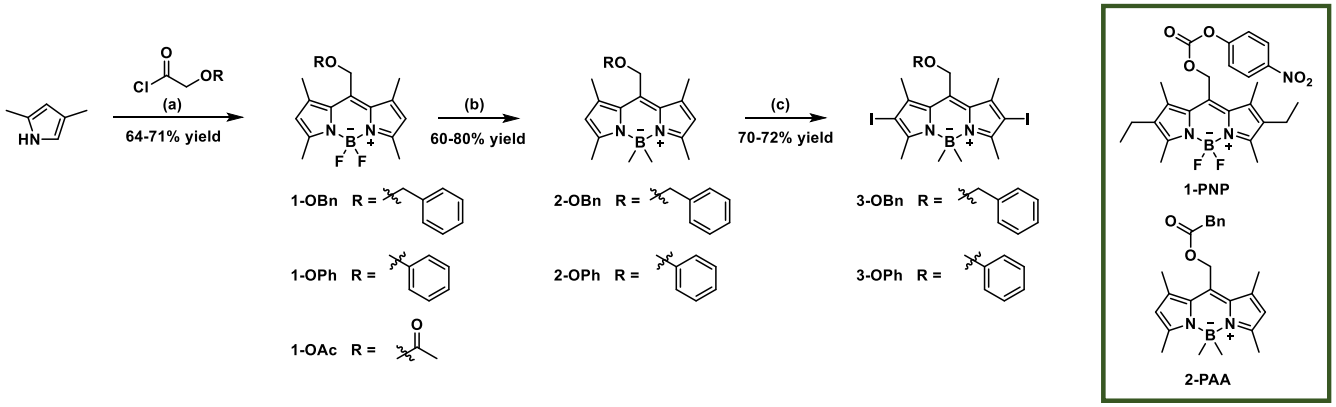

Scheme 4.1. Synthesis of BODIPY compounds ether linkages from acetyl chlorides to investigate the release of alcohols. Conditions: (a) DCM, reflux. Triethyamine, boron trifluoride diethyl etherate. (b) DCM, methylmagnesium bromide, r.t. (c) THF, N-iodosuccinimide, r.t. Compound 1-PNP is an example of a carbonate linkage previously published by Weinstain's group.[16] Compound 2-PAA is an example of a B-methylated derivative published by our group in a collaborative study with Weinstain and Klan.[18]

Table 4.1. Photophysical Properties

	λ_{ex} (nm)	λ_{em} (nm)	ε x 10^4 ($M^{-1}cm^{-1}$)	Φ (%)	Chemical Yield (time)[c]	Remaining ethers (time)	εΦ ($M^{-1}cm^{-1}$)
1-OAc[a]	517	529	7.1	0.099	--	--	70
2-PAA[b]	512	550	6.9	5.5 ± 0.02	--	--	3800
1-PNP[c]	547	--	4.8	0.16	>95%	--	77
1-OBn[d]	514	528	6.9	0.10 ± 0.02	12% (20 h)	83% (20 h)	69
1-OPh[d]	516	529	6.6	0.38 ± 0.04	30% (9 h)	56% (9 h)	251
2-OBn[d]	510	528	5.2	1.0 ± 0.5	71% (24 h)	0% (24 h)	340
2-OPh[d]	511	529	5.1	1.0 ± 0.1	45% (4 h)	53% (4 h)	510
3-OBn[d]	535	547	5.7	0.15 ± 0.03	32% (4 h)	0% (4 h)	86
3-OPh[d]	537	560	6.1	0.8 ± 0.1			104

Photophysical properties of compounds in this study. [a]Values taken from a previous study, quantum yields were calculated in methanol.[12] [b]Values taken from a previous study, quantum yield was calculated in methanol.[18] [c]Values taken from a previous study, quantum yields were calculated in a pH 7.4 aqueous solution with 5% acetonitrile.[16] [d]Compounds synthesized in this study, quantum yields were calculated in 1:1 $CDCl_3$:CD_3OD using quantitative NMR to follow the release of the substrate using dimethyl sulfone as an internal standard and **1-OAc** as the actinometer. [e]Chemical yields and remaining ether were determined by irradiating NMR tubes with 1 mL of 2 mM solutions of substrates dissolved in in 1:1 $CDCl_3$:CD_3OD with a 500 W halogen lamp. Dimethyl sulfone was used as an internal standard for quantitative NMR.

1-OBn and **1-OPh** were formed in a one pot synthesis first refluxing 2,4-dimethylpyrrole in dry DCM with benzyloxyacetyl chloride for **1-OBn**, or phenoxyacetyl chloride for **1-OPh**. The reaction was then cooled to room temperature and triethylamine and boron trifluoride diethyl etherate were added sequentially. **1-OBn** and **1-OPh** were transformed to **2-OBn** and **2-OPh** by reaction with excess methylmagnesium bromide. N-iodosuccinimide was used to iodinate the compounds to generate **3-OBn** and **3-OPh**. These photocages have high extinction coefficients (>50,000 $M^{-1}cm^{-1}$) and λ_{max} values >500 nm (**Table 1**). Photocages **2-OBn** and **2-OPh** were irradiated with a 500 W Halogen lamp and release of phenol or benzyl alcohol occurred, as demonstrated by following the photoreaction by ^{1}H NMR (**Figure C.1-C.2**).

Due to low solubility in methanol, a 1:1 mixture with a cosolvent was necessary to dissolve the substrates in this study. Interestingly, in solutions of **2-OBn** dissolved using acetonitrile or DMSO as cosolvents with methanol, benzaldehyde was observed in the NMR after irradiation with a 532 nm

Nd:YAG laser. However, benzaldehyde formation was not detected with either a 500 W halogen lamp or a low intensity green LED (**Figure C.5**). Additionally it was not detected in a 50:50 mixture using chloroform as the cosolvent (**Table C.1**). The mechanism of this oxidation is currently unknown, and it is unclear why benzaldehyde is only present under certain conditions. To avoid this curiosity, quantum yields were determined using chloroform as the cosolvent for the purpose of this study.

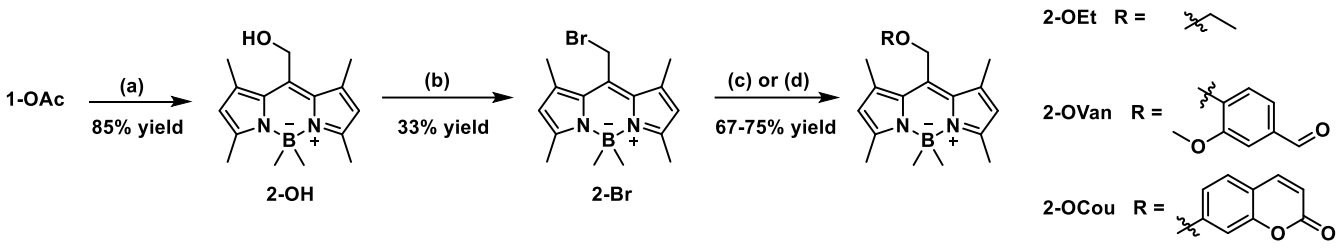

Scheme 4.2. Synthesis of BODIPY ethers with Williamson ether synthesis from **2-Br**. Conditions: (a) DCM, methylmagnesium bromide, r.t. (b) DCM, phosphorous tribromide, 0 ºC, (c) ACN, potassium carbonate, r.t. (d) ACN, cesium carbonate, r.t.

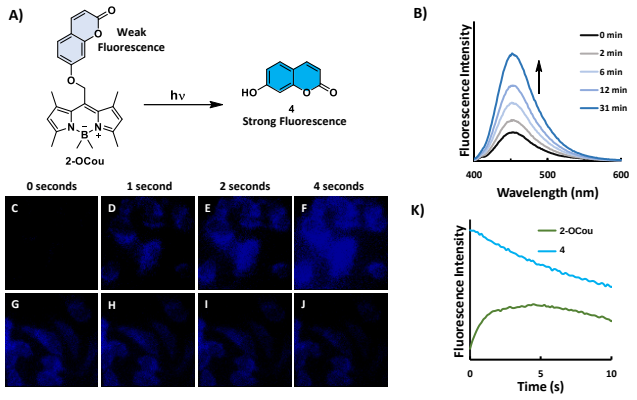

Figure 4.2. A) Scheme of **2-OCou** which has a fluorescence increase upon photorelease of 4. B) Fluorescence increase in imaging buffer following the photorelease of 7-hydroxycoumarin upon irradiation with a green LED. C-F) Fluorescence images of HeLa cells incubated with 25 µM compound **2-OCou** and continuously irradiated with 350 nm light while collecting 450 nm emission. G-J) Fluorescence images using 25 µM of 4 as a control. K) Fluorescence intensity with continuous irradiation of cells incubated with **2-OCou** and 4.

To determine quantum yields of photorelease for the compounds of this study, samples dissolved in 50:50 CD_3OD:$CDCl_3$ were irradiated with a 532 nm Nd:YAG laser. The amount of release over time was calculated using quantitative NMR with dimethyl sulfone as an internal standard and using **1-OAc** as the actinometer (Φ = 0.099%).[12]

The boron-fluorinated ethers surprisingly have decent quantum yields of photorelease in a 50:50 methanol:chloroform mixture (**Table 1**). Upon methylating the boron of the BODIPY ethers, the quantum yield of photorelease increases 2.5-10-fold compared to the corresponding boron-fluorinated ethers. We hypothesized that appending iodines to the BODIPY core would lead to a further increase in the quantum yield by promoting intersystem crossing to a longer-lived triplet excited state. This strategy was previously shown to be effective for increasing the photorelease quantum yields for carboxylic acids.[12, 17, 18] Curiously, instead of increased quantum yields of release, we observed a lower quantum yield of release and an accelerated rate of photodecomposition compared to the uniodinated derivatives (**Figure C.6**).

Direct photorelease of alcohols with a visible light photoremovable protecting group is an exciting avenue for studies of biologically relevant alcohols, or as protecting groups for multistep syntheses. There are three obvious synthetic methods for attaching alcohols to the meso position of BODIPY. First, as used for the synthesis of **1-OBn** and **1-OPh**, the phenoxy or alkyloxy acid chloride could be used for the BODIPY synthesis (**Scheme 3.1**). This method is useful for simple alcohols that are readily available. However, it may not be practical to make the acid chloride from sensitive or expensive alcohols. Another potential method of attaching alcohols to the meso BODIPY is via Williamson ether synthesis, using the BODIPY alcohol as the nucleophile and having the desired alcohol replaced with a good leaving group.[13] While this is a reasonable approach, it would be difficult to use this method for precious materials which are not available with leaving groups in the appropriate positions.

The most generally useful method is to perform a Williamson ether synthesis using the alcohol of interest as the nucleophile. However, we found that addition of alkoxides to boron-fluorinated BODIPY can lead to decomposition of the starting material with very low or no yield. However, first substituting the boron with methyl groups allowed this reaction to occur with fair yields (**Scheme 2**).[19] **1-OAc** was converted to **2-OH** using excess methylmagnesium bromide which both methylated the boron and

deprotected the acetyl group. Then, **2-Br** was synthesized by reacting **2-OH** with 0.33 equivalents of phosphorous tribromide at 0 ºC. This reaction gave a 33% yield when done on a 50 mg scale of **2-OH**. Attempts to scale up the reaction or add more phosophorous tribromide resulted in lowered yields. Unfortunately, because of low yields of the conversion of **2-OH** to **2-Br** we were limited in the amount of **2-Br** we could use in the synthesis. Therefore, we chose to use an excess of the alcohols, which may not be practical for precious materials. Our group is currently investigating routes to make **2-Br** in larger batches. Using the alcohols in excess afforded fair (67-75%) yields of **2-OEt**, **2-OVan**, and **2-OCou** under mild conditions. For the phenolic compounds, potassium carbonate was used as the base. However under these conditions no reaction was observed between **2-Br** and ethanol after 12 h. When cesium carbonate was used instead, the reaction was complete after stirring overnight. **2-OEt** and **2-OVan** released ethanol and vanillin respectively upon irradiation with white light (**Figures C.3-4**).

2-OCou was used as a proof of concept to demonstrate the viability for direct photorelease of alcohols in biological studies. The fluorescence of 7-hydroxycoumarin (**4**) is known to be highly dependent on substitutions on the hydroxy group. The protected coumarin (**2-OCou**) should have a diminished fluorescence which is recovered after irradiation. HeLa cells were incubated with **2-OCou** and irradiated. Cells irradiated with green light for intervals showed an increase in fluorescence at 450 nm using short 365 nm excitation (**Figure C.7**). In order to obtain the best signal to noise ratio, the cells were irradiated with 350 nm light. This doubled as the activation wavelength for BODIPY, as well as the excitation wavelength for 7-hydroxycoumarin so the fluorescence could be collected continuously at 450 nm (**Figure 3.2**). An increase in fluorescence followed by photobleaching was observed for irradiation of cells incubated with **2-OCou**, while only a decrease in fluorescence (photobleaching) was measured in a control experiment irradiating cells incubated only with 7-hydroxycoumarin. These studies indicate that the use of ethers as a linkage to directly photorelease alcohols is a viable strategy in biological systems.

In conclusion, the synthesis of meso-substituted BODIPY ethers was demonstrated, and direct photorelease of the corresponding alcohols has been reported. Swapping the fluorines on the boron for methyls effectively increases the quantum yield of release, while iodination does not. Williamson-ether synthesis between **2-Br** and an alcohol of interest may be a good path for making these ethers, but more work needs to be done to find a better path for the synthesis of **2-Br** itself. Practical use was demonstrated by direct photorelease of the fluorescent dye 7-hydroxycoumarin in living HeLa cells.

Experimental

General Information

Unless otherwise stated, all purchased chemicals were used without further purification. Solvents were dried for 3 days over activated 4 Å molecular sieves. Compound **1-OAc** was prepared as previously reported.[20]

Light Sources

Irradiation with white light was carried out using a Utilitech brand 500 W model #MPL1025-C500K9030 halogen work lamp. A 500 mL beaker filled with water was placed in front of the lamp and a fan was blown on the lamp and the sample to prevent overheating. Samples were irradiated in NMR tubes approximately 25 cm away from the light source.

Irradiation with green LED was carried out using a Luzchem EXPO-LED photoreactor equipped with 5 LED-GR (4 W) lamps. The photoreactor was placed on its side and samples were irradiated in NMR tubes approximately 10 cm away from the light source.

Irradiation with green laser was carried out using a Nd:YAG laser equipped with a 532 nm crystal. Samples were irradiated in quartz cuvettes equipped with stir bars.

Procedure for Determination of Quantum Yields. 2-20 mg of BODIPY compounds were dissolved in 5 mL of deuterated chloroform. The solutions were spiked with a known amount of dimethylsulfone as an internal standard and diluted to 10 mL with deuterated methanol. The solutions were checked to ensure that they had an absorbance of greater than 2 at 532 nm. 3 mL of the solutions were transferred to quartz cuvettes and irradiated with a ND:YAG 532 nm laser under air. At varying time intervals of irradiation, 0.6 mL of the samples were transferred to NMR tubes and ^{1}H NMR spectra were obtained. The solutions were then returned to the cuvettes for further irradiation. Photorelease was monitored at six time points for each compound by ^{1}H NMR, following the growth of the leaving group. The concentration of the released compound was calculated using the internal standard and the quantum yield was calculated using **1-OAc** (8-Acetoxymethyl-1,3,5,7-tetramethyl pyrromethene fluoroborate) as the actinometer. **1-OAc** was irradiated in the same manner as the other photocages.

General procedure for synthesis of 1-OBn and 1-OPh. To a solution of 2,4-dimethylpyrrole (2 eq) stirring in 3 mL dry dichloromethane in a 2-neck flask equipped with a condenser under argon was added 1 eq of acid chloride. The mixture was stirred at reflux in an oil bath for 2 h and turned dark red. The mixture was cooled to room temperature and triethylamine was added followed by boron trifluoride diethyl etherate. The solvent was reduced under vacuum to give a dark oily liquid. Methanol was added to precipitate the product, which was then filtered and washed with methanol until the solid was bright orange.

*8-Phenoxymethyl-1,3,5,7-tetramethyl pyrromethene fluoroborate (**1-OPh**)*. Obtained from 2,4-dimethyl pyrrole (400μL, 3.9 mmol, 2 eq) and phenoxyacetyl chloride (270 μL, 1.95 mmol, 1 eq) as a bright orange solid in 73% yield (511 mg). ^{1}H NMR (400 MHz, $CDCl_3$) δ 7.34 (t, J = 6 Hz, 2H), 7.04 (t, J = 6 Hz, 1H), 6.98 (d, J = 6 Hz, 2H), 6.07 (s, 2H), 5.15 (s, 2H), 2.54 (s, 6H), 2.30 (s, 6H); ^{13}C{^{1}H} NMR (93 MHz, $CDCl_3$): δ 158.3, 156.5, 141.7, 134.1, 133.0, 129.8, 122.1, 121.7, 114.1, 60.7, 15.4, 14.7; HRMS (ESI/QTOF) m/z: $[M + H]^+$ Calcd for $C_{20}H_{21}BF_2N_2O$ 355.1793; Found 355.1787.

*8-Benzoxymethyl-1,3,5,7-tetramethyl pyrromethene fluoroborate (**1-OBn**).* Obtained from 2,4-dimethyl pyrrole (400μL, 3.9 mmol, 2 eq) and benzyloxyacetyl chloride (310 μL, 1.95 mmol, 1 eq) as a bright orange solid in 64% yield (447 mg). ^{1}H NMR (400 MHz, $CDCl_3$) δ 7.31-7.37 (m, 5 H), 6.04 (s, 2 H), 4.65 (s, 2 H), 4.61 (s, 2 H), 2.52 (s, 6 H), 2.31 (s, 6 H); $^{13}C\{^{1}H\}$ NMR (93 MHz, $CDCl_3$) δ 155.9, 141.9, 137.1, 136.2, 133.1, 128.6, 128.4, 128.3, 122.0, 73.1, 63.1, 15.4; HRMS (ESI/QTOF) m/z: $[M + H]^+$ Calcd for $C_{21}H_{23}BF_2N_2O$ 369.1944; Found 369.1952.

General Procedure for methylation of BODIPY etherate photocages. To a solution of **1-OBn** or **1-OPh** in 5 mL dry dichloromethane was added 11 eq of methylmagnesium bromide. The solutions were stirred for 1 h, quenched with ammonium chloride, washed 3 times with water, once with brine, and dried over sodium sulfate. The solvent was removed under vacuum and the mixtures were purified as listed below.

*1,3,5,7-tetramethyl-8-Phenoxymethyl pyrromethene methylborate (**2-OPh**).* Obtained from **1-OPh** (100 mg, 0.28 mmol, 1 eq) and methylmagnesium bromide (1 mL 3 M solution in THF, 3.0 mmol, 11 eq). The crude solid was purified with silica gel column chromatography using 90:10 hexanes:methylene chloride as the eluent to give the product as a bright orange solid in 80% yield (75 mg). ^{1}H NMR (400 MHz, $CDCl_3$) δ 7.36 (t, J = 8 Hz, 2H), 7.05 (t, J = 8 Hz, 2H), 7.00 (d, J = 8 Hz, 2H), 5.20 (s, 2H), 2.56 (s, 6H), 2.35 (s, 6H), 0.22 (s, 6H); $^{13}C\{^{1}H\}$ NMR (93 MHz, $CDCl_3$) δ 158.5, 153.1, 137.4, 134.2, 131.6, 129.8, 122.6, 121.5, 114.2, 61.3, 16.7, 15.8, 1.2; HRMS (ESI/QTOF) m/z: $[M + H]^+$ Calcd for $C_{22}H_{27}BN_2O$ 346.2295; Found 347.2288.

*8-Benzoxymethyl-1,3,5,7-tetramethyl pyrromethene methylborate (**2-OBn**).* Obtained from **1-OBn** (100 mg, 0.27 mmol, 1 eq) and methylmagnesium bromide (1 mL 3 M solution in THF, 3.0 mmol, 11 eq). The crude solid was purified with silica gel column chromatography using 90:10 hexanes:methylene chloride as the eluent to give the product as a bright orange solid in 60% yield (60 mg). **1**H NMR (400 MHz, $CDCl_3$) δ 7.40 (m, 5H), 6.09 (s, 2H), 4.77 (s, 2H), 4.65 (s, 2H), 2.49 (s 6H), 2.40 (s, 6H), 0.24 (s,

6H); $^{13}C\{^{1}H\}$ NMR (93 MHz, $CDCl_3$) δ 152.5, 137.4, 137.3, 136.1, 131.7, 128.6, 128.5, 128.2, 122.4, 73.4, 63.9, 16.7, 15.7. HRMS (ESI/QTOF) m/z: $[M + H]^+$ Calcd for $C_{23}H_{29}BN_2O$ 361.2446 Found 361.2454.

General iodination procedure. To a solution of **2-OBn** or **2-OPh** dissolved in 10 mL dry THF was added 3 eq of N-iodosuccinimide. The solution was stirred until the color changed to dark pink after which dichloromethane and water were added. The organic layer was washed with water three times and dried over sodium sulfate. The solvent was removed under vacuum and the crude product was purified as listed below.

*8-Benzoxymethyl-2,6-diiodo-1,3,5,7-tetramethyl pyrromethene methylborate (**3-OBn**).* Obtained from **2-OBn** (50 mg, 0.14 mmol, 1 eq) and N-iodosuccinimide (95 mg, 0.42 mmol, 3 eq). The crude product was purified with silica gel column chromatography using hexanes to 90:10 hexanes:dichloromethane gradient as the eluent to give the product as a red solid in 70% yield (59 mg). ^{1}H NMR (400 MHz, $CDCl_3$): δ 7.35 (m, 5 H), 4.73 (s, 2H), 4.63 (s, 2H), 2.52 (s, 6H), 2.42 (s, 6H), 0.17 (s, 6H). $^{13}C\{^{1}H\}$ NMR (93 MHz, CDCl3): δ 153.2, 139.9, 136.8, 135.2, 131.6, 128.7, 128.7, 128.5, 87.1, 73.7, 64.5, 18.5, 18.0, 1.2. HRMS (ESI/QTOF) m/z: $[M - H]^-$ Calcd for $C_{22}H_{25}BI_2N_2O$ 597.0077; Found 597.0059.

*2,6-Diiodo-1,3,5,7-tetramethyl-8-Phenoxymethyl pyrromethene methylborate (**3-OPh**).* Obtained from **2-OPh** (50 mg, 0.14 mmol, 1 eq) and N-iodosuccinimide (95 mg, 0.42 mmol, 3 eq). The crude product was purified with silica gel column chromatography using hexanes to 90:10 hexanes:dichloromethane gradient as the eluent to give the product as a red solid in 72% yield (62 mg). ^{1}H NMR (400 MHz, $CDCl_3$): δ 7.36 (dd, J = 8, 7.6, 2H), 7.06 (t, J = 7.6, 1H), 7.00 (d, J = 8, 2H), 5.20 (s, 2H), 2.56 (s, 6H), 2.35 (s, 6H), 0.23 (s, 6H). $^{13}C\{^{1}H\}$ NMR (93 MHz, $CDCl_3$): δ 158.0, 153.7, 139.8, 133.3, 131.4, 129.9, 121.8, 114.1, 87.3, 61.8, 18.4, 18.1, 1.1. HRMS (ESI/QTOF) m/z: $[M + H]^+$ Calcd for $C_{23}H_{27}BI_2N_2O$ 613.0379; Found 613.0380.

*8-Hydroxymethyl-1,3,5,7-tetramethyl pyrromethene methylborate (**2-OH**).* To a solution of **1-OAc** (100 mg, 0.31 mmol, 1 eq) dissolved in dichloromethane was added 15 eq of methyl magnesium bromide (4.7 mL 1 M solution in diethyl ether, 4.7 mmol, 15 eq). The solution was stirred for 1 h after which the reaction was complete by TLC. The reaction was quenched with ammonium chloride and ethyl acetate was added. The organic layer was washed 3 times with ammonium chloride, with brine, and dried over sodium sulfate. The solvent was reduced under vacuum and the product was purified via silica gel column chromatography using methylene chloride as the eluent to give **2-OH** in a 85% yield (71 mg). Characterization matched those previously reported.[20]

*8-Bromomethyl-1,3,5,7-tetramethyl pyrromethene methylborate (**2-Br**).* To a solution of **2-OH** (50 mg, 0.18 mmol, 1 eq) stirring in 5 mL dry dichloromethane at 0 °C was added phosphorous tribromide (6 µL, 0.06 mmol, 0.3 eq). The solution was stirred for 30 minutes after which it had turned dark red. Ice water was added and the organic layer was extracted with dichloromethane. The organic layer was washed with water and brine, dried over sodium sulfate, and the solvent was removed under vacuum. The mixture was purified with column chromatography on silica gel using 90:10 hexanes:dichloromethane as the eluent to give product as an red-orange solid in a 33% yield (20 mg). ^{1}H NMR (400 MHz, $CDCl_3$): δ 6.09 (s, 2H), 4.77 (s, 2H), 2.58 (s, 6H), 2.46 (s, 6H), 0.21 (s, 3H), 0.15 (s, 3H). $^{13}C\{^{1}H\}$ NMR (93 MHz, $CDCl_3$): δ 153.2, 137.6, 136.7, 129.6, 122.9, 26.1, 16.7, 16.5. HRMS (ESI/QTOF) m/z: $[M + H]^+$ Calcd for $C_{16}H_{22}BN_2Br$ 333.1132; Found 333.1133.

*8-Ethoxymethyl-1,3,5,7-tetramethyl pyrromethene methylborate (**2-OEt**).* To a solution of 1 mL ethanol in 5 mL acetonitrile stirring with cesium carbonate (5 mg, 0.015, 1 eq) was added **2-Br** (5 mg, 0.015 mmol, 1 eq). The solution was stirred at room temperature in the dark overnight. The solvent was evaporated and the residue was extracted with dichloromethane and washed withwater. The organic layer was dried over sodium sulfate and the solvent was removed under vacuum. The residue was purified by silica gel chromatography using 50:50 hexanes:dichloromethane as the eluent to give product as an orange

solid in 67% yield (3 mg). ^{1}H NMR (400 MHz, $CDCl_3$): δ 6.06 (s, 2H), 4.65 (s, 2H), 3.63 (t, J = 7, 2H), 2.44 (s, 12H), 1.30 (t, J = 7, 3H), 0.17 (s, 6H). $^{13}C\{^{1}H\}$ NMR (93 MHz, $CDCl_3$): δ 152.4, 137.3, 136.0, 131.6, 122.1, 66.5, 64.2, 29.7, 15.6, 15.3, 1.0. HRMS (ESI/QTOF) m/z: $[M + H]^+$ Calcd for $C_{18}H_{27}BN_2O$ 299.2289; Found 299.2299.

2-OVan. To a solution of **2-Br** (15 mg, 0.04 mmol, 1 eq) stirring in 5 mL dry acetonitrile was added 7 mg *p*-vanillin (7 mg, 0.046 mmol, 1.1 eq) followed by potassium carbonate (10 mg, 0.07 mmol, 1.8 eq). The solution was stirred overnight after which **2-Br** had been consumed by TLC. The mixture was diluted with water and extracted three times with dichloromethane. The combined organic layers were dried over sodium sulfate, and the solvent was removed under vacuum. The crude mixture was purified via silica gel column chromatography using 20:80 dichloromethane:hexanes as the eluent to give product as a pink-orange solid in a 75% yield (12 mg). **1**H NMR (400 MHz, $CDCl_3$): δ 9.89 (s, 2H), 7.50 (dd, J = 8, 2, 1H), 7.45 (d, J = 2, 1H), 7.11 (d, J = 8, 1H), 6.07 (s, 2H), 5.31 (s, 2H), 3.89 (s, 3H), 2.47 (s, 6H), 2.28 (s, 6H), 0.21 (s, 6H). $^{13}C\{^{1}H\}$ NMR (93 MHz, $CDCl_3$): δ 191.00, 153.52, 153.39, 150.17, 137.39, 132.91, 131.93, 130.97, 126.62, 122.76, 111.60, 109.82, 62.98, 56.18, 16.75, 15.68, 1.17. HRMS (ESI/QTOF) m/z: $[M + H]^+$ Calcd for $C_{24}H_{29}BN_2O_3$ 404.238; Found 404.2375.

2-OCou. To a solution of 7-hydroxycoumarin (20 mg, 0.12 mmol, 1.7 eq) stirring in 5 mL acetonitrile was added potassium carbonate (10 mg, 0.07 mmol, 1 eq) followed by **2-Br** (24 mg, 0.07 mmol, 1 eq). The solution was stirred until the starting material was consumed by TLC, after which it was diluted with water and ethyl acetate. The organic layer was washed with water 10 times to remove unreacted 7-hydroxycoumarin. The organic layer was dried over sodium sulfate and the solvent was removed under vacuum. The crude product was purified via silica gel column chromatography using dichloromethane as the eluent to give product as a pink solid in 69% yield (20 mg). ^{1}H NMR (400 MHz, $CDCl_3$): δ 7.67 (d, J = 8, 1H), 7.43 (d, J = 8, 1H), 6.96 (m, 2H), 6.30 (d, J = 8, 1H), 6.09 (s, 2H), 5.27 (s, 2H), 2.48 (s, 6H), 2.29 (s, 6H), 0.22 (s, 6H). $^{13}C\{^{1}H\}$ NMR (140 MHz, $CDCl_3$): δ 161.64, 161.05, 156.10,

153.62, 143.39, 137.20, 132.75, 131.55, 129.33, 122.94, 113.84, 112.94, 101.26, 62.34, 16.77, 15.87, 1.17. HRMS (ESI/QTOF) m/z: $[M + H]^+$ Calcd for $C_{25}H_{27}BN_2O_3$ 415.2187; Found 415.2197.

References

1. Bardhan, A.; Deiters, A., Development of photolabile protecting groups and their application to the optochemical control of cell signaling. *Current Opinion in Structural Biology* **2019,** *57,* 164-175.

2. Stanton-Humphreys, M. N.; Taylor, R. D. T.; McDougall, C.; Hart, M. L.; Brown, C. T. A.; Emptage, N. J.; Conway, S. J., Wavelength-orthogonal photolysis of neurotransmittersin vitro. *Chemical Communications* **2012,** *48* (5), 657-659.

3. Toupin, N. P.; Arora, K.; Shrestha, P.; Peterson, J. A.; Fischer, L. J.; Rajagurubandara, E.; Podgorski, I.; Winter, A. H.; Kodanko, J. J., BODIPY-Caged Photoactivated Inhibitors of Cathepsin B Flip the Light Switch on Cancer Cell Apoptosis. *ACS Chemical Biology* **2019,** *14* (12), 2833-2840.

4. Sarode, B. R.; Kover, K.; Friedman, S. H., Visible-Light-Activated High-Density Materials for Controlled in Vivo Insulin Release. *Molecular Pharmaceutics* **2019,** *16* (11), 4677-4687.

5. Alexandre Specht , F. B., Ziad Omran , Jean-François Nicoud; Goeldner, M., Photochemical tools to study dynamic biological processes. *HFSP Journal* **2009,** *3* (4), 255-264.

6. Haitao Yu, J. L., Dongdong Wu, Zhenjun Qiu, Yan Zhang, Chemistry and biological applications of photo-labile organic molecules. *Chem. Soc. Rev.* **2010,** *39*, 464-473.

7. Wen-hong Li, G. Z., Photoactivatable fluorophores and techniques for biological imaging applications. *Photochem. Photobiol. Sci.* **2012,** *11*, 460.

8. Klan, P.; Solomek, T.; Bochet, C. G.; Blanc, A.; Givesns, R.; Rubina, M.; Popik, V.; Kostikov, A.; Wirz, J., Photoremovable Protecting Groups in Chemistry and Biology: Reaction Mechanisms and Efficacy. *Chem. Rev.* **2013,** *113*, 119-191.

9. Shembekar, V. R.; Chen, Y.; Carpenter, B. K.; Hess, G. P., A Protecting Group for Carboxylic Acids That Can Be Photolyzed by Visible Light. *Biochemistry* **2005,** *44* (19), 7107-7114.

10. Olson, J. P.; Banghart, M. R.; Sabatini, B. L.; Ellis-Davies, G. C. R., Spectral Evolution of a Photochemical Protecting Group for Orthogonal Two-Color Uncaging with Visible Light. *Journal of the American Chemical Society* **2013,** *135* (42), 15948-15954.

11. Gorka, A. P.; Nani, R. R.; Zhu, J.; Mackem, S.; Schnermann, M. J., A near-IR uncaging strategy based on cyanine photochemistry. *Journal of the American Chemical Society* **2014,** *136* (40), 14153-14159.

12. Goswami, P.; Syed, A.; Beck, C. L.; Albright, T. R.; Mahoney, K. M.; Unash, R.; Smith, E. A.; Winter, A. H., BODIPY-Derived Photoremovable Protecting Groups Unmasked with Green Light. *J. Am. Chem. Soc* **2015,** *137*, 3783-3786.

13. Kand, D.; Pizarro, L.; Angel, I.; Avni, A.; Friedmann-Morvinski, D.; Weinstain, R., Organelle-Targeted BODIPY Photocages: Visible-Light-Mediated Subcellular Photorelease. Angewandte Chemie International Edition, 2019; Vol. 58, pp 4659-4663.

14. Palao, E.; Salanina, T.; Muchova, L.; Solomek, T.; Vitek, L.; Klan, P., Transition-Metal-Free CO-Releasing BODIPY Derivatives Activatable by Visible to NIR Light as Promising Bioactive Molecules. *J. Am. Chem. Soc* **2015,** *138* (1), 126–133.

15. Peterson, J. A.; Wijesooriya, C.; Gehrmann, E. J.; Mahoney, K. M.; Goswami, P. P.; Albright, T. R.; Syed, A.; Dutton, A. S.; Smith, E. A.; Winter, A. H., Family of BODIPY Photocages Cleaved by Single Photons of Visible/Near-Infrared Light. Journal of the American Chemical Society, 2018; Vol. 140, pp 7343-7346.

16. Rubinstein, N.; Liu, P.; Miller, E. W.; Weinstain, R., meso-Methylhydroxy BODIPY: a scaffold for photo-labile protecting groups. *Chem. Commun.* **2015,** *51*, 6369-6372.

17. Sitkowska, K.; Feringa, B. L.; Szymański, W., Green-Light-Sensitive BODIPY Photoprotecting Groups for Amines. *The Journal of Organic Chemistry* **2018,** *83* (4), 1819-1827.

18. Slanina, T.; Shrestha, P.; Palao, E.; Kand, D.; Peterson, J. A.; Dutton, A. S.; Rubinstein, N.; Weinstain, R.; Winter, A. H.; Klan, P., In Search of the Perfect Photocage: Structure-Reactivity Relationships in *meso*-Methyl BODIPY Photoremovable Protecting Groups. Journal of the American Chemical Society, 2017; Vol. 139, pp 15168-15175.

19. More, A. B.; Mula, S.; Thakare, S.; Sekar, N.; Ray, A. K.; Chattopadhyay, S., Masking and Demasking Strategies for the BF2–BODIPYs as a Tool for BODIPY Fluorophores. *The Journal of Organic Chemistry* **2014,** *79* (22), 10981-10987.

20. Krumova, K.; Cosa, G., Bodipy Dyes with Tunable Redox Potentials and Functional Groups for Further Tethering: Preparation, Electrochemical, and Spectroscopic Characterization. *Journal of the American Chemical Society* **2010,** *132* (49), 17560-17569.

CHAPTER 5. WAVELENGTH DEPENDENT CONTROL OF VISIBLE LIGHT PHOTOREMOVABLE PROTECTING GROUPS

Julie A. Peterson, Ding Yuan, Arthur H. Winter

Modified from a publication in preparation for submission to *Journal of Americal Chemical Society*

Abstract

Selective deprotection of functional groups using different wavelengths of light is needed for materials synthesis as well as for achieving independent photocontrol over substrates in biological systems. However, wavelength-selective activation has been difficult to achieve with common UV-absorbing photoremovable protecting groups (PRPGs) because it is difficult to separate the chromophore absorption profiles. Here, we investigated the ability of recently-developed visible light absorbing BODIPY-derived PRPGs and a known coumarin-derived PRPG to undergo wavelength selective activation in order to identify well-behaved pairs of PRPGs that allow independent optical control over a mixture of photocaged substrates. The three pairs of PRPGs tested have perfect selectivities for cleaving the longer-wavelength absorbing photocage first, and fair to excellent selectivities for releasing the lower-wavelength absorbing photocage first when mixtures were irradiated in solution. When the PRPGs are attached to the same substrate, the shorter-wavelength absorbing PRPG cannot be removed first due to energy transfer, but the PRPGs could be cleaved in a sequential manner starting by deprotecting the longest wavelength absorbing photocage first and then removing the lower-wavelength absorbing PRPG.

Introduction

Biological systems consist of a multitude of systems acting in conjunction with each other. Orthogonal control of separate biological processes could be key in investigating complex biological phenomena. Light is an ideal method of activation for control of biological targets. It is cheap,

noninvasive, and allows spatial and temporal control of activation. There are a plethora of potential applications for wavelength controlled release including orthogonal control of separate processes in biological systems,[1, 2] materials chemistry,[3] drug delivery,[4, 5] and selective release of different protecting groups on a substrate with multiple reactive sites.[6, 7]

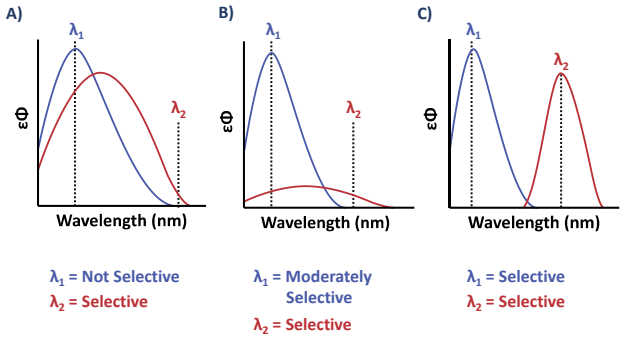

Figure 5.1. A) Two separate chromophores with overlapping absorbances that can be activated sequentially, B) Chromophores that have selectivity based on differences in quantum efficiencies. C) Chromophores with separated absorbances that can be released orthogonally.

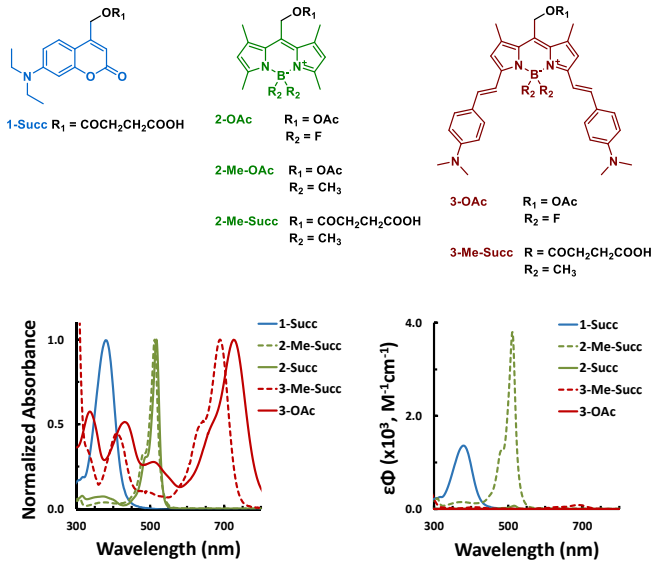

Figure 5.2. Photocages investigated in this study based on coumarin, a green absorbing BODIPY and a red-absorbing BODIPY. These three chromophores have well separated absorbances. In addition, the BODIPY compounds have tunable quantum efficiencies.

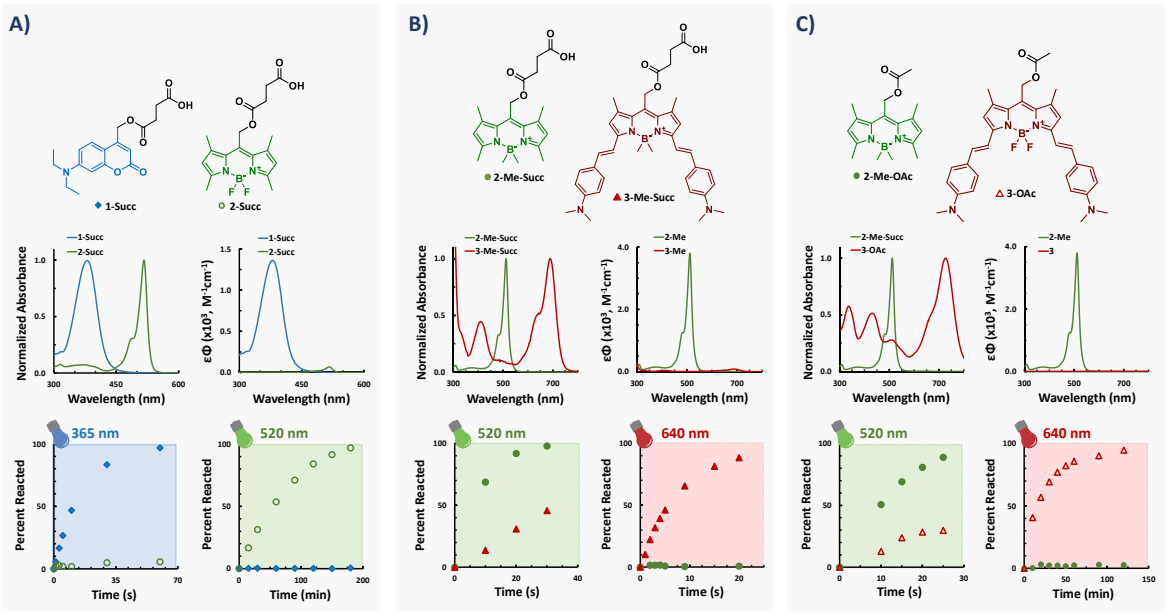

Figure 5.3. Structures of the photocages dissolved in a 1:1 ratio in 50:50 DMSO:MeOH for irradiation (top), Normalized absorbance, quantum efficiencies[a] of photocages mixed together (middle), and reactivity over time of the mixtures irradiated with LEDs centered around 365 nm, 520 nm, or 640 nm.

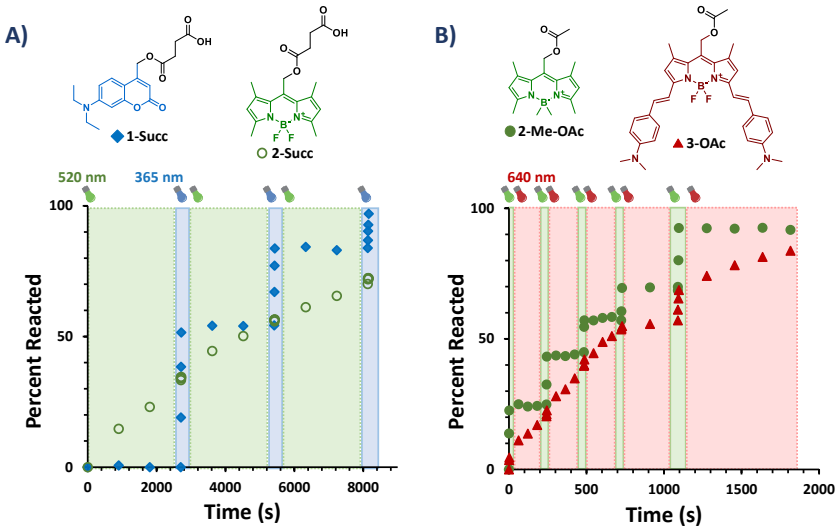

Figure 5.4. A) Solution of 1-Succ and 2-Succ dissolved in 50:50 DMSO:MeOH intermittently irradiated with a 520 nm LED and a 365 nm LED. B) Solution of **2-Me-OAc** and **3-OAc** intermittently irradiated with a 520 nm LED and a 640 nm LED.

Most of the commonly used photoremovable protecting groups have broad absorbance bands that are not well separated from each other.[1, 8-10] These photocages can be cleaved sequentially if a band for one extends to a longer wavelength than another (**Figure 4.1a**). While these work for sequential activation of two substrates of interest, they do not provide independent photocontrol over each individually.

Assuming that the chromophores do not interact during the lifetime of the excited state (e.g. no electron transfer, energy transfer, or exciplex formation occurs), the selectivity is governed by the relative quantum yields of photorelease if both chromophores absorb light equally. Under conditions of photon scarcity, which is more often the case in biological experiments, the selectivity is determined instead by the relative quantum efficiency at the irradiation wavelength. The quantum efficiency takes into account both how strongly the photocage chromophore absorbs light and the photorelease quantum yield and is defined quantitatively as the product of the quantum yield of photorelease and the extinction coefficient at the excitation wavelength.

One way to allow for better independent selectivity when the absorbances of the PRPGs overlap is if the quantum efficiency of the shorter wavelength photocage is much higher than the photocage which has a longer wavelength band (**Figure 4.1b**). In this case, assuming the chromophores do not interact during the lifetime of the excited state, there is still complete selectivity for cleaving the longer-wavelength-absorbing PRPG as well as improved selectivity for cleaving the shorter wavelength-absorbing PRPG. The extent of selectivity with the shorter wavelength can be tuned based on the difference in quantum efficiencies between the two compounds. Both of these cases require judicious selection of the irradiation wavelengths, and the photocage that absorbs the longer wavelength often cannot be irradiated at its λ_{max}. The

perfect scenario that could provide orthogonality between the two photocages would occur if there is no overlap between the two at the wavelength of irradiation (**Figure 4.1c**). Unfortunately, organic chromophores in solution typically have broad absorbances and generally cannot be perfectly separated. However, we envisioned that the narrow absorption bands of BODIPY chromophores at various wavelengths[11] (**Figure 4.2**) may have the potential to achieve near orthogonality, with very high selectivities for photoreleasing one PRPG over another.

Results and Discussion

For our investigation we compared three PRPGs—one, based on coumarin PRPG **1**,, which has a strong absorbance in the UV-blue range; a BODIPY-derived PRPG **2**, which has a strong absorbance in the green region of the visible ~500 nm, and a redshifted BODIPY PRPG **3**, which has a strong absorbance in the red to near IR region ~690 nm. These three PRPGs feature separated λ_{max} values. PRPGs **2** and **3** also have the advantage of being able to adjust their quantum efficiencies based on the substituents on the boron, providing another handle with which to achieve selectivity.[11, 12]

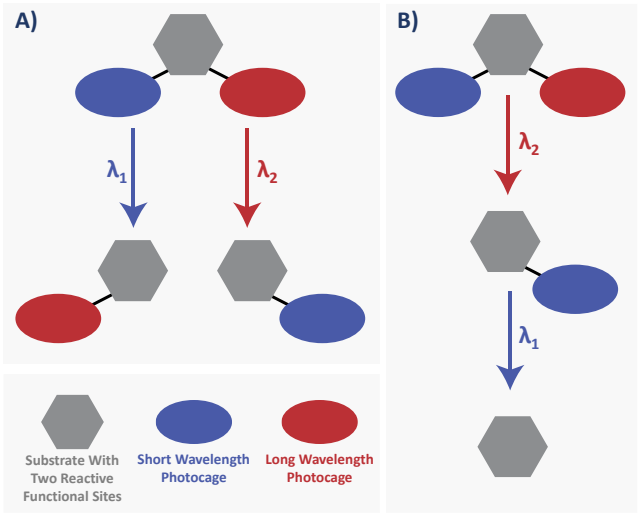

Figure 5.5. Scheme of a substrate with two functional sites that can be protected with orthogonal photocages that are A) independently selective or B) sequentially selective.

The plots of the absorbance and quantum efficiencies for each of the three sets of pairs are shown in **Figure 4.3**. As can be seen, all of them have reasonably separated absorbance bands. More importantly, plots of the quantum efficiencies for each pair suggests the possibility for very high selectivities. When a mixture of **2-Succ** and **1-Succ** were irradiated with green light, **2-Succ** reacted with no evidence of reaction of **1-Succ**. When the mixture was irradiated with an LED centered around 365 nm, **1-Succ** was reacted quickly with only a small amount of **2-Succ** reacted. This pair has excellent selectivity with both long and short wavelengths (**Figure 4.3a)**.

For **2-Me-Succ** with **3-Me-Succ** (**Figure 4.3b**), the methylation of the boron on the BODIPY chromophores has been shown to increase quantum yields of release.[11, 13] We envisioned that selectivity could be obtained based on the much higher quantum efficiency of **2-Me-Succ** compared to that of **3-Me-Succ**. This mixture had a good selectivity from red to green irradiation, however was only about 2:1 selectivity for **2-Me-Succ** over **3-Me-Succ** at full completion of **2-Me-Succ** when irradiated with an LED centered around 520 nm. We then tested a mixture of **2-Me-OAc** with **3-OAc** (**Figure 4.3c**). Since the fluorinated

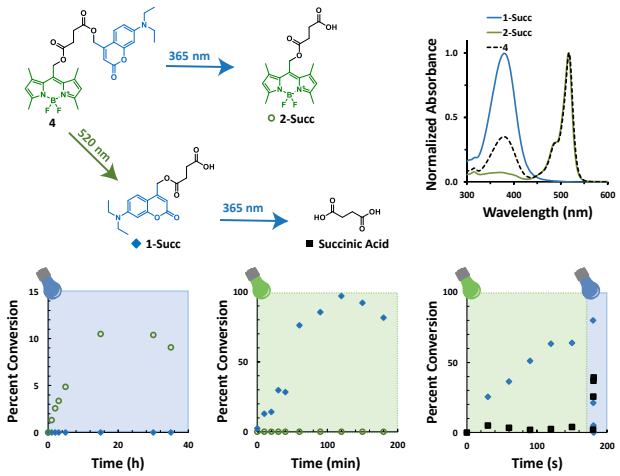

Figure 5.6. Predicted reactivity of **4** with different wavelengths of light (top left); normalized absorbance of **1-Succ**, **2-Succ**, and **4** (top right); percent of **1-Succ**, **2-Succ** grown in in after irradiation of **4** with UV (bottom left) and green (bottom middle) light; percent of **1-Succ** and succinic acid grown in after irradiation of **4** sequentially with green followed by UV light (bottom right).

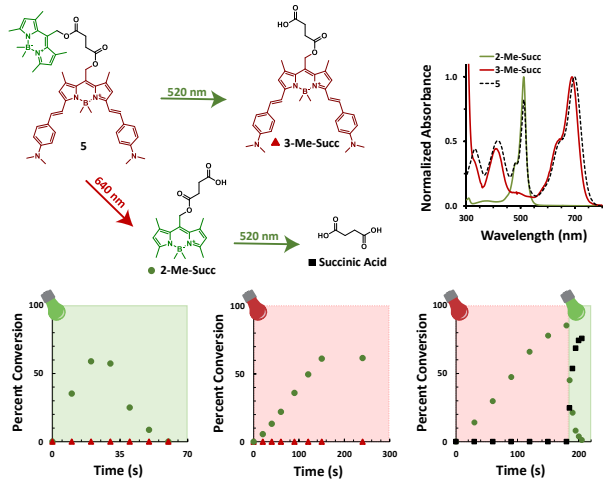

Figure 5.7. Predicted reactivity of **5** with different wavelengths of light (top left); normalized absorbance of **2-Me-Succ**, **3-Me-Succ**, and **5** (top right); percent of **2-Me-Succ** and **3-Me-Succ** grown in in after irradiation of **5** with green (bottom left) and red (bottom middle) light; percent of **2-Me-Succ** and succinic acid grown in after irradiation of **4** sequentially with red followed by green light (bottom right).

derivative has an even lower quantum efficiency compared to the methylated derivative, the mixture should give better selectivity. Indeed, this pair does give better selectivity (~4:1 selectivity after completion of **2-Me-OAc**). However, in both of these cases, the selectivity is

lower than that predicted based on the quantum efficiencies at the wavelengths of irradiation, suggesting that there may be interaction of the chromophores during the lifetime of the excited state (e.g. energy transfer between the chromophores of **2** and **3)**. We then chose the two pairs that had the best selectivity in order to demonstrate the ability for them to do alternating activation upon irradiation of different wavelengths of light. Both pairs (**1-Succ** with **2-Succ** and **2-Me-OAc** with **3-OAc**) showed good selectivity with intermittent activation (**Figure 4.4)**.

After observing good selectivity with irradiation of a mixture in solution, we envisioned that we could protect two different functional groups on the same substrate and orthogonally release one over the other (**Figure 4.5a**). We chose to investigate the pairs of **1** and **2** as well as **2-Me** and **3-Me**, using succinic acid as a linker.

When irradiating **4** with green light, the BODIPY photocage was selectively cleaved to release **1-Succ** (**Figure 4.6**). Interestingly, when irradiating **4** with UV light, the compound reacted much slower. **2-Succ** was observed and **1-Succ** was never observed; however, the percent of conversion was less than 10% over a much longer time period than **1-Succ** had reacted before. Likely, energy transfer from coumarin to BODIPY caused the reactivity of the coumarin to be diminished. At the same time, **1-Succ** may have been formed, but was not observed because it was able to react much faster than it was formed. Indeed, succinic acid was increasing steadily over time with UV irradiation (SI). When irradiated with green light, however, there was good selectivity. The green light-absorbing BODIPY chromophore was able to react and release **1-Succ** almost quantitatively. Though **4** is not able to be selective with 365 nm light, it can be activated sequentially, first with the activation of BODIPY with green light, then with the activation of coumarin with UV light to release succinic acid.

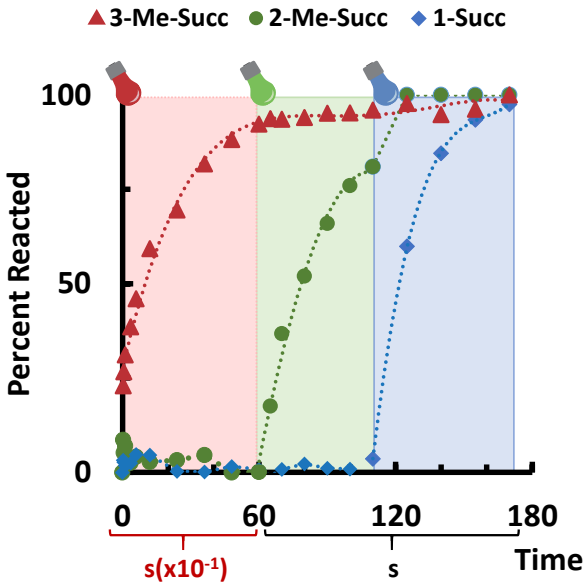

Figure 5.8. Irradiation of a 1:1:1 mixture (0.02 mM) of **1-Succ**, **2-Me-Succ**, and **3-Me-Succ** dissolved in 50:50 DMSO:MeOH. Samples were taken at time intervals and run through LC/MS. Solution was irradiated for 0-600 s with red light, followed by 50 s with green light and 60 s with UV light. Percent reacted was calculated by looking at the disappearance of the starting materials.

We then chose to look at **5** which has **2-Me** linked with **3-Me** (**Figure 4.7**). We chose this pair over the fluorinated **3** because it reacts much faster and the mixture was still selective. However, when irradiating **5** with green light no selectivity was observed. In fact, we only observed the growth of **2-Me-Succ** and none of the **3-Me-Succ**, suggesting that energy transfer was even more efficient in this case than the case for **4**. However, selectivity was obtained when first using red light to cleave **3-Me**. As was the case for **4**, we were able to sequentially cleave **5** by first irradiating with red light followed by green light to release succinic acid.

In both cases of **4** and **5** there was selectivity when the chromophores were separated, but not when linked together, presumably due to the higher efficiency of intramolecular energy transfer that leads to loss of selectivity. More studies need to be done to elucidate the mechanism

behind the lost of selectivity and to design systems that can selectively cleave the lower wavelength photocage attached to the same substrate as a higher wavelength chromophore.

While these photocages do not demonstrate orthogonality, they can be sequentially cleaved. In order to demonstrate their viability to be sequentially cleaved, compounds **1-Succ**, **2-Me-Succ**, and **3-Me-Succ** were irradiated together in a cuvette with red, green, and UV light to show that they demonstrate excellent sequential selectivity (**Figure 4.8**). As expected, red light selectively cleaved **3-Me-Succ**, green light selectively cleaved **2-Me-Succ**, and UV light cleaved the remaining **1-Succ**.

Conclusion

In conclusion, we have demonstrated that BODIPY PRPGs can be used for selective release with visible light LEDs. While excellent selectivity was obtained in mixed solutions, the linked compounds did not exhibit selectivity for irradiating the lower-wavelength PRPG first; however, the PRPGs could be removed sequentially starting with removal of the longer-wavelength absorbing PRPG. New strategies to allow for complete orthogonal control over PRPGs linked to the same molecule are needed.

References

1. Olson, J. P.; Banghart, M. R.; Sabatini, B. L.; Ellis-Davies, G. C. R., Spectral Evolution of a Photochemical Protecting Group for Orthogonal Two-Color Uncaging with Visible Light. *Journal of the American Chemical Society* **2013,** *135* (42), 15948-15954.

2. Azagarsamy, M. A. a. A. K. S., Wavelength-Controlled Photocleavage for the Orthogonal and Sequential Release of Multiple Proteins. *Angewandte Chemie International Edition* **2013,** *52* (51), 13803-13807.

3. Gumbley, P.; Koylu, D.; Pawle, R. H.; Umezuruike, B.; Spedden, E.; Staii, C.; Thomas, S. W., Wavelength-Selective Disruption and Triggered Release with Photolabile Polyelectrolyte Multilayers. *Chemistry of Materials* **2014,** *26* (3), 1450-1456.

4. Truong, V. X.; Li, F.; Forsythe, J. S., Photolabile Hydrogels Responsive to Broad Spectrum Visible Light for Selective Cell Release. *ACS Applied Materials & Interfaces* **2017,** *9* (38), 32441-32445.

5. Marturano, V.; Marcille, H.; Cerruti, P.; Bandeira, N. A. G.; Giamberini, M.; Trojanowska, A.; Tylkowski, B.; Carfagna, C.; Ausanio, G.; Ambrogi, V., Visible-Light Responsive Nanocapsules for Wavelength-Selective Release of Natural Active Agents. *ACS Applied Nano Materials* **2019,** *2* (7), 4499-4506.

6. Bochet, C. G., Orthogonal Photolysis of Protecting Groups. *Angewandte Chemie International Edition* **2001,** *40* (11), 2071-2073.

7. Blanc, A.; Bochet, C. G., Wavelength-Controlled Orthogonal Photolysis of Protecting Groups. *The Journal of Organic Chemistry* **2002,** *67* (16), 5567-5577.

8. Wavelength-selective cleavage of photolabile protecting groups. *Tetrahedron Letters* **2000,** *41* (33), 6341 - 6346.

9. Hansen, M. J.; Velema, W. A.; Lerch, M. M.; Szymanski, W.; Feringa, B. L., Wavelength-selective cleavage of photoprotecting groups: strategies and applications in dynamic systems. *Chemical Society Reviews* **2015,** *44* (11), 3358-3377.

10. San Miguel, V.; Bochet, C. G.; del Campo, A., Wavelength-Selective Caged Surfaces: How Many Functional Levels Are Possible? *Journal of the American Chemical Society* **2011,** *133* (14), 5380-5388.

11. Peterson, J. A.; Wijesooriya, C.; Gehrmann, E. J.; Mahoney, K. M.; Goswami, P. P.; Albright, T. R.; Syed, A.; Dutton, A. S.; Smith, E. A.; Winter, A. H., Family of BODIPY Photocages Cleaved by Single Photons of Visible/Near-Infrared Light. Journal of the American Chemical Society, 2018; Vol. 140, pp 7343-7346.

12. Slanina, T.; Shrestha, P.; Palao, E.; Kand, D.; Peterson, J. A.; Dutton, A. S.; Rubinstein, N.; Weinstain, R.; Winter, A. H.; Klán, P., In Search of the Perfect Photocage: Structure–Reactivity Relationships in meso-Methyl BODIPY Photoremovable Protecting Groups. *Journal of the American Chemical Society* **2017,** *139* (42), 15168-15175.

13. Slanina, T.; Shrestha, P.; Palao, E.; Kand, D.; Peterson, J. A.; Dutton, A. S.; Rubinstein, N.; Weinstain, R.; Winter, A. H.; Klan, P., In Search of the Perfect Photocage: Structure-Reactivity Relationships in *meso*-Methyl BODIPY Photoremovable Protecting Groups. Journal of the American Chemical Society, 2017; Vol. 139, pp 15168-15175.

CHAPTER 6. GENERAL CONCLUSION

Boron-alkylated derivatives allow for higher quantum yields of photorelease compared to their boron-fluorinated counterparts. Taking advantage of this effect has allowed us to achieve reasonable quantum yields of photorelease for red-absorbing photoremovable protecting groups as well as for direct release of alcohols from BODIPY ethers. The difference in photoreactivity between the fluorinated and methylated derivatives can be exploited in order to achieve wavelength-selective release. The boron-alkyl bond is thermally stable, but is photolabile and irradiation in alcoholic solvents results in a solvent adduct on the boron which has a higher quantum yield of fluorescence than the alkylated derivatives. This photoreactivity can be used for designing photoactivatable probes for single molecule localization microscopy.

It is currently unclear how the photolability of the boron-alkyl bond effects the quantum yield of photorelease. It may be the case that the two are competing photoreactions, in which case designing a derivative that has a more photostable boron-alkyl bond may further work to increase photochemical quantum yields. In addition, while we have designed derivatives which release substrates with red light, the quantum yields of these derivatives remain low. More work needs to be done to design red derivatives with enhanced quantum yields of release.

APPENDIX A. SUPPORTING INFORMATION FOR CHAPTER 1

Synthetic procedures

8-Acetoxymethyl-1,3,5,7-tetramethyl pyrromethene fluoroborate[1] **1** and 4-(1,4,7,10-tetraoxaundecyl)benzaldehyde[2] were synthesized as previously reported.

Synthetic Scheme

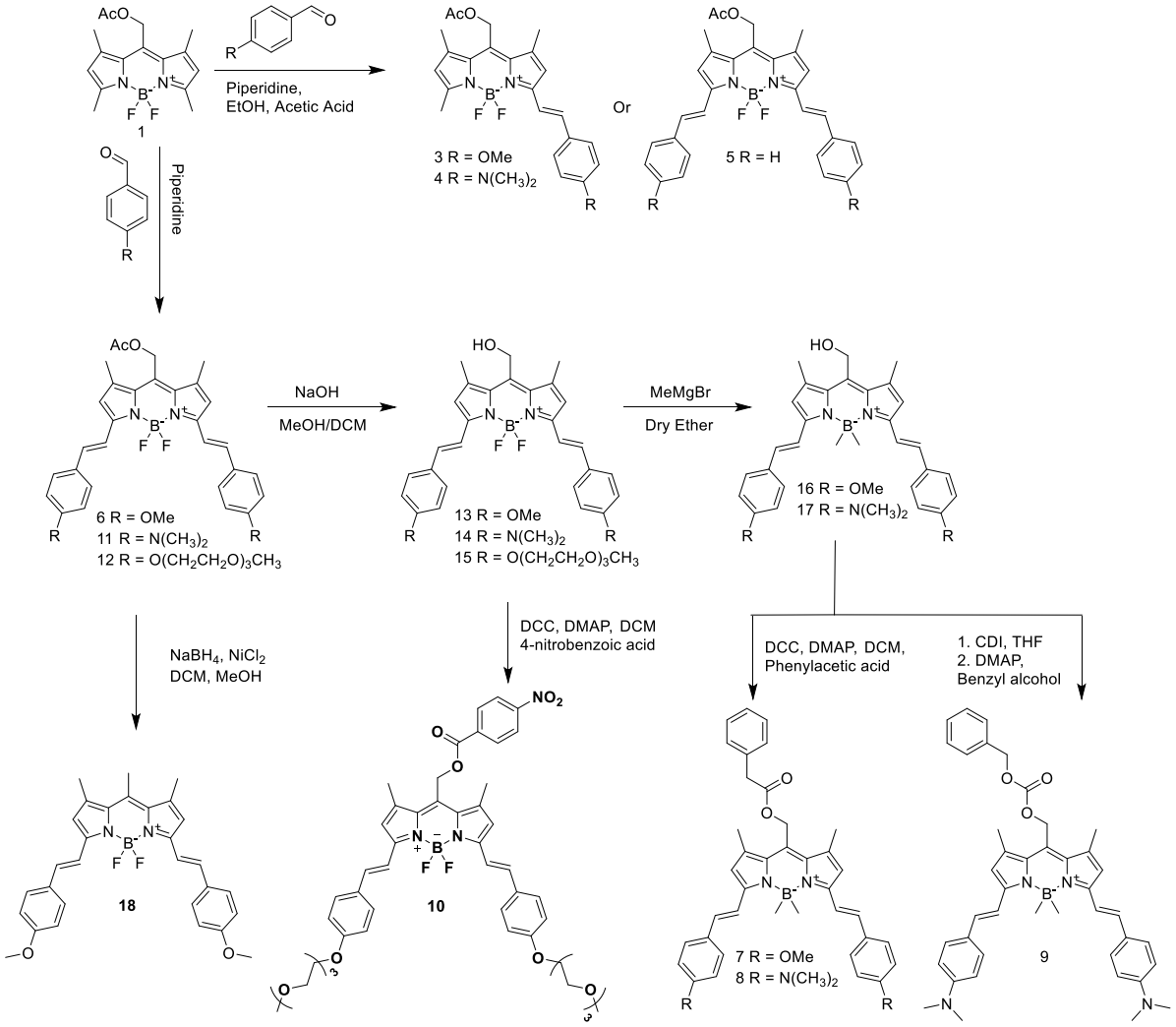

General Procedure for Compounds 3-5. 8-acetoxymethyl-1,3,5,7-tetramethyl pyrromethene fluoroborate **1** (50 mg, 0.016 mmol, 1 eq) and the respective benzaldehyde (0.032

mmol, 2 eq) were added to 8 mL of ethanol which had been previously dried over 3 Å molecular sieves for 24 h. This suspension was then placed in a dry, glass microwave reaction vessel. Acetic acid (120 µL) and piperidine (120 µL) were then added and the vessel was sparged with argon. The microwave vessel was irradiated at 113 °C and 800 W for the times listed below. The solvent was evaporated under reduced pressure and purified as detailed below.

8-Acetoxymethyl-3-(4-methoxy)styryl-1,5,7-trimethyl pyrromethene fluoroborate 3. 8-Acetoxymethyl-1,3,5,7-tetramethyl pyrromethene fluoroborate (50 mg, 0.016 mmol, 1 eq) and 4-methoxybenzaldehyde (4.4 mg, 0.032 mmol, 2 eq) were irradiated for 10 min. The solid residue was loaded onto a silica gel flash column and eluted with 50:50 hexanes:ethyl acetate. The dark purple product (32 mg, 0.009 mmol, 58%) was recovered and further purified using a prep TLC plate and 80:20 hexanes:ethyl acetate. ^{1}H NMR (400 MHz, $CDCl_3$): δ = 7.55 (d, *J* = 4 Hz, 2H), 7.52 (d, *J* = 8 Hz, 1H), 7.24 (d, *J* = 8 Hz, 1H), 6.91 (d, *J* = 4 Hz, 2H), 6.71 (s, 1H), 6.10 (s, 1H), 5.32 (s, 2H), 3.85 (s, 3H), 2.57 (s, 3H), 2.42 (s, 3H), 2.37 (s, 3H), 2.14 (s, 3H) ppm; ^{13}C NMR (200 MHz, $CDCl_3$): δ = 170.7, 160.8, 155.5, 154.5, 141.1, 140.4, 137.3, 135.4, 134.5, 132.9, 131.4, 129.4, 122.2, 118.9, 117.0, 114.5, 58.2, 55.2, 20.8, 16.1, 15.7, 14.9 ppm; HRMS (ESI) for $C_{24}H_{25}BF_2N_2O_3$ = 438.2035 (calc.), found 438.2040.

8-Acetoxymethyl-3-(4-dimethylamino)styryl-1,5,7-trimethyl pyrromethene fluoroborate 4. 8-Acetoxymethyl-1,3,5,7-tetramethyl pyrromethene fluoroborate (50 mg, 0.016 mmol, 1 eq) and 4-(dimethylamino)benzaldehyde (4.8 mg, 0.032 mmol, 2 eq) were irradiated for 20 min. The solid residue was loaded onto a silica gel flash column and eluted with 80:20 hexanes:ethyl acetate to give **4** as a dark blue solid (9.1 mg, 24% yield). ^{1}H NMR (400 MHz, $CDCl_3$): δ = 7.50 (d, *J* = 8 Hz, 2H), 7.45 (d, *J* = 16 Hz, 1H), 7.24 (d, *J* = 16 Hz, 1H), 6.72 (s, 1H), 6.68 (d, *J* = 8 Hz, 2H), 6.06 (s, 1H), 5.31 (s, 2H), 3.03 (s, 6H), 2.56 (s, 3H), 2.41 (s, 3H),

2.36 (s, 3H), 2.15 (s, 3H) ppm; ^{13}C NMR (200 MHz, $CDCl_3$): δ = 170.9, 156.1, 153.4, 151.4, 141.4, 139.2, 138.6, 134.9, 132.3, 129.7, 124.6, 121.4, 119.2, 114.3, 112.1, 58.3, 40.4, 24.0, 20.9, 16.1, 15.6 ppm; HRMS (ESI) for formula $C_{25}H_{28}BF_2N_3O_2$ = 451.2352 (calc.), found 451.2322

8-Acetoxymethyl-3,5-bisstyryl-1,7-dimethyl pyrromethene fluoroborate 5. 8-Acetoxymethyl-1,3,5,7-tetramethyl pyrromethene fluoroborate (50 mg, 0.016 mmol, 1 eq) and benzaldehyde (3.4 mg, 0.032 mmol, 2 eq) were irradiated in the microwave for 20 min. The solid residue was loaded onto a silica gel flash column and eluted with 80:20 hexanes:ethyl acetate to give **5** as a dark blue solid (23.7 mg, 38% yield). ^{1}H NMR (400 MHz, $CDCl_3$): δ = 7.71 (d, *J* = 8 Hz, 2H), 7.64, (d, *J* = 4 Hz, 4 H), 7.42 (t, *J* = 8 Hz, 4H), 7.34 (t, *J* = 8 Hz, 2H), 7.30 (d, *J* = 8 Hz, 2H), 6.76 (s, 2H), 5.35 (s, 2H), 2.44 (s, 6H), 2.16 (s, 3H) ppm; ^{13}C NMR (200 MHz, $CDCl_3$): δ = 170.6, 153.4, 140.4, 137.1, 136.4, 134.8, 130.2, 129.2, 128.8, 127.7, 118.9, 58.0, 22.7, 15.9, 14.1 ppm; HRMS (ESI) for formula $C_{30}H_{27}BF_2N_2O_2H^+$ = 497.2212 (calc.), found 497.2220.

General Procedure for Compounds 6, 11-12. Compound **1** was added to a 20 mL scintillation vial with 10-50 equivalents of respective benzaldehyde and one drop of piperidine. The vial was rotated under vacuum while heated at the temperatures listed below. The reaction was monitored by TLC, and upon completion the residue was purified by silica gel flash chromatography with the solvents listed below.

8-Acetoxymethyl-3,5-bis(4-methoxy)styryl-1,7-dimethyl pyrromethene fluoroborate 6. Compound **1** (25 mg, 0.078 mmol, 1 eq) was reacted with *p*-anisaldehyde (0.5 mL, 4.1 mmol, 50 eq.) at 60 °C for 2 h until the color changed from red to blue-green. The mixture was returned to room temperature and loaded onto silica gel flash column and eluted with 80:20 hexanes:ethyl acetate followed by 50:50 hexanes:ethyl acetate to give **6** (30 mg, 69% yield). ^{1}H NMR (400 MHz, $CDCl_3$): δ = 7.59 (d, *J* = 4 Hz, 4H), 7.58 (d, *J* = 8 Hz, 2H), 7.24 (d, *J* = 8 Hz, 2H), 6.94 (d,

J = 4 Hz, 4H), 6.73 (s, 2H), 5.35 (s, 2H), 3.87 (s, 6H), 2.43 (s, 6H), 2.16 (s, 3H) ppm; ^{13}C NMR (200 MHz, $CDCl_3$): δ = 170.8, 160.7, 153.5, 140.1, 136.7, 134.7, 129.6, 129.4, 118.8, 117.2, 114.5, 58.3, 55.5, 20.9, 16.0 ppm; HRMS (ESI) for formula $C_{32}H_{31}BF_2N_2O_4$ = 556.2454 (calc.), found 556.2449.

8-Acetoxymethyl-3,5-bis(4-dimethylamino)styryl-1,7-dimethyl pyrromethene fluoroborate 11. Compound **1** (100 mg, 0.3 mmol, 1 eq) was reacted with 4-dimethylaminobenzaldehyde (500 mg, 3.5 mmol, 11 eq) at 75 ºC until the color changed from red to dark brown. The mixture was returned to room temperature and loaded onto silica gel flash column and eluted with 70:30 toluene:methylene chloride to give 120 mg (68%) **11** as a forest green solid**.** ^{1}H NMR (500 MHz, DMSO-D_6): δ 7.49 – 7.44 (m, 6H), 7.27 (d, *J* = 17.1 Hz, 2H), 7.00 (s, 2H), 6.79 (d, *J* = 9.1 Hz, 4H), 5.29 (s, 2H), 3.01 (s, 12H), 2.38 (s, 6H), 2.13 (s, 3H). ^{13}C NMR (500 MHz, CD_2Cl_2) δ 171.09, 153.66, 151.80, 140.06, 137.81, 134.86, 129.64, 127.97, 125.10, 118.71, 114.63, 112.55, 58.66, 54.00, 40.56, 21.11, 16.14.; HRMS (ESI) for formula $C_{34}H_{37}BF_2N_2O_2$ = 582.2978 (calc.), found 582.2964.

8-Acetoxymethyl-3,5-bis(4-(1,4,7,10-tetraoxaundecyl)styryl-1,7-dimethyl pyrromethene fluoroborate 12. Compound **1** (22 mg, 0.068 mmol, 1 eq) was reacted with 4-(1,4,7,10-Tetraocaundecyl)benzaldehyde (182 mg, 0.68 mmol, 10 eq) at 60 º C until the reaction was complete by TLC. The oil was purified by silica gel flash chromatography with 100:1 dichloromethane:methanol to give pure **9** (27 mg, 49%). ^{1}H NMR (500 MHz, $CDCl_3$): δ = 7.56 (m, 6H), 7.23 (d, *J* = 16 Hz, 2H), 6.94 (d, *J* = 8 Hz, 4H), 6.71 (s, 2H), 5.33 (s, 2H), 4.18 (t, *J* = 5 Hz, 4H), 3.88 (t, *J* = 5 Hz, 4H), 3.75 (m, 4H), 3.71 (m, 4H), 3.70 (m, 4H), 3.67 (m, 4H), 3.56 (m, 4H), 3.38 (s, 6H), 2.41 (s, 6H), 2.15 (s, 3H) ppm; ^{13}C NMR (125 MHz, $CDCl_3$): δ = 170.8, 159.9, 153.5, 140.0, 136.7, 134.7, 129.7, 129.3, 129.2, 118.8, 117.2, 115.1, 72.1, 71.0, 70.8, 70.7,

69.8, 67.9, 67.8, 67.7, 59.2, 58.3, 29.8, 20.9, 16.0 ppm; HRMS (ESI) for formula $C_{44}H_{55}BF_2N_2O_{10}Na^+$ = 842.3846 (calc.), found 842.3845.

General Procedure for Compounds 13-15 Compound **6** and **11-12** in the amounts listed below were dissolved in 1:1 dichloromethane:methanol to which was added 0.1 M aqueous sodium hydroxide. The reaction mixtures were stirred at room temperature for the times listed below after which they were diluted with 20 mL dichlochloromethane, washed with 40 mL brine 3x, dried over sodium sulfate, filtered, and the solvent was evaporated under vacuum. The remaining solids were purified as listed below.

3,5-Bis(4-methoxy)styryl-1,7-dimethyl-8-hydroxymethyl pyrromethene fluoroborate 13. Compound **6** (55 mg, 0.10 mmol, 1 eq) was dissolved in 20 mL 1:1 dichloromethane:methanol to which was added 3 mL 0.1 M aqueous sodium hydroxide. The reaction was stirred for 2 h and after the workup listed above yields a dark blue solid that was purified by flash chromatography with dichloromethane as the eluent to give **10** (35 mg, 70% yield). ^{1}H NMR (400 MHz, $CDCl_3$): δ = 7.59 (m, 6H), 7.26 (d, *J* = 16 Hz, 2H), 6.94 (d, *J* = 8 Hz, 4H), 6.73 (s, 2H), 4.95 (s, 2H), 3.86 (s, 6H), 2.57 (s, 6H). ^{13}C NMR (200 MHz, $CDCl_3$): δ = 160.74, 153.43, 140.13, 136.43, 134.41, 134.22, 139.72, 139.3, 118.6, 117.4, 117.4, 117.4, 114.5, 90.2, 56.2, 55.6, 29.9, 16.0, 1.2 ppm; HRMS (ESI) for formula $C_{30}H_{29}BF_2N_2O_3H^+$= 515.2310 (calc.), found 515.2308.

8-Hydroxymethyl-3,5-bis(4-dimethylamino)styryl-1,7-dimethyl pyrromethene fluoroborate (14). Compound **11** (100 mg, 0.17 mmol, 1 eq) was dissolved in 100 mL 1:1 dichloromethane:methanol to which was added 10 mL 0.1 M (1 mmol, 5.9 eq) aqueous sodium hydroxide. The reaction was stirred at room temp. for 6 h. Following the workup, the remaining solid was purified on silica gel flash chromatography using 5% ethyl acetate in dichloromethane

to give pure **14 (**85 mg, 92%)**.** ^{1}H NMR (500 MHz, $CDCl_3$): δ = 7.44 (m, 6H), 7.27 (d, *J* = 15 Hz, 2H), 6.94 (s, 2 H), 6.79 (d, *J* = 10 Hz, 4H), 5.46 (t, *J* = 5 Hz, 1H), 4.74 (d, *J* = 5 Hz, 2H), 3.00 (s, 12H), 2.54 (s, 6H) ppm; ^{13}C NMR (125 MHz, $CDCl_3$): δ = 152.0, 151.1, 140.1, 137.0, 135.0, 133.6, 128.9, 124.2, 118.1, 113.6, 112.4, 31.5, 22.3, 15.6 ppm; HRMS (ESI) for formula $C_{32}H_{35}BF_2N_4O$ = 540.2981 (calc.), found 540.2969.

3,5-Bis(4-(1,4,7,10-tetraoxaundecyl)styryl-1,7-dimethyl-8-hydroxymethyl pyrromethene fluoroborate 15. Compound **12** (35 mg, 0.04 mmol, 1 eq) was dissolved in 40 mL 1:1 dichloromethane:methanol to which was added 5 mL 0.1 M aqueous sodium hydroxide and stirred at room temperature for 3 h. Following the workup, the remaining solid was purified on silica gel flash chromatography using a gradient from 0.5-2% methanol in dichloromethane as the eluent to give pure **11** (19 mg, 57%). ^{1}H NMR (500 MHz, $CDCl_3$): δ = 7.53 (m, 6H), 7.17 (d, *J* = 17 Hz, 2H), 6.91 (d, *J* = 9 Hz, 4H), 4.85 (s, 2H), 4.15 (t, *J* = 5 Hz, 4H) 3.87 (t, *J* = 5 Hz, 4H), 3.74 (m, 4H), 3.69 (m, 4H), 3.65 (m, 4H) 3.55 (m, 4H), 3.37 (s, 6H), 2.50 (s, 6H) ppm; ^{13}C NMR (125 MHz, $CDCl_3$): δ = 159.8, 153.1, 140.2, 136.3, 134.4, 134.2, 132.1, 129.7, 129.2, 118.5, 117.2, 115.0, 72.1, 71.0, 70.8, 70.7, 69.8, 67.6, 59.2, 55.9, 29.8, 15.88 ppm; HRMS (ESI) for formula $C_{42}H_{53}BF_2N_2O_9$ = 779.3885 (calc.), found 779.3878.

General Procedure for Boron-alkylation for compounds 16-17. The respective compound was stirred under argon in dry ether. 10 equivalents of 3 M methylmagnesium bromide in tetrahydrofuran was added dropwise. The reaction was stirred for the times listed below. Saturated ammonium chloride was added dropwise to quench the reaction. 50 mL methylene chloride was added and the solution was washed three times with ammonium chloride and once with brine. The organic layer was dried over sodium sulfate and the solvent was removed under vacuum. The resulting solids were purified as listed below.

3,5-bis(4-methoxy)styryl-1,7-dimethyl-8-hydroxymethyl pyrromethene dimethylborate 16 Compound **13** (170 mg, 0.33 mmol, 1 eq) was reacted with 1.1 mL 3 M methylmagnesium bromide (3.3 mmol, 10 eq) for 3 h. After the workup listed above, the resulting solid was purified on silica gel chromatography using methylene chloride as an eluent to give pure 16 (92 mg, 55% yield) as a blue solid. ^{1}H NMR (400 MHz, $CDCl_3$): δ = 7.50 (m, 6H), 7.07 (d, *J* = 16 Hz, 2H), 6.94 (d, *J* = 8 Hz, 4H, 6.73 (s, 2H), 5.01 (d, *J* = 4 Hz, 2H), 3.86 (s, 6H), 2.60 (s, 6H), 0.45 (s, 6H) ppm; ^{13}C NMR (125 MHz, $CDCl_3$): δ = 160.4, 150.9, 136.9, 135.9, 133.0, 132.9, 130.4, 128.8, 119.6, 119.0, 114.8, 56.8, 55.8, 30.1, 16.6 ppm; HRMS (ESI) for formula $C_{32}H_{35}BN_2O_3$ = 506.285 (calc.), found 506.2805.

3,5-bis(4-dimethylamino)styryl-1,7-dimethyl-8-hydroxymethyl pyrromethene dimethylborate 17 Compound **14** (95 mg, 0.17 mmol, 1 eq) was reacted with 0.6 mL 3 M methylmagnesium bromide (1.7 mmol, 10 eq) overnight. The resulting solid after the workup listed above was purified on silica gel chromatography using methylene chloride as an eluent to give pure **17** (52 mg, 57% yield) as a green solid. ^{1}H NMR (500 MHz, $CDCl_3$): δ = 7.46 (d, *J* = 8.9 Hz, 4H), 7.40 (d, *J* = 16.2 Hz, 2H), 7.05 (d, *J* = 17.3 Hz, 2H), 6.77 – 6.69 (m, 6H), 4.98 (d, *J* = 6.1 Hz, 2H), 3.02 (s, 12H), 2.59 (s, 6H), 0.45 (s, 6H) ppm. ^{13}C NMR (125 MHz, $CDCl_3$) δ 150.81, 150.70, 136.08, 134.25, 133.29, 132.61, 128.51, 125.73, 118.50, 117.24, 112.46, 56.65, 40.50, 29.86, 16.30 ppm; HRMS (ESI) for formula $C_{34}H_{40}BN_4O$ = 531.3404 (calc.), found 531.3411.

3,5-bis(4-methoxy)styryl-1,7-dimethyl-8-phenylacetoxy pyrromethene dimethylborate 7. A 100 mL dry round bottom flask was charged with 35 mg (0.069 mmol, 1 eq) **16**, 4-dimethylaminopyridine (13 mg, 0.10 mmol, 1.5 eq), N,N'-dicyclohexylcarbodiimide (21 mg, 0.10 mmol, 1.5 eq), and phenylacetic acid (14 mg, 0.10 mmol, 1.5 eq) in dry methylene

chloride. The reaction was stirred for 5 h after which the solvent was removed under vacuum and the residue was purified with silica gel chromatography with 70:30 toluene:methylene chloride to yield **7** (23 mg, 53%)**.** ^{1}H NMR (500 MHz, $CDCl_3$): δ = 7.49 (m, 6H), 7.32 (m, 5H), 7.08 (d, *J* = 15, 2H), 6.95 (d, *J* = 5, 4H), 6.70 (s, 2H), 5.38 (s, 2H), 3.86 (s, 6H), 3.72 (s, 2H), 2.30 (s, 6H), 0.46 (s, 6H) ppm. ^{13}C NMR (125 MHz, $CDCl_3$): δ = 171.6, 160.2, 150.8, 136.7, 133.6, 133.5, 133.0, 130.4, 130.1, 129.4, 128.8, 128.6, 127.5, 119.2, 118.9, 114.5, 59.3, 55.5, 41.4, 22.9, 16.0 ppm. HRMS (ESI) for formula $C_{40}H_{41}BN_2O_4$ = 624.3268 (calc.), found 624.325.

3,5-bis(4-dimethylamino)styryl-1,7-dimethyl-8-phenylacetoxy pyrromethene dimethylborate 8 A 250 mL dry round bottom flask was charged with 45 mg (0.069 mmol, 1 eq) **16**, 4-dimethylaminopyridine (13 mg, 0.10 mmol, 1.5 eq), N,N'-dicyclohexylcarbodiimide (21 mg, 0.10 mmol, 1.5 eq), and phenylacetic acid (14 mg, 0.10 mmol, 1.5 eq) in 50 mL dry methylene chloride. The reaction was stirred overnight after which the solvent was removed under vacuum and the residue was purified with silica gel chromatography with 70:30 toluene:methylene chloride to yield **8** (23 mg, 40%)**.** ^{1}H NMR (400 MHz, $CDCl_3$) δ = 7.47 (d, *J* = 8.8 Hz, 4H), 7.41 (d, *J* = 16.1 Hz, 2H), 7.32 (d, *J* = 2.8 Hz, 5H), 7.05 (d, *J* = 16.1 Hz, 2H), 6.74 (d, *J* = 8.8 Hz, 4H), 6.69 (s, 2H), 5.38 (s, 2H), 3.71 (s, 2H), 3.03 (s, 13H), 2.29 (s, 6H), 0.46 (s, 6H) ppm; ^{13}C NMR (125 MHz, $CDCl_3$) δ = 171.55, 150.83, 150.60, 135.96, 133.57, 133.41, 133.19, 129.24, 128.67, 128.66, 128.41, 127.27, 125.53, 118.50, 118.48, 117.02, 112.30, 59.37, 41.24, 40.33, 29.70, 15.88 ppm; HRMS (ESI) for formula $C_{42}H_{46}BN_4O_2$ = 649.3823 (calc.), found 649.3826.

3,5-Bis(4-(1,4,7,10-tetraoxaundecyl)styryl-1,7-dimethyl-8-(4-nitrobenzoato) pyrromethene fluoroborate 10. N,N'-dicyclohexylcarbodiimide (10 mg, 0.04 mmol, 1.6 eq) dissolved in 2 mL dichloromethane was added slowly to a solution of 4-nitrobenzoic acid (7 mg,

0.04 mmol, 1.6 eq) and 4-dimethylaminopyridine (1 mg, 0.008 mmol, 0.4 eq) stirring in dry dichloromethane under argon. Next, **11** (19 mg, 0.025 mmol, 1 eq.), dissolved in 2 mL dichloromethane, was added dropwise to the solution and it was stirred for 30 min. The solvent was removed under vaccum and the remaining mixture was purified by prep HPLC to give pure **7** (20 mg, 84% yield). ^{1}H NMR (400 MHz, $CDCl_3$): δ = 8.30 (d, *J* = 9 Hz, 2H), 8.25 (d, *J* = 9 Hz, 2H), 7.58 (m, 6H), 7.25 (d, *J* = 16 Hz, 2H), 6.95 (d, *J* = 7 Hz, 4H), 6.74 (s, 2H), 5.64 (s, 2H), 4.19 (t, *J* = 5 Hz, 4H), 3.89 (t, *J* = 5 Hz, 4H), 3.76 (m, 4H), 3.69 (m, 8H), 3.57 (m, 4H), 3.39 (s, 6H), 2.43 (s, 6H) ppm; ^{13}C NMR (125 MHz, $CDCl_3$): δ =164.6, 160.1, 153.8, 151.0, 139.9, 137.1, 134.8, 134.5, 131.2, 129.6, 129.4, 127.9, 123.9, 119.0, 117.1, 115.1, 90.1, 72.1, 71.0, 70.8, 70.7, 69.8, 67.7, 59.6, 59.2, 16.1 ppm; HRMS (ESI) for formula $C_{49}H_{56}BF_2N_3O_{12}Na^+$ = 949.3854 (calc.), found 949.3831.

3,5-Bis(4-methoxy)styryl-1,7,8-trimethyl pyrromethene fluoroborate 18. Compound **6** (30 mg, 0.054 mmol, 1 eq), dissolved in 2 mL dry dichloromethane, was added to a suspension of nickel (II) chloride (16 mg, 0.12 mmol, 2.2 eq) in 10 mL freshly distilled methanol. Sodium borohydride (10 mg, 0.24 mmol, 4.4 eq) was added slowly. The reaction was stirred for 2 h at room temperature after which 10 mL saturated ammonium chloride was added. The solution was extracted 3 times with methylene chloride. The combined organic layers were dried over sodium sulfate, filtered, and the solvent was removed under vacuum. The remaining mixture was purified by flash chromatography with 70:30 dichloromethane:toluene to give **8** (8.4 mg, 28% yield). ^{1}H NMR (400MHz, $CDCl_3$) δ = 7.58 (m, 6H), 7.20 (d, *J* = 16 Hz, 2H), 6.92 (d, *J* = 8 Hz, 4H), 6.69 (s, 2H), 3.85 (s, 6H), 2.63 (s, 3H), 2.48 (s, 6H) ppm; ^{13}C NMR (175 MHz, $CDCl_3$): δ = 160.6, 151.7, 141.8, 140.3, 137.8, 135.5, 134.1, 130.0, 129.2, 127.9, 118.0, 117.6, 114.6, 55.7,

17.9, 16.7 ppm; Hi-res MS (ESI) for formula $C_{30}H_{28}BF_2N_2O_2$ = 497.2321 (calc.), found 497.2393.

Benzyl 3,5-Bis(4-dimethylamino)styryl-1,7-dimethyl pyrromethene fluoroborate 8-methyl carbonate 9. To a solution of **17** (50 mg, 0.09 mmol, 1 eq) stirring in dry THF was added carbonyldiimidazole (23 mg, 0.14 mmol, 1.5 eq). The reaction was stirred under argon for 1 h or until the starting material was gone and a new spot had formed. Then, 4-dimethylaminopyridine (11 mg, 0.09 mmol, 1 eq) and benzyl alcohol (0.1 mL, 0.9 mmol, 10 eq) were added. The reaction was stirred at room temperature overnight. The reaction mixture was washed with water and brine. The organic layer was dried over sodium sulfate, the solvent was removed under vacuum, and the mixture was purified using silica gel column chromatography with toluene as the eluent to yield 12 mg 20%yield of **8** as a green solid. ^{1}H NMR (400 MHz, $CDCl_3$) δ = 7.45 (d, *J* = 8.5 Hz, 4H), 7.42 – 7.32 (m, 7H), 7.04 (d, *J* = 16.1 Hz, 2H), 6.73 (d, *J* = 8.5 Hz, 4H), 6.69 (s, 2H), 5.47 (s, 2H), 5.22 (s, 2H), 3.02 (s, 12H), 2.61 (s, 3H), 2.41 (s, 6H), 0.43 (s, 6H) ppm; ^{13}C NMR (100 MHz, $CDCl_3$) δ 168.10, 154.89, 150.93, 150.59, 145.77, 135.89, 135.07, 133.44, 133.19, 128.57, 128.41, 128.09, 125.55, 118.64, 117.05, 112.29, 69.95, 61.86, 40.32, 29.69, 16.10 ppm; HRMS (ESI) for formula $C_{42}H_{46}BN_4O_3$ = 665.3772 (calc.), found 665.3773.

Photorelease of acetic acid followed by NMR

The BODIPY compound was dissolved in a minimum amount of $CDCl_3$ to dissolve and then CD_3OD was added to make 600 µL of a 2 mM solution. A Xenon arc lamp was used to irradiate the sample and it was followed by ^1H NMR over time. Solvent peaks are cut from the spectrum for clarity. In most cases, the byproduct of the photocage is insoluble at the high concentrations required for an ^1H NMR study and precipitates.

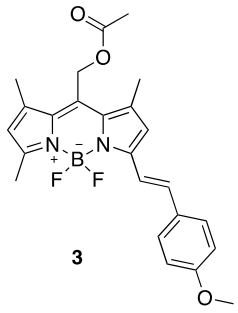

3

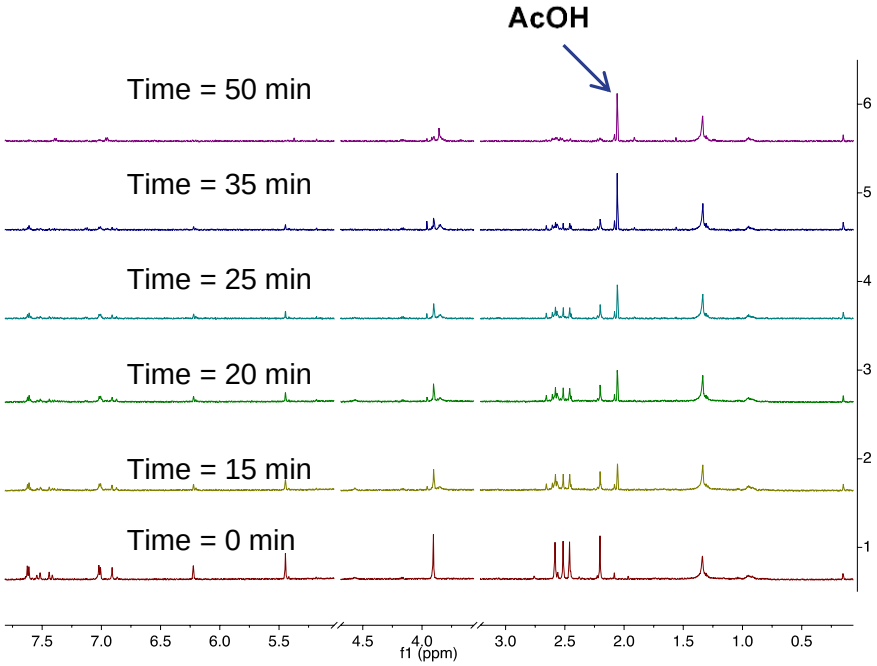

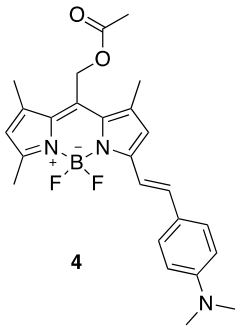

4

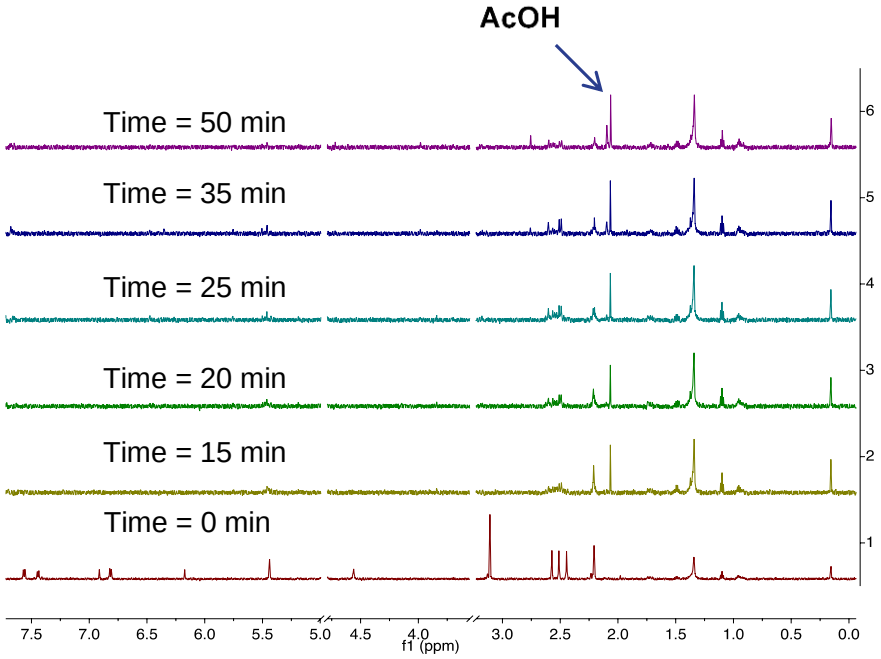

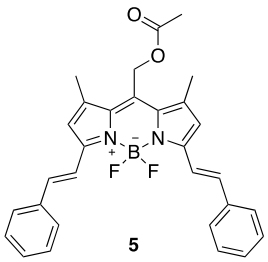

5

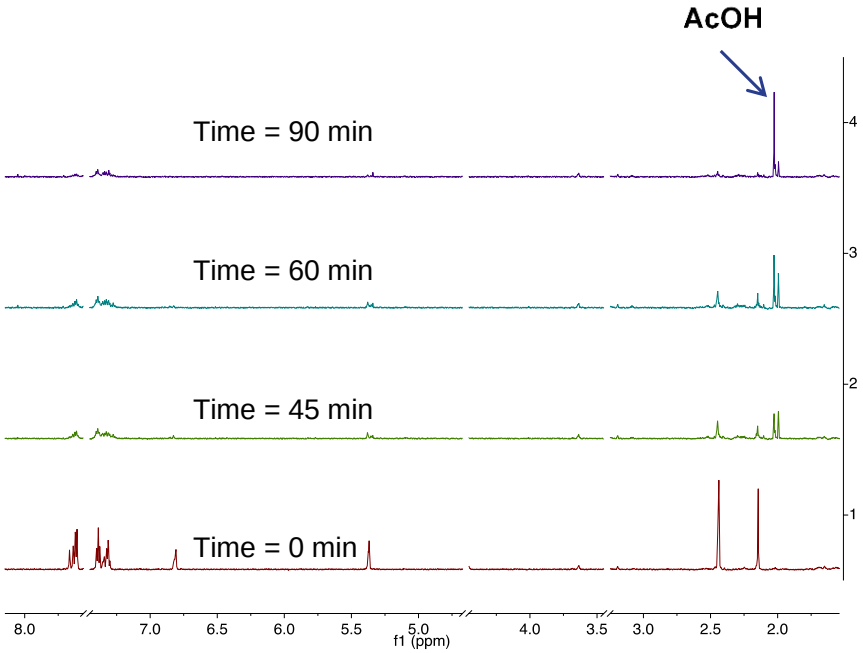

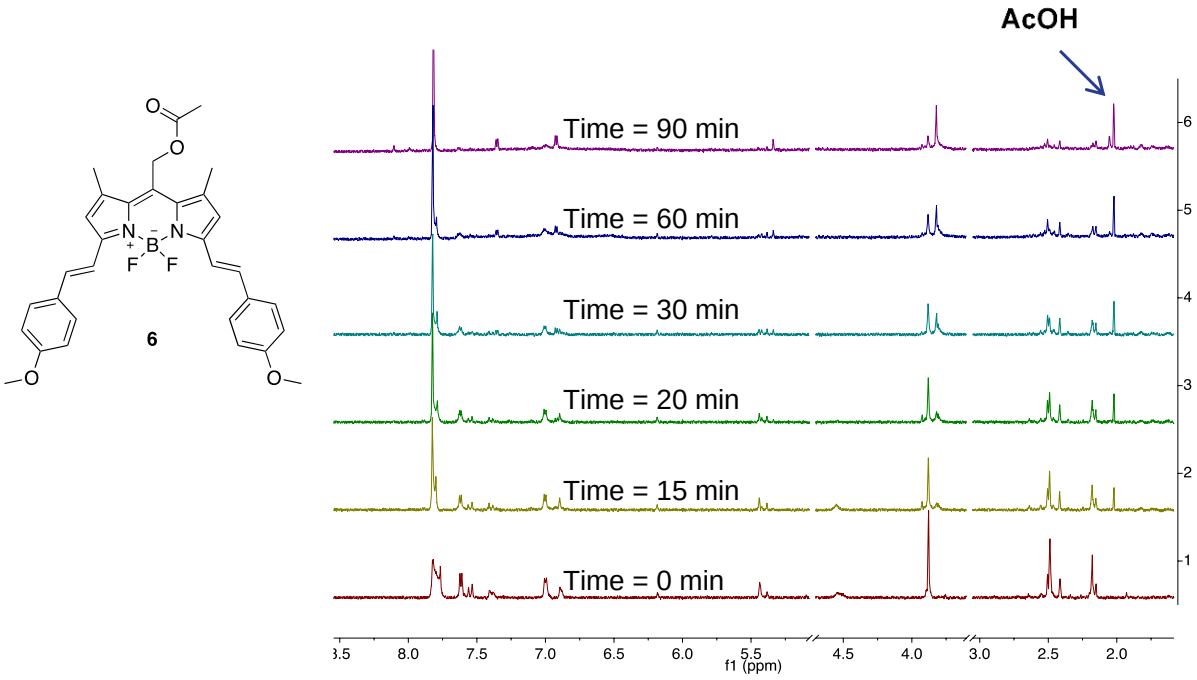

In order to test the oxygen-dependence of the reactivity of **6** upon irradiation, the photolysis of a degassed sample was followed by ^{1}H NMR. 2 mg of compound **6** was dissolved in 2 mL 1:1 DMSO-d_6: CD_3OD. 1 mL portions of the solution were taken into two different NMR tubes. One was purged for 30 minutes with argon. The solutions were then irradiated side by side with a 500 W halogen lamp with a water-based IR cutoff filter to prevent sample heating. ^{1}H NMR spectra were taken at different irradiation times. The sample irradiated under air (A) showed a small growth of 4-methoxybenzaldehyde (characteristic peak at ~9.8 ppm) while no benzaldehyde was observed in the degassed sample (B). Inset are the zoomed regions from 1.7-2.2 ppm and 9.5-10.0 ppm to show the growth of acetic acid and *p*-anisaldehyde.

A. Compound **6** irradiated under air

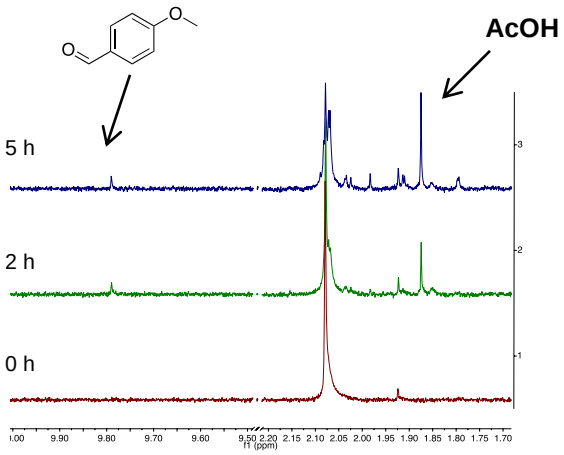

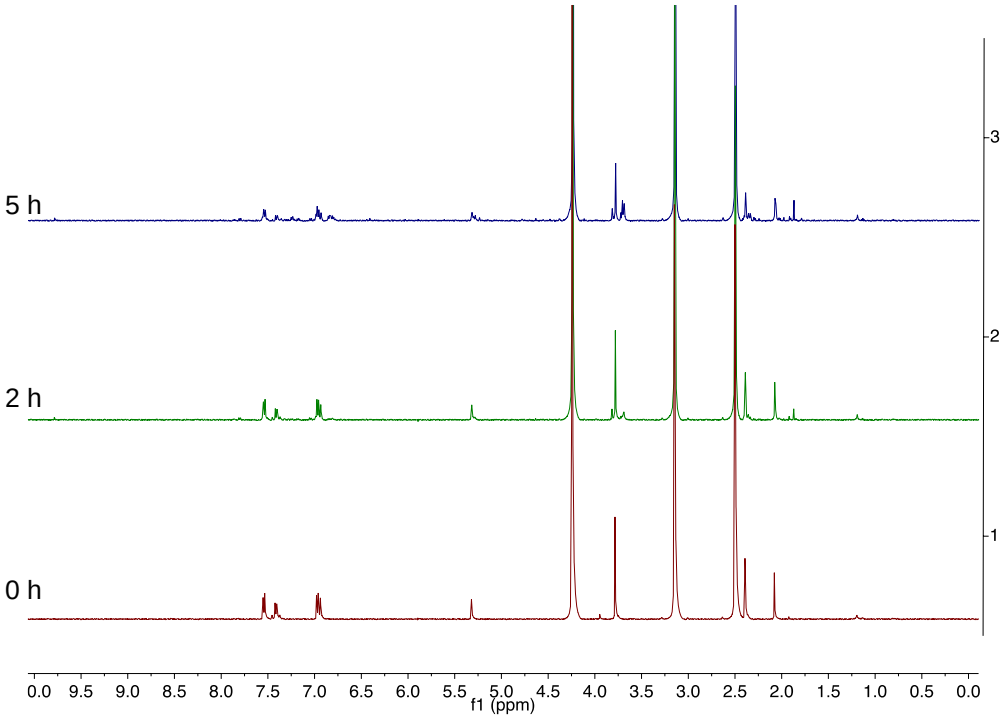

B. Compound **6** irradiated under argon

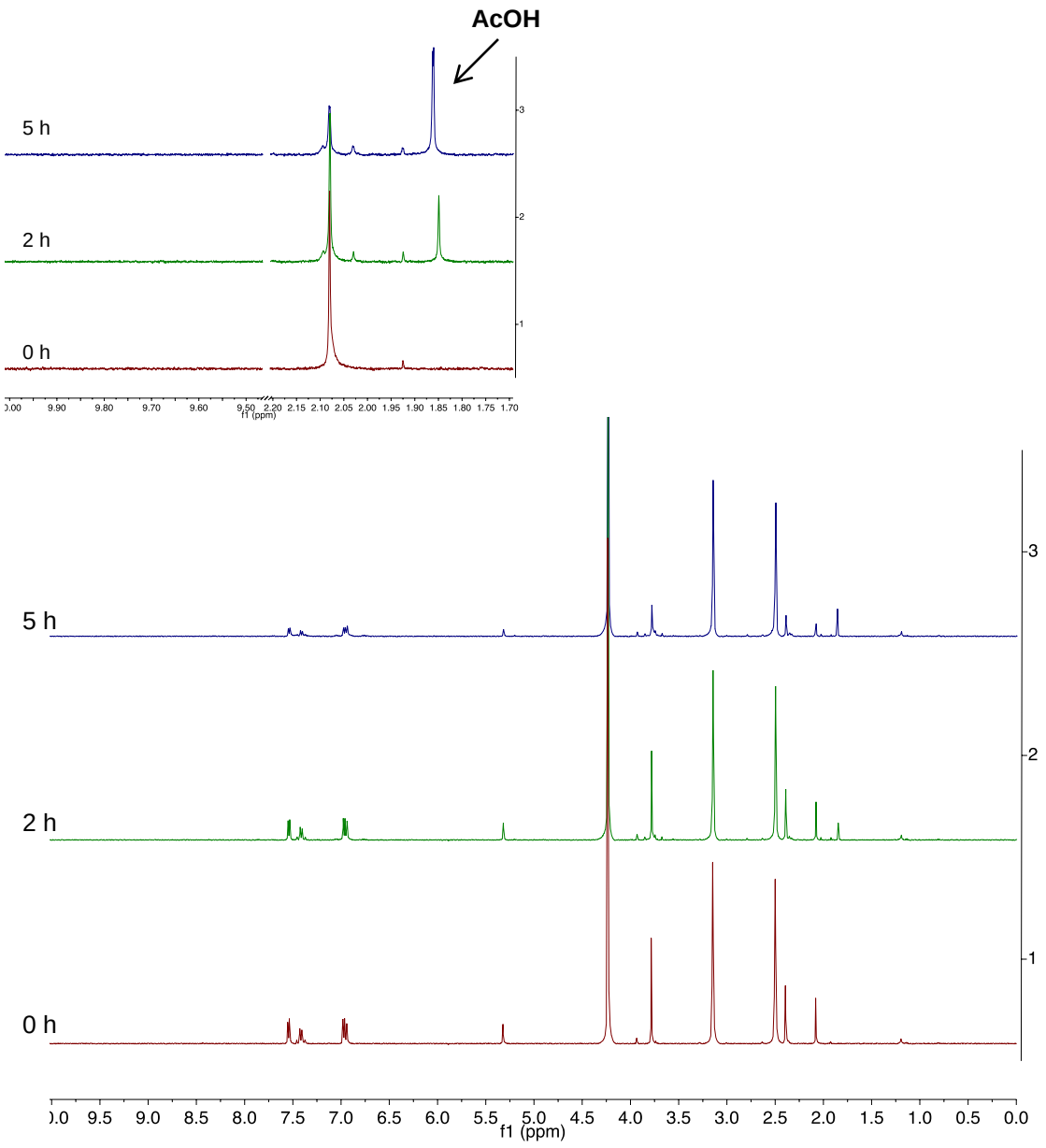

Similarly, 1 mg compound **18** was dissolved in 1 mL 1:1 $CDCl_3$:MeOD exposed to air. The solution was irradiated with a with a 500 W halogen lamp with a water-based IR cutoff filter and ^1H NMR spectra were taken at different irradiation times. Comound **18** quickly decomposes and a small amount of *p*-anisaldehyde grows in. Solvent peaks are cut for clarity.

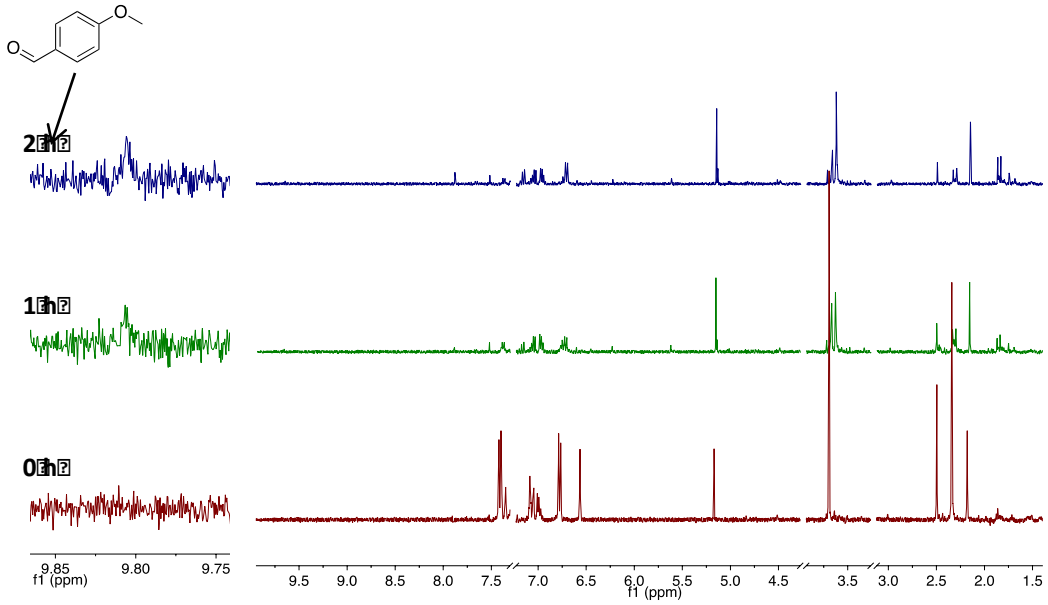

Compound **7** (1 mg in 1 mL 1:1 DMSO:MeOH) was irradiated under air with a 500 W halogen lamp behind a water-based IR filter. After 10 minutes, release of phenylacetic acid was complete, and *p*-anisaldehyde was not yet detected in the NMR.

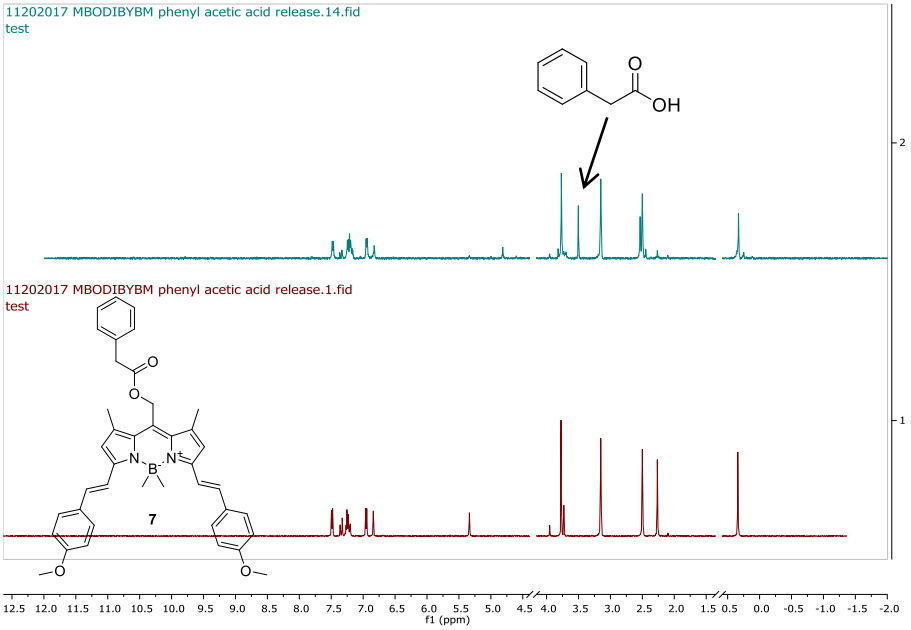

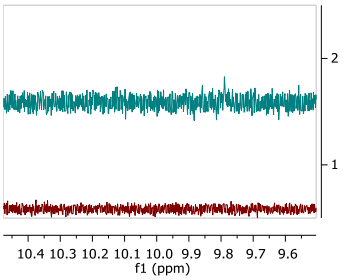

Quantitative NMR studies of the release of acetic acid for compound 6

1 mg of compound **6** was dissolved in 1:1 DMSO-d_6: CD_3OD with 0.1% 1,4-dioxane as an internal standard. The sample was irradiated with an ORIEL white lamp. ^1H NMR spectrum were taken at 0, 30, 90, 180, and 600 minutes. The percent conversion over time was plotted,

showing a total of 75% release of acetic acid with 95% conversion of the starting material. This shows a correlation of the release of acetic acid with the disappearance of **6**.

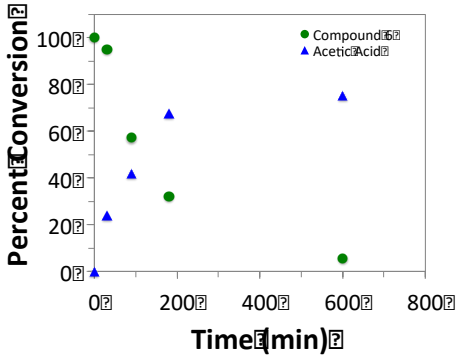

Irradiation of compounds 6 and 18 followed by fluorescence

Two identical 2 μM solutions of **6** were made in 3.5 mL methanol and placed in one regular and one stemmed fluorescence cuvette. The solution in the stemmed cuvette was purged for 30 minutes **(A)** while the other was left open to atmosphere **(B).** The two solutions were irradiated with a 500 W halogen lamp using a water-based IR cutoff filter to prevent heating. Fluorescence measurements were taken at time increments with 400 nm excitation. The unpurged photolysis **(B)** shows a marked increase in fluorescence at 608 nm. The photolysis mixture under inert atmostphere (**A**) showed little increase of fluorescence at 608 nm within 3

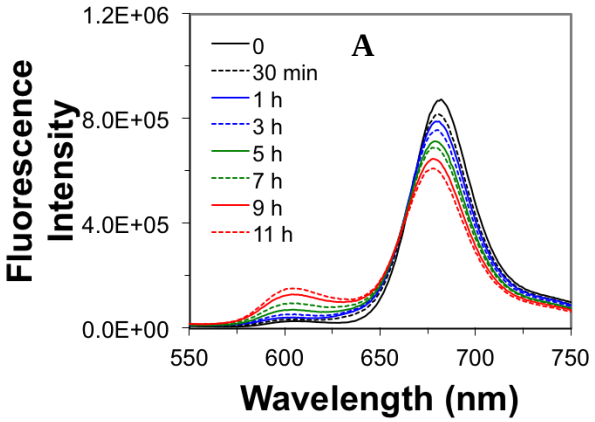

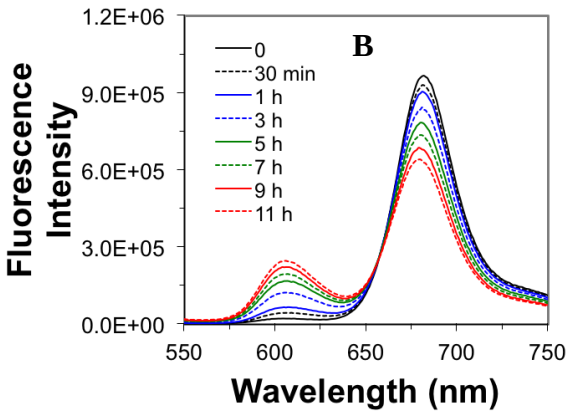

In order to determine whether this fluorescence increase at 608 nm is related to the photorelease process, an unpurged 2 □M solution of **18** (lacking a leaving group) was irradiated under the same conditions and no corresponding increase (~600 nm) was seen in the fluorescence spectrum (below).

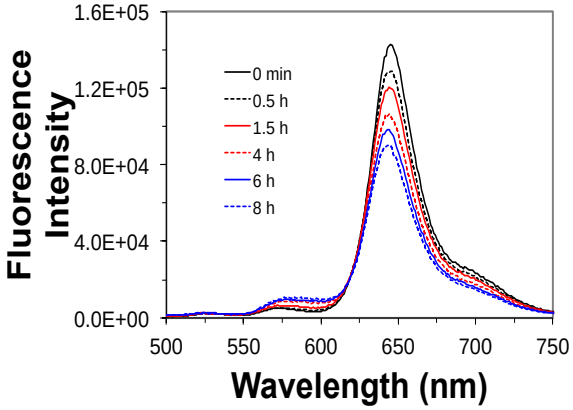

Photoproduct studies of compounds 6 and 10

25 mg of **6** was dissolved in 20 mL 1:1 Dichloromethane:Methanol. The solution was irradiated for a total of 50 h with a 500 W Halogen lamp with a water-based IR cutoff filter, exposed to air. The solvent was removed under vacuum and the resulting product was loaded onto a silica gel column and eluted with 80:20 hexanes:ethyl acetate with 1% methanol (gave pure product **B**). Product **A** was further purified with prep TLC using dichloromethane with 1% methanol as the eluent. Water trapped at the *meso* position (**A:** spectrum match compound **13**) was isolated, as well as a compound which has oxidative cleavage of a styryl group (**B**). Both of these isolated compounds appear to be very minor products. The major products proved to be difficult to isolate due to poor solubility and unstability.

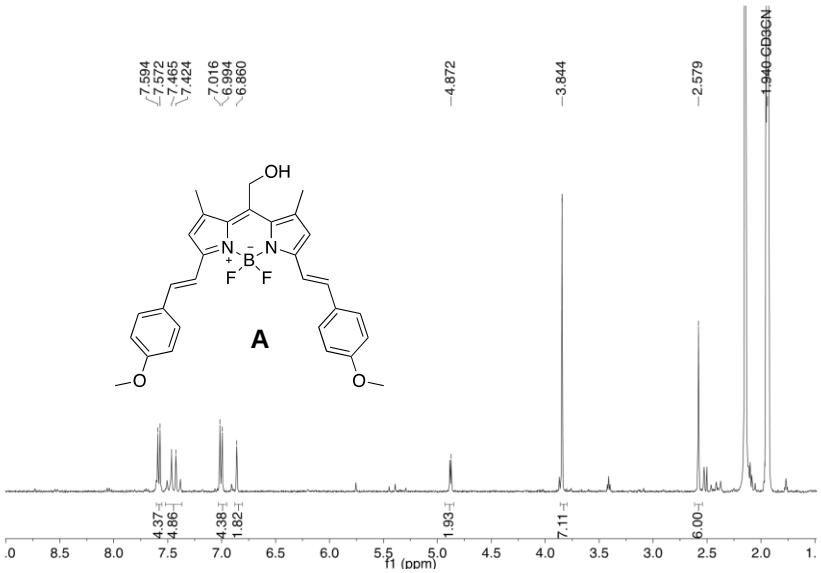

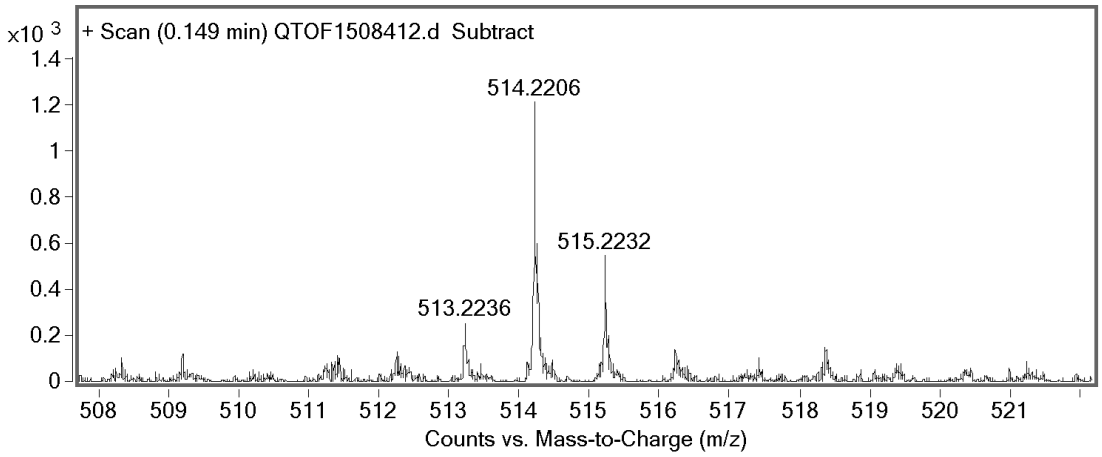

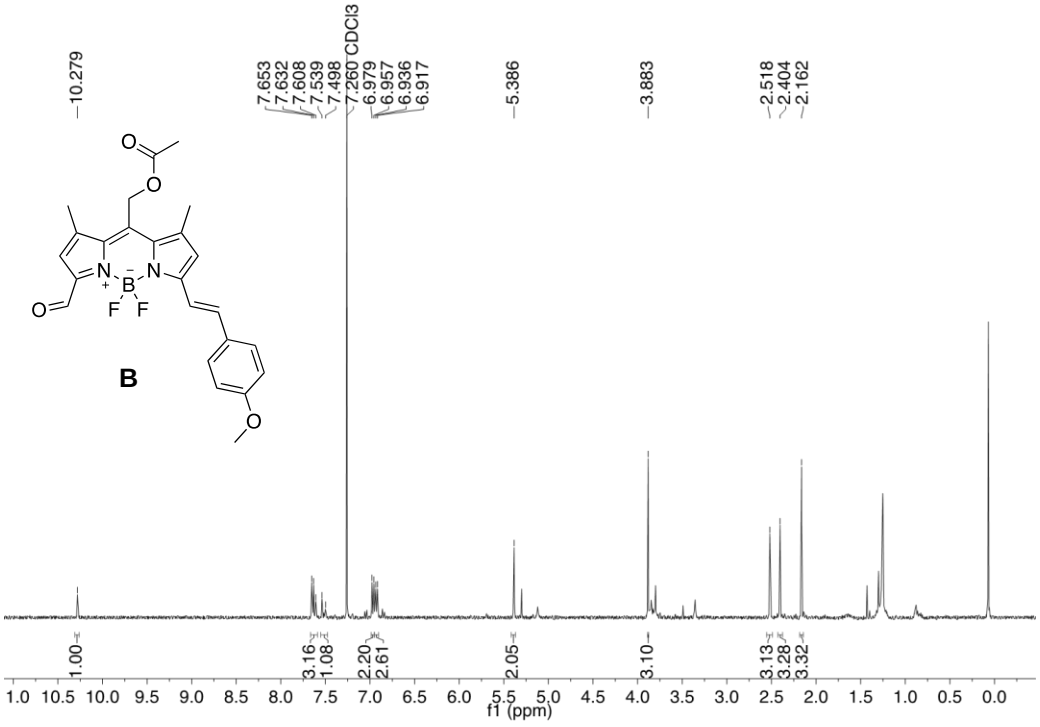

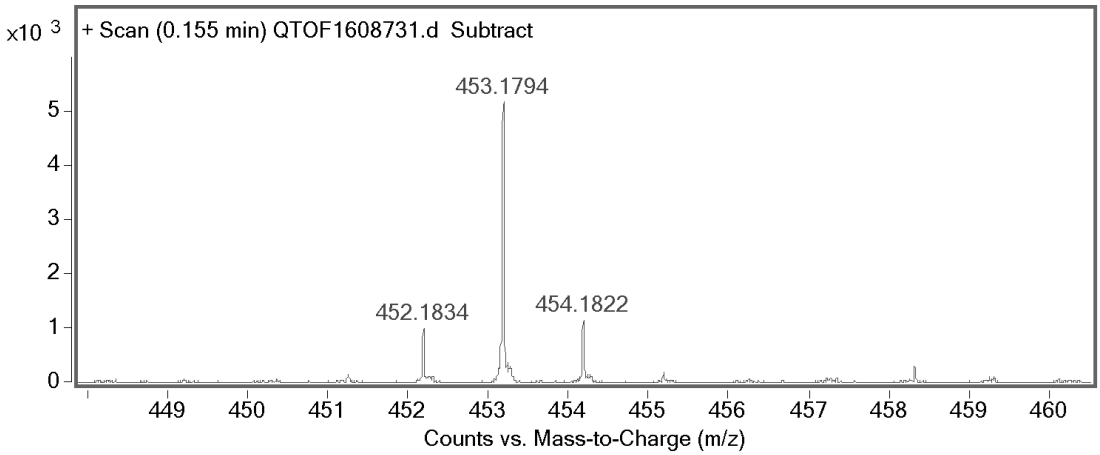

Compound **10** (1.3 mg) was dissolved in 1 mL 1:1 CD_3CN:CD_3OD and irradiated with a 500 W Halogen lamp with a water-based IR cutoff filter for 16 h, after which compound **10** had completely reacted. ^{1}H NMR shows the release of 4-nitrobenzoic acid, as well as the 4-(1,4,7,10-Tetraoxaundecyl)benzaldehyde. MS was used to confirm the release of 4-nitrobenzoic acid.

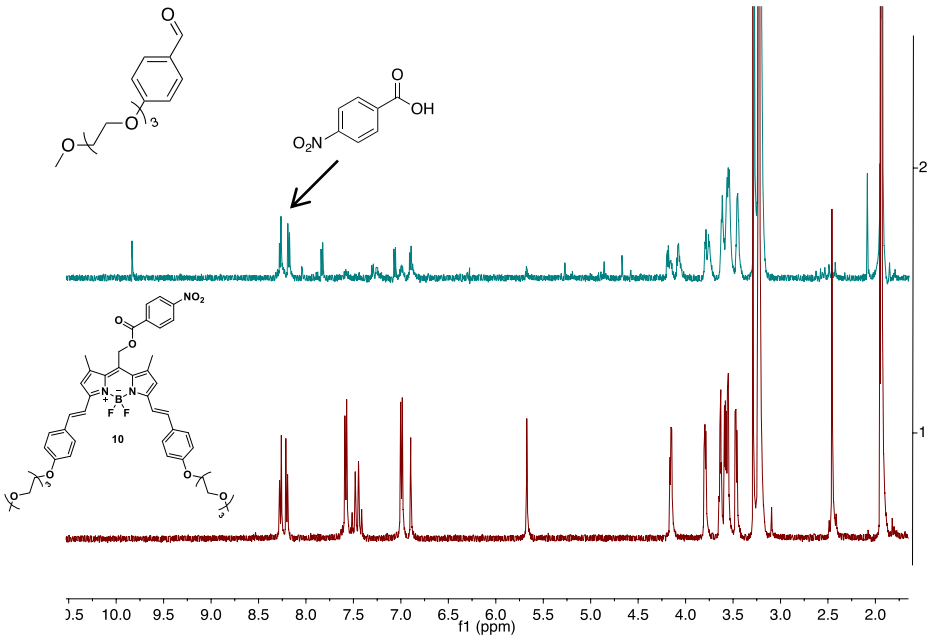

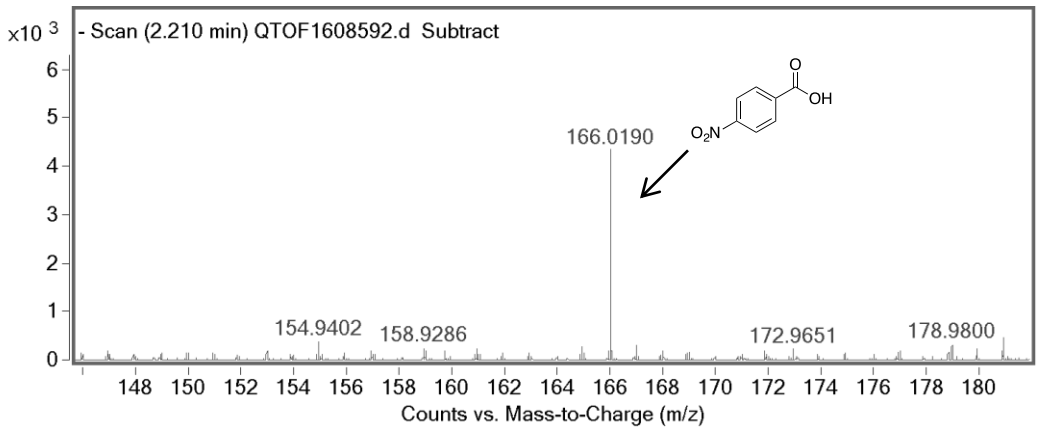

Thermal stability studies of compounds 3-6

Compounds **3-6** (1 mg) were each dissolved in 20 µL of CD_3OD and 600 µL of MeOD. ^1H NMR (600 MHz) were recorded for these compounds at room temperature. They were then heated at 60 °C in the dark for 1 h and allowed to cool to room temperature. ^1H NMR was then retaken to test their thermal stability. In all cases the spectra before and after heating are essentially unchanged.

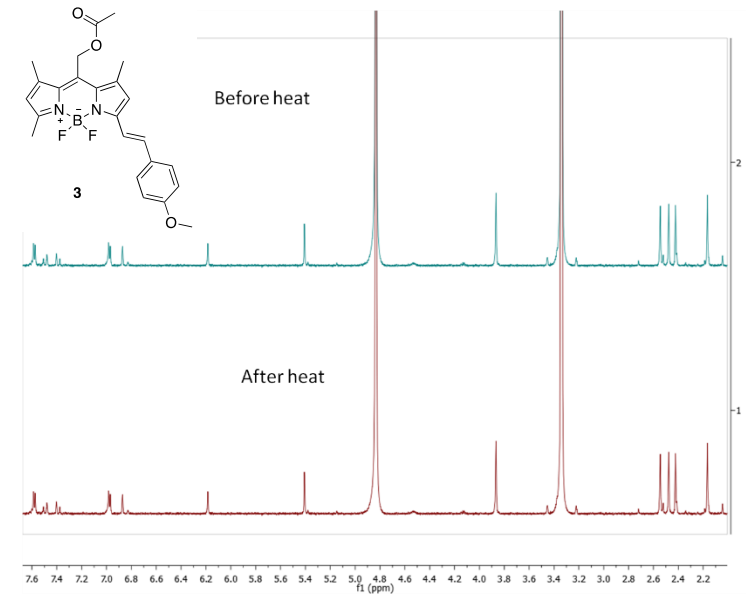

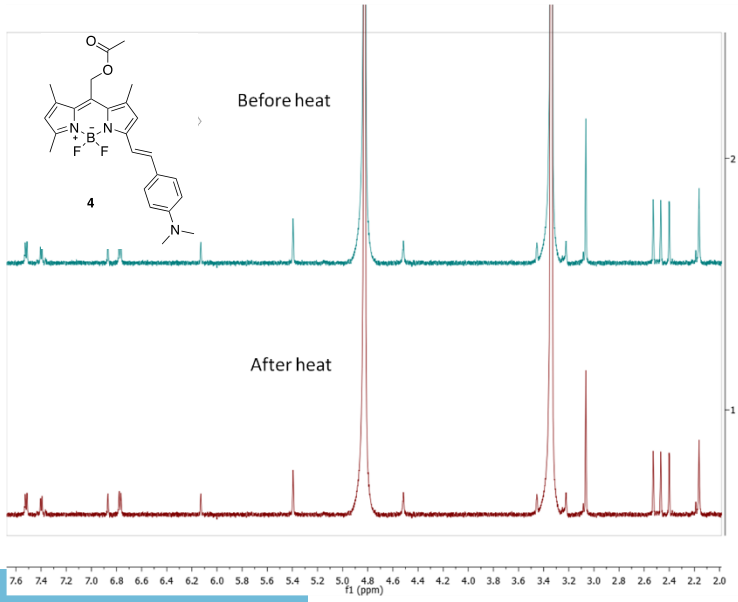

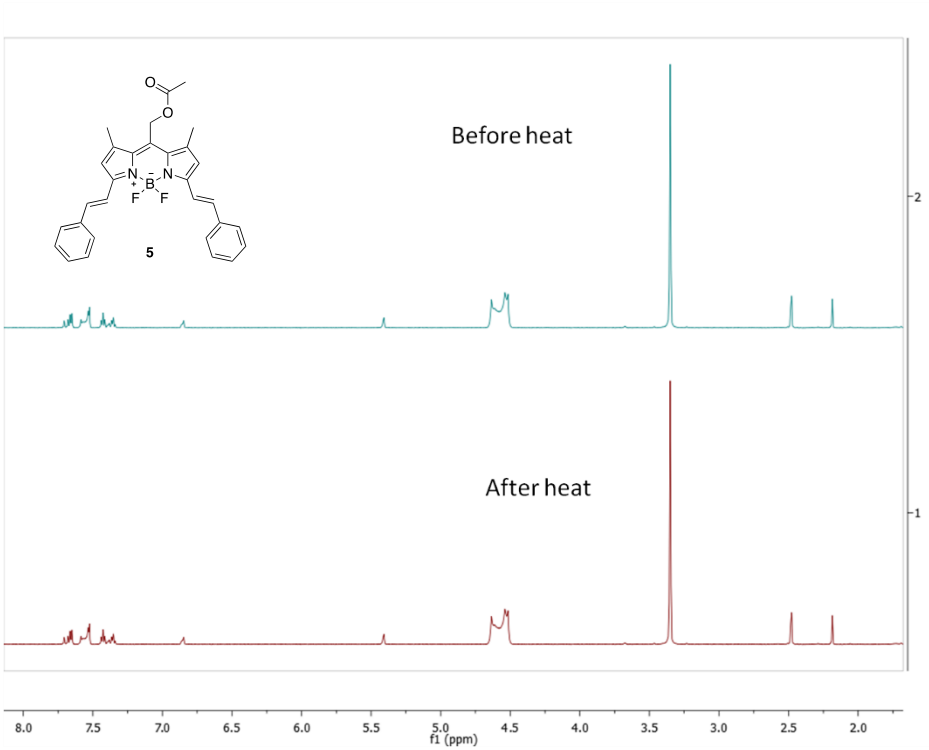

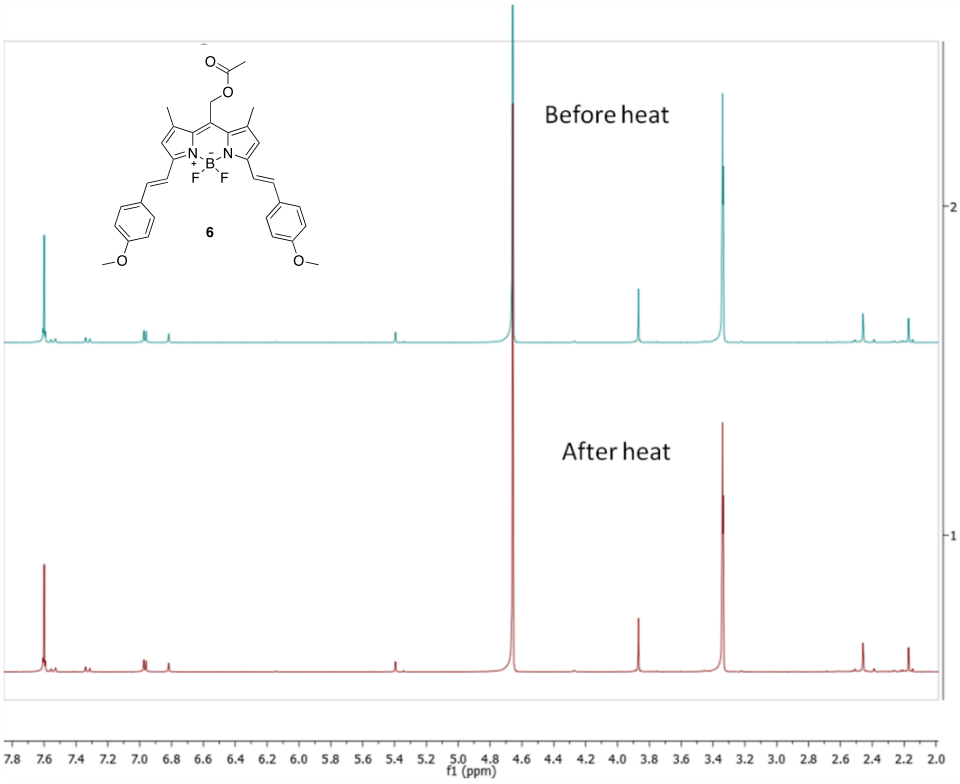

Quantum yield determination for compounds 3-6.

All quantum yields were calculated using potassium ferrioxalate actinometry. A dark room was used for the preparation and manipulation of all actinometry solutions. A 0.15 M solution of potassium ferrioxalate was prepared as previously reported.[3]

For each measurement a methacrylate cuvette was filled with 3 mL of 0.15 M ferrioxalate solution. The cuvettes were irradiated with a 532 nm ND:YAG laser for specified times so as not to exceed 20% conversion. The irradiated samples were transferred to 25 mL volumetric flasks to which were added 6 mL developing solution (0.05 mol% phenanthroline, 0.75 M acetate, and 0.2 M sulfuric acid), and 5 mL 1.0 M aqueous sodium fluoride and diluted to 25 mL with water. The absorbances at 510 nm of the solutions were taken after 10 minutes.

The amounts of reacted ferrioxalate were determined using a calibration curve of the iron(II)-phenanthroline complex that absorbs at 510 nm (generated using known concentrations of $FeSO_4$ and 1,10-phenanthroline).[3]

The flux of the laser was calculated with the following equations:

$$I = \frac{\Delta n}{(10^{-3} \bullet \Phi \bullet V_1 \bullet t)}$$

where I is the flux (Einstein/L/s), Δn is the Fe^{2+} photogenerated (mole), ϕ is the quantum yield at 532 nm, V_1 is the irradiated volume (mL), and t = irradiation time (seconds).

$$\Delta n = \frac{10^{-3} \bullet V_1 \bullet V_3 \bullet C_T}{V_2}$$

where V_2 is the volume taken from the irradiated sample (mL), V_3 is the volume after dilution for concentration determination (mL), and C_T is the concentration of Fe^{2+} after dilution (M)

$$C_T = \frac{abs}{e \cdot l}$$

where *abs* is the absorbance at 510 nm, ε is the molar absorptivity ($M^{-1}cm^{-1}$) and *l* is the path length

Due to the low absorbance of the potassium ferrioxalate solution at 532 nm, a correction was made to account for an absorbance less than 2 (via multiplying the flux by 0.0967).

For compounds 3-9

For each compound, a solution of 1000 ppm was prepared. Due to their poor solubility compounds **3-9** were predissolved in the minimal amount of acetonitrile or methylene chloride to dissolve and diluted to 1 mL of methanol. Each sample was irradiated in a cuvette for a specified period of time (so as not to exceed 30% cleavage). At each time point selected, 20 μL of the irradiated solution was removed and placed into an LC vial fitted with a 250 μL glass vial insert.

The concentrations of acetic acid (for **3-6**), phenylacetic acid (for **7-8**), and benzyl alcohol (for **8**) were determined using HPLC with UV detection at 210 nm and comparing with calibration curves of known concentrations of the given compounds between 5-1000 ppm.

Photolysis of compound 10 followed by fluorescence

1 mg of compound **10** was dissolved in 100 µL methanol and injected into 3.5 mL 0.5% BSA (w/v). The sample was placed in a quartz cuvette and irradiated with a halogen lamp through a water filter. Fluorescence measurements were taken over time using an excitation wavelength of 400 nm (**A**).

In order to test the thermal stability of compound **10** under the conditions of *in vivo* imaging, compound **10** (0.5 mg) was dissolved in 50 □L of methanol and injected into 3.5 mL imaging media (see cell studies, below) with 0.5% BSA (w/v). The solution was heated at 38 ºC for a total of 5 h, periodically monitoring the fluorescence. After heating, the sample was irradiated with a halogen lamp (**B**).

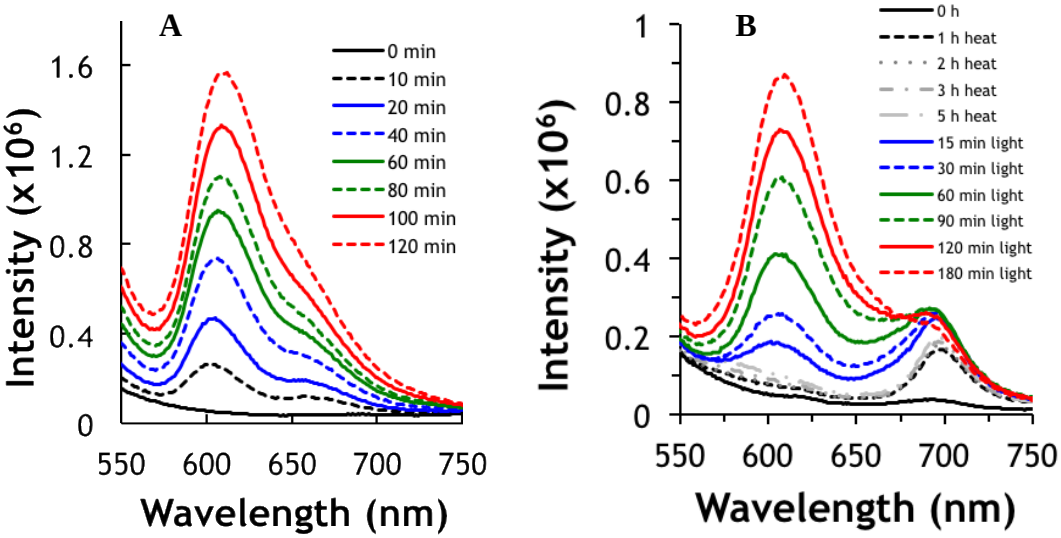

Cell studies

Cell sample preparation for fluorescence imaging

In vivo cell experiments were performed with HeLa (human), GM07373 (bovine) or S2 (*Drosophila*) cells. HeLa and GM07373 cells were cultured in DMEM medium supplemented with 10% fetal bovine serum, 12.5 mM streptomycin, and 36.5 mM penicillin (Fisher Scientific, Pittsburgh, PA) in a 37 °C water jacketed CO_2 incubator (Thermo Scientific, Waltham, MA). HeLa and GM07373 cells were sub-cultured using 0.25% (w/v) trypsin-EDTA (Life Technology, Carlsbad, CA) solution every two days. Cells were sub-cultured onto custom-made glass bottom culture dishes two days before the microscopy experiment. On the day of the microscopy experiment, the growth media was replaced with 20 µM compound **10** in serum-free DMEM for one hour. Cells were rinsed with the imaging medium (pH = 7.2, 155 mM NaCl, 5 mM KCl, 2 mM $CaCl_2$, 1 mM $MgCl_2$, 2 mM NaH_2PO_4, 10 mM HEPES and 10 mM Glucose) prior to collecting microscopy images. S2 cells were cultured in Shields and Sang M3 insect medium (Sigma-Aldrich, St. Louis, MO) with heat-inactivated 10% fetal bovine serum (Irvine Scientific, Santa Ana, CA), 12.5 mM streptomycin, and 36.5 mM penicillin in a 22 °C incubator (Fisher Scientific, Pittsburgh, PA).[4] S2 cells were incubated with 20 µM of the compound **10** in M3 media for one hour and then washed twice with serum free M3 medium. Incubated S2 cells were allowed to spread on cover glass for half an hour at room temperature, and were then rinsed with BES buffer (pH = 7.0) multiple times prior to collecting microscopy images.

Live cell fluorescence imaging

All microscopy experiments were performed on a Nikon Eclipse TE2000U microscope (Melville, NY) operating in wide-field, epi-fluorescence mode and equipped with a 100× Apo, 1.49 numerical aperture oil-immersion objective. HeLa or GM07373 cells were imaged at 36±2

ºC in a home-built housing around the microscope. S2 cells were imaged at room temperature. For photolysis, the cells were illuminated with 635±15 nm wavelength light from a mercury lamp (X-Cite 120 PC, EXFO Photonic Solutions Inc., Mississauga, Ontario, Canada) operating at 100% lamp power. Increased fluorescence due to quencher release during the photolysis reaction was collected through excitation (425±45nm) and emission (605±20nm) filters from Omega Optical (XF304-1, Brattleboro, VT). Fluorescence images were collected every 2 minutes using a PhotonMAX 512 EMCCD camera (Princeton Instruments, Trenton, NJ) and WinView 2.6 imaging software (Princeton Instruments, Trenton, NJ). The control experiments were performed without the 635±15 nm light illumination. Images were further analyzed with imageJ (National Institute of Health) and IGOR Pro V 6.32A (WaveMetrices Inc., Lake Oswego, OR).

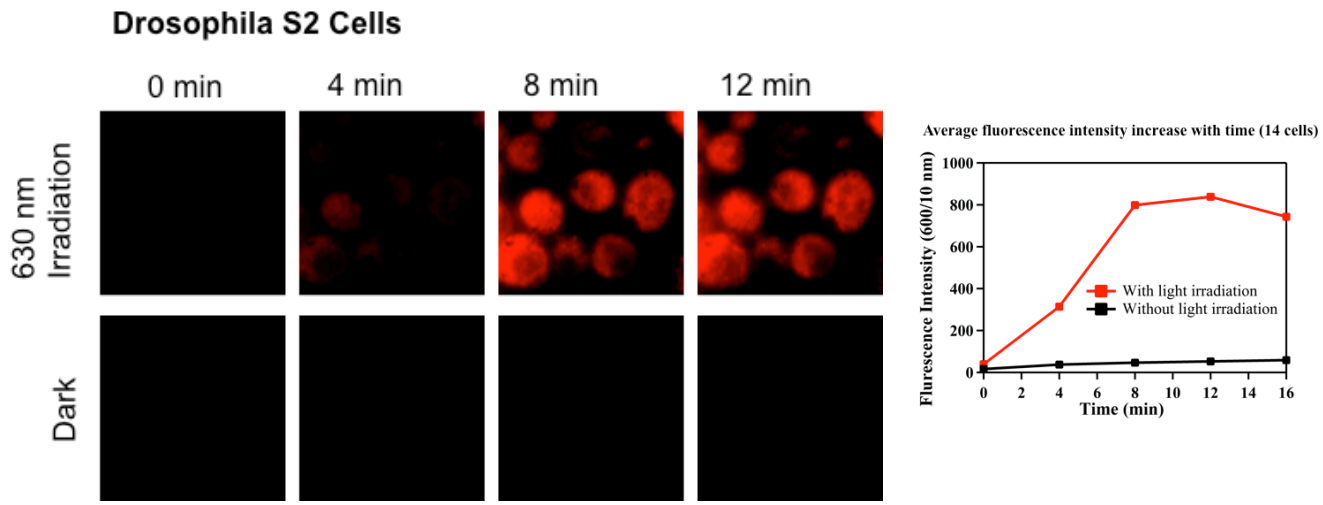

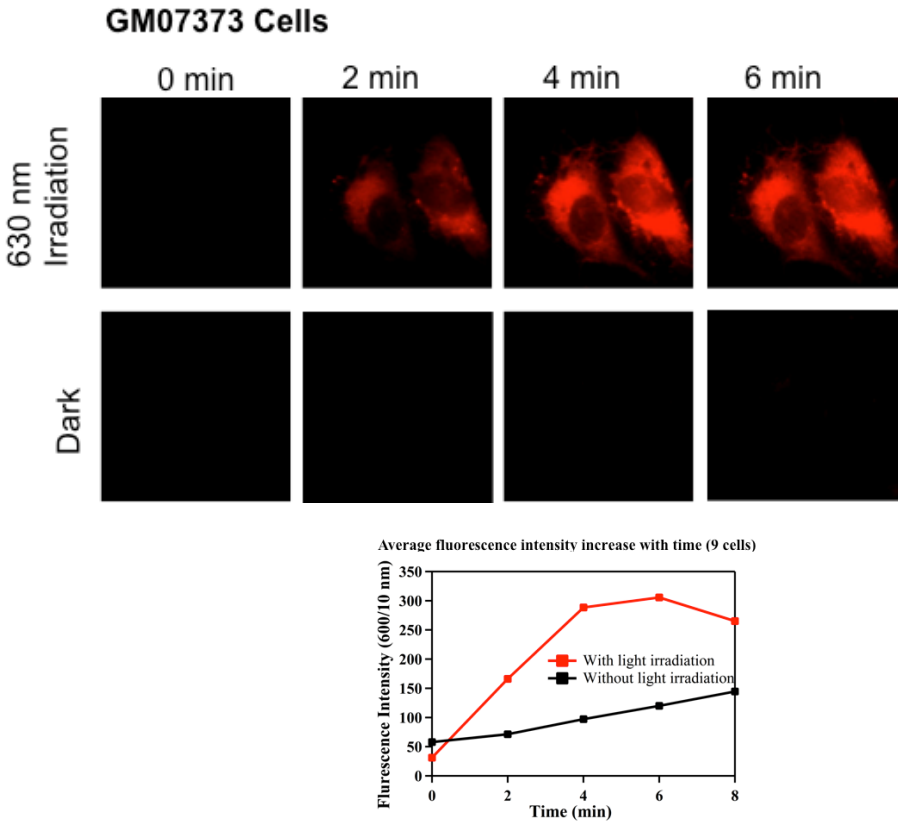

Cytotoxicity assay

HeLa, GM07373 and S2 cells were each incubated with 20 µM of the compound **10** for an hour. Cytotoxicity of the compound was measured using trypan blue exclusion assays.[5] Equal volumes of the cell suspension and 0.4% trypan blue stain (Thermo ScientificTM HycloneTM Trypan Blue, Waltham, MA) were incubated for 3 minutes at room temperature. The number of viable cells that excluded the dye was counted using a hemacytometer (Hausser Bright-Line, Hausser scientific, Horsham, PA) and an optical microscope.

Cytotoxicity of compounds as measured with trypan blue exclusion assay

	% of Viable cells
HeLa cells	
No treatment	90±3
Cells incubated with 20 μM compound **10**	92±5
S2 cells	
No treatment	95±2
Cells incubated with 20 μM compound **10**	93±2
GM07373 cells	
No treatment	90±1
Cells incubated with 20 μM compound **10**	92±5

Uncertainty represents standard deviation from two measurements

DFT calculations

The restricted singlet and triplet geometries of compound **6** were optimized using UB3LYP/6-31G(d) with the Gaussian 09[6] software. An unrestricted broken-symmetry calculation was done on the singlet state using the guess=(mix,always,save) command. The spin contamination was corrected using the following equation.[7-10]

$$E_{singlet} = \frac{2E_{<S_z>=0} - < S^2 > E_{<S_z>=1}}{2 - < S^2 >}$$

Where E_{singlet} is the corrected singlet energy, $E_{<S_z>=0}$ is the broken-symmetry singlet state energy, $< S^2 >$ is the expectation value of the total-spin operator for the broken-symmetry singlet calculation, and $E_{<S_z>=1}$ is the energy of the triplet state at the singlet geometry.

Below are shown the SOMOs of the triplet (**A**-**B**) and unrestricted singet (**C**-**D**) UB3LYP/6-31G(d) optimized geometries (isovalue = 0.05 for triplet and 0.065 for singlet).

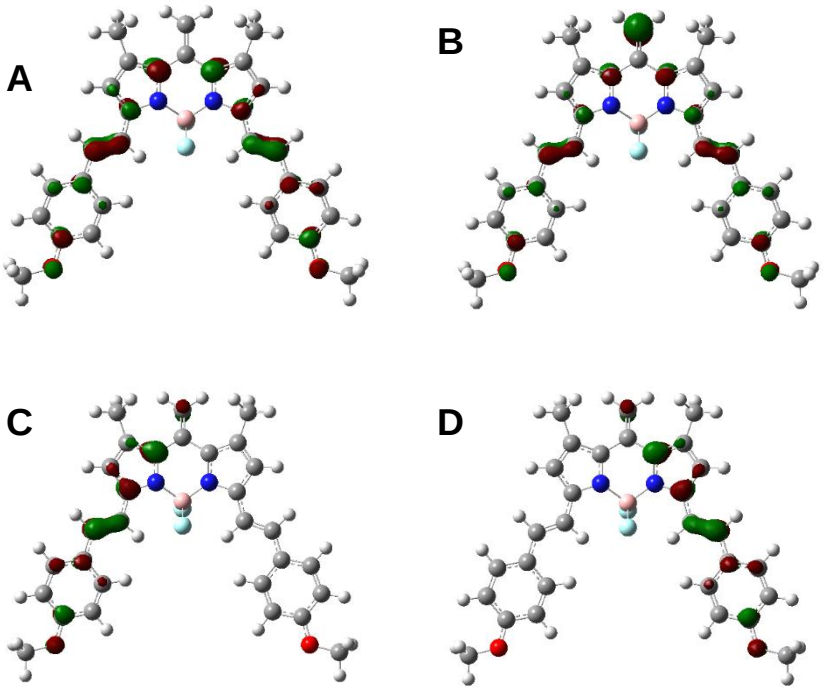

Compound 6 (optimized singlet geometry)

Center Number	Atomic Number	Atomic Type	Coordinates (Angstroms) X	Y	Z
1	6	0	-1.248889	-3.687758	0.029341
2	6	0	-0.000029	-4.435820	0.180475
3	6	0	1.248826	-3.687759	0.029281
4	5	0	-0.000019	-1.470982	0.509799
5	9	0	-0.000008	-1.231581	1.866186
6	9	0	-0.000035	-0.282981	-0.219540
7	6	0	2.588647	-4.156197	-0.228428
8	6	0	-2.550575	-1.881005	-0.062935
9	6	0	-2.588728	-4.156188	-0.228300
10	6	0	3.374781	-3.026957	-0.278952
11	6	0	-3.374858	-3.026942	-0.278787
12	6	0	-0.000015	-5.758370	0.482747
13	6	0	2.902948	-0.518421	-0.019742
14	6	0	-2.902968	-0.518400	-0.019715
15	6	0	4.203975	-0.060883	-0.118981

16	6	0	-4.203987	-0.060835	-0.118932
17	6	0	-4.633074	1.302934	-0.083175
18	6	0	-6.016477	1.588125	-0.200577
19	6	0	-3.746481	2.407072	0.065739
20	6	0	-6.505038	2.883297	-0.175662
21	1	0	-6.714936	0.763059	-0.313950
22	6	0	-4.218893	3.698130	0.092188
23	1	0	-2.679342	2.236777	0.162030
24	6	0	-5.605098	3.956421	-0.028276
25	1	0	-7.570015	3.058257	-0.268939
26	1	0	-3.549616	4.544362	0.206076
27	6	0	4.633094	1.302875	-0.083187
28	6	0	3.746529	2.407029	0.065779
29	6	0	6.016502	1.588038	-0.200604
30	6	0	4.218971	3.698075	0.092263
31	1	0	2.679388	2.236755	0.162081
32	6	0	6.505093	2.883198	-0.175654
33	1	0	6.714940	0.762961	-0.314018
34	6	0	5.605180	3.956338	-0.028215
35	1	0	3.549715	4.544318	0.206190
36	1	0	7.570072	3.058137	-0.268944
37	1	0	-0.918143	-6.308822	0.632510
38	1	0	0.918130	-6.308810	0.632457
39	1	0	-4.437432	-3.006430	-0.479631
40	1	0	4.437345	-3.006450	-0.479853
41	7	0	-1.247160	-2.332318	0.104531
42	1	0	2.090291	0.187801	0.093440
43	1	0	4.998716	-0.795629	-0.232394
44	1	0	-2.090291	0.187809	0.093416
45	1	0	-4.998747	-0.795567	-0.232300
46	7	0	1.247110	-2.332321	0.104500
47	6	0	2.550527	-1.881018	-0.063003
48	8	0	5.955298	5.250948	0.010404
49	8	0	-5.955185	5.251041	0.010307
50	6	0	7.335446	5.612308	-0.100869
51	6	0	-7.335326	5.612429	-0.100962
52	1	0	-7.919303	5.186346	0.722257
53	1	0	-7.356783	6.700316	-0.041431
54	1	0	-7.749001	5.287267	-1.061929
55	1	0	7.356930	6.700192	-0.041295
56	1	0	7.919423	5.186179	0.722326
57	1	0	7.749101	5.287173	-1.061853
58	6	0	-3.063815	-5.560902	-0.451560
59	1	0	-2.416895	-6.107161	-1.146863
60	1	0	-3.107187	-6.135947	0.482330
61	1	0	-4.073767	-5.552313	-0.870859

62	6	0	3.063704	-5.560914	-0.451733
63	1	0	3.107190	-6.135955	0.482155
64	1	0	2.416695	-6.107176	-1.146952
65	1	0	4.073605	-5.552332	-0.871156

Energy = -1644.47028613 Hartrees
Spin-corrected energy = -1644.467865 Hartrees

Compound 6 (optimized triplet geometry)

Center Number	Atomic Number	Atomic Type	Coordinates (Angstroms) X	Y	Z
1	6	0	1.244588	-3.684012	0.026705
2	6	0	0.000075	-4.429452	0.157892
3	6	0	-1.244424	-3.684015	0.026551
4	5	0	0.000052	-1.457887	0.487122
5	9	0	0.000137	-0.277128	-0.253974
6	9	0	-0.000032	-1.203998	1.841276
7	6	0	-2.591861	-4.151955	-0.209899
8	6	0	2.546970	-1.875581	-0.061225
9	6	0	2.592071	-4.151939	-0.209518
10	6	0	-3.376049	-3.023522	-0.258847
11	6	0	3.376219	-3.023480	-0.258581
12	6	0	0.000065	-5.772128	0.417771
13	6	0	-2.901850	-0.512169	-0.023309
14	6	0	2.901903	-0.512117	-0.023242
15	6	0	-4.204702	-0.061374	-0.107890
16	6	0	4.204732	-0.061250	-0.107789
17	6	0	4.640950	1.301168	-0.076795
18	6	0	6.026647	1.577952	-0.178887
19	6	0	3.758323	2.410306	0.052607
20	6	0	6.521737	2.871004	-0.157660
21	1	0	6.722328	0.748579	-0.277238
22	6	0	4.236978	3.699339	0.075219
23	1	0	2.689214	2.245951	0.136874
24	6	0	5.625712	3.949588	-0.029785
25	1	0	7.588689	3.039759	-0.238842
26	1	0	3.570621	4.549725	0.174309
27	6	0	-4.641002	1.301016	-0.076806
28	6	0	-3.758449	2.410195	0.052747
29	6	0	-6.026709	1.577727	-0.178957
30	6	0	-4.237182	3.699197	0.075442
31	1	0	-2.689335	2.245895	0.137065

32	**6**	**0**	**-6.521878**	**2.870747**	**-0.157648**
33	**1**	**0**	**-6.722336**	**0.748321**	**-0.277422**
34	**6**	**0**	**-5.625924**	**3.949373**	**-0.029624**
35	**1**	**0**	**-3.570881**	**4.549614**	**0.174647**
36	**1**	**0**	**-7.588834**	**3.039446**	**-0.238880**
37	**1**	**0**	**0.917785**	**-6.326271**	**0.549926**
38	**1**	**0**	**-0.917664**	**-6.326272**	**0.549862**
39	**1**	**0**	**4.441156**	**-3.003280**	**-0.446162**
40	**1**	**0**	**-4.440979**	**-3.003339**	**-0.446474**
41	**7**	**0**	**1.245570**	**-2.323819**	**0.091996**
42	**1**	**0**	**-2.089580**	**0.196888**	**0.073027**
43	**1**	**0**	**-4.997910**	**-0.800201**	**-0.204938**
44	**1**	**0**	**2.089585**	**0.196901**	**0.072989**
45	**1**	**0**	**4.997990**	**-0.800038**	**-0.204727**
46	**7**	**0**	**-1.245426**	**-2.323817**	**0.091833**
47	**6**	**0**	**-2.546842**	**-1.875610**	**-0.061387**
48	**8**	**0**	**-5.982416**	**5.242570**	**0.003648**
49	**8**	**0**	**5.982124**	**5.242809**	**0.003398**
50	**6**	**0**	**-7.365748**	**5.595439**	**-0.092842**
51	**6**	**0**	**7.365441**	**5.595754**	**-0.093035**
52	**1**	**0**	**7.936599**	**5.173076**	**0.740899**
53	**1**	**0**	**7.789692**	**5.260750**	**-1.046008**
54	**1**	**0**	**7.392243**	**6.683957**	**-0.041809**
55	**1**	**0**	**-7.789918**	**5.260492**	**-1.045871**
56	**1**	**0**	**-7.936934**	**5.172653**	**0.741019**
57	**1**	**0**	**-7.392619**	**6.683636**	**-0.041522**
58	**6**	**0**	**-3.078936**	**-5.554895**	**-0.417883**
59	**1**	**0**	**-2.461727**	**-6.101468**	**-1.139443**
60	**1**	**0**	**-3.087839**	**-6.131626**	**0.515752**
61	**1**	**0**	**-4.104236**	**-5.541310**	**-0.797816**
62	**6**	**0**	**3.079204**	**-5.554885**	**-0.417325**
63	**1**	**0**	**3.088593**	**-6.131365**	**0.516458**
64	**1**	**0**	**2.461725**	**-6.101719**	**-1.138459**
65	**1**	**0**	**4.104333**	**-5.541292**	**-0.797716**

Energy = -1644.47281641 Hartrees

Compound characterization data

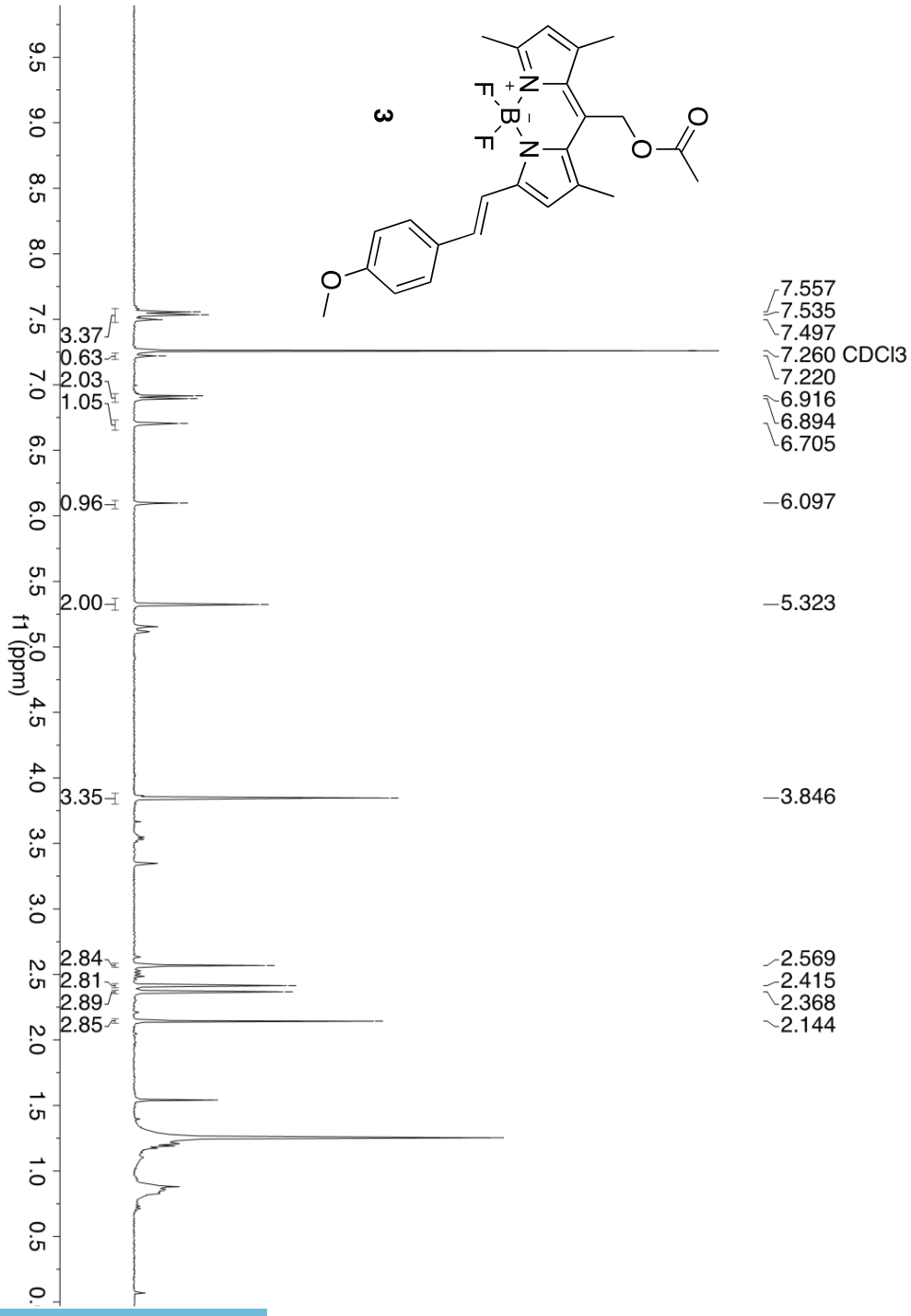

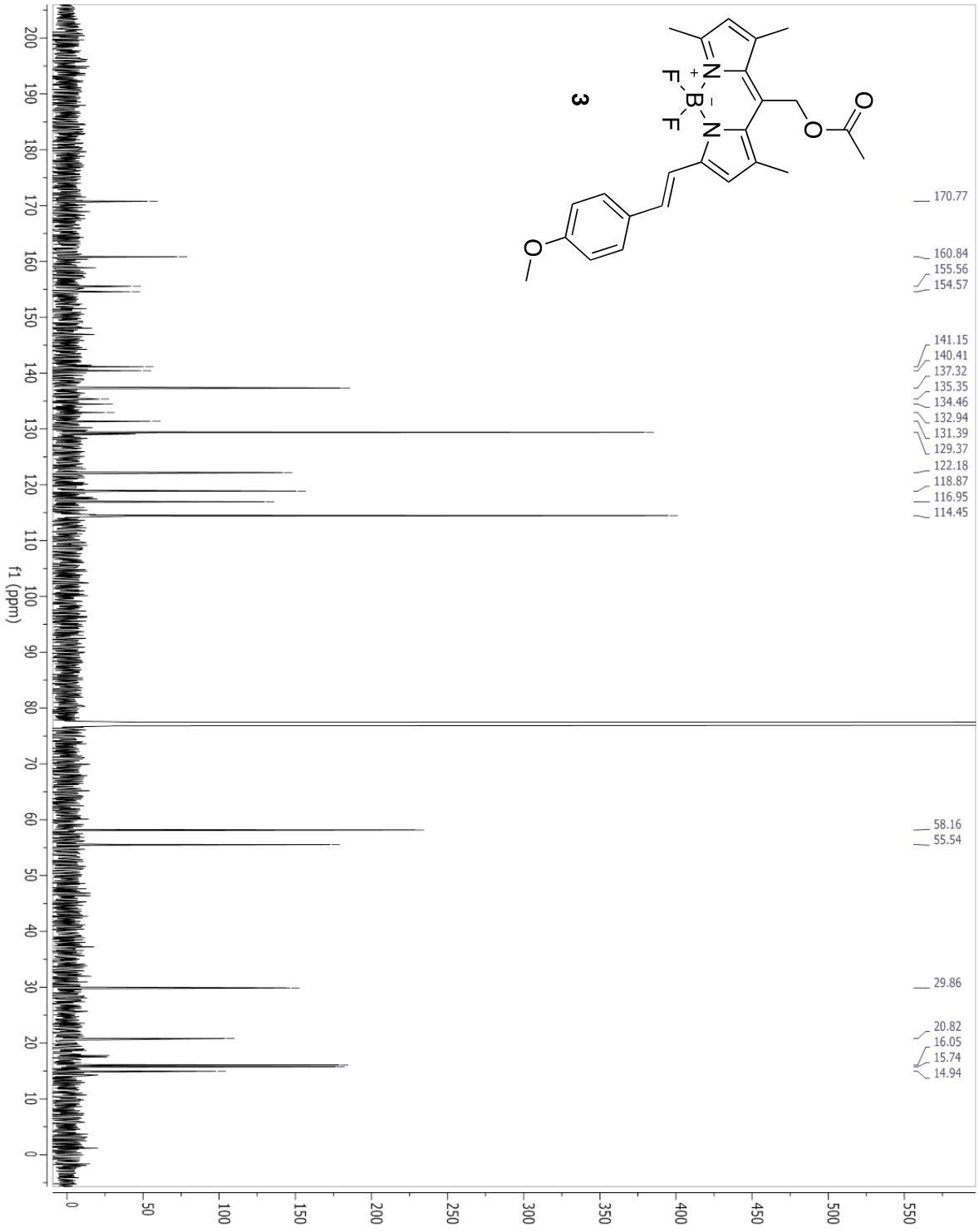

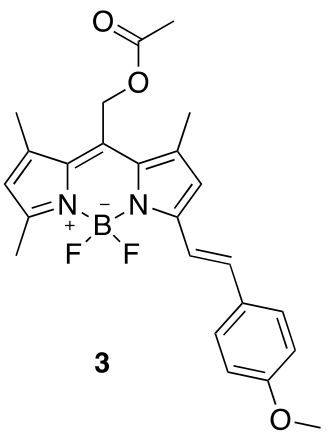

3

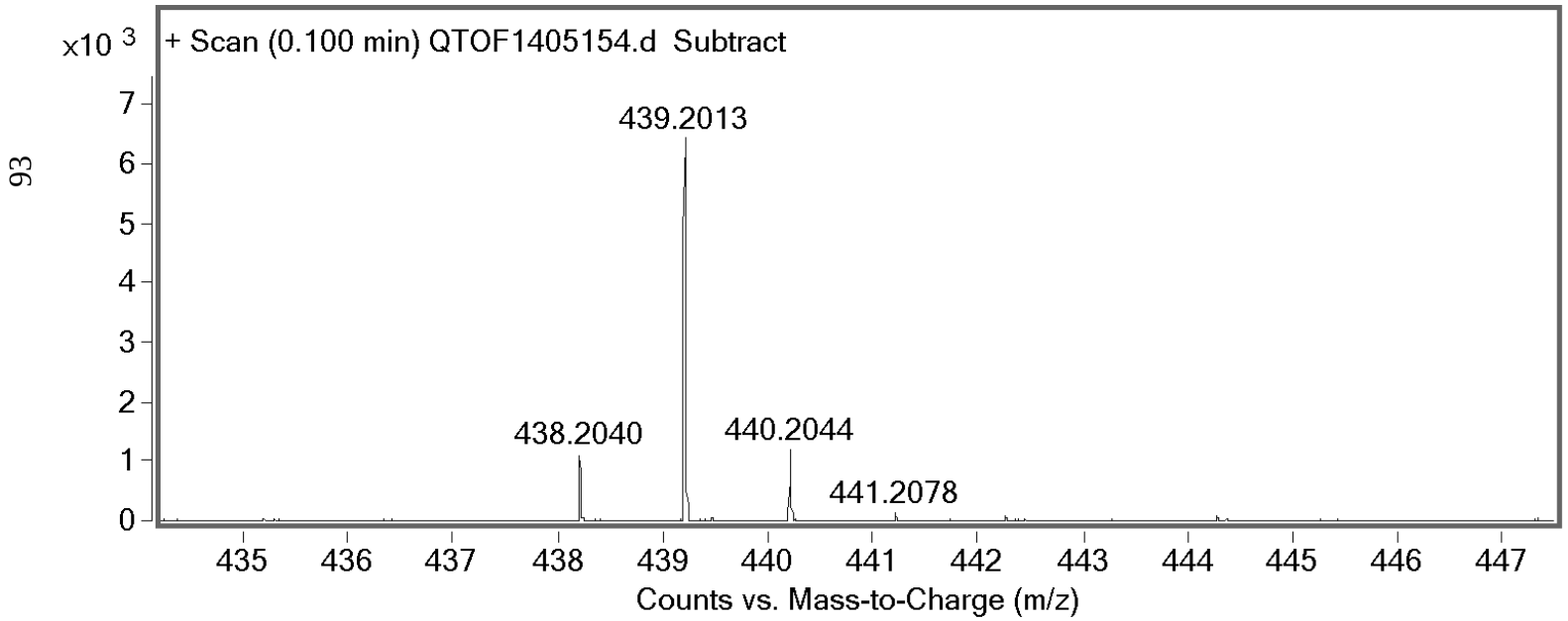

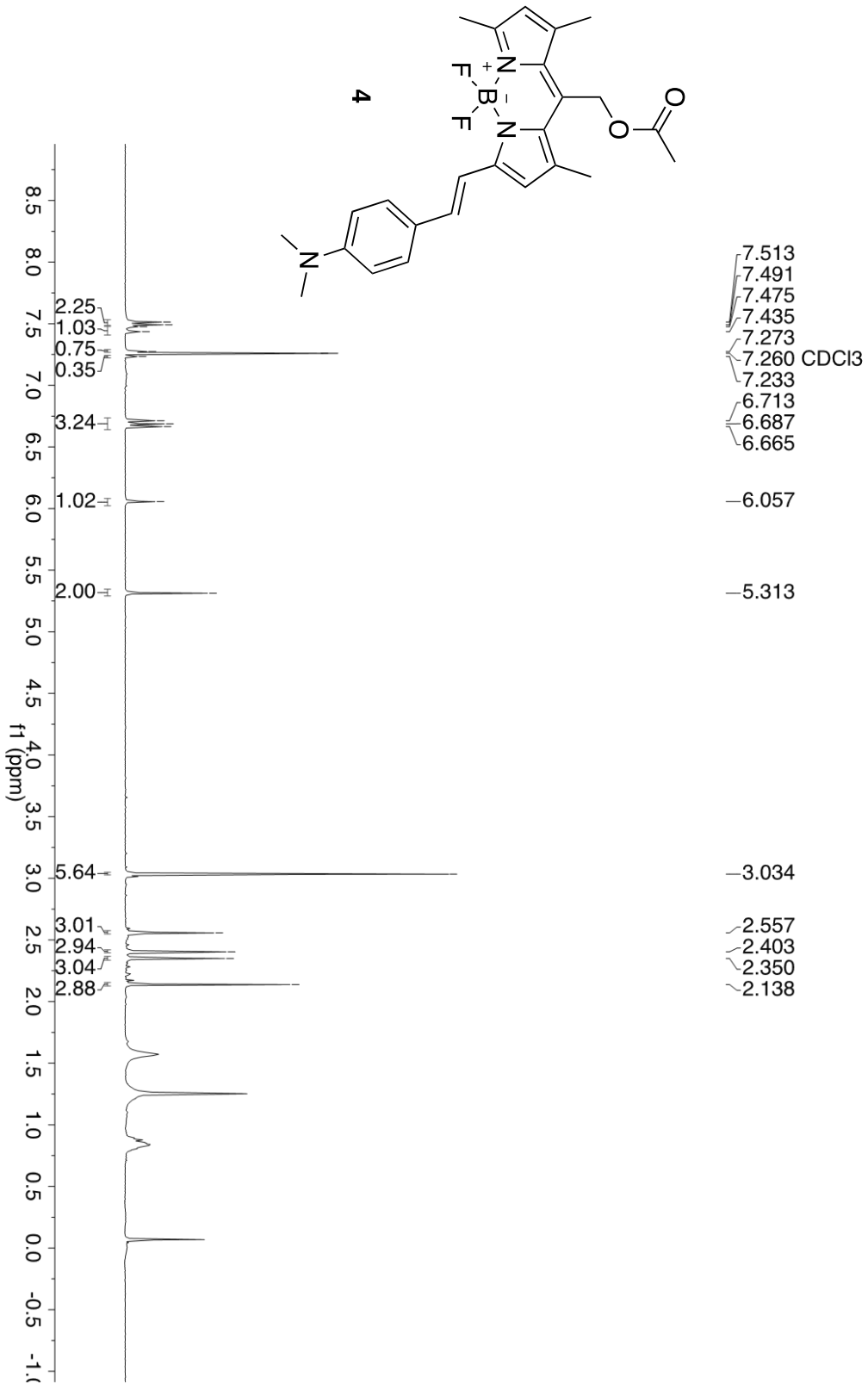

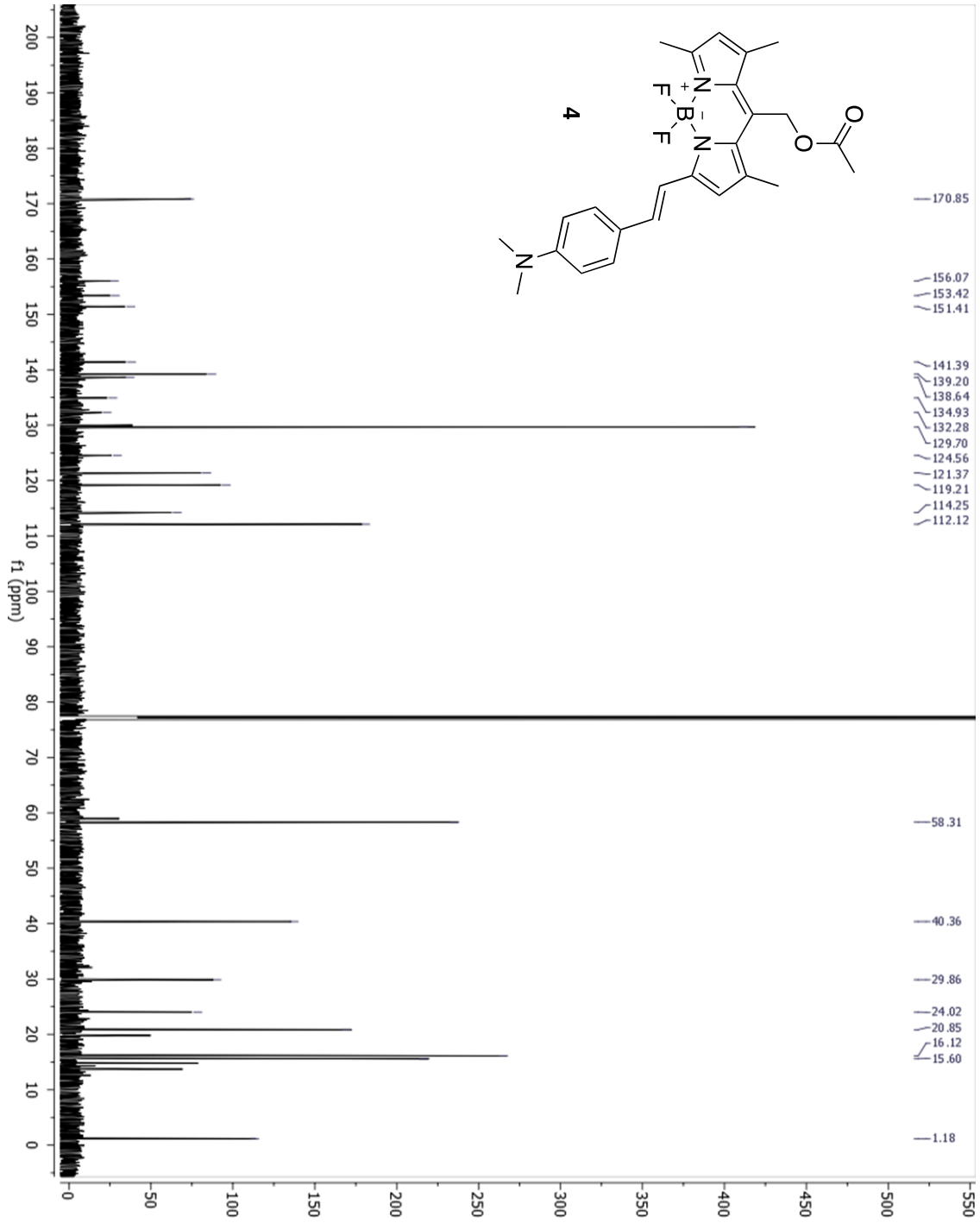

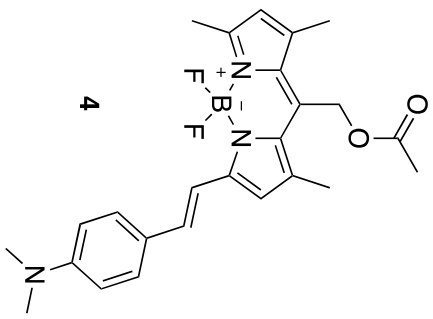

4

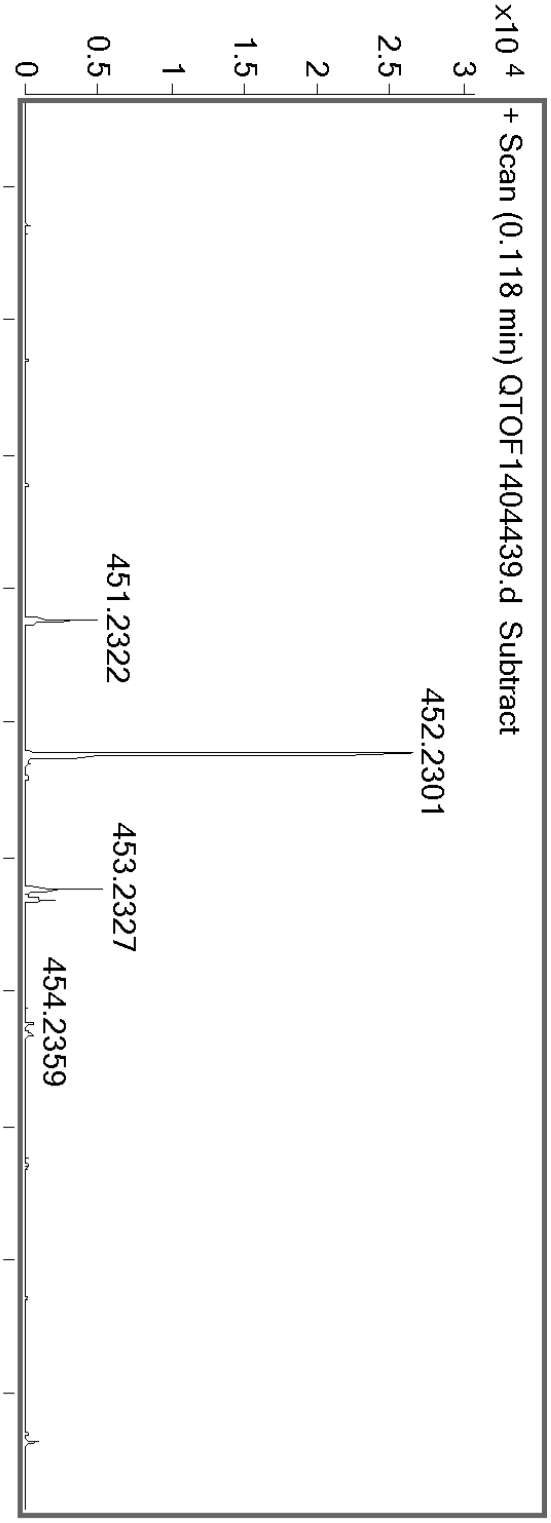

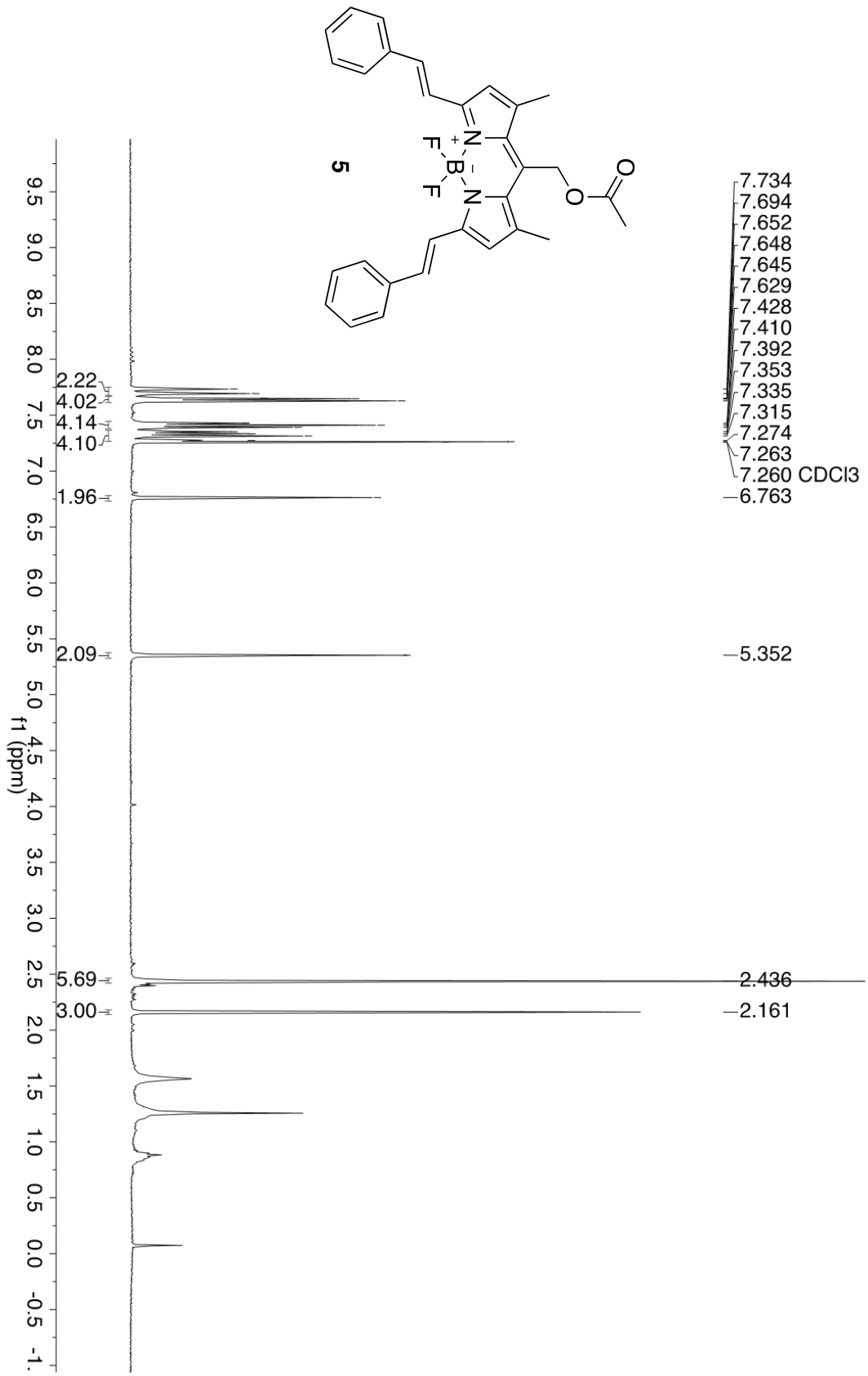

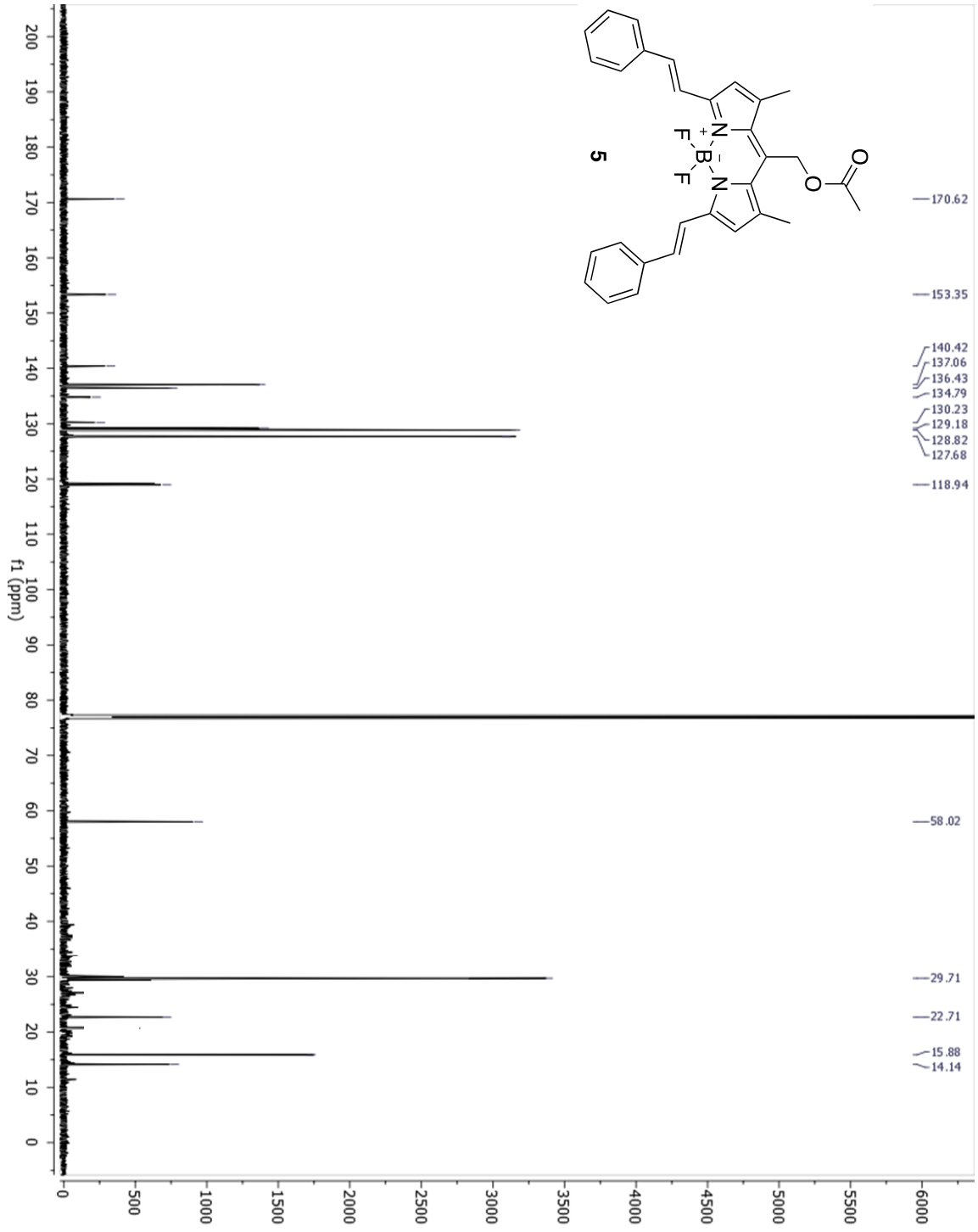

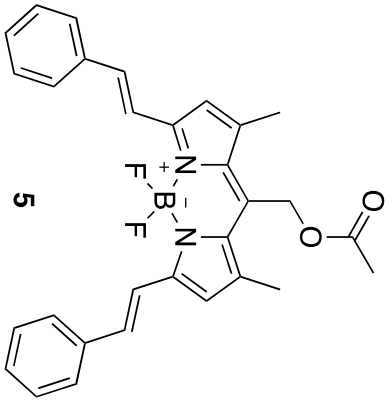

5

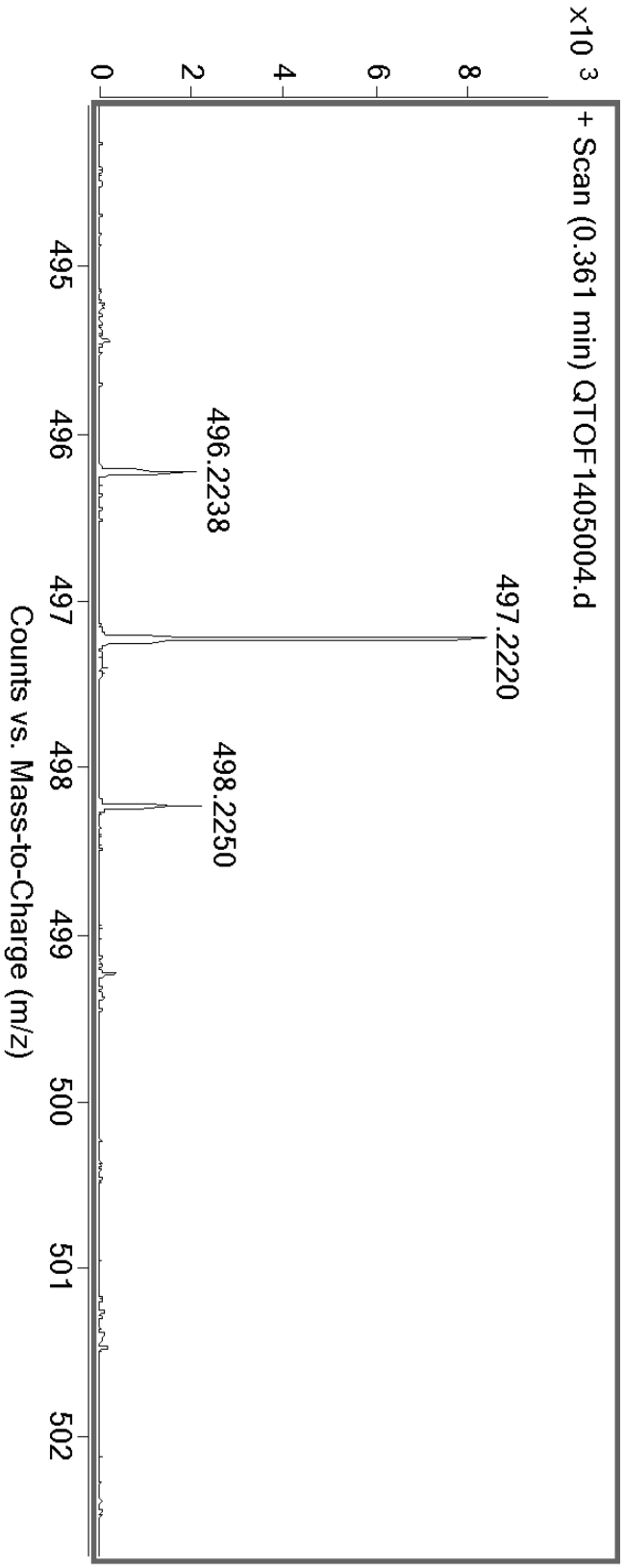

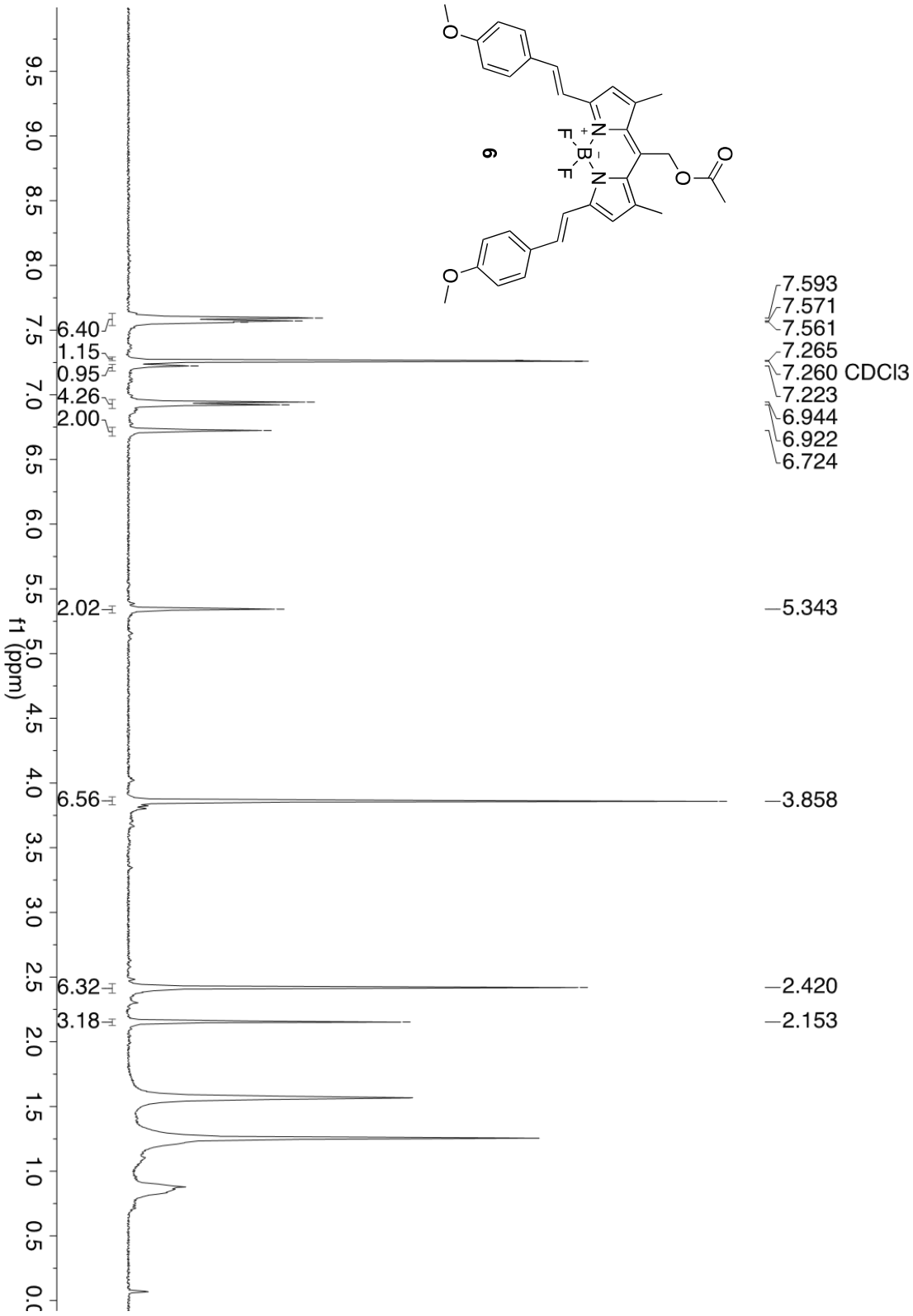

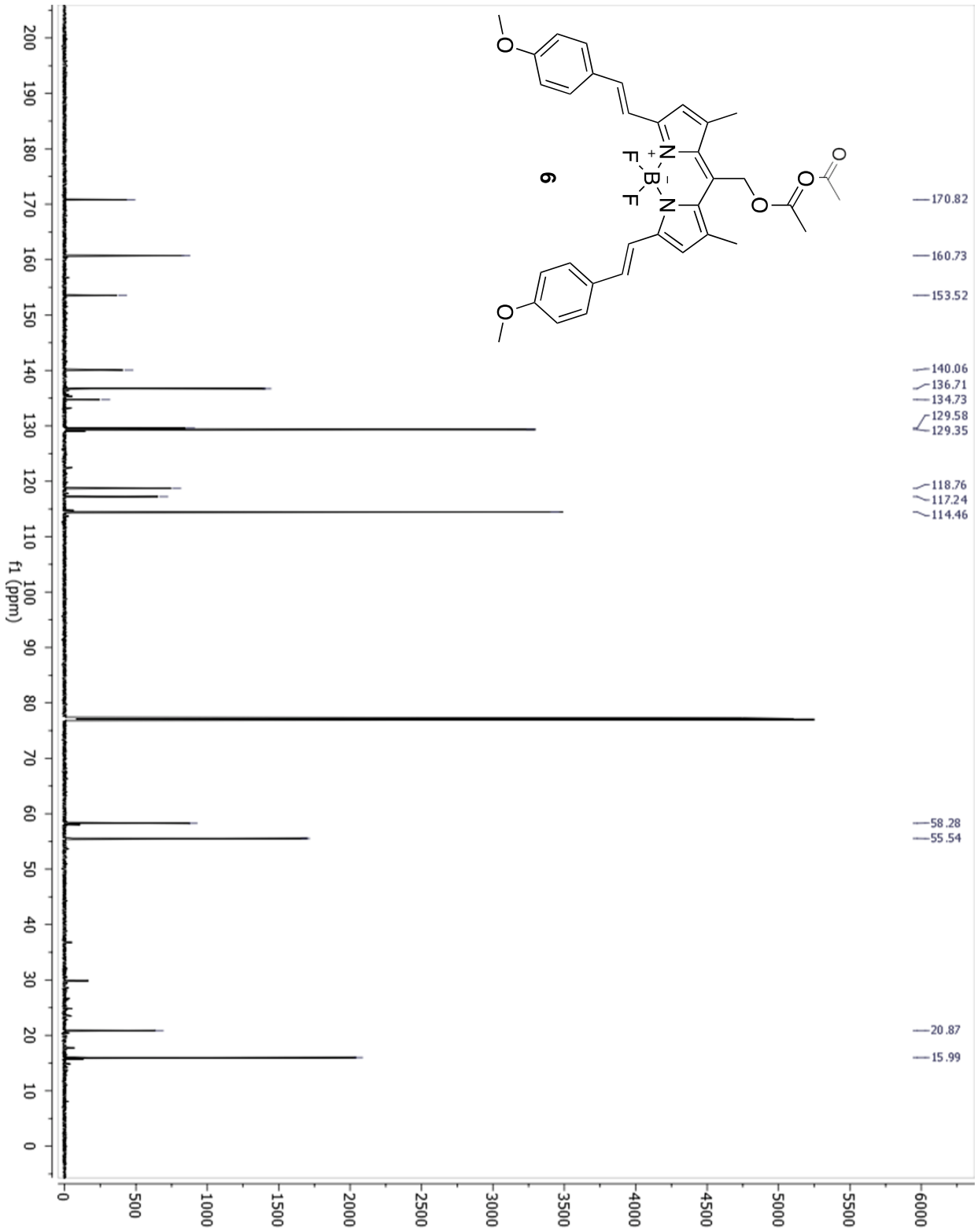

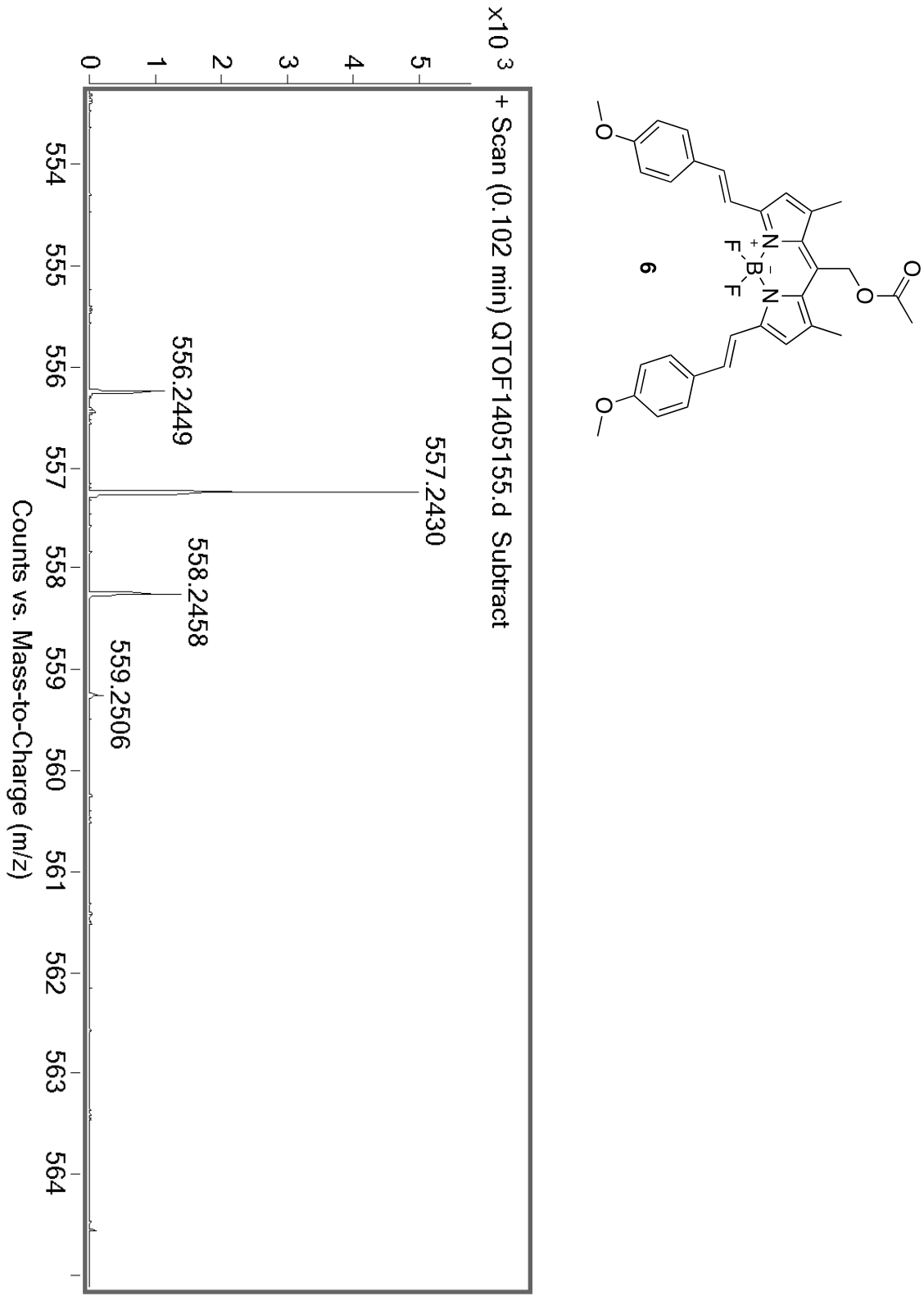

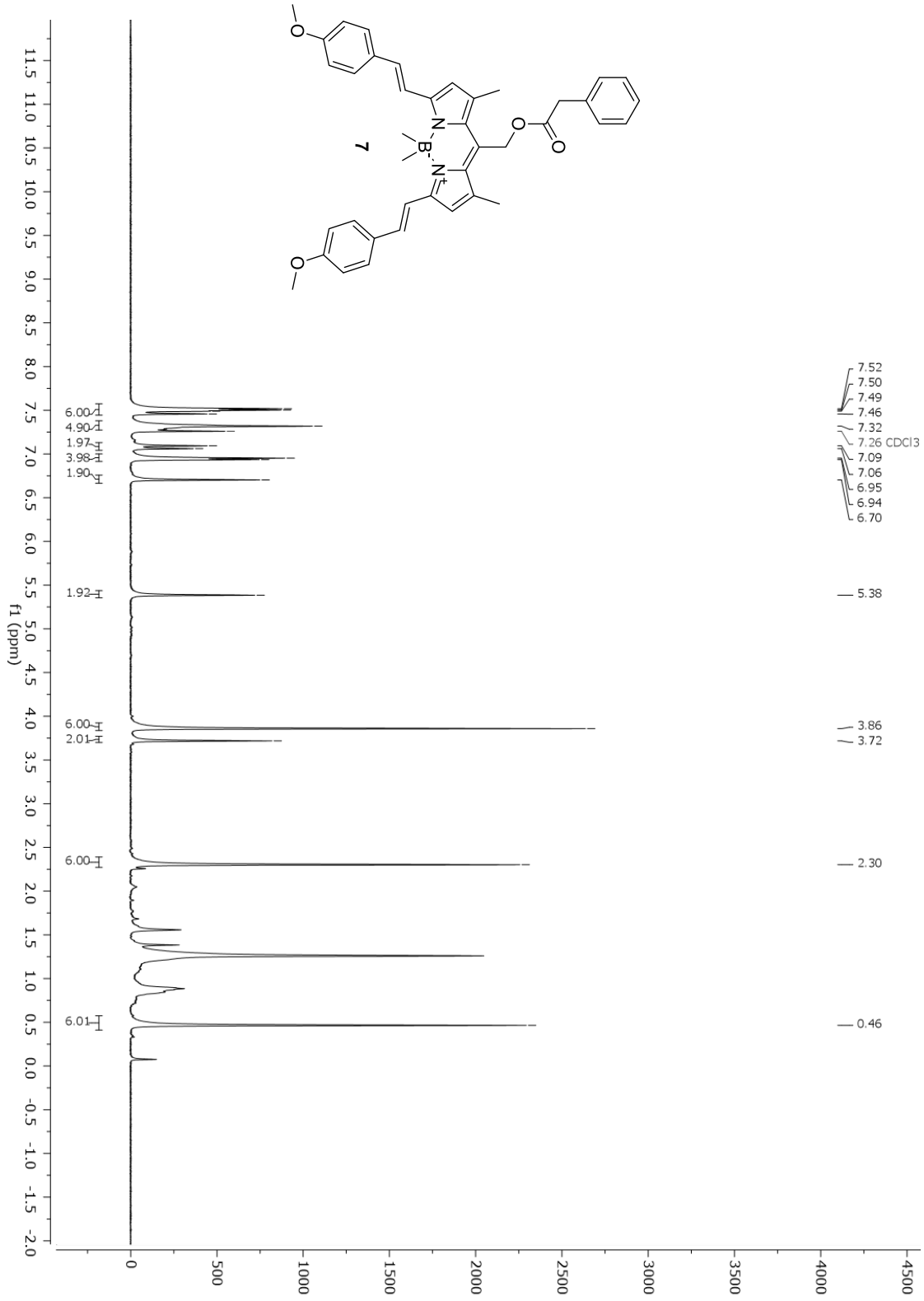

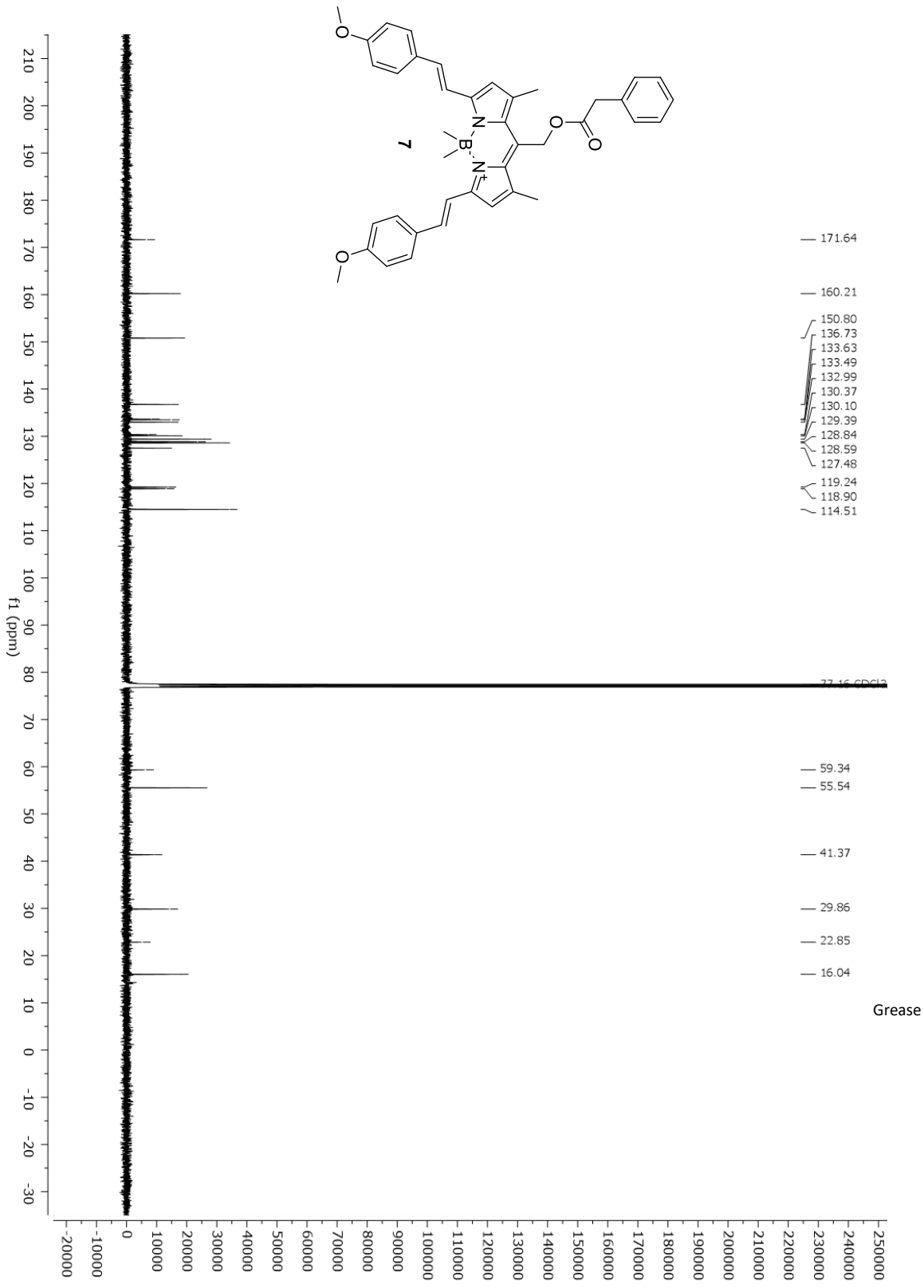

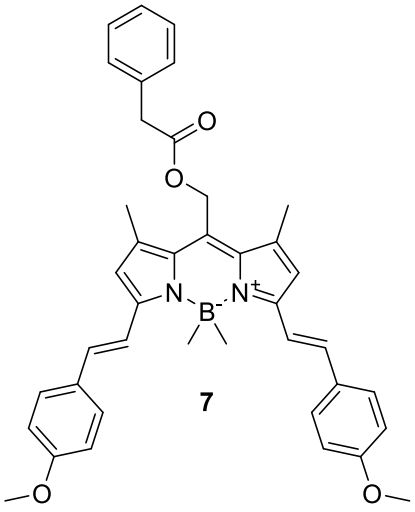

7

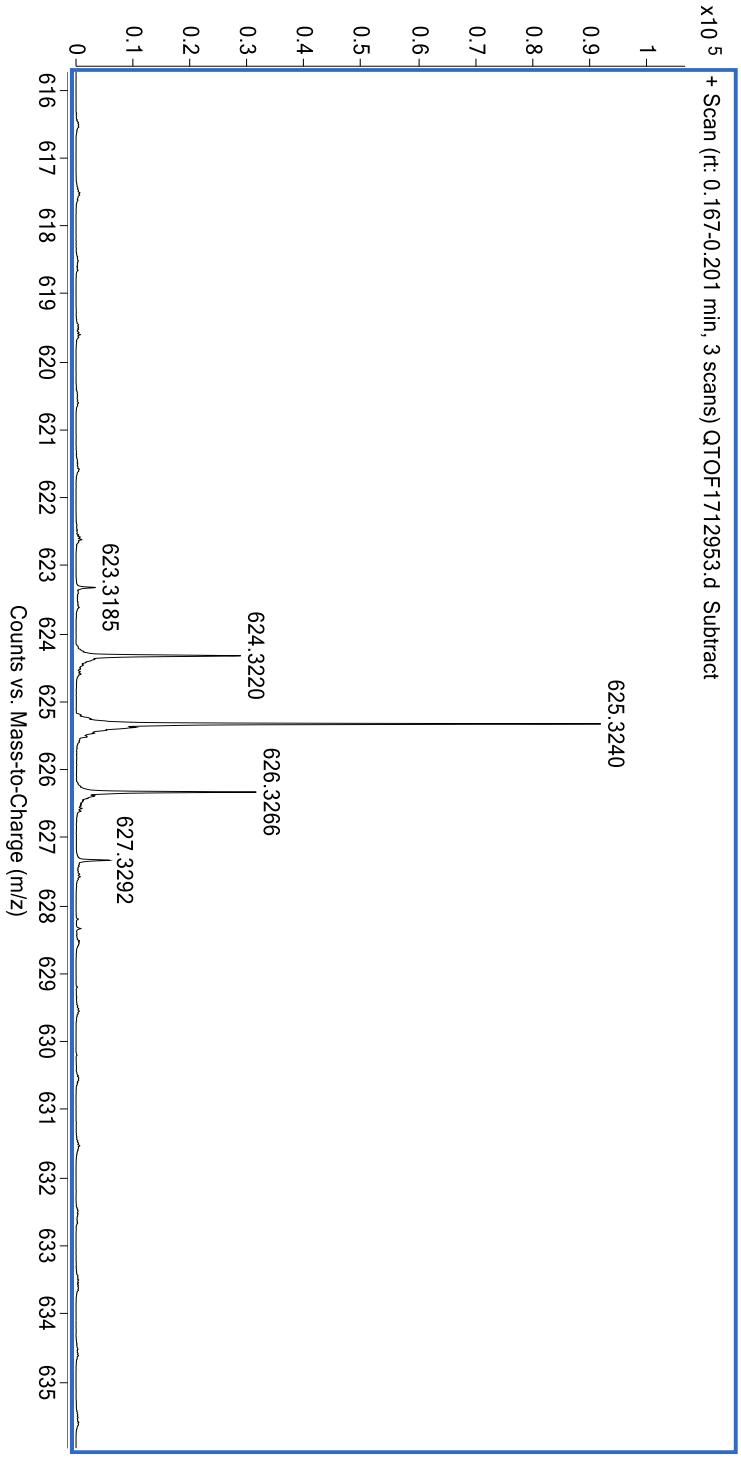

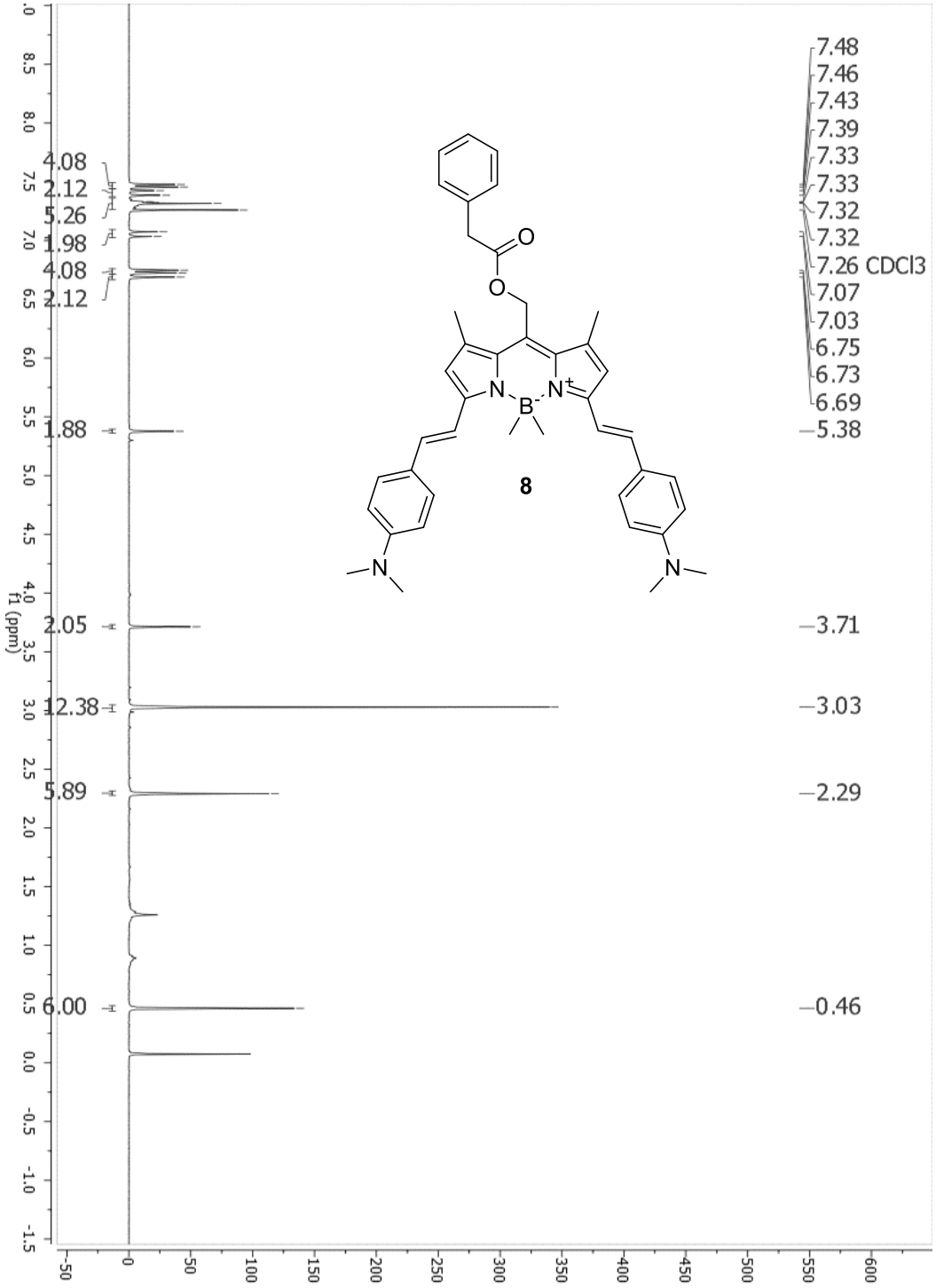

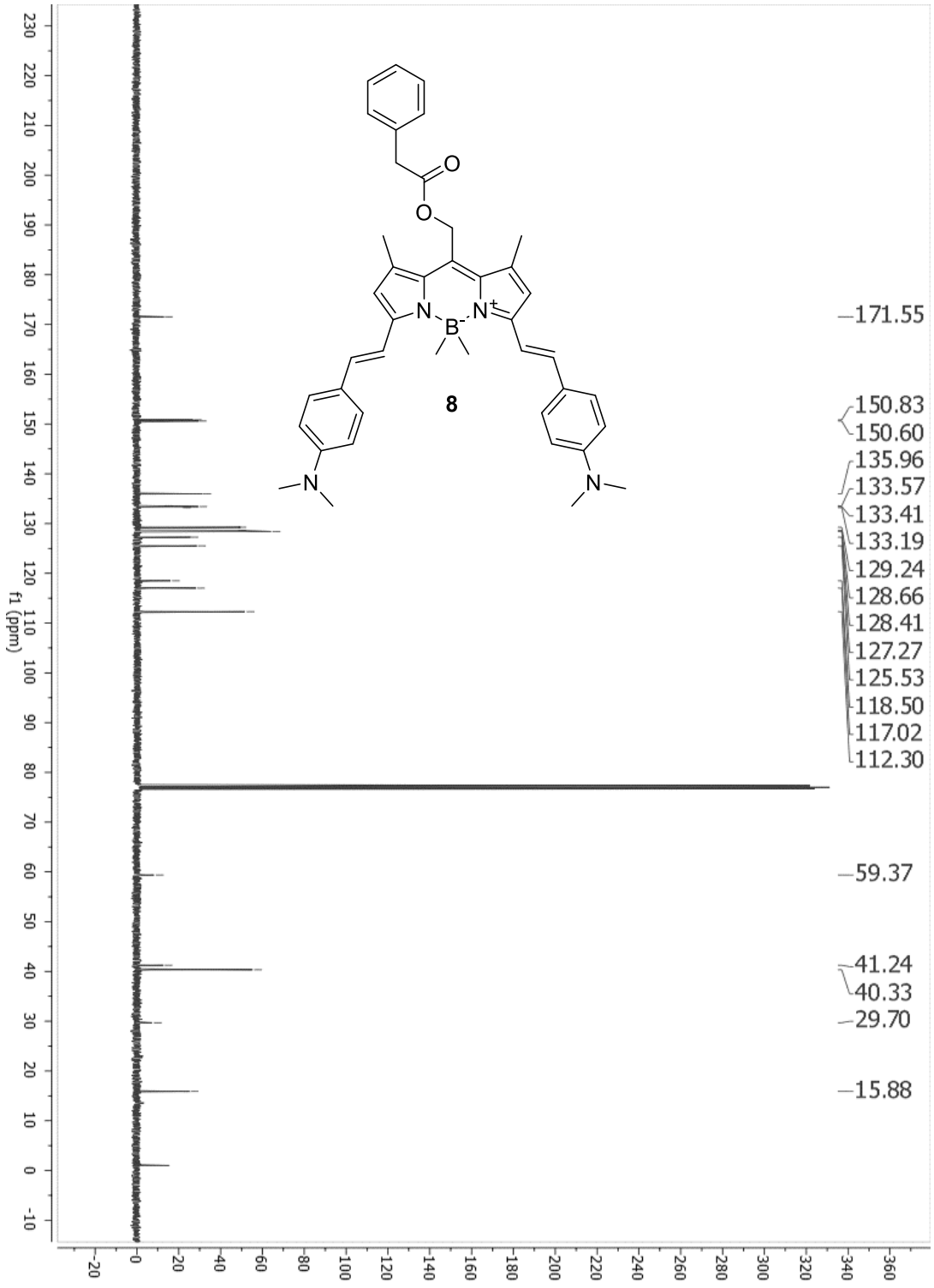

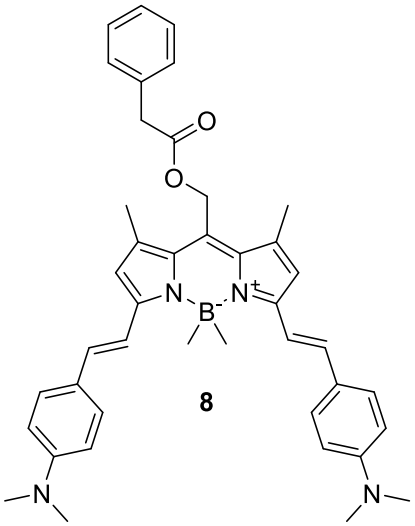

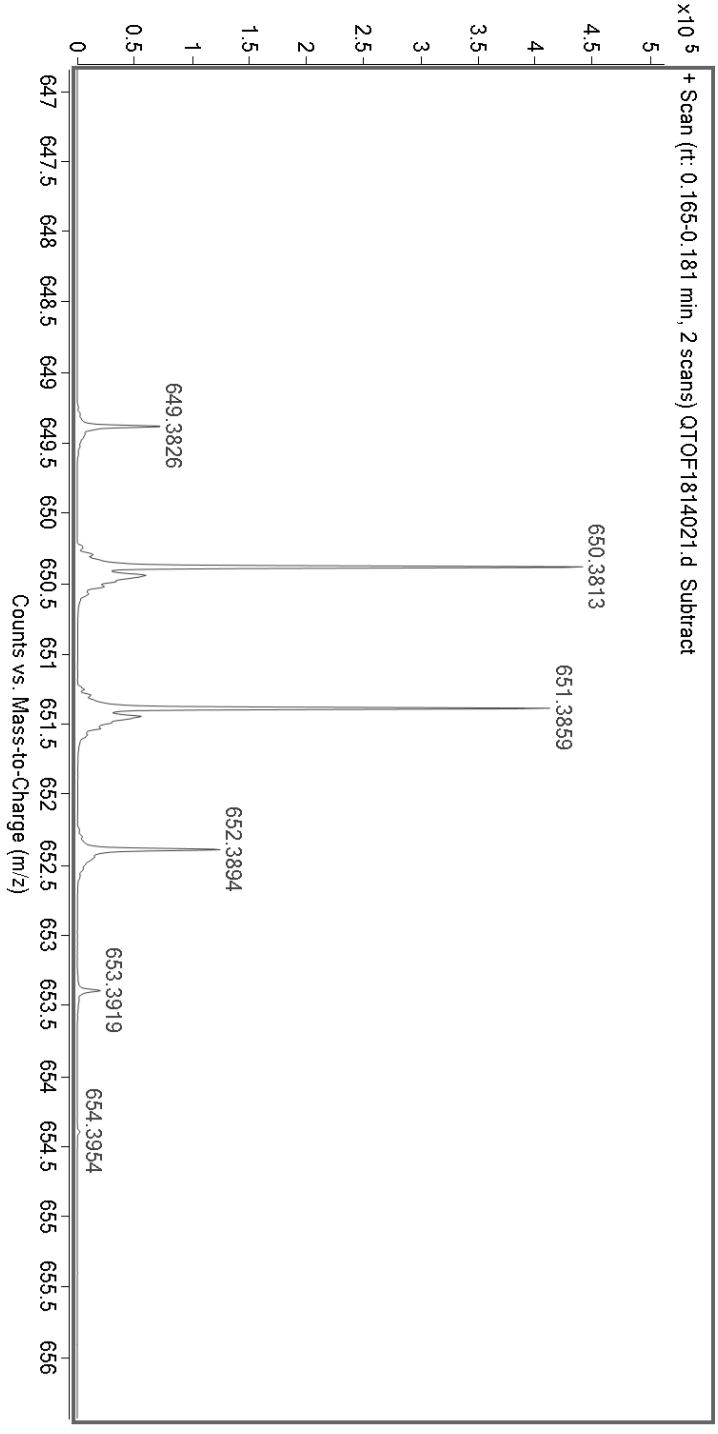

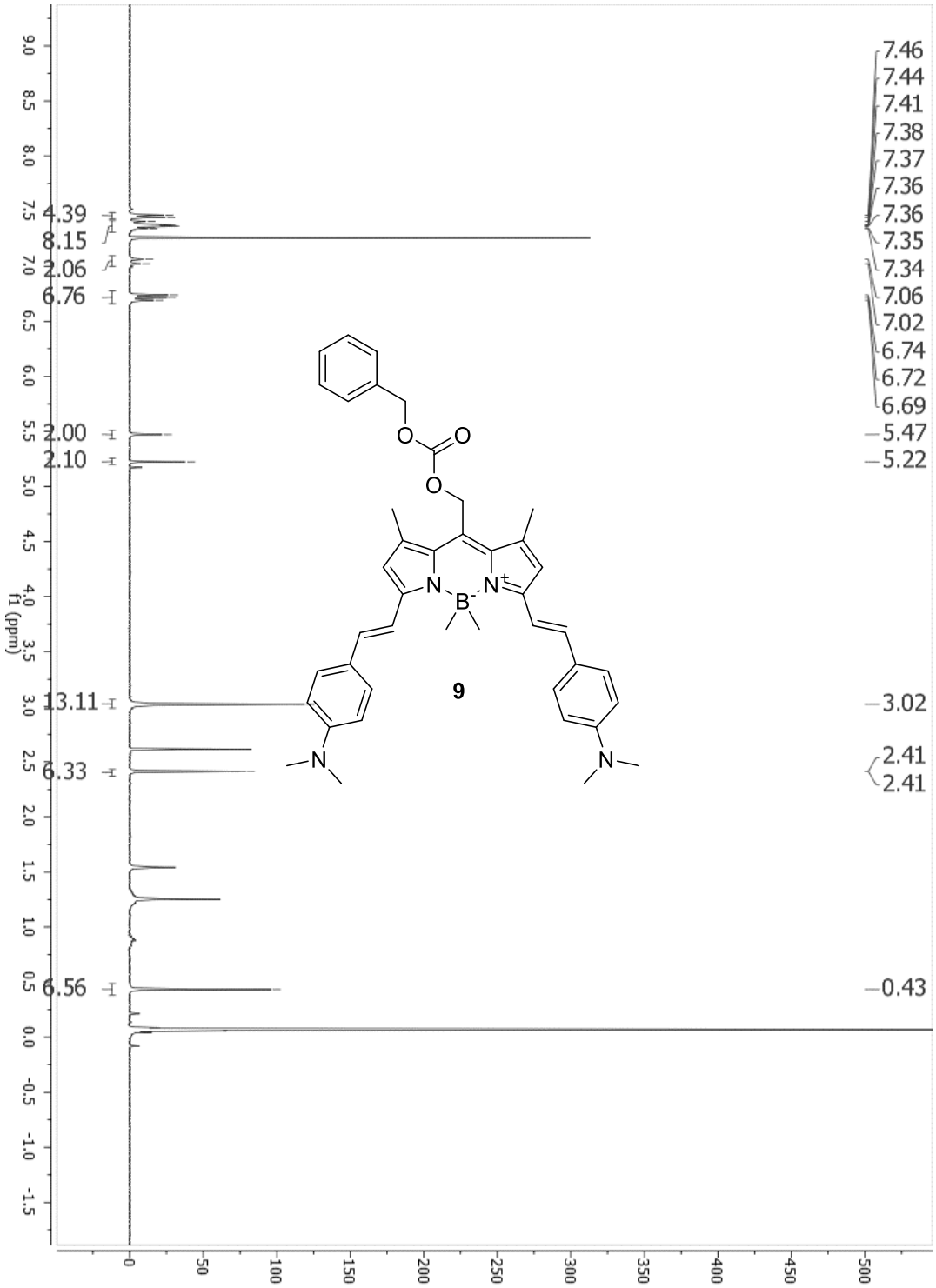

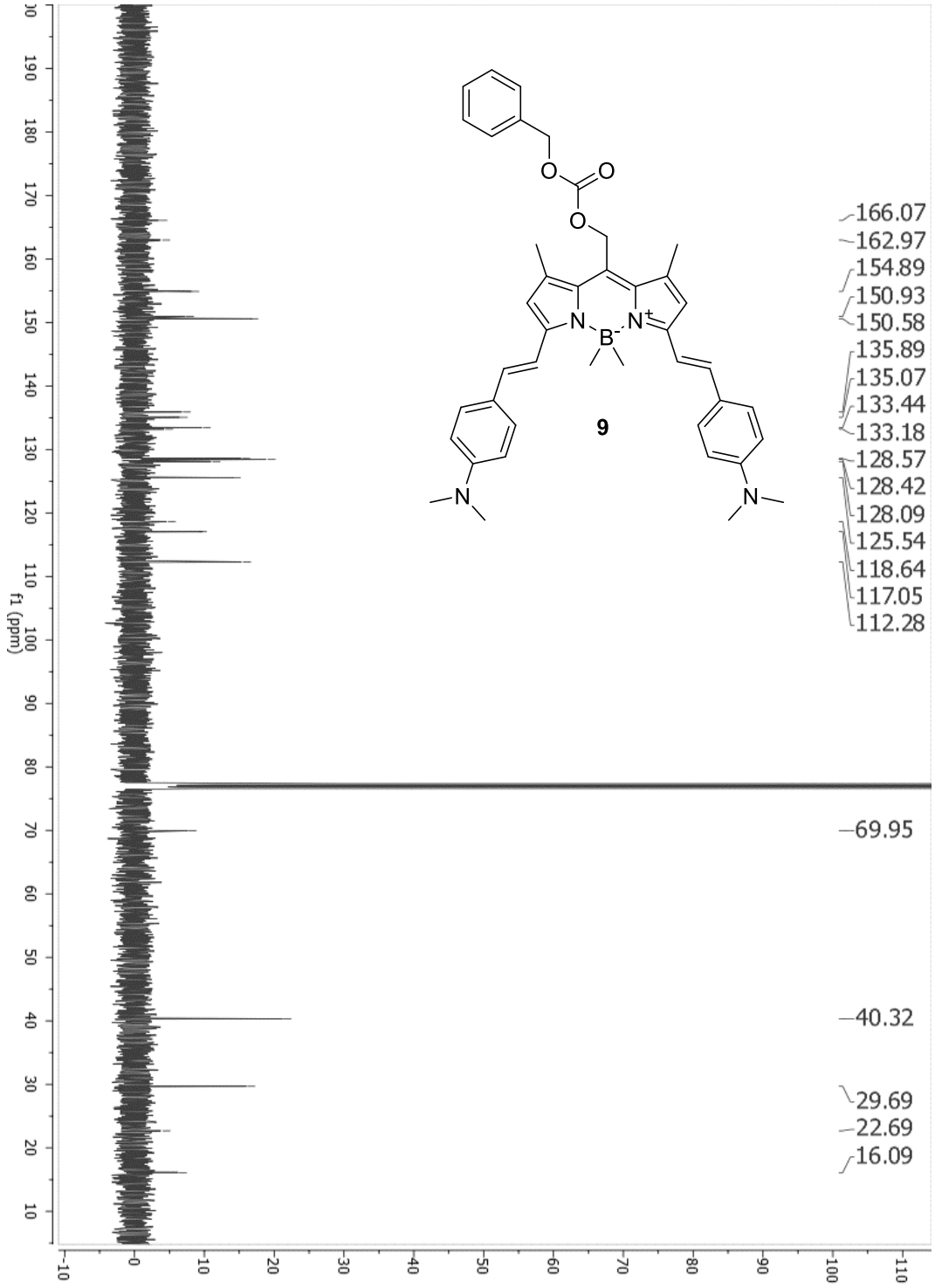

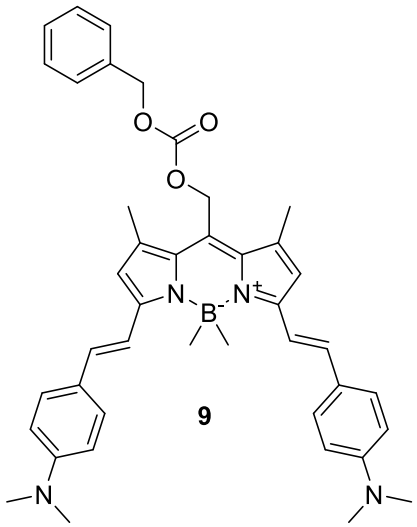

9

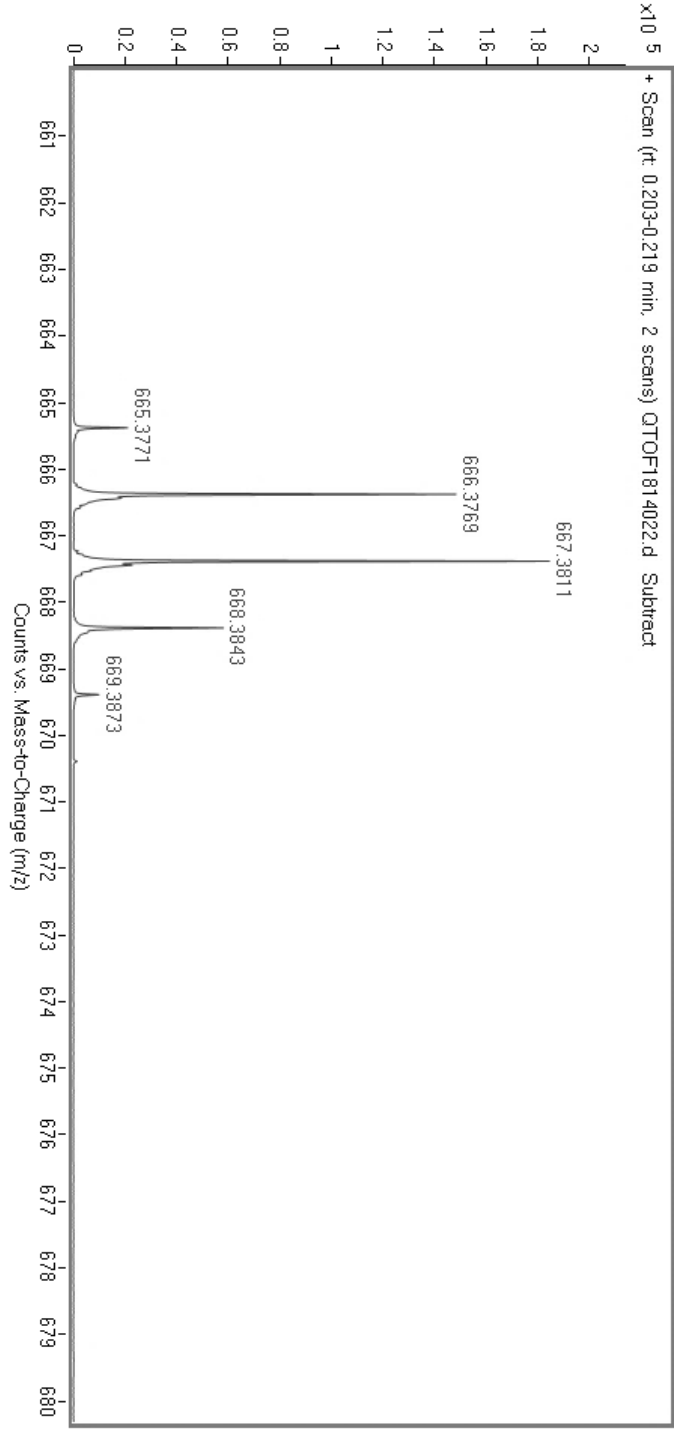

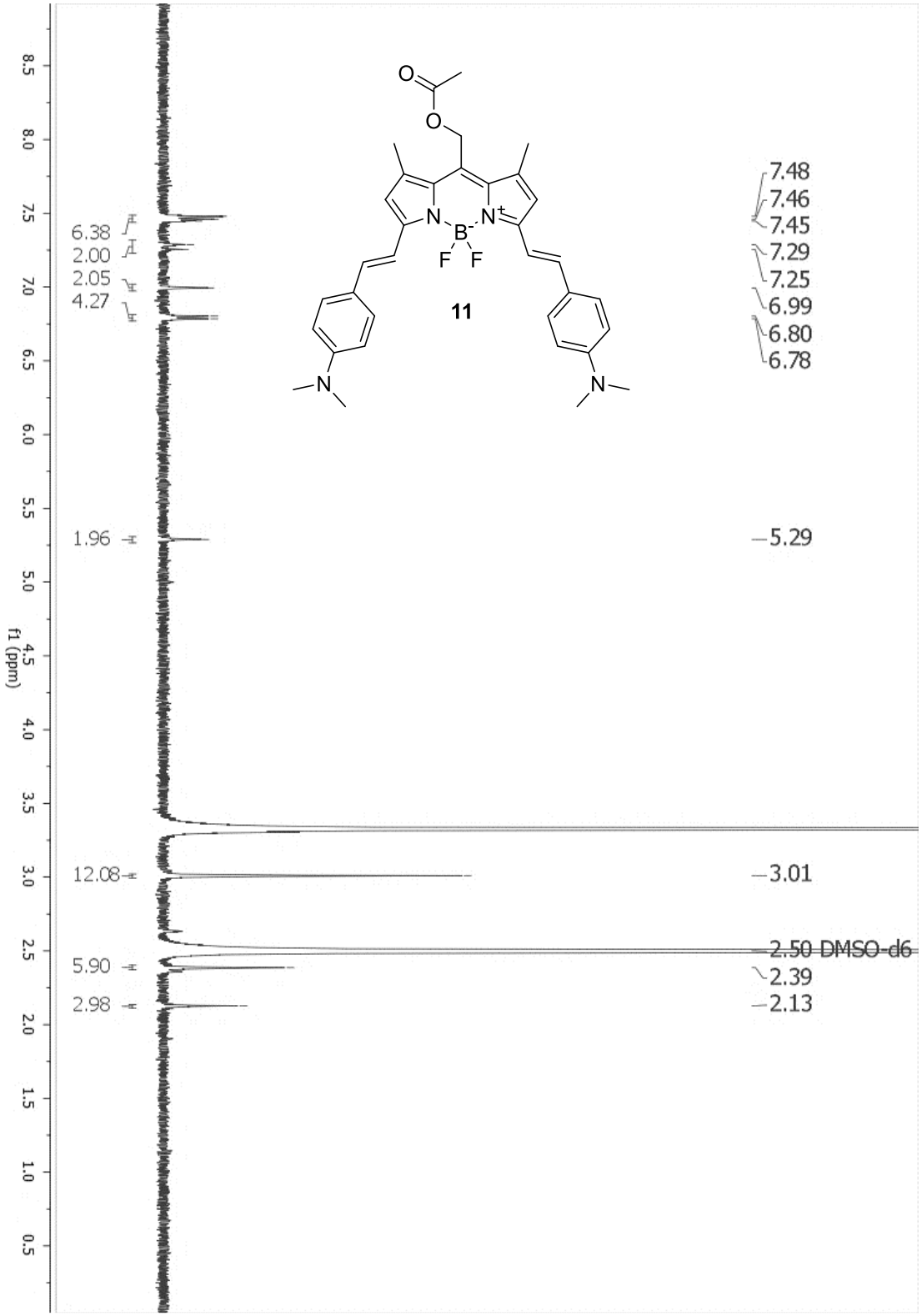

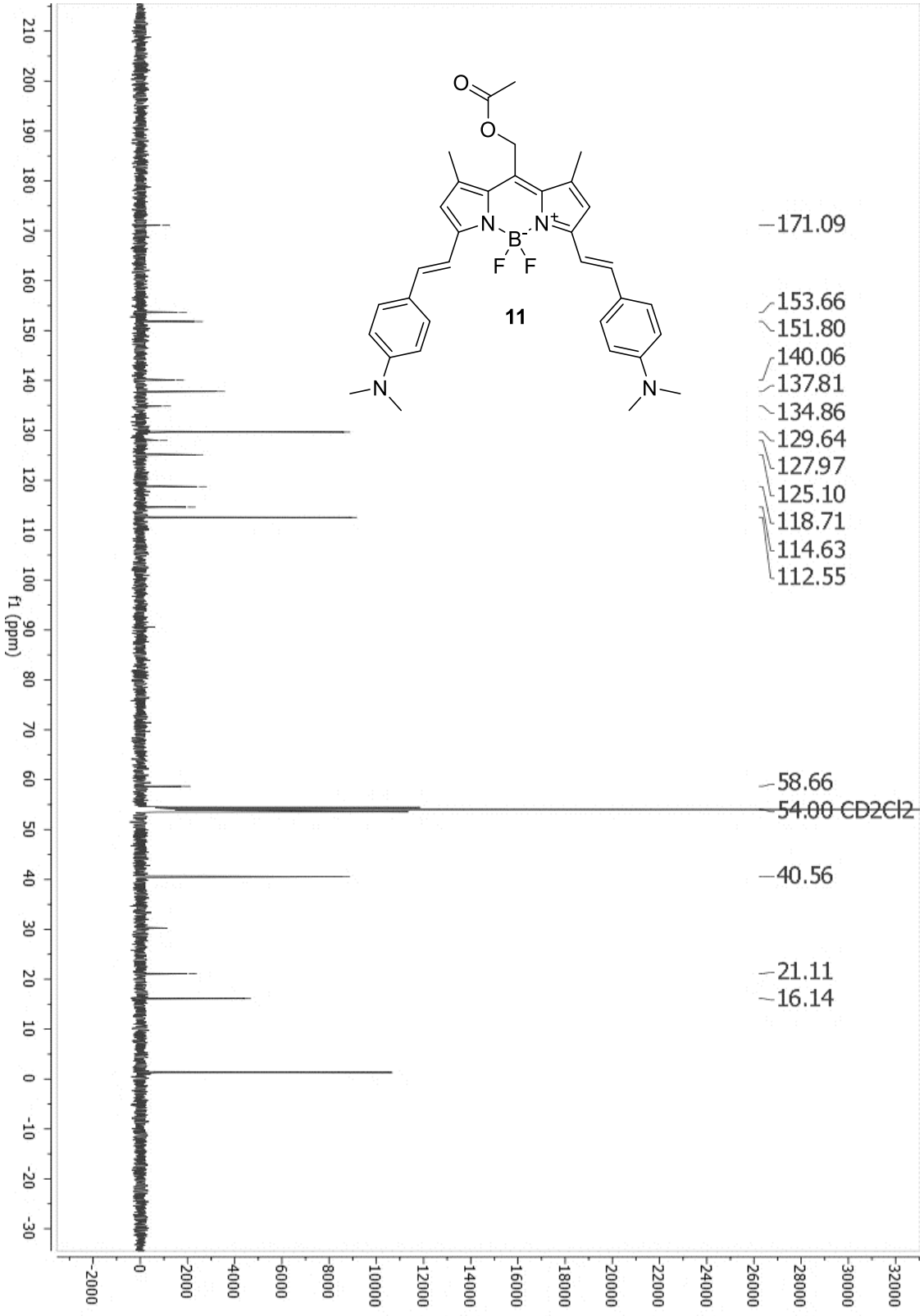

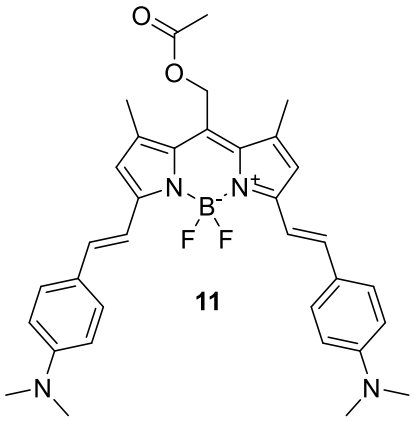

11

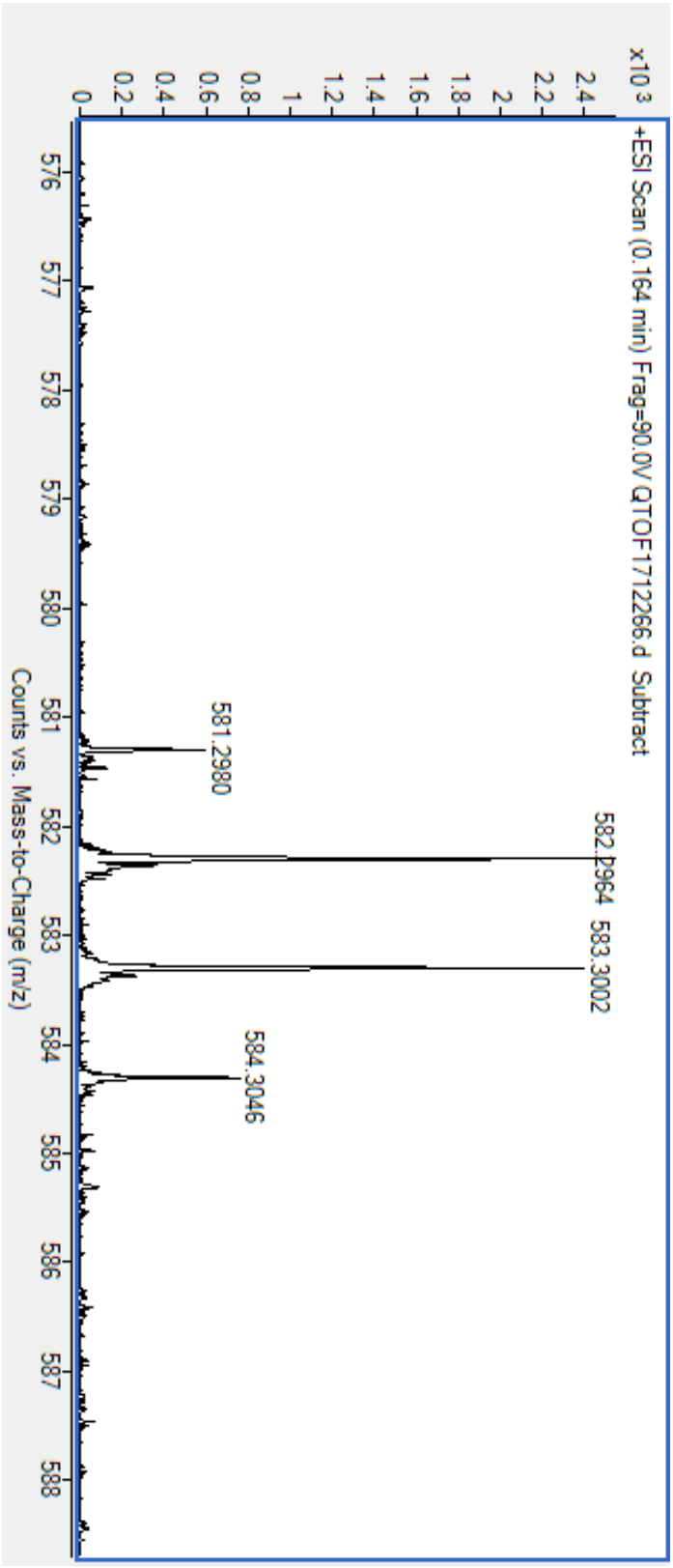

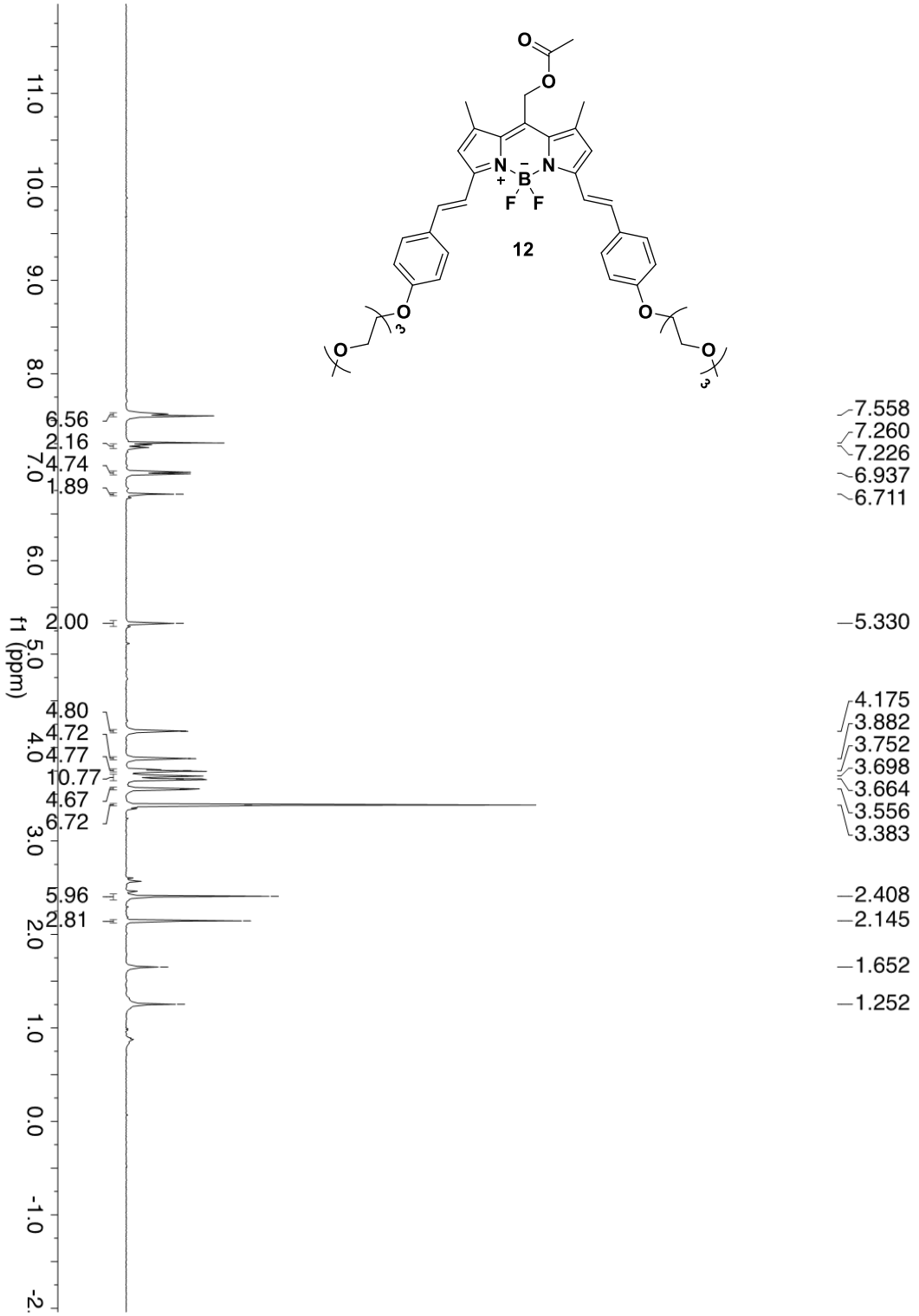

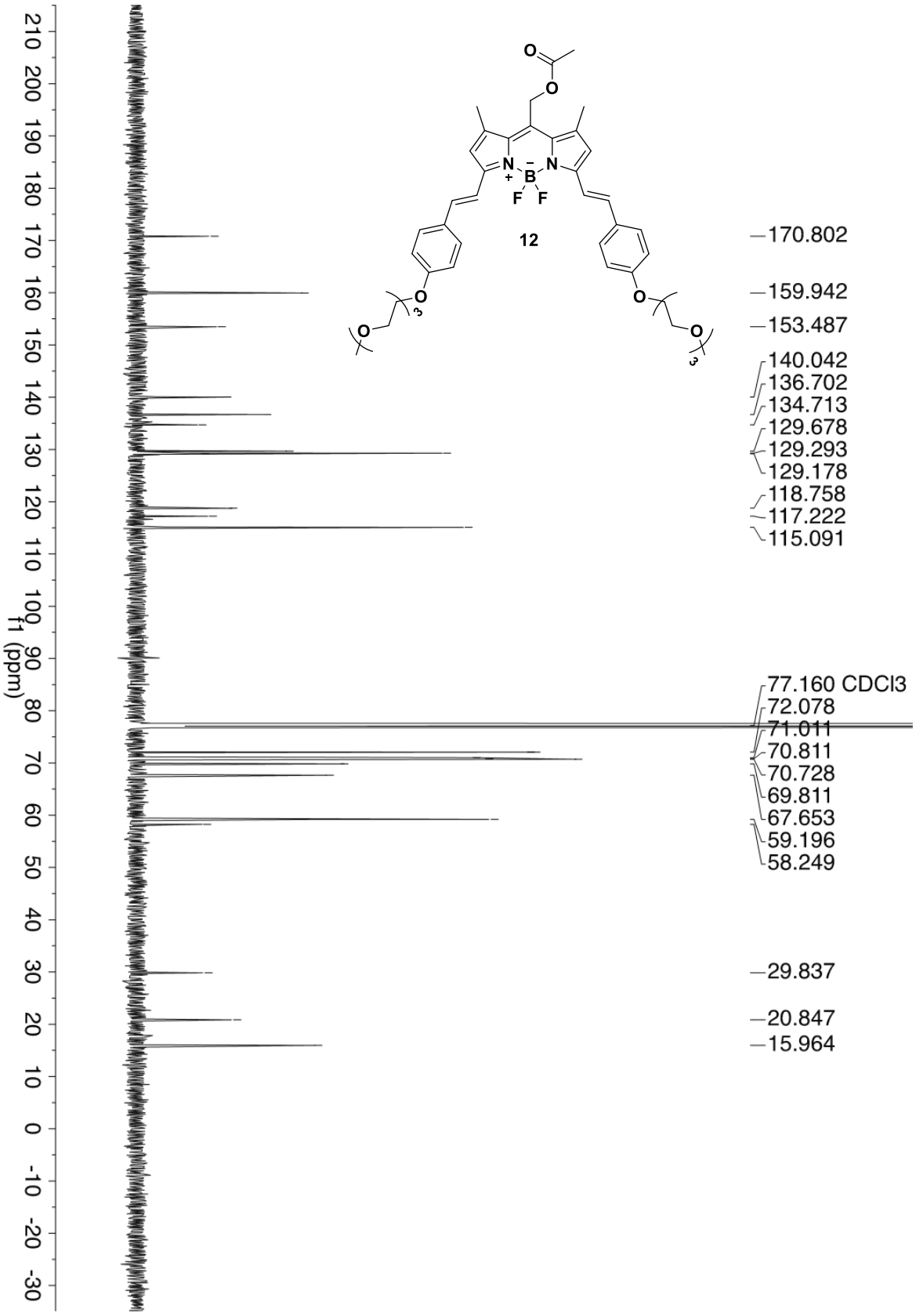

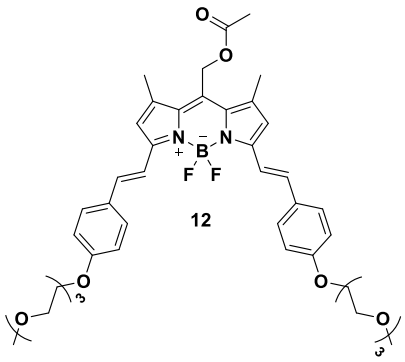

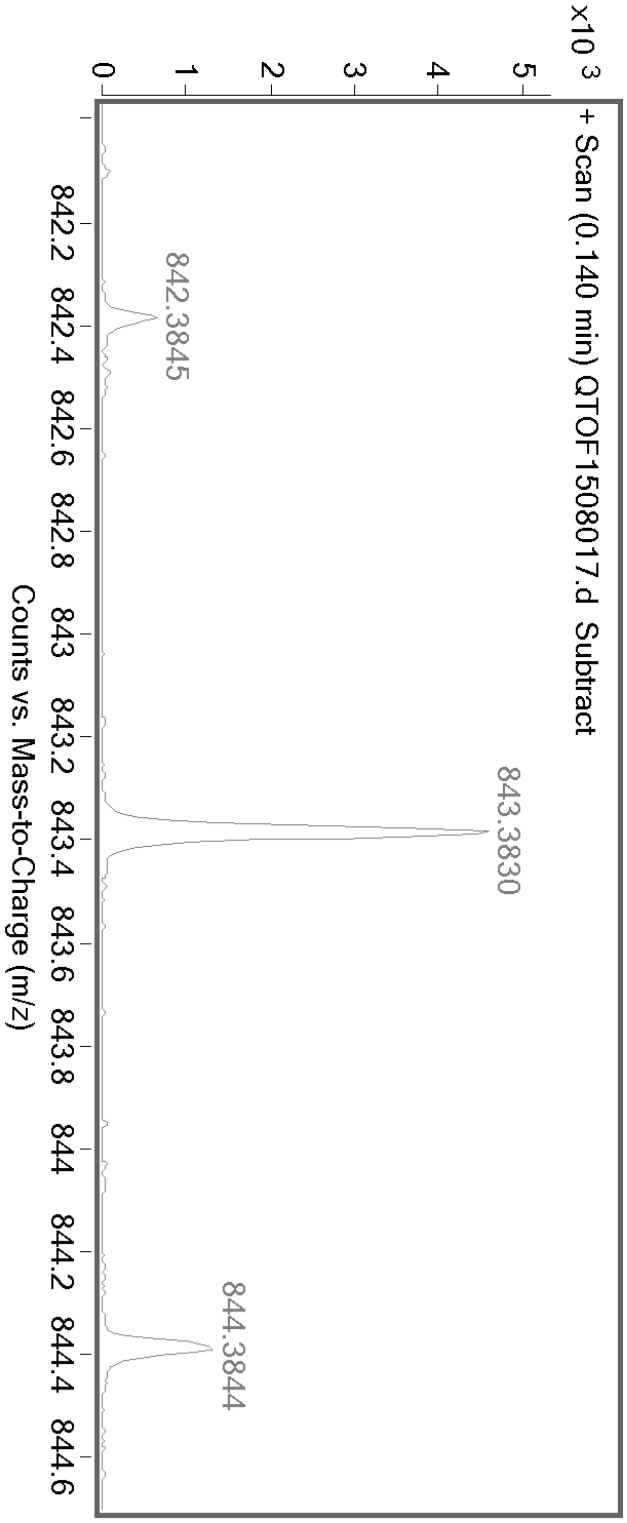

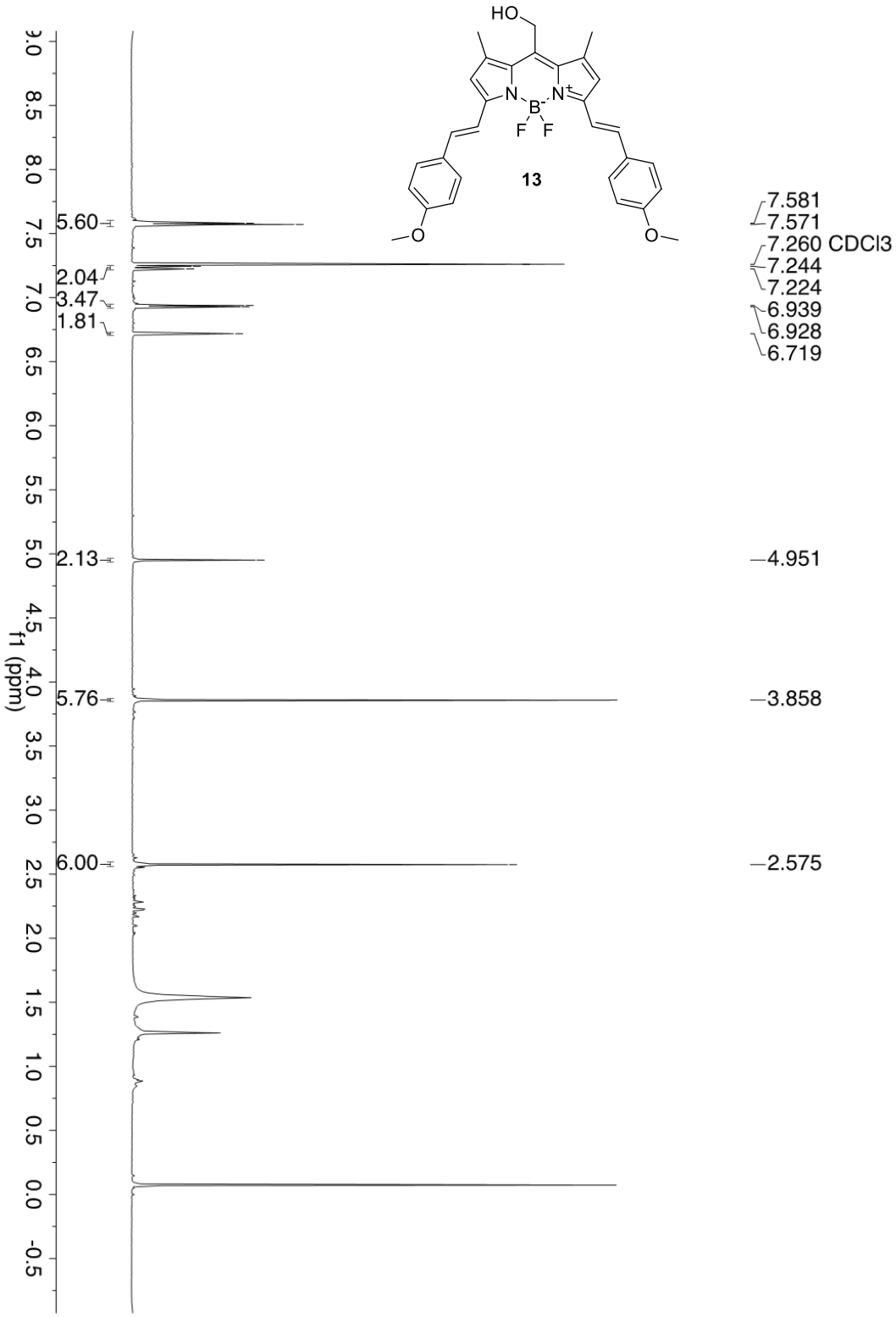

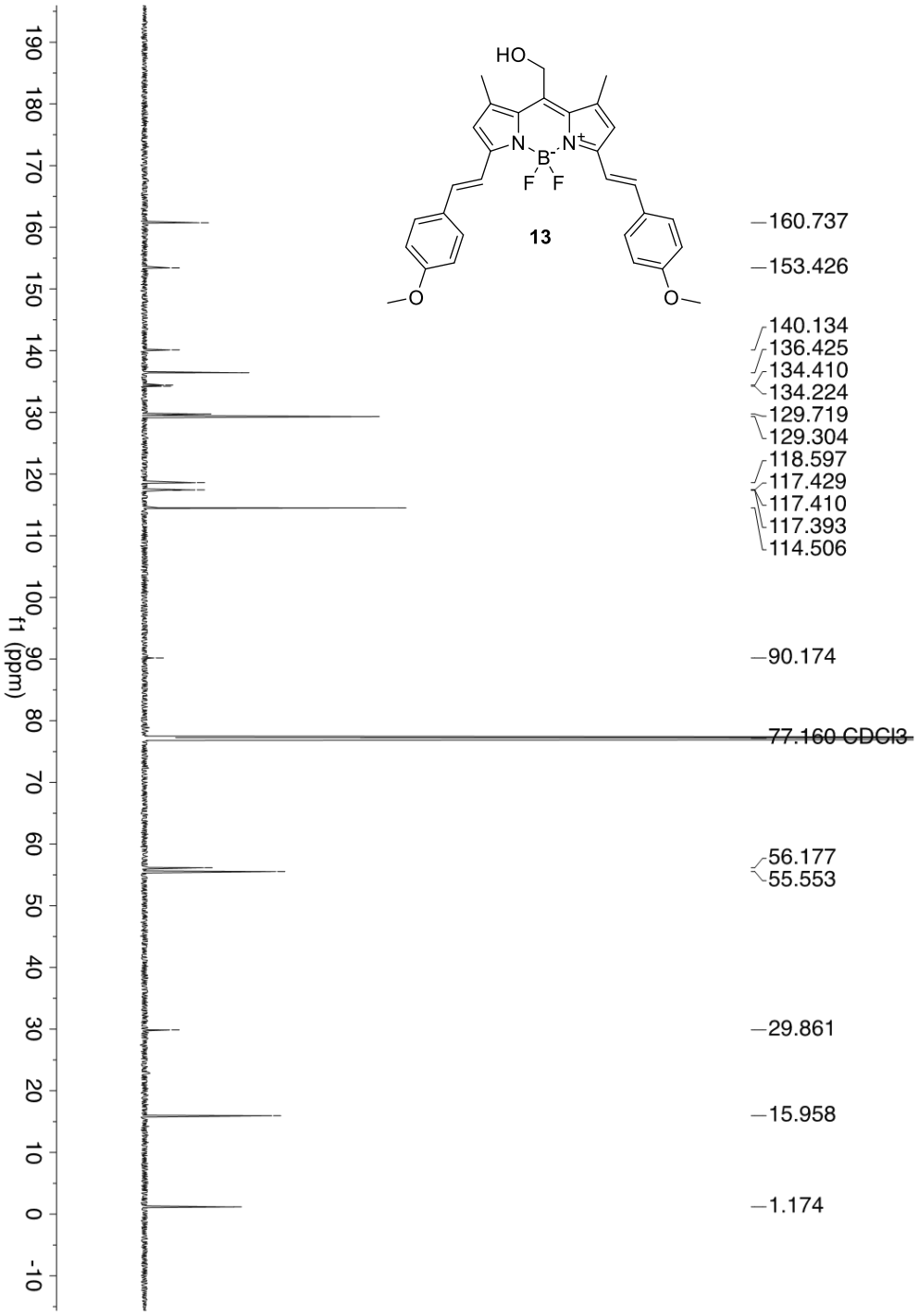

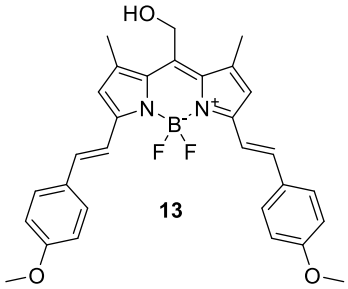

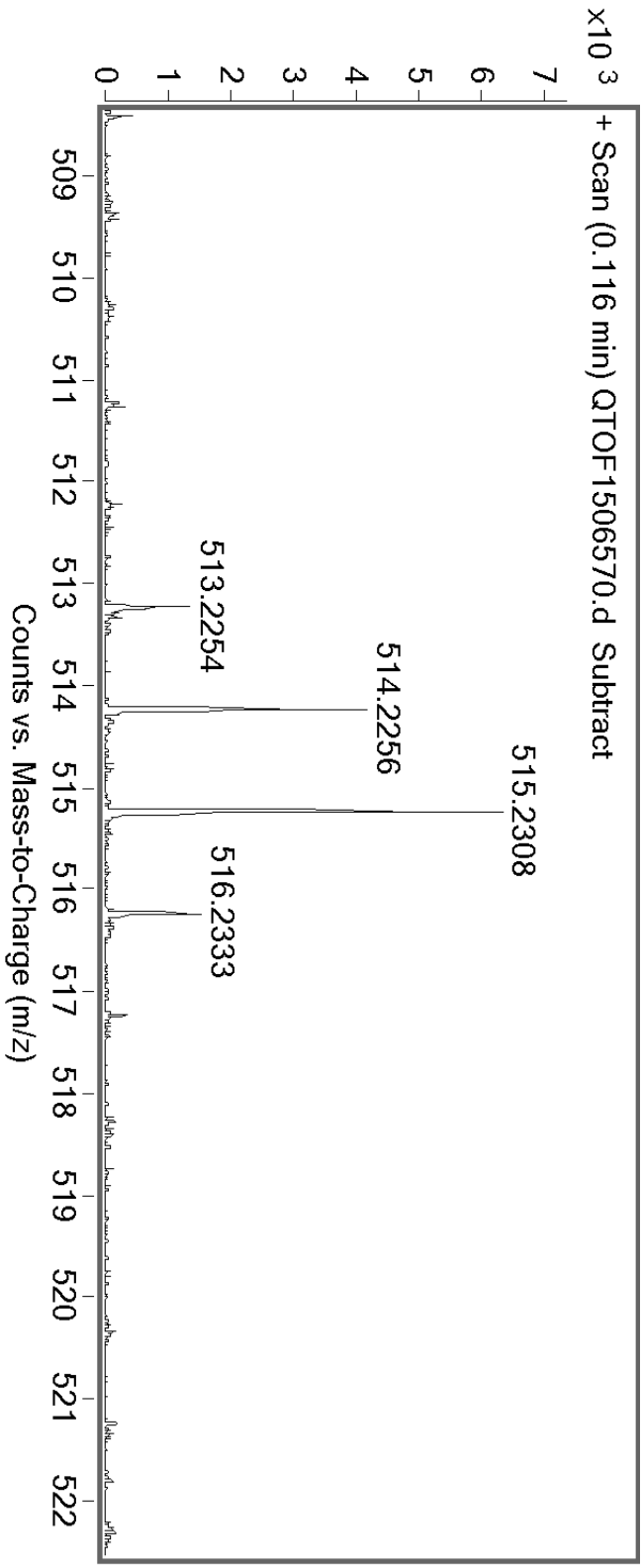

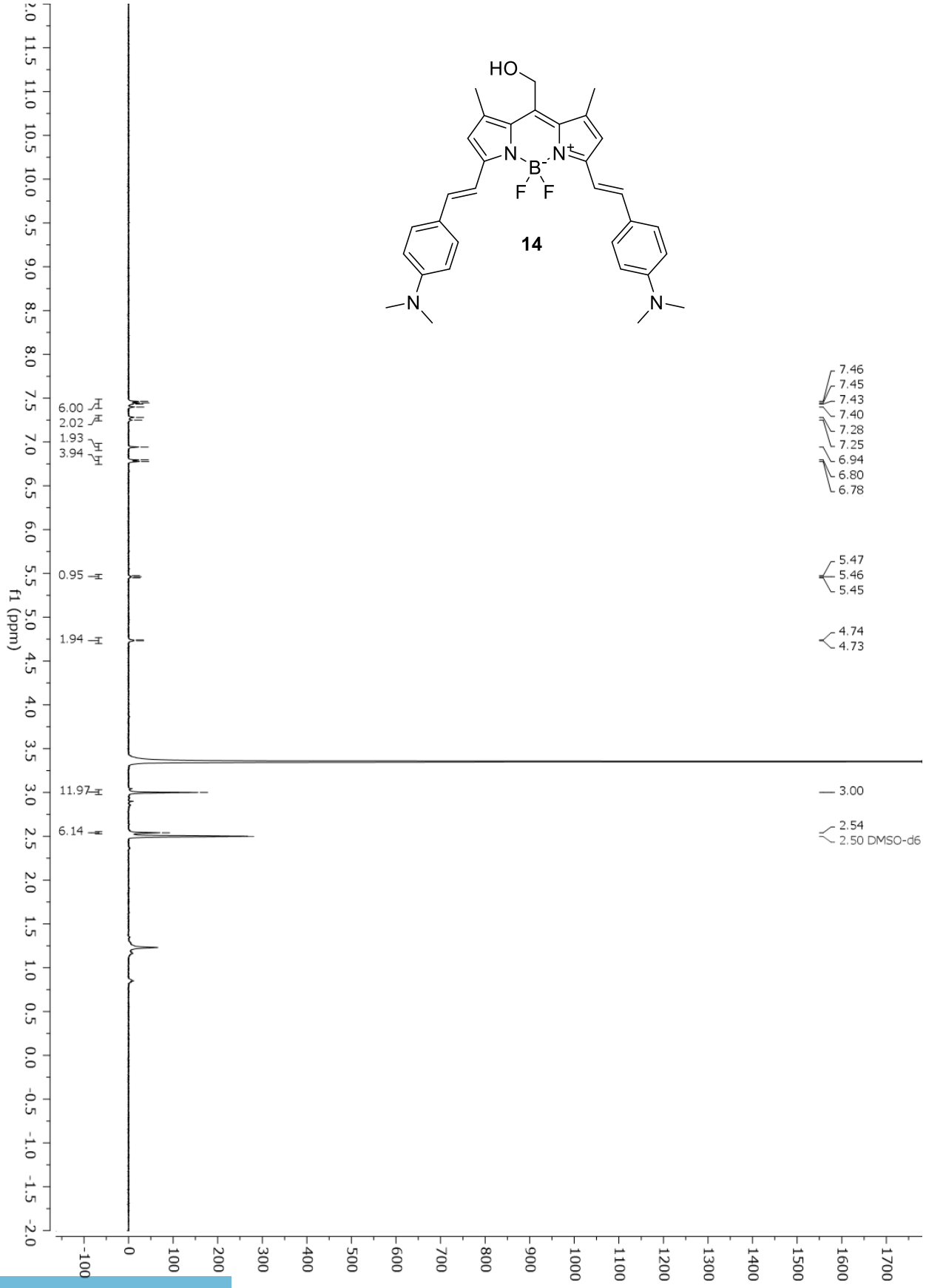

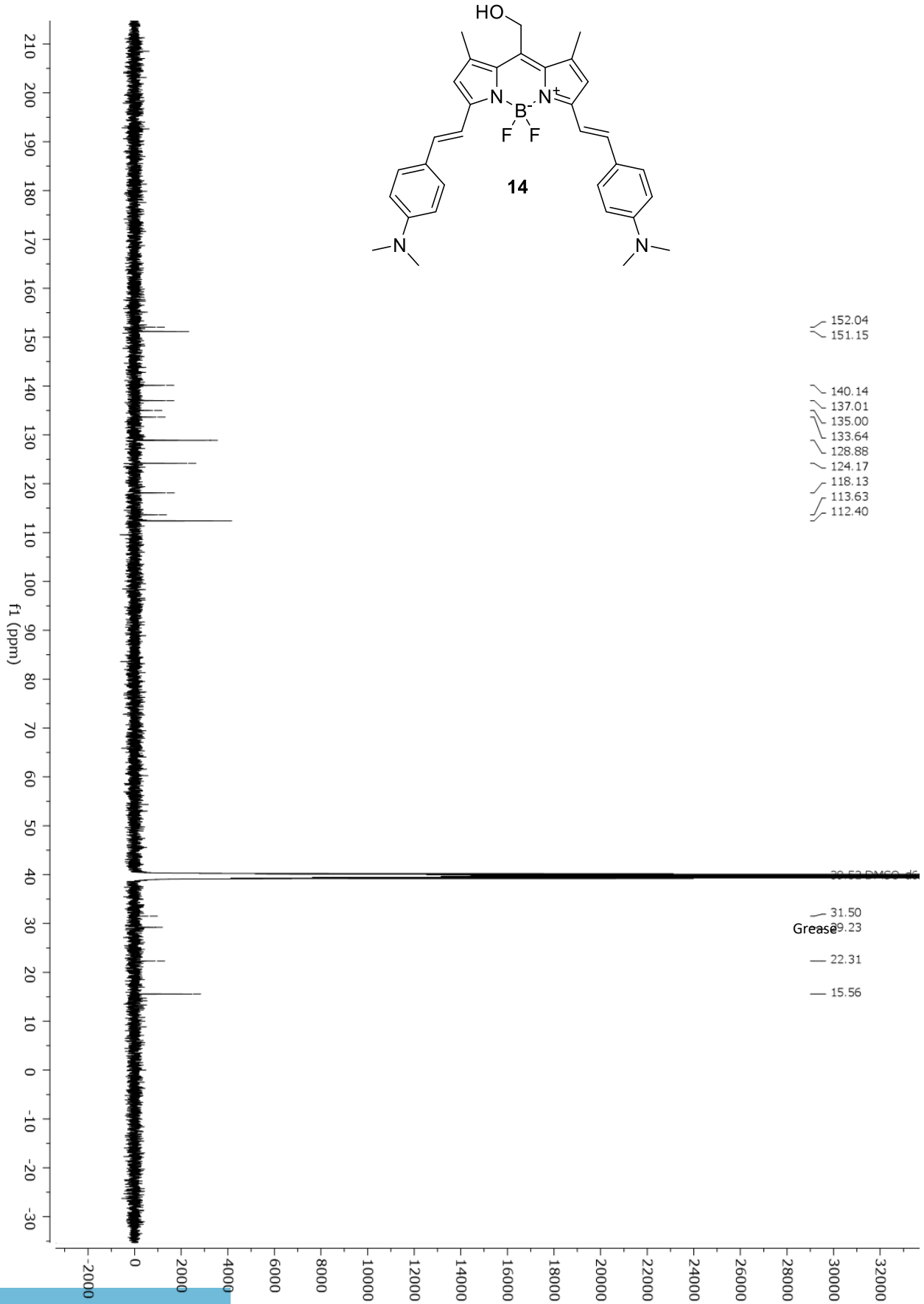

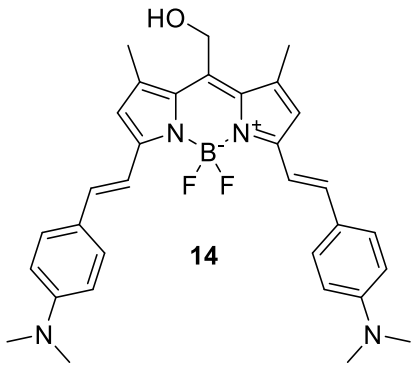

14

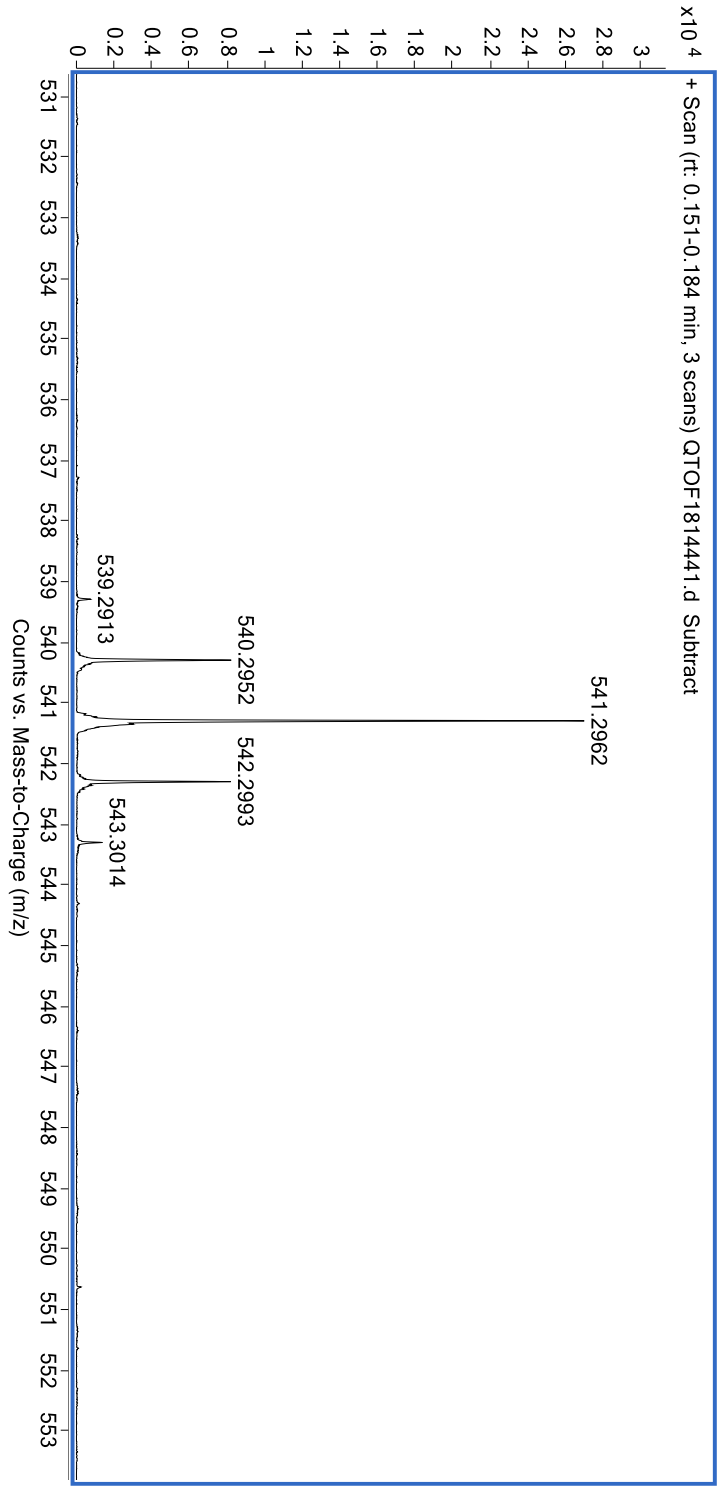

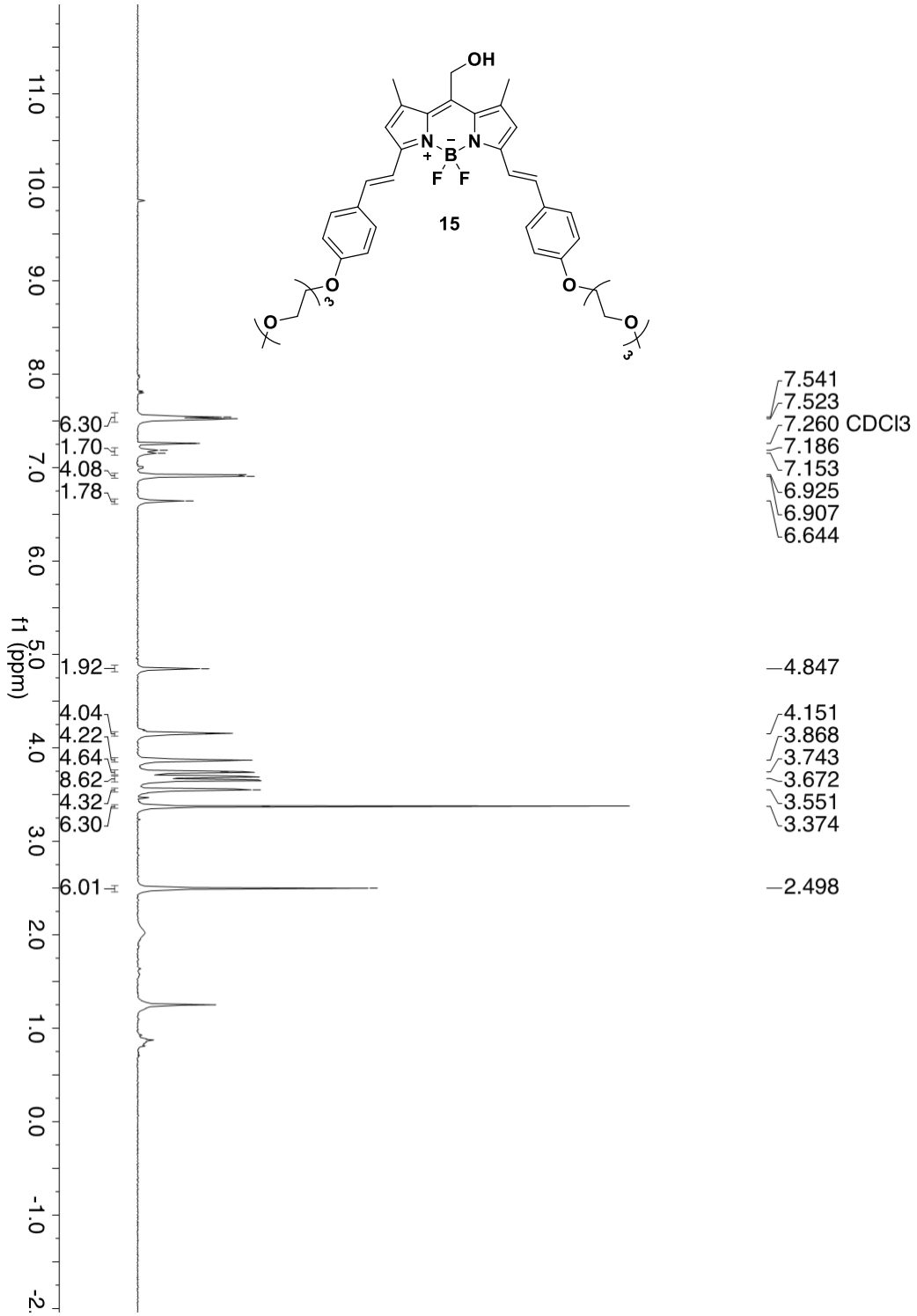

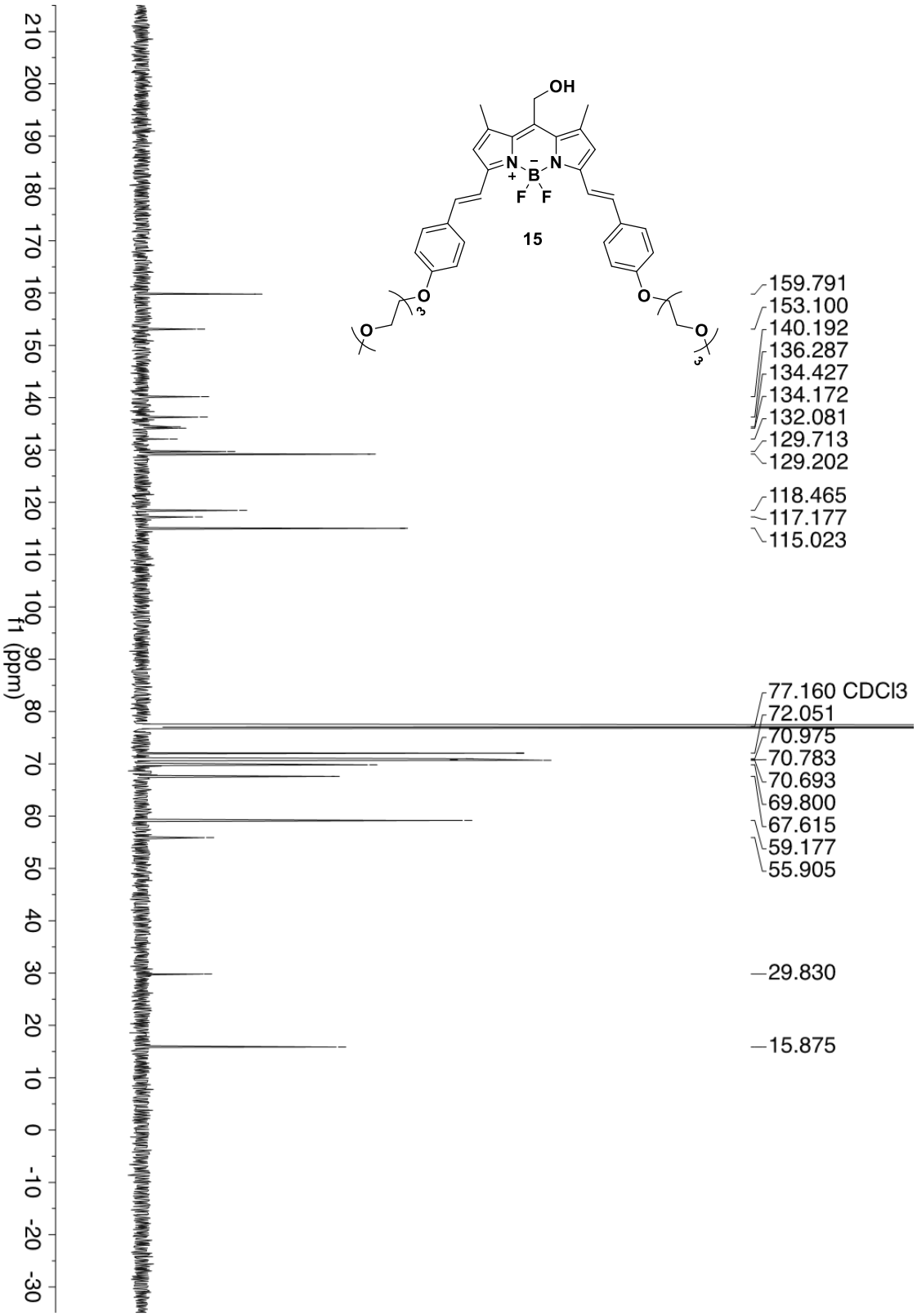

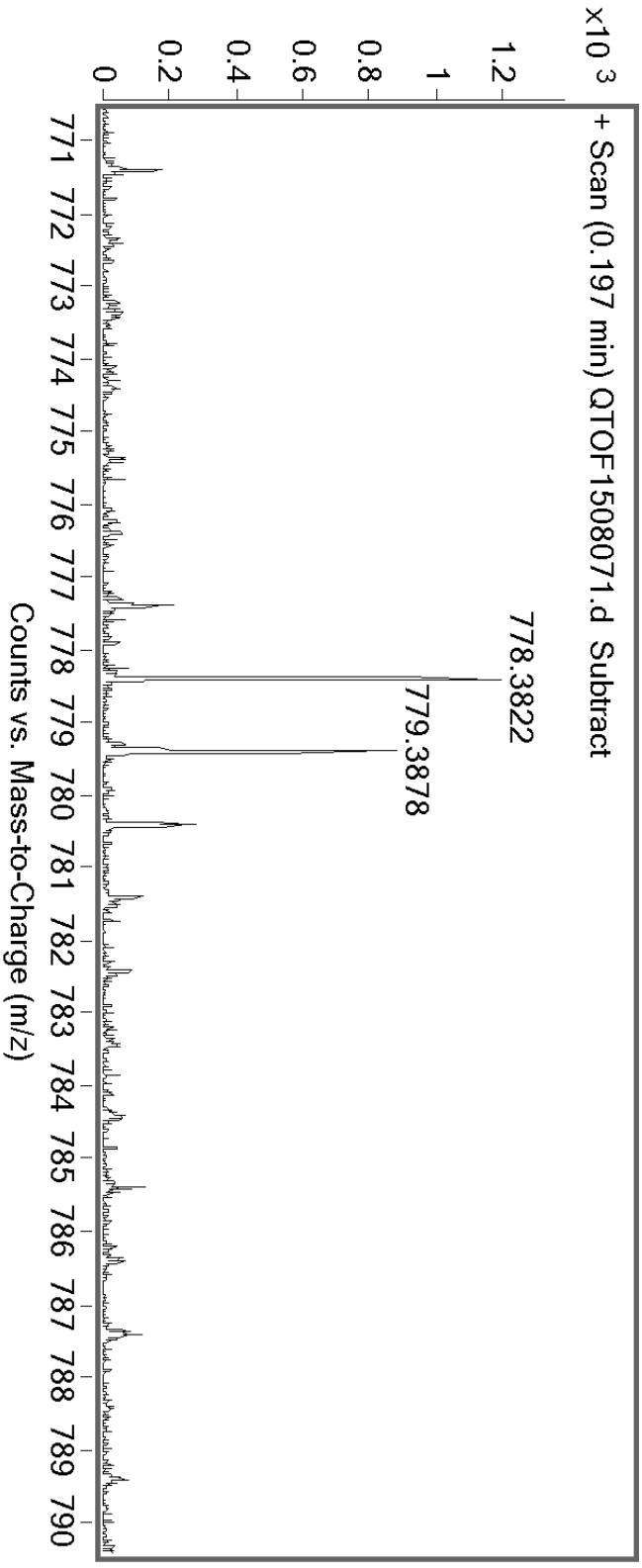

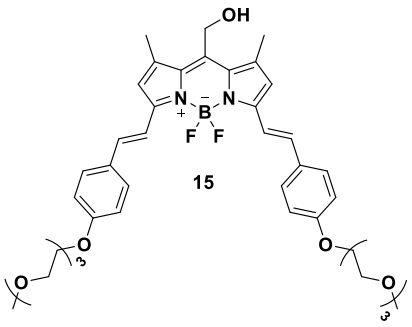

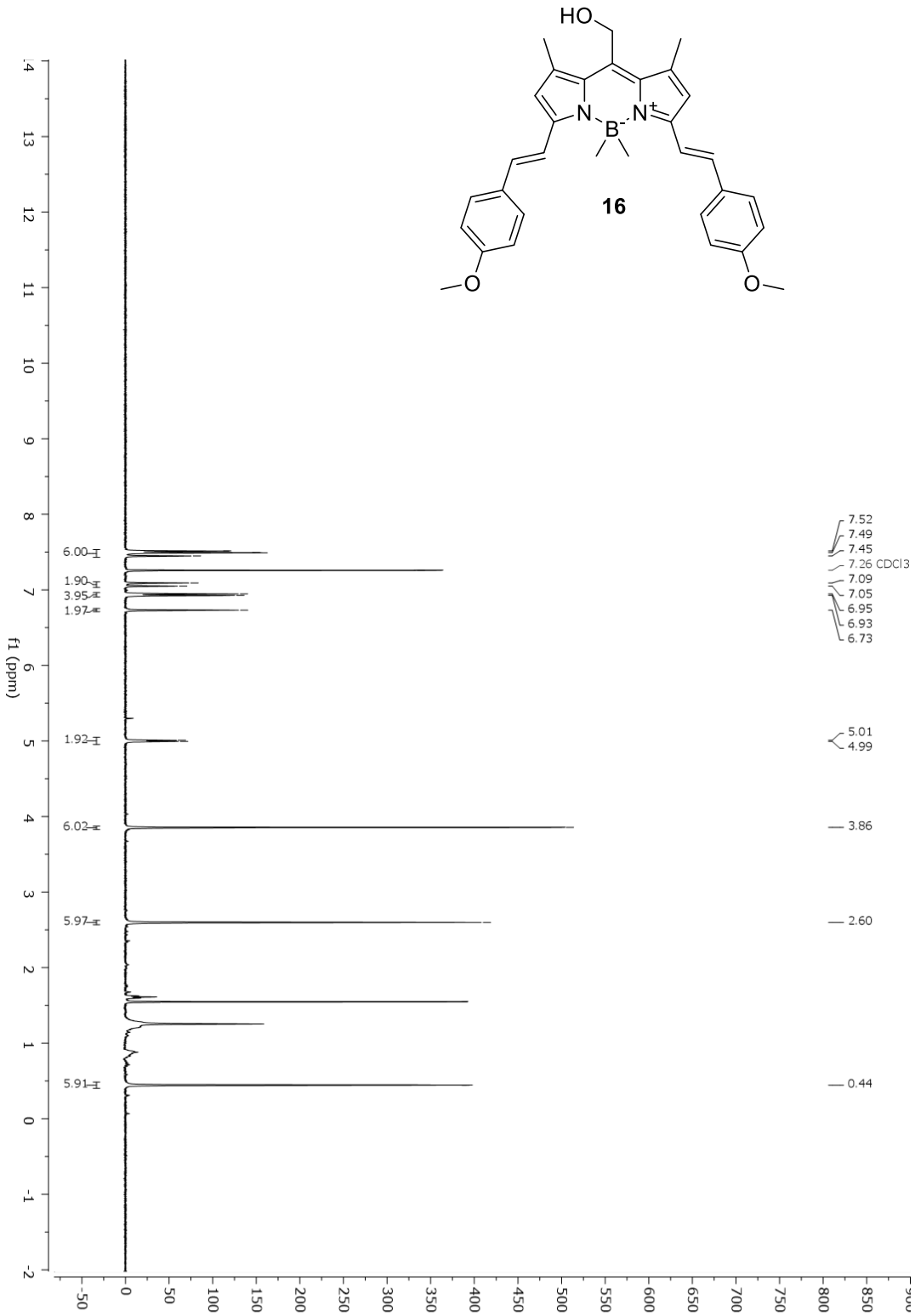

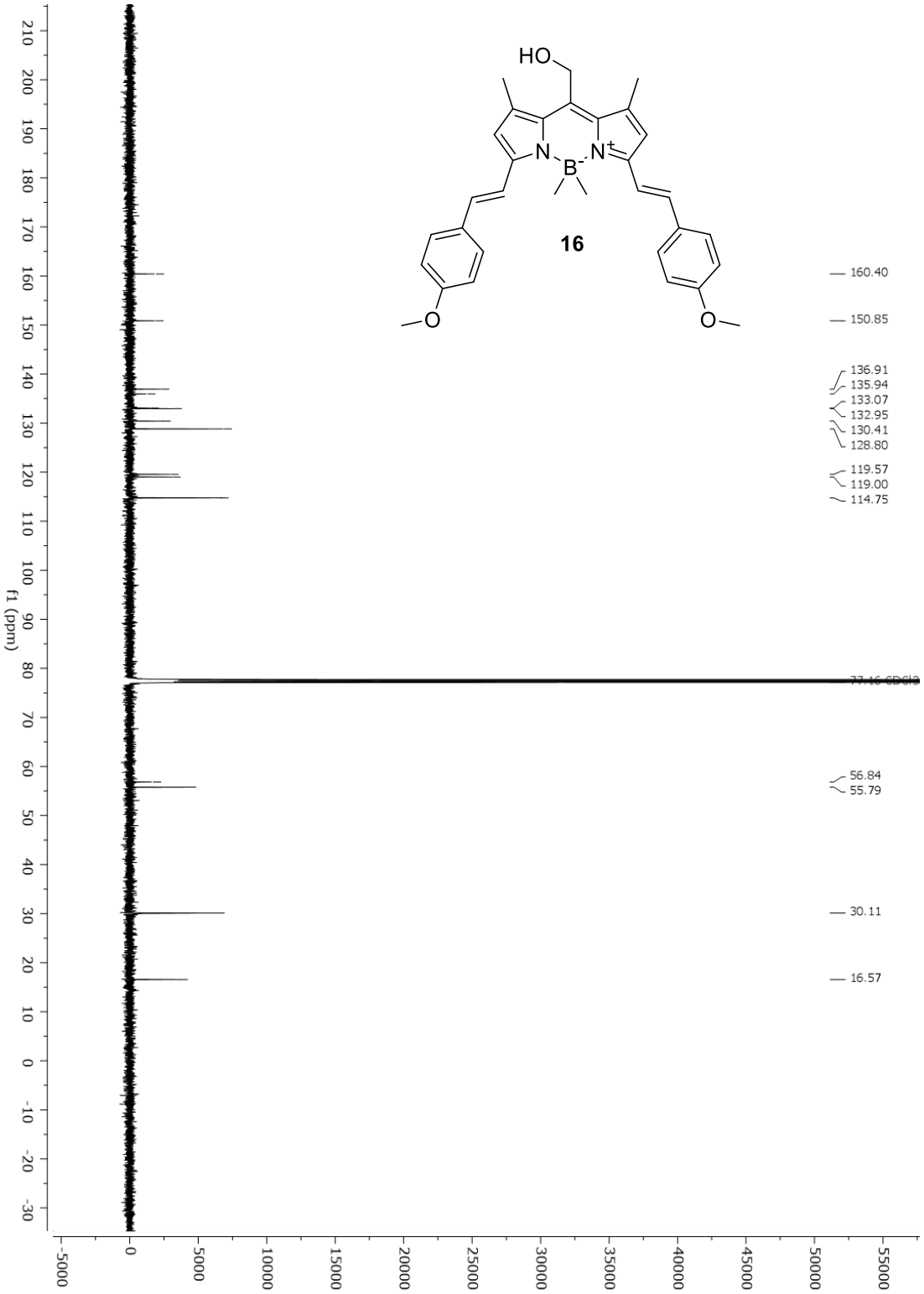

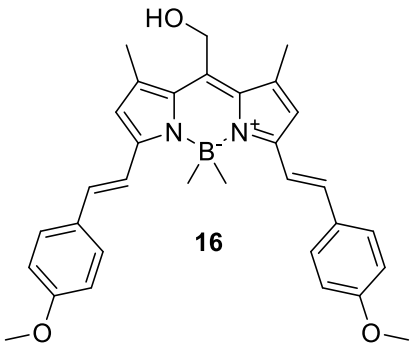

16

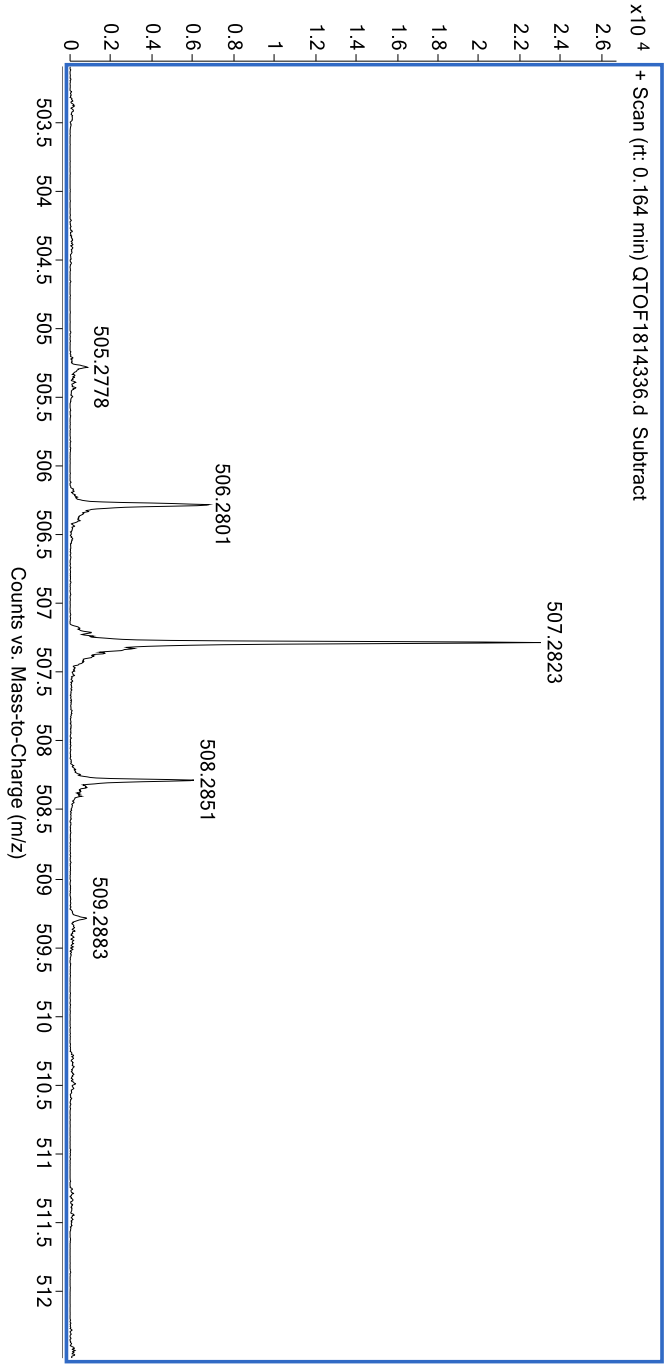

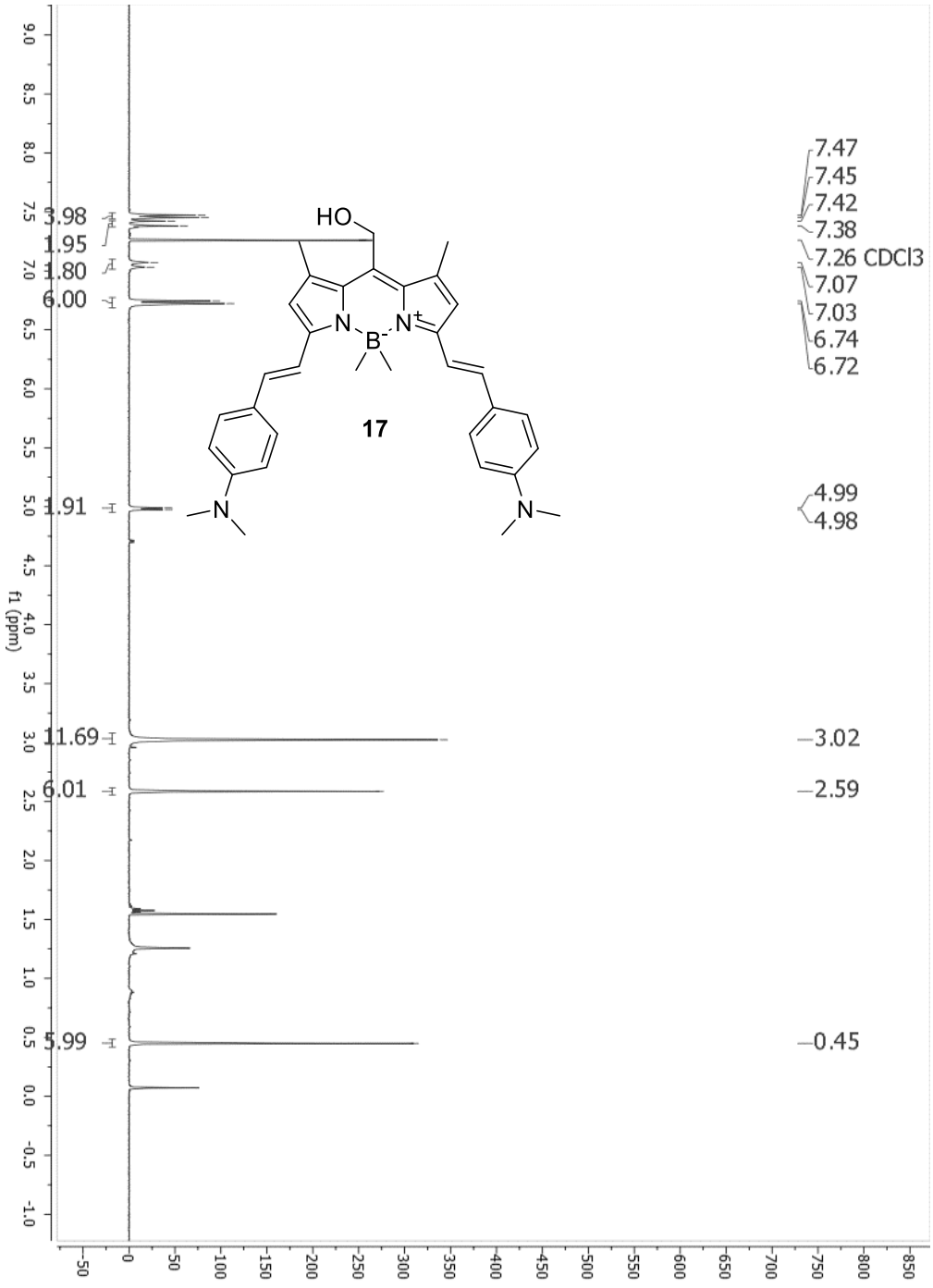

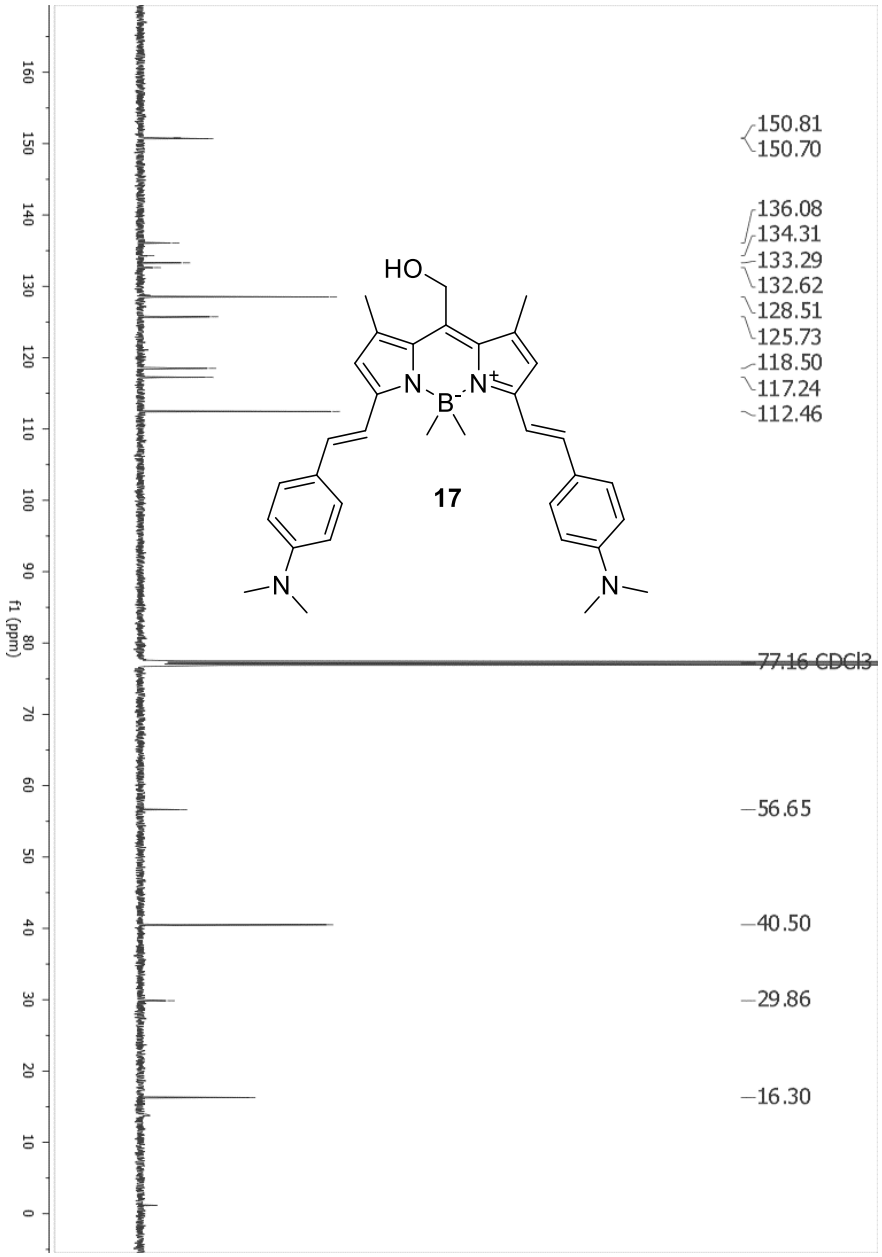

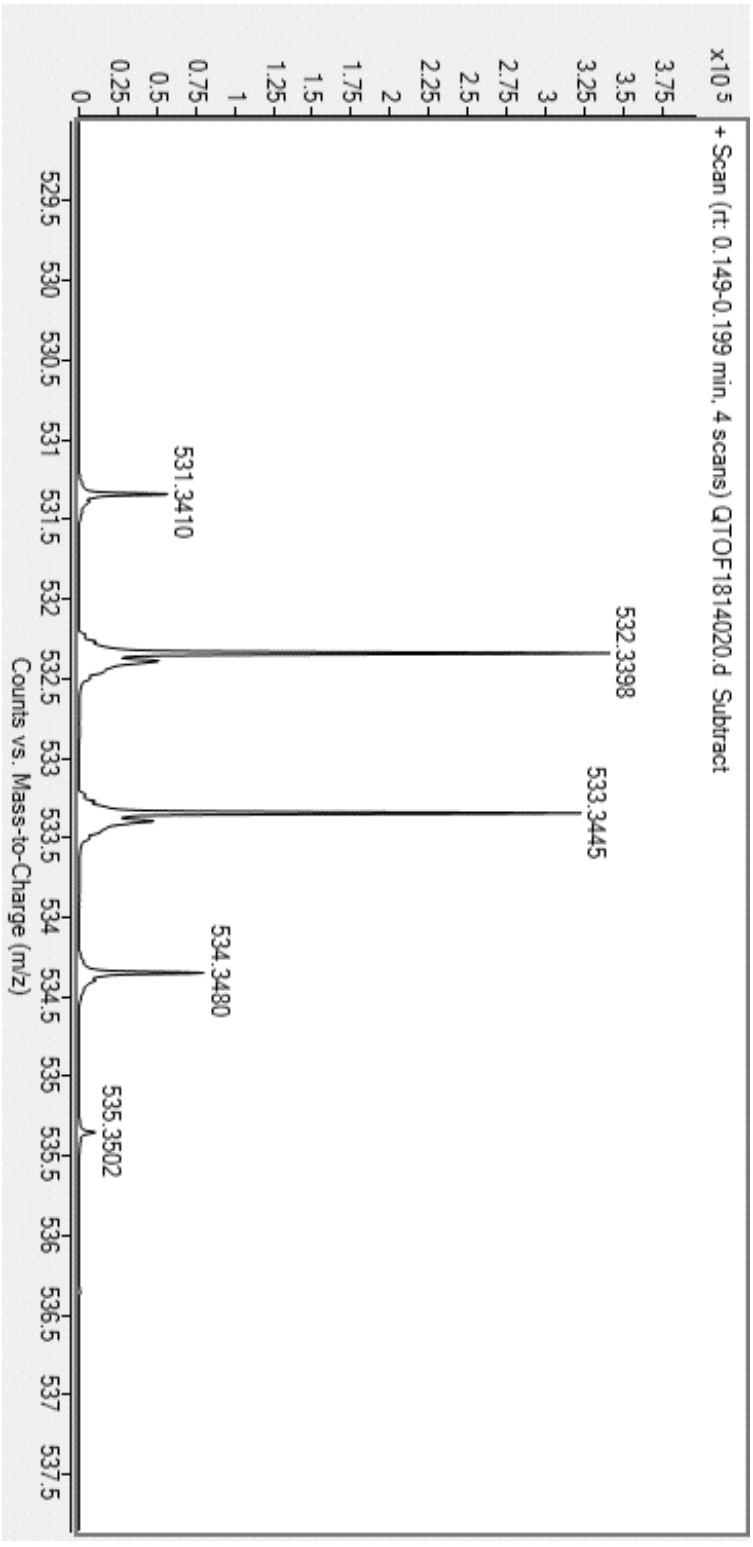

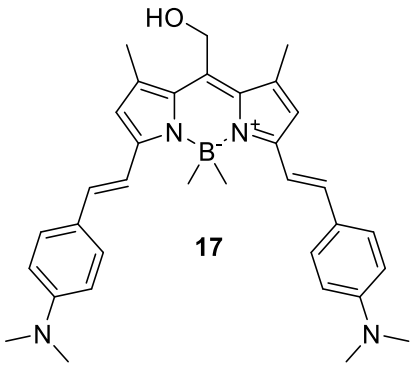

17

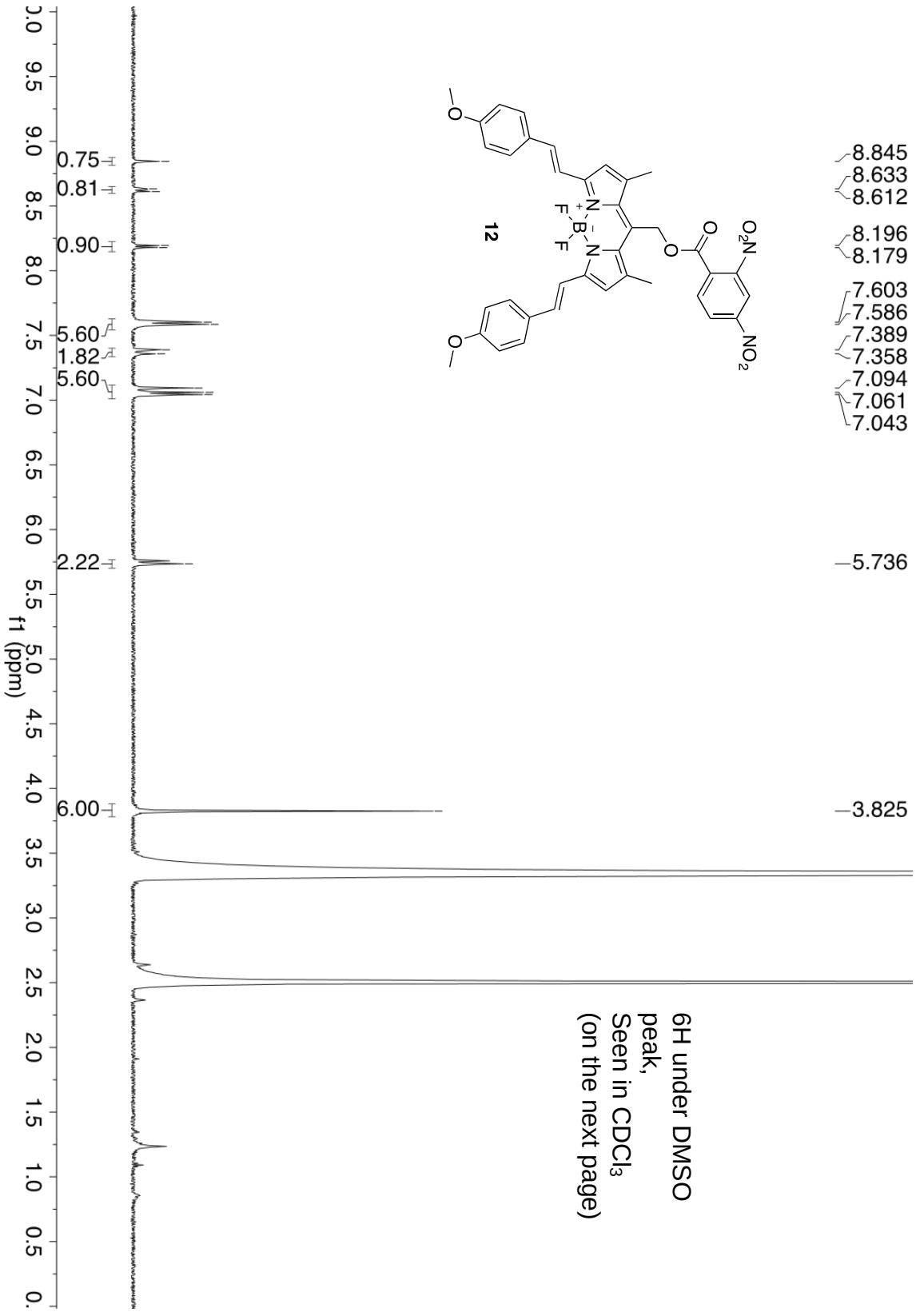

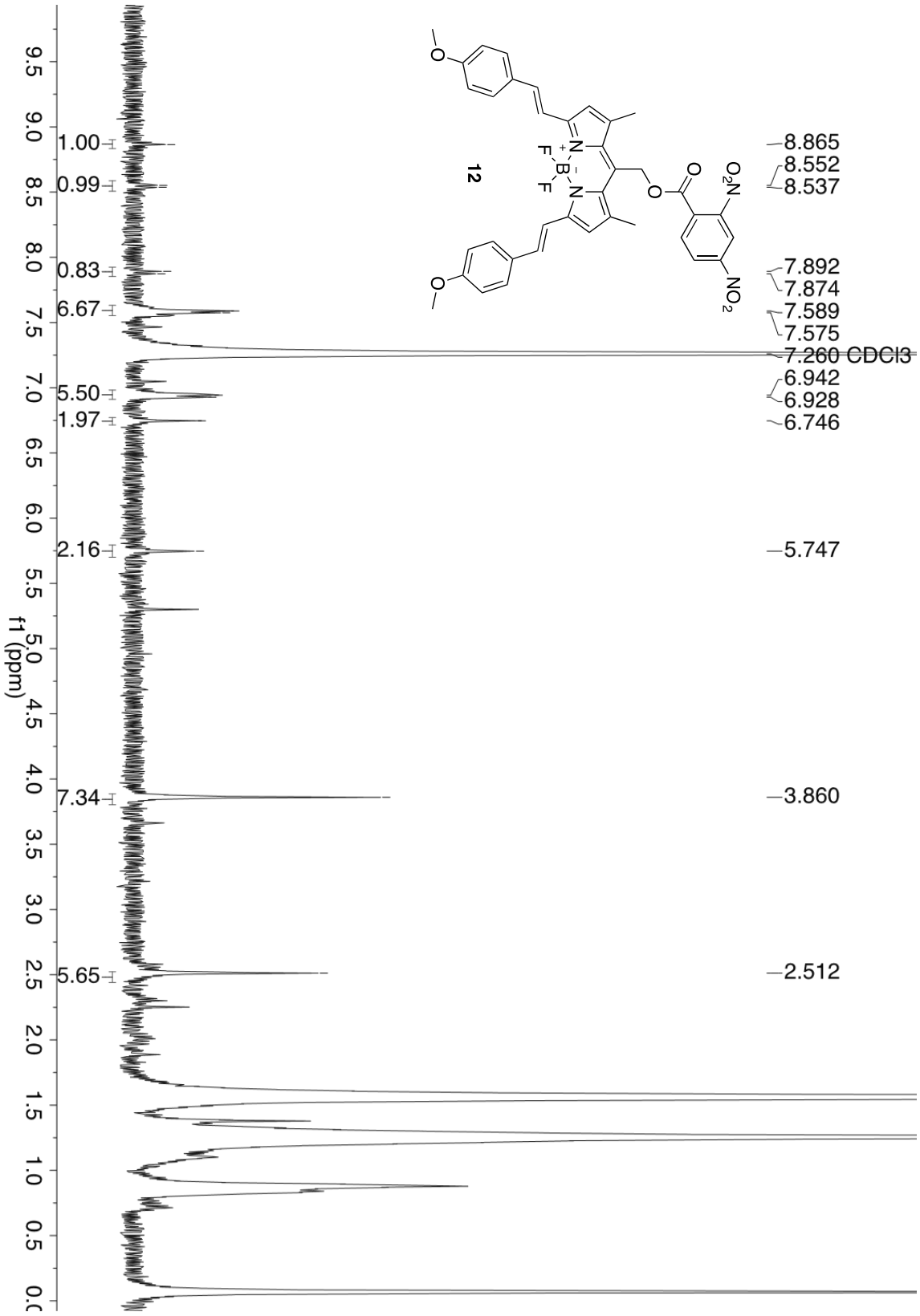

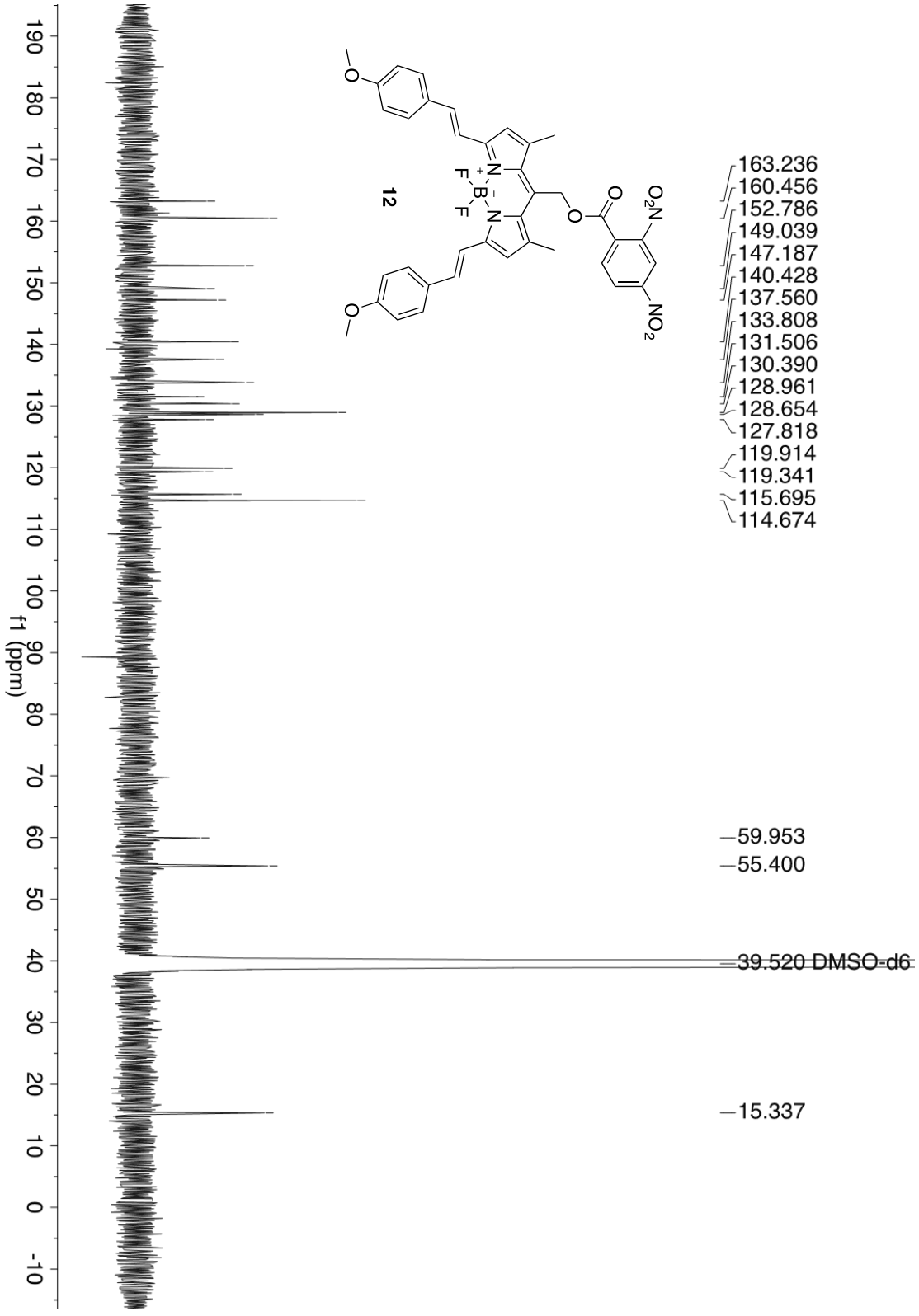

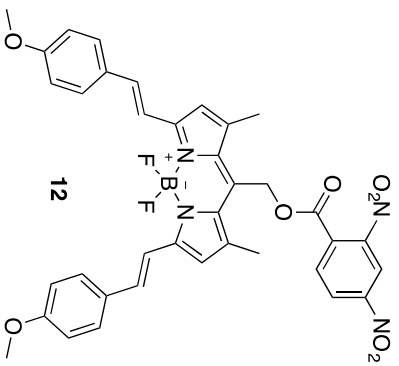

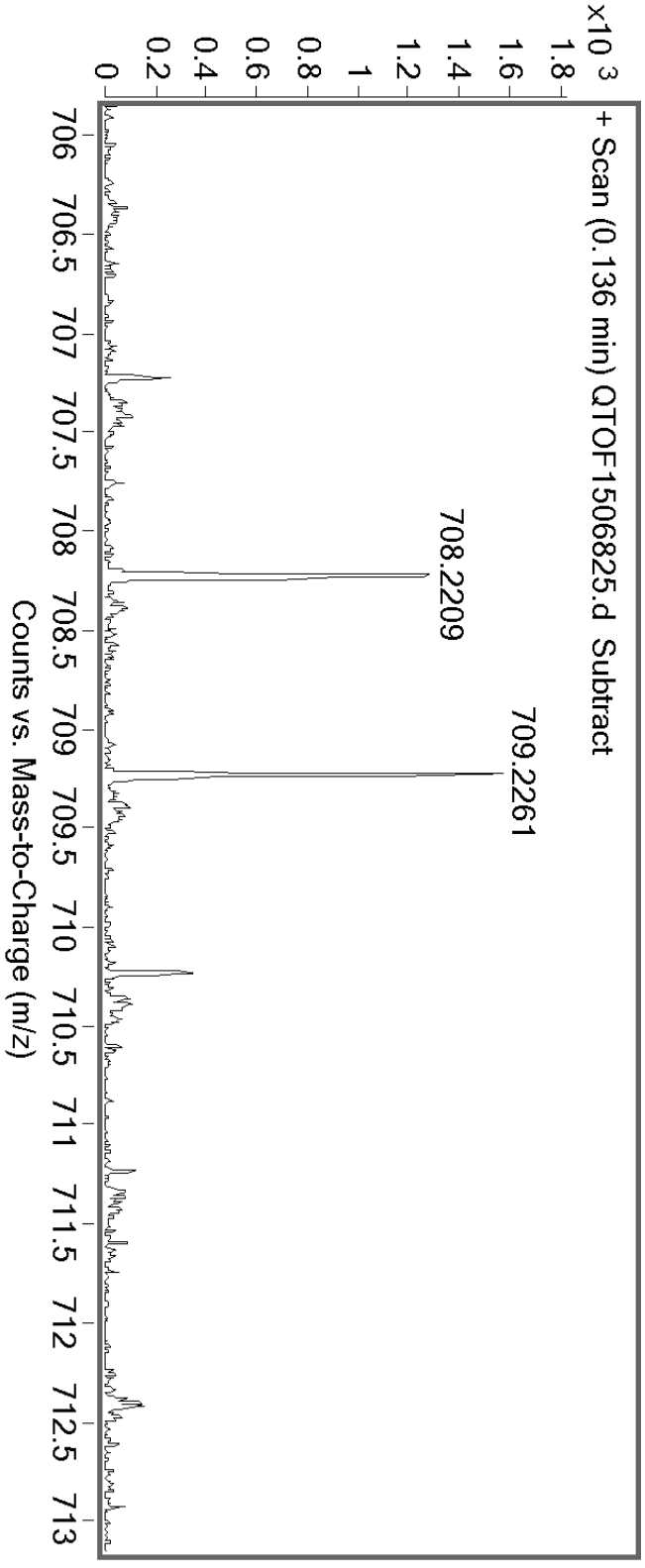

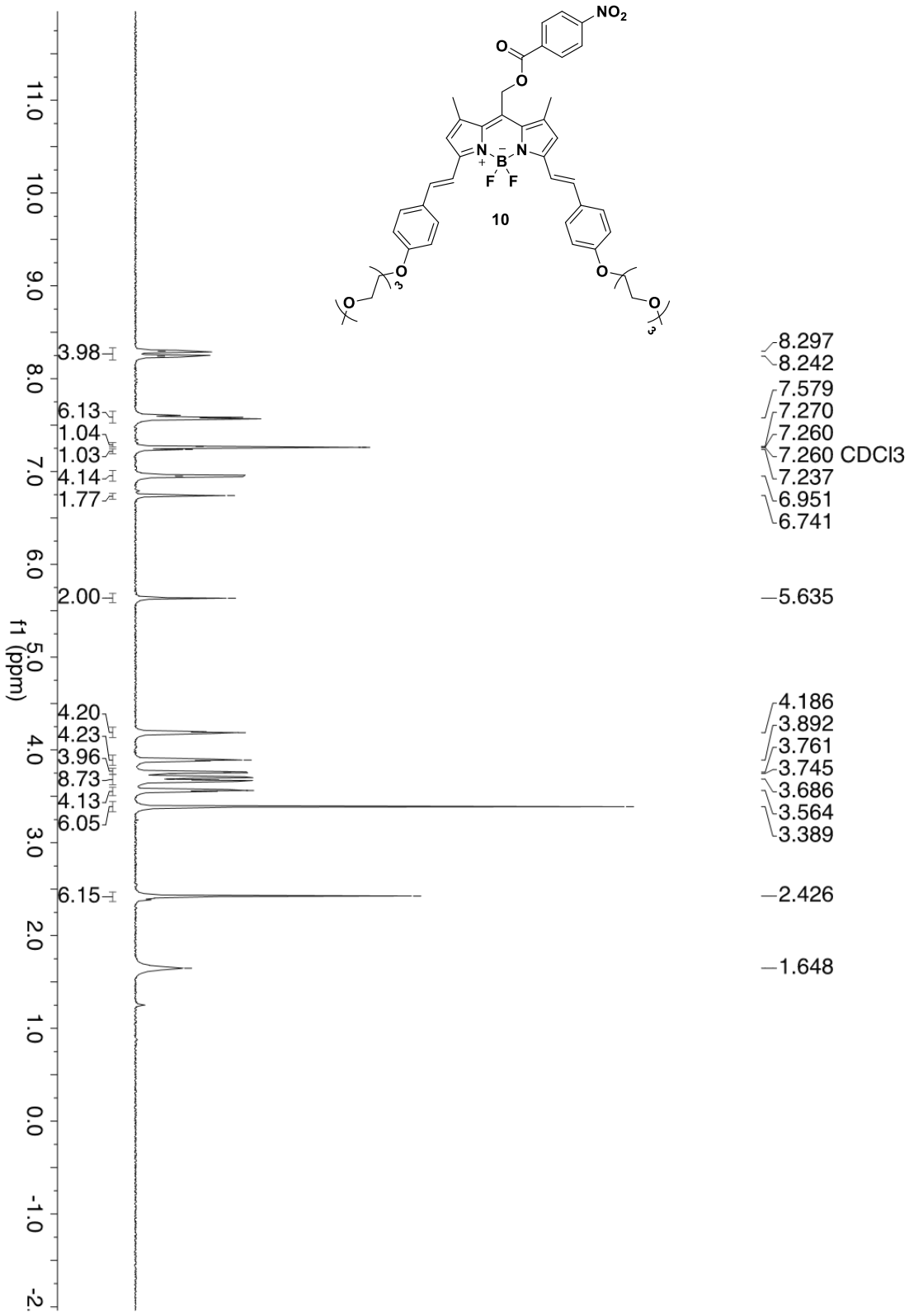

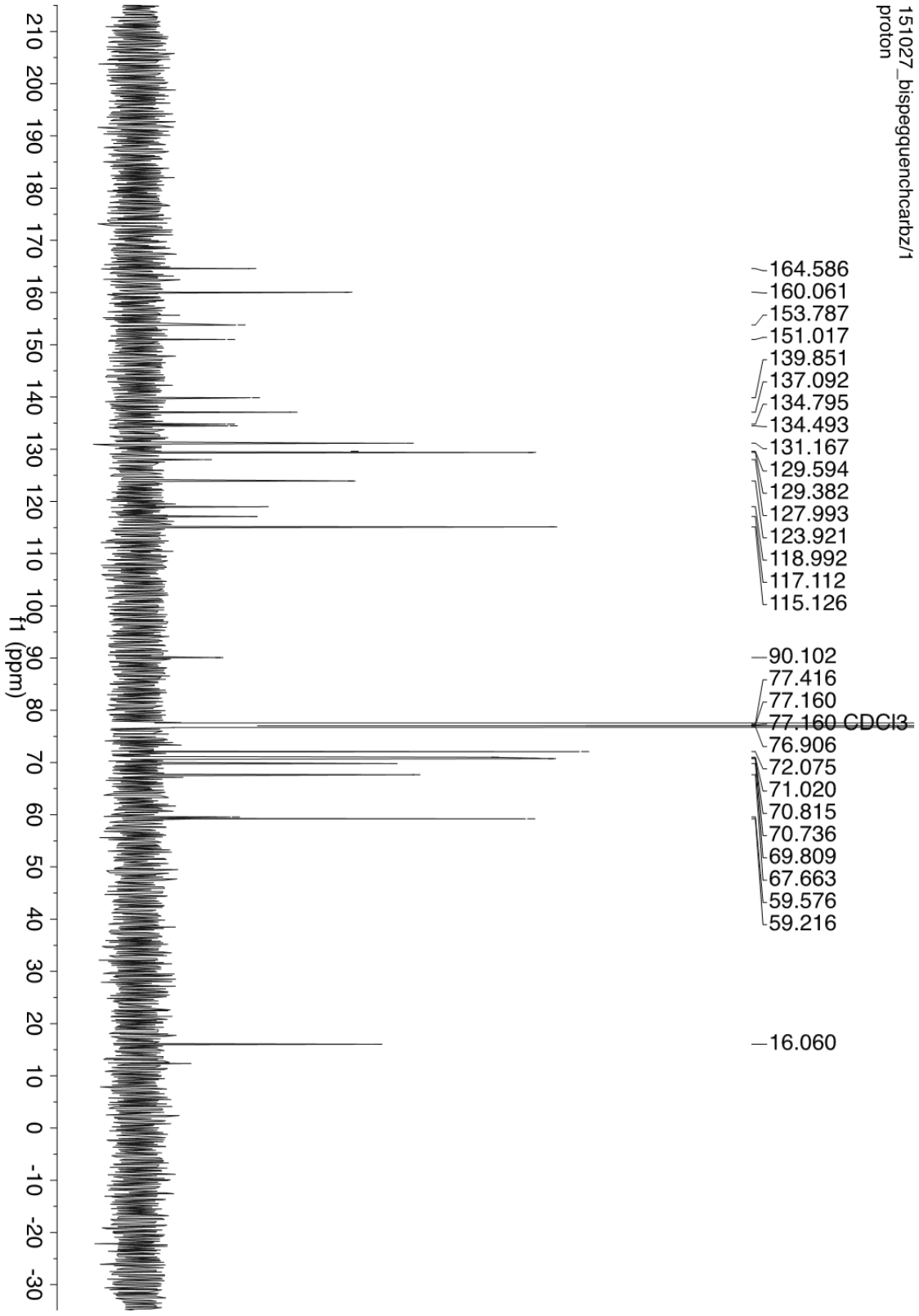

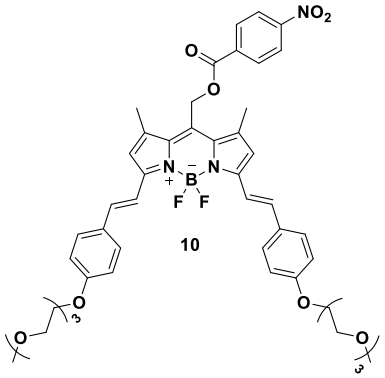

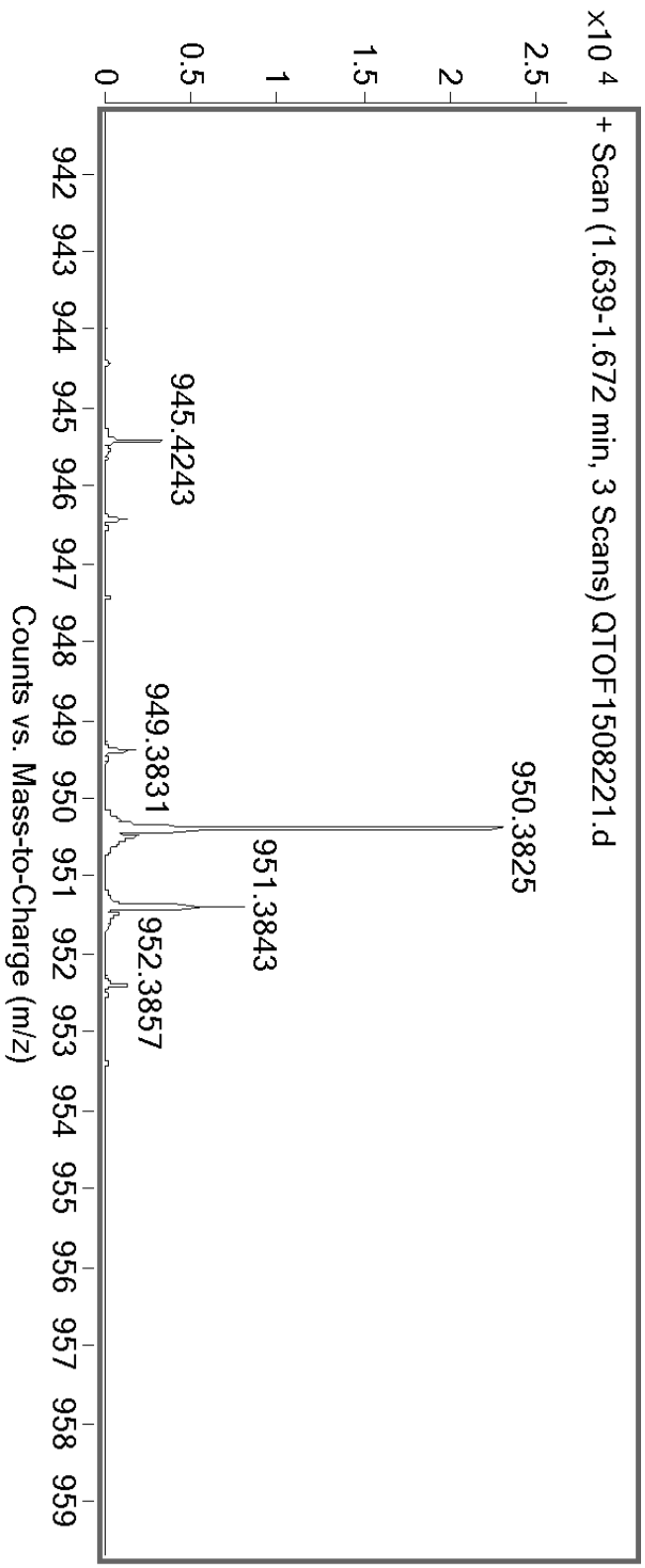

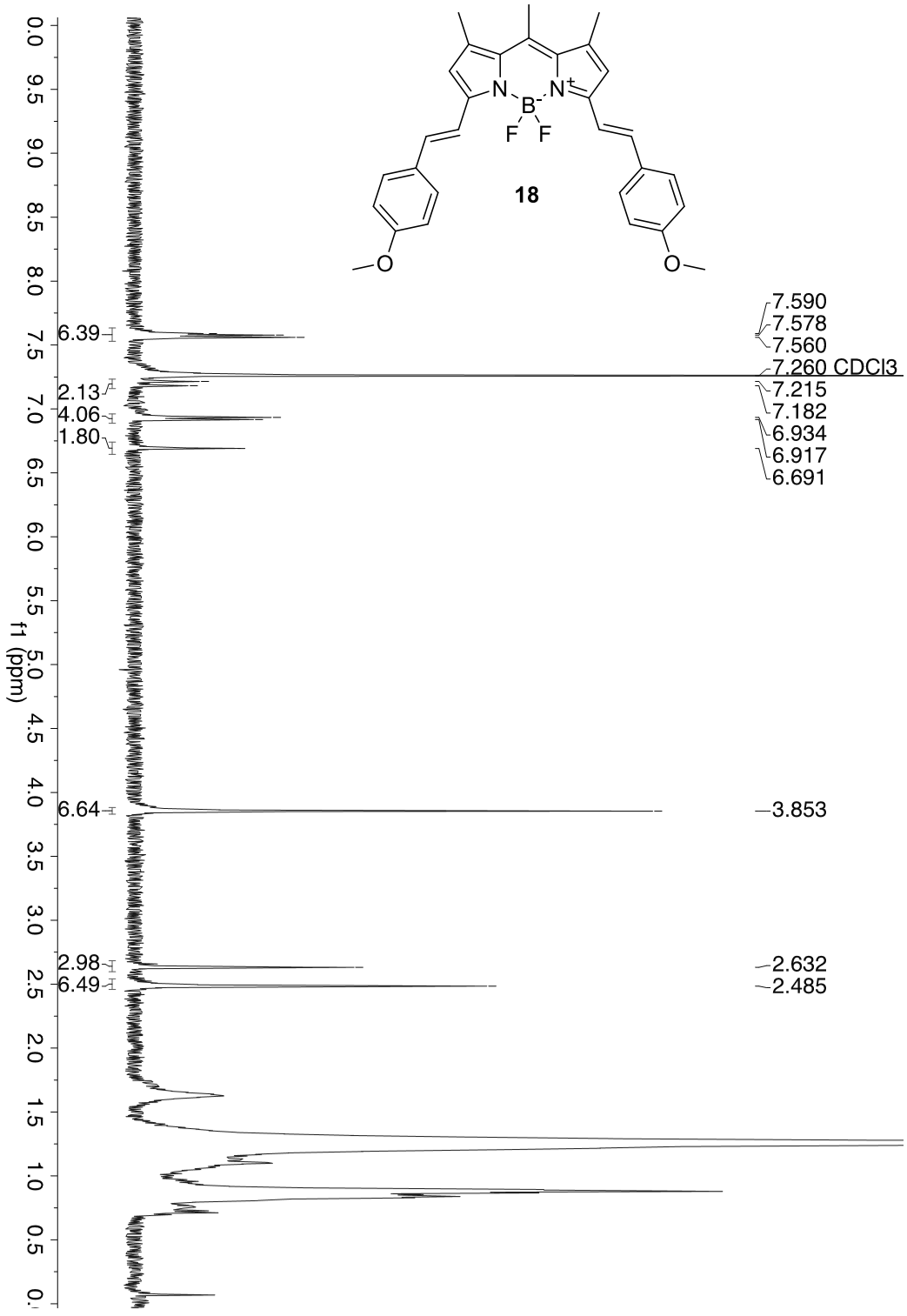

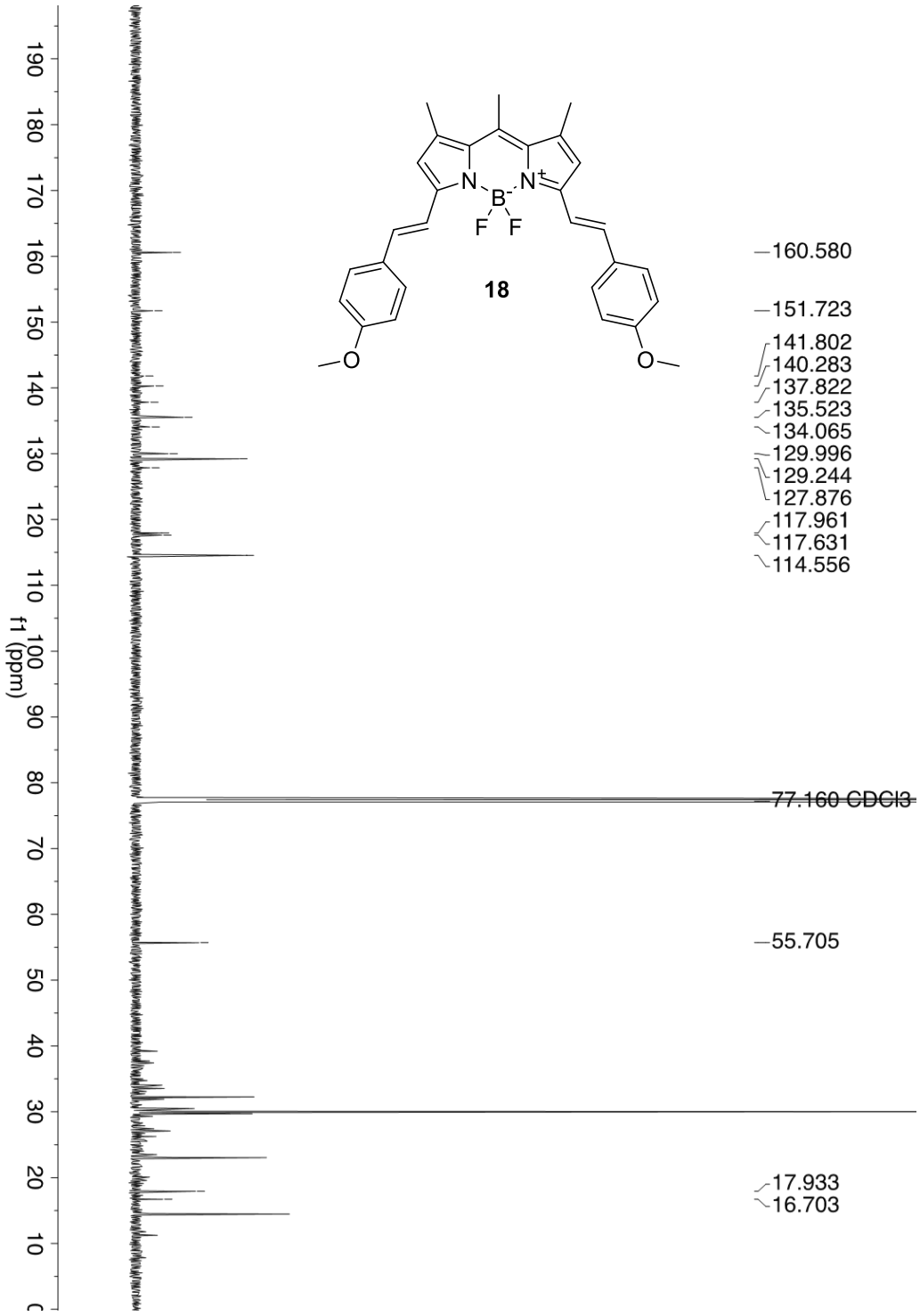

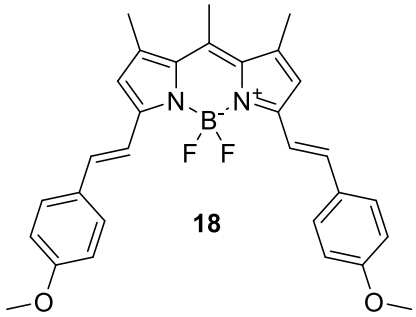

18

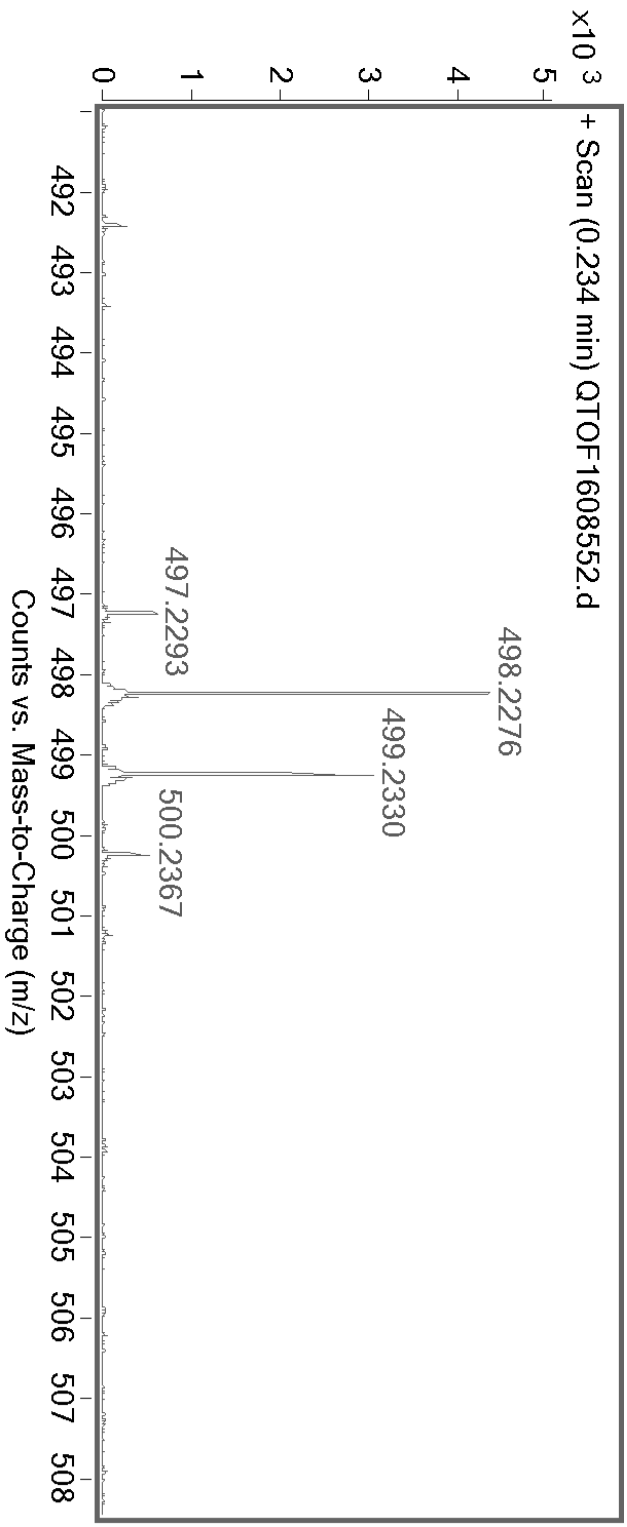

References

1. Krumova, K.; Cosa, G. *J. Am. Chem. Soc.* **2010**, 132, 17560.

2. Lottner, C.; Bart, K.-C.; Bernhardt, G.; Brunner, H. *J. Med. Chem.* **2002**, 45, 2079-2089

3. Hatchard, C. G.; Parker, C. A. *Proceedings of the Royal Society of London. Series A, Mathematical and Physical Sciences* **1956**, 235, 518.

4. (a) Bunch, T. A.; Brower, D. L. *Development* **1992,** *116*, 239; (b) Bunch, T. A.; Grinblat, Y.; Goldstein, L. S. *Nucleic Acids Res* **1988,** *16*, 1043.

5. Strober, W. *Curr Protoc Immunol* **2001,** *Appendix 3,* Appendix 3B.

6. Frisch, M. J.; Trucks, G. W.; Schlegel, H. B.; Scuseria, G. E.; Robb, M. A.; Cheeseman, J. R.; Scalmani, G.; Barone, V.; Mennucci, B.; Petersson, G. A.; Nakatsuji, H.; Caricato, M.; Li, X.; Hratchian, H. P.; Izmaylov, A. F.; Bloino, J.; Zheng, G.; Sonnenberg, J. L.; Hada, M.; Ehara, M.; Toyota, K.; Fukuda, R.; Hasegawa, J.; Ishida, M.; Nakajima, T.; Honda, Y.; Kitao, O.; Nakai, H.; Vreven, T.; Jr., J. A. M.; Peralta, J. E.; Ogliaro, F.; Bearpark, M.; Heyd, J. J.; Brothers, E.; Kudin, K. N.; Staroverov, V. N.; Kobayashi, R.; Normand, J.; Raghavachari, K.; Rendell, A.; Burant, J. C.; Iyengar, S. S.; Tomasi, J.; Cossi, M.; Rega, N.; Millam, J. M.; Klene, M.; Knox, J. E.; Cross, J. B.; Bakken, V.; Adamo, C.; Jaramillo, J.; Gomperts, R.; Stratmann, R. E.; Yazyev, O.; Austin, A. J.; Cammi, R.; Pomelli, C.; Ochterski, J. W.; Martin, R. L.; Morokuma, K.; Zakrzewski, V. G.; Voth, G. A.; Salvador, P.; Dannenberg, J. J.; Dapprich, S.; Daniels, A. D.; Farkas, O.; Foresman, J. B.; Oritz, J. V.; Cioslowski, J.; Fox, D. J. *Gaussian 09, Revision A.02*; Gaussian, Inc.: Wallingford, CT, 2009.

7. Isobe, H.; Takano, Y.; Kitagawa, Y.; Kawakami, T.; Yamanaka, S.; Yamaguchi, K.; Houk, K. N. *Mol. Phys*. **2002**, 100, 717.

8. Yamaguchi, K.; Jensen, F.; Dorigo, A.; Houk, K. N. *Chem. Phys. Lett.* **1988**, 149, 537.

9. Noodleman, L.; Case, D. A. *Adv. Inorg. Chem*. **1992**, 38, 423.

10. Lim, M. H.; Worthington, S. E.; Dulles, F. J.; Cramer, C. J. In *Chemical Applications of Density-Functional Theory*; Laird, B. B., Ross, R. B., Ziegler, T., Eds.; Amer Chemical Soc: Washington, 1996; Vol. 629, p 402.

APPENDIX B. SUPPORTING INFORMATION FOR CHAPTER 2

Probe Synthesis

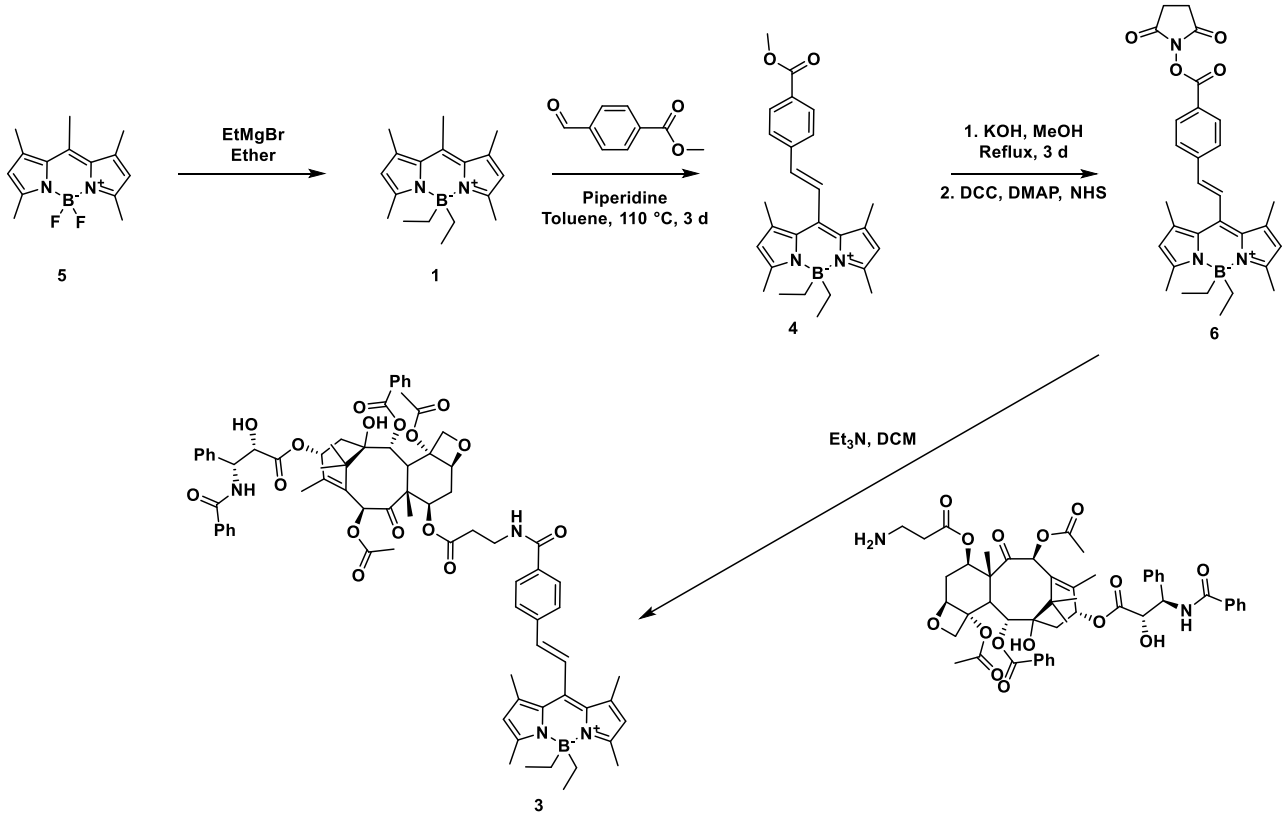

Scheme B.1. Synthesis of BODIPY-paclitaxel conjugate for use in single molecule localization microscopy (SMLM).

General: 1,3,5,7,8-pentamethylBODIPY (**5**)[1] and 7-β-alanyl-taxol[2] were synthesized using previously reported procedures.

B,B-diethyl-1,3,5,7,8-pentamethyl BODIPY (1): To a solution of 1,3,5,7,8-pentamethylBODIPY **5** (200 mg, 0.76 mmol, 1 eq) stirring in 10 mL dry ether under argon was added 3M ethylmagnesium bromide (2.5 mL, 10 eq.) dissolved in dry THF. The solution was stirred for 2 h at room temperature. The reaction was quenched with a small portion of saturated ammonium chloride and washed 3 times with ammonium chloride and once with brine. The

combined organic layer was dried over sodium sulfate, filtered, and the solvent was removed under vacuum. The resulting mixture was purified with silica gel chromatography (hexanes), affording 150 mg (70%) of the bright orange-yellow product. Characterization matched the previously reported compound.[3]

B,B-diethyl-8-(*E*)-(4-(methoxycarbonyl)styryl)**-1,3,5,7-tetramethylBODIPY (4):** To a solution of **1** (100 mg, 0.35 mmol, 1 eq) in 2 mL toluene was added methyl 4-formylbenzoate (500 mg, 3.0 mmol, 8.5 eq) and 1 mL piperidine. The solution was equipped with a dean stark trap and refluxed for 72 h. The toluene was removed under vacuum and the mixture was purified by column chromatography with silica gel (80:20 toluene:DCM), affording **4** as a red solid (70 mg, 47%). ^{1}H NMR (500 MHz, $CDCl_3$) δ, 0.38 (t, *J* = 8, 6 H), 0.83 (q, *J* = 8, 4 H), 2.19 (s, 6 H), 2.47 (s, 6 H), 3.93 (s, 3 H), 6.06 (s, 2 H), 6.70 (d, *J* = 16, 1 H), 7.26 (d, *J* = 16, 1 H), 7.55 (d, *J* = 8, 2 H), 8.07 (d, *J* = 8, 2 H). ^{13}C NMR (500 MHz, $CDCl_3$) δ, 0.04, 9.20, 16.49, 17.68, 52.26, 121.64, 126.38, 126.55, 129.94, 130.34, 131.59, 135.58, 137.36, 139.61, 140.65, 151.77, 166.71; HRMS-ESI (*m/z*): [$C_{27}H_{33}BN_2O_2$] calc, 428.2744; found, 428.2742.

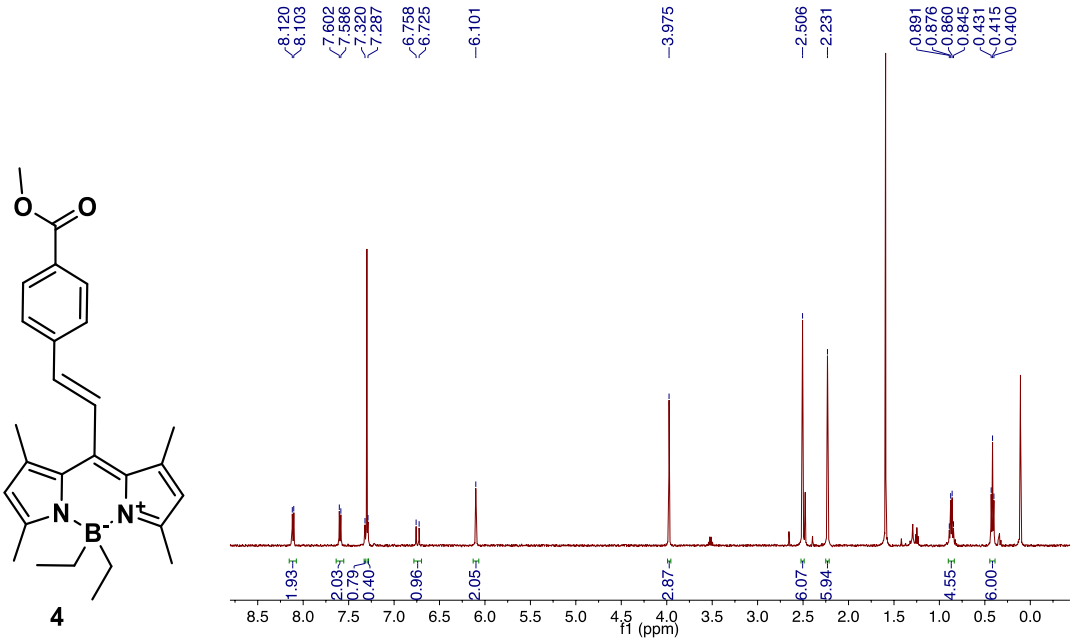

4

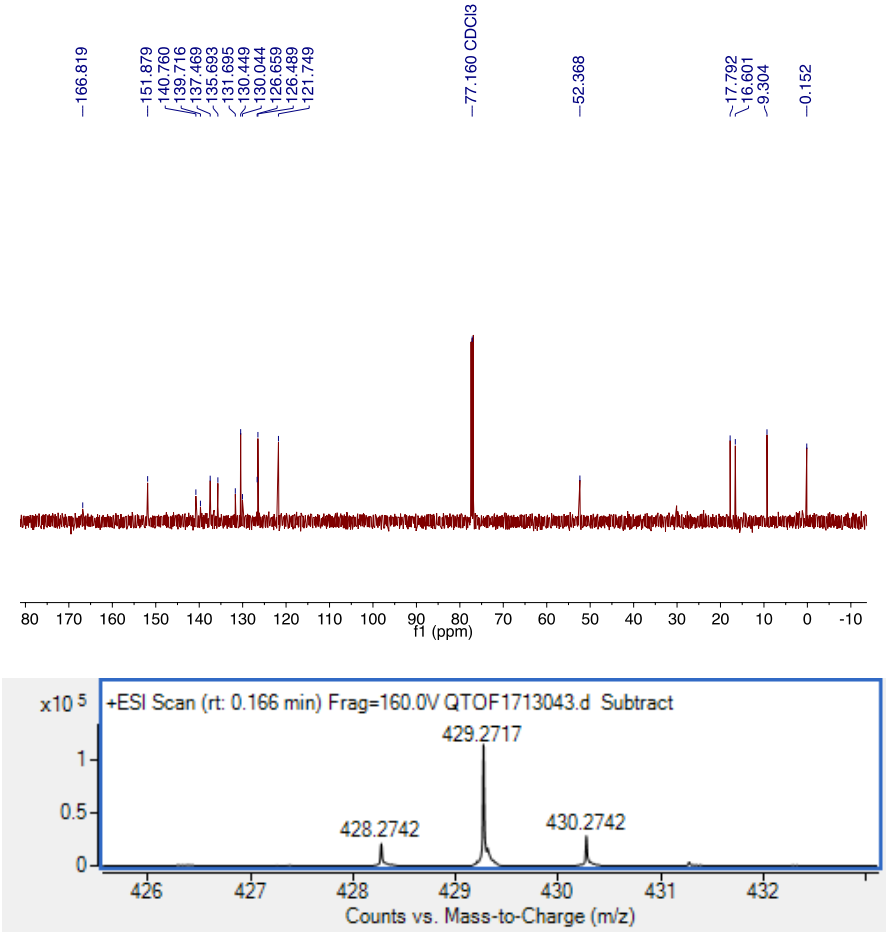

B,B-diethyl-8-(*E*)-(4-(**N-hydroxysuccinamidyl**carbonyl)styryl)**-1,3,5,7-tetramethylBODIPY (6):** To a solution of **4** (50 mg, 0.12 mmol, 1 eq) in 1 mL methanol was added 1 g KOH. The mixture was refluxed for 72 h. The solution was brought to room temperature and acidified with 1 mL HCl, diluted with 10 mL dichloromethane and extracted with dichloromethane 3 times and washed with brine. The organic layer was dried over sodium sulfate, filtered, and the solvent was removed under vacuum to yield 30 mg (60%) of a red solid. The resulting compound was dissolved in dry dichloromethane, to which was added 4-(dimethylamino)pyridine (1 mg, 0.01 mmol, 0.1 eq), dicyclohexylcarbodiimide (22.3 mg, 0.11 mmol, 1.5 eq), and N-hydroxysuccinimide (13 mg, 0.11 mmol, 1.5 eq). The solution was stirred

overnight at room temperature. The mixture was left in the freezer for 1 h, and filtered, after which solvent was removed under vacuum. **6** was purified with silica chromatography (DCM) to yield 17 mg (29% yield over two steps) of a red solid. ^{1}H NMR (500 MHz, $CDCl_3$) δ, 0.42 (t, *J* = 8, 6 H), 0.87 (q, *J* = 8, 4 H), 2.23 (s, 6 H), 2.51 (s, 6 H), 2.96 (s, 4 H), 6.11 (s, 2 H), 6.76 (d, *J* = 16, 1 H) 7.36 (d, *J* = 16, 1 H), 7.66 (d, *J* = 8, 2 H), 8.22 (d, *J* = 8, 2 H). ^{13}C NMR (500 MHz, $CDCl_3$) δ, 0.15, 9.30, 16.61, 17.75, 25.84, 121.186, 124.81, 126.84, 128.13, 131.52, 135.21, 137.42, 139.19, 141.78, 142.70, 152.09, 161.62, 169.34. HRMS-ESI (m/z) [$C_{30}H_{34}BN_3O_4$ + H^+] calc, 512.2715; found,512.2732.

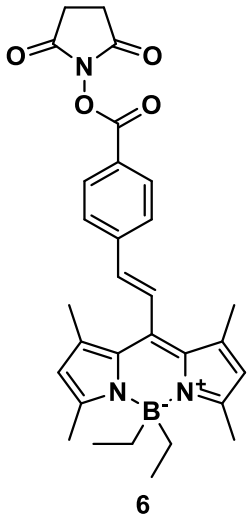

6

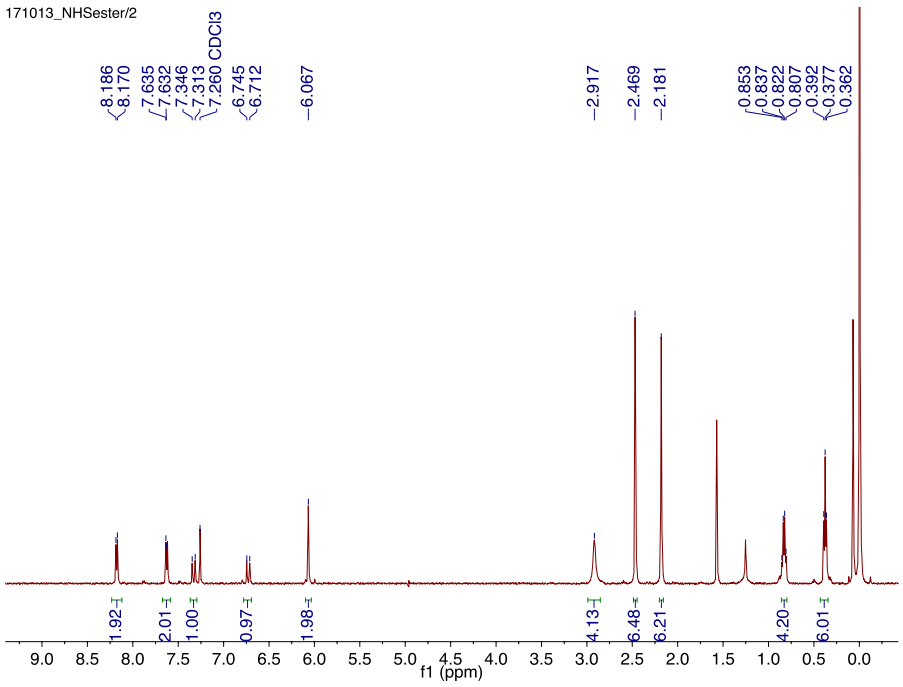

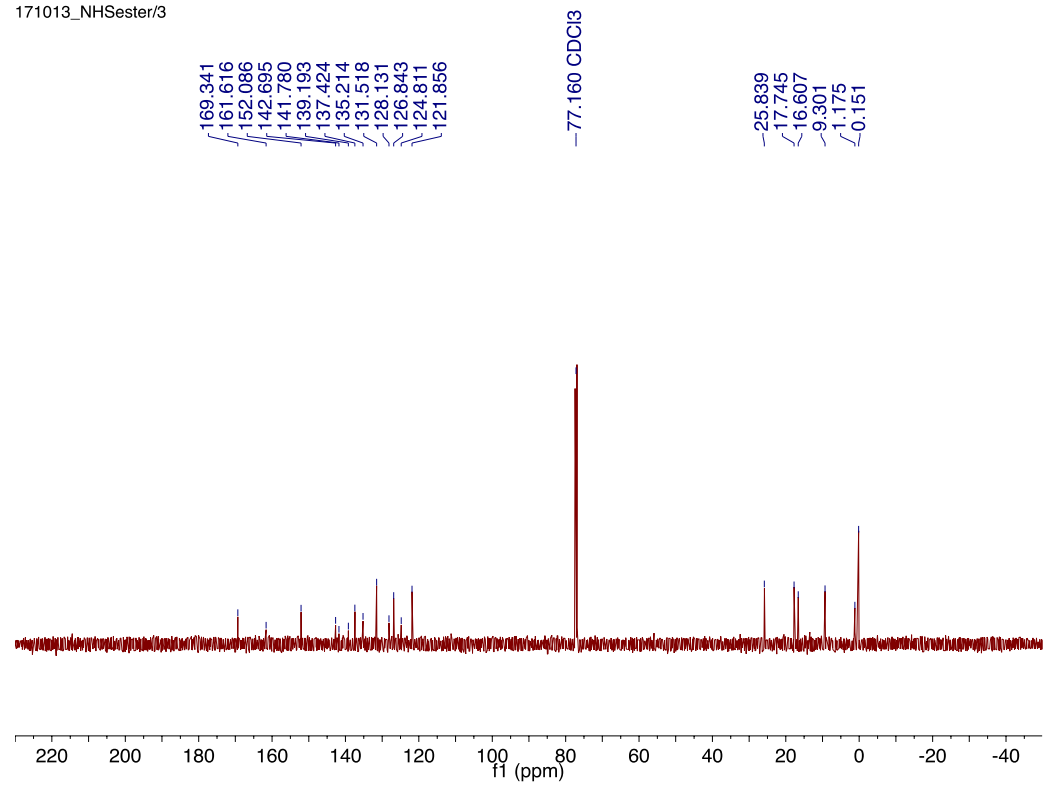

Compound 3: To a solution of **6** (10 mg, 0.02 mmol, 1 eq) stirring in 5 mL dry dichloromethane was added 7-β-alanyltaxol (20 mg, 0.022 mmol, 1.1 eq) and 100 µL triethylamine. The solution was stirred 12 h at room temperature. The solvent was removed under vacuum and the solid was purified by column chromatograpy (99:1 DCM:MeOH) yielding 7 mg of **3** (26% yield). The solid was additionally purified by prep-HPLC for use in fluorescent imaging studies. ^{1}H NMR

(500 MHz, $CDCl_3$) δ, 0.37 (t, *J* = 8, 6 H), 0.83 (q, *J* = 8, 4 H), 1.14 (m, 6 H), 1.68 (s, 3 H), 1.85-2.05 (m, 2 H), 1.99 (s, 3 H), 2.13 (s, 1 H), 2.18 (s, 6 H), 2.23 (s, 3 H), 2.36 (s, 3 H), 2.47 (s, 6 H), 2.49-2.62 (m, 3 H), 3.15 (m, 1 H), 3.35 (s, 1 H), 3.83 (m, 1 H), 4.20 (d, *J* = 9, 1 H), 4.32 (d, *J* = 9, 1 H), 4.98 (m, 1 H), 5.68 (m, 2 H), 6.05 (m, 3 H), 6.28 (m, 2 H), 6.70 (d, *J* = 20, 1 H), 7.00 (d, *J* = 9, 1 H,) 7.17 (m, 2 H), 7.30-7.65 (band, 13 H), 7.76 (d, *J* = 8, 2 H), 8.03 (d, *J* = 9), 8.13 (d, *J* = 8, 2 H)). ^{13}C NMR (500 MHz, $CDCl_3$) δ, 8.86, 9.29, 9.77, 14.26, 15.06, 16.60, 17.76, 20.97, 22.85, 25.10, 25.79, 29.86, 32.09, 34.12, 43.35, 46.51, 49.35, 56.14, 58.71, 72.09, 72.30, 73.39, 74.91, 75.30, 75.77, 76.60, 79.44, 81.25, 84.63, 121.86, 126.79, 127.07, 127.24, 128.82, 128.92, 129.32, 130.37, 130.77, 131.66, 132.18, 132.95, 133.85, 133.90, 135.38, 137.10, 137.38, 139.37, 141.80, 143.02, 152.09, 156.84, 165.35, 167.23, 168.24, 169.94, 171.41, 173.58, 203.96; HRMS-ESI (*m/z*) [$C_{76}H_{85}BN_4O_{16}$ + H^+] calc, 1321.6126; found, 1321.6146.

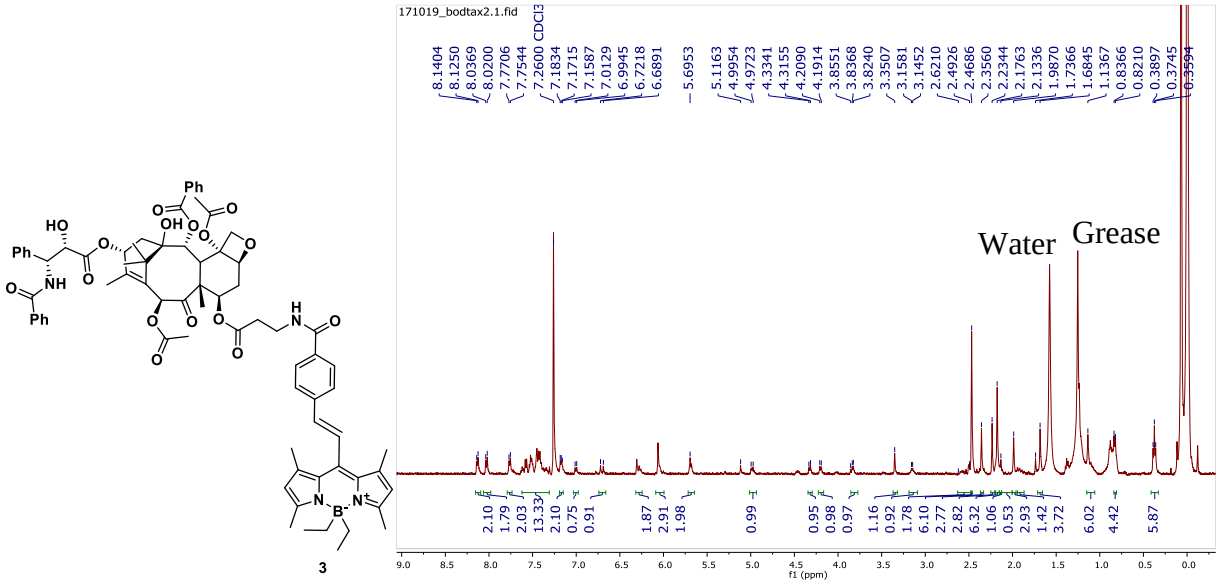

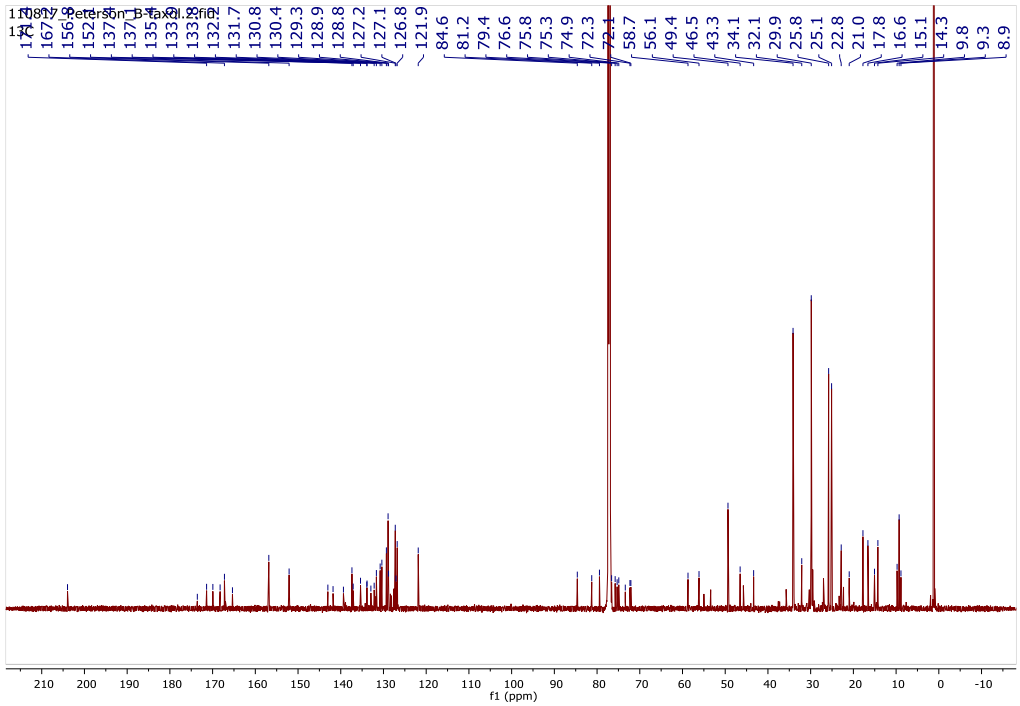

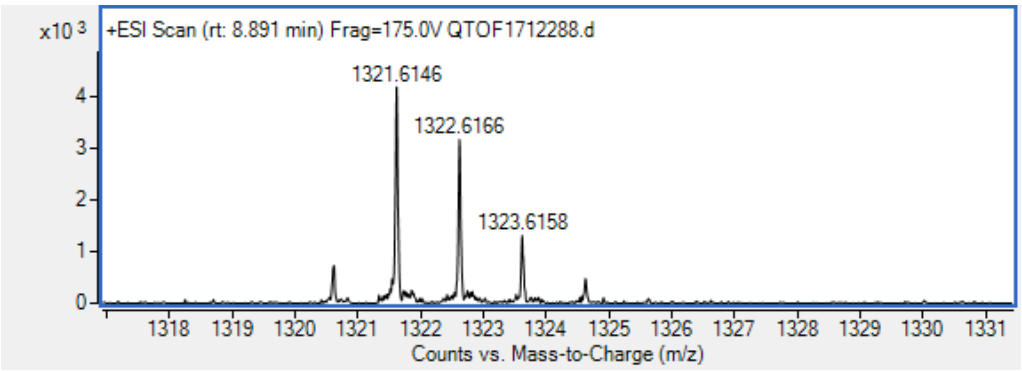

Fluorescence quantum yields (Φ_f)

Fluorescence quantum yields were determined as an average of three trials. Compounds **1-3** were prepared in methanol at concentrations between 1-30 µM. The absorbance at 450 nm was recorded and the fluorescence spectra was collected using 450 nm excitation. Calibration plots were constructed using the integrated fluorescence peak area from 475-600 nm versus the absorbance at 450 nm. Calibration curves were compared to those for a fluorescein standard. In

addition, the quantum yield of the aqueous photoproduct of **1** was determined by irradiating a solution of **1** in 90:10 acetonitrile:water for 30 minutes. As described above, the calibration curve was plotted using the integrated fluorescence peak area from 475-600 nm and the absorbance at 450 nm.

Photoactivation quantum yield

The photoactivation quantum yield was determined using an average of three trials. Compounds **1** and **4** (an analogue of **3** without paclitaxel attached) between 1-4 mg were dissolved in 1 mL dichloromethane and diluted to 25 mL with methanol, or 45 mL acetonitrile and diluted to 50 mL with water. 3 mL of the solutions were transferred to a quartz cuvette. The initial absorbance was recorded at 532 nm. The solutions were then irradiated with a 532 nm Nd:YAG laser or a 530 nm 5 lamp Luzchem LED setup. At intervals, 10 µL of the solutions were removed and diluted to 25 mL with methanol or 90:10 acetonitrile:water and the fluorescence intensity at 510 nm was measured with 450 nm excitation. Time points were taken until the fluorescence began to decrease due to photobleaching, at which time it was assumed that the maximum fluorescence intensity was 100% conversion. The percent conversion was converted into moles reacted, which was plotted versus irradiation time. The photoactivation quantum yield was determined against a ferrioxalate actinometer, taking into account the low absorbance of compounds **1**, **4** and ferrioxalate at 532 nm. The quantum yield of photoactivation for compound **1** was 0.79 ± 0.02% in methanol and 0.8 ± 0.1% in 90:10 acetonitrile:water. The quantum yield of photoactivation for **4** was found to be 0.12 ± 0.02% in 90:10 acetonitrile:water.

Photoproduct studies

Compound **1** (25 mg) was dissolved in 10 mL dichloromethane, which was diluted to 100 mL with methanol. The solution was stirred in an Erlenmeyer flask overnight under a 532 nm LED. The solvent was removed under vacuum and the remaining solid was purified via column chromatography with silica gel (60:40 Hex:EtOAc). Two major photoproducts were isolated and characterized by NMR (Figure S1), corresponding to the single and disubstituted compounds. 2 mg (8% yield) of **7** and 21 mg (83% yield) of **2** were isolated, suggesting that the photoactivation to **2** is a sequential two-photon process.

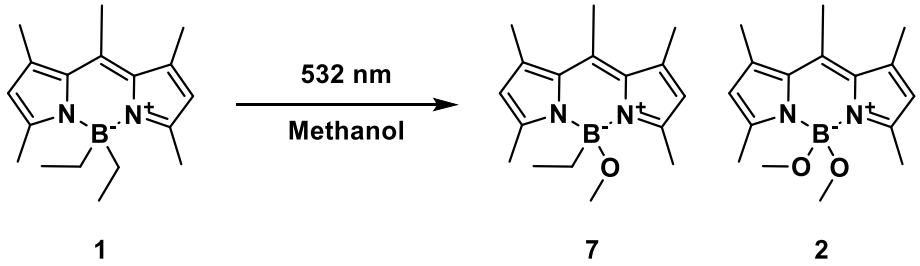

Scheme B.2. Photoproducts of **1** in methanol when irradiated with green light.

The solubility of **1** in water is low, so verification that the dihydroxy product is formed in water was performed by collecting a mass spectrum of the compound after irradiation in 90:10 acetonitrile:water. Photoproduct studies were conducted by dissolving 1 mg of **1** in 9 mL of acetonitrile to which was added 1 mL of water. The solution was irradiated in a pyrex test tube with green light for 3 h. A high resolution mass spectrum (HRMS, Figure S2) was measured of the solution to confirm that the dihydroxy species is formed upon irradiation in water. HRMS, ESI: C_{14} H_{19} B N_2 O_2 Na + Calc: 281.1437 Found: 281.1431

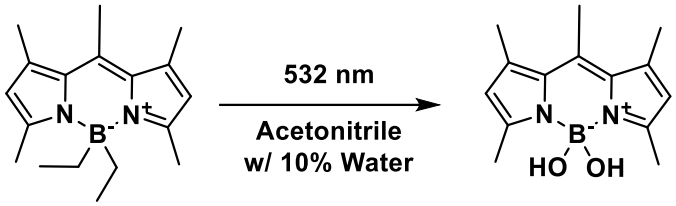

1 8

Scheme B.3. Photoproduct of **1** when irradiated with green light in acetonitrile with 10% water.

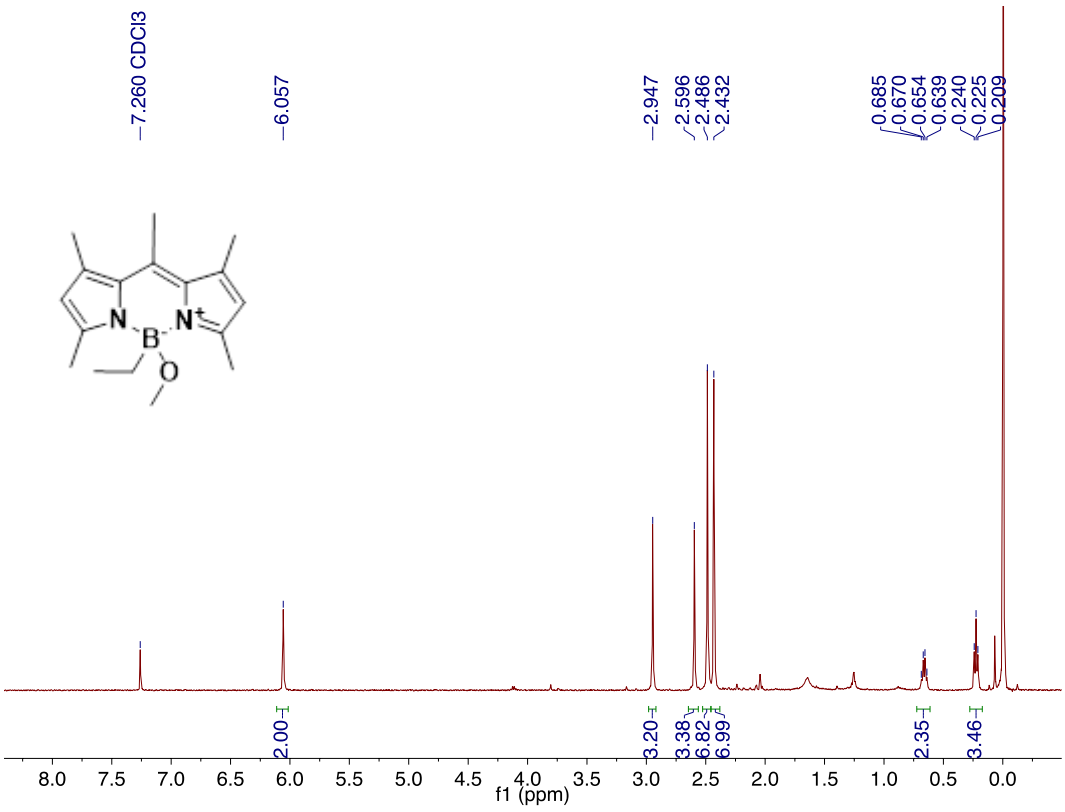

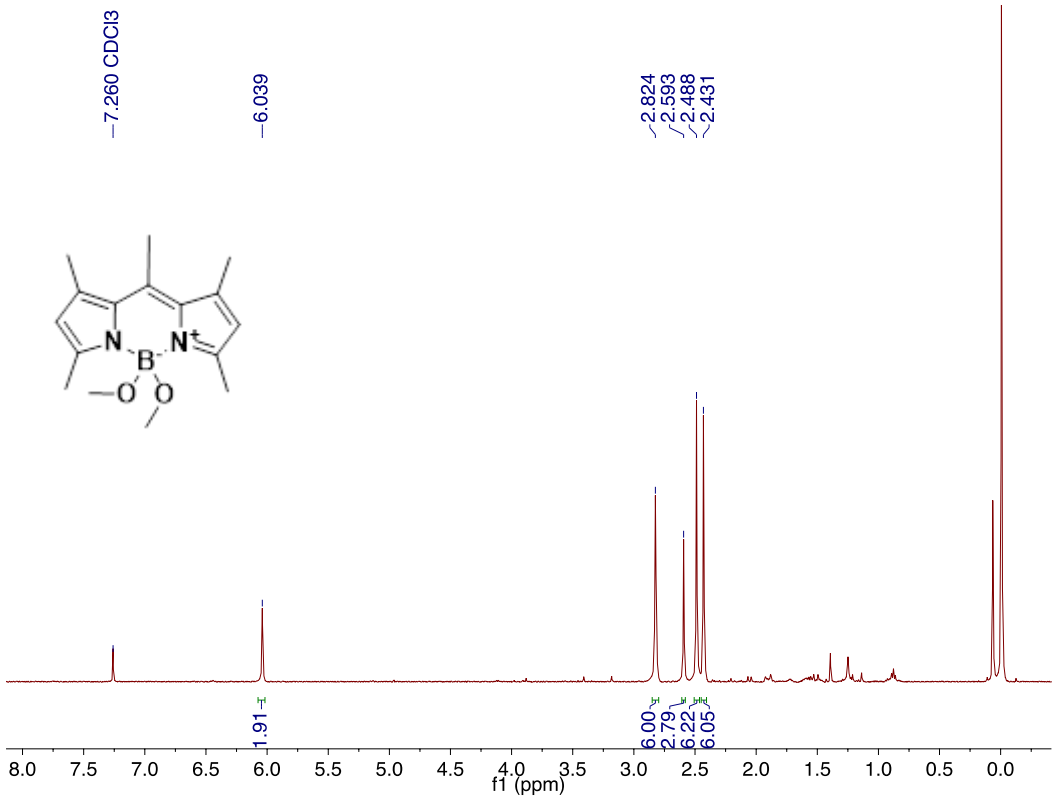

Figure B.1. NMR spectra of the photoproducts of **1** in methanol: (top) **7** and (bottom) **2**.

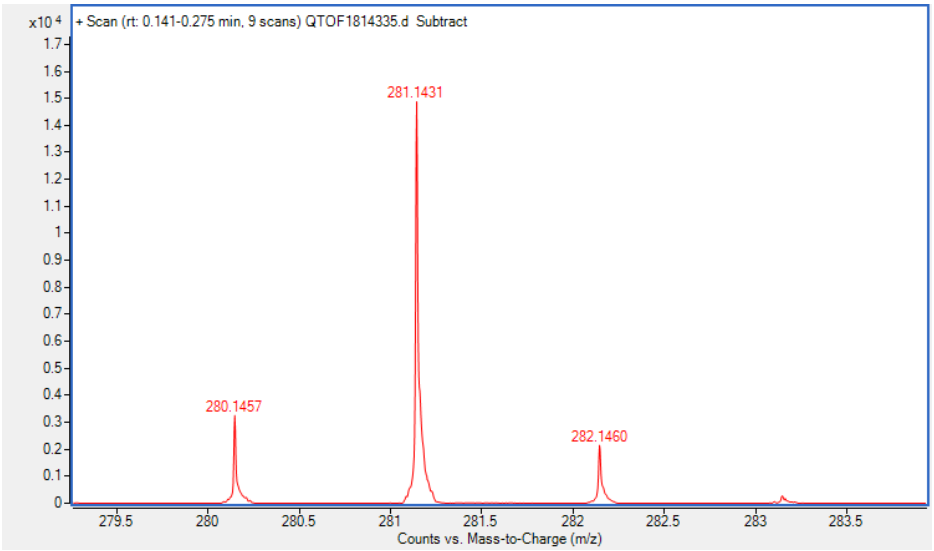

Figure B.2. High resolution mass spectrum of the photoproduct of **1** in an aqueous medium showing the formation of the dihydroxy product **8**.

Single Molecule Localization Microscopy

Table B.1. Examples of the laser irradiances used for SMLM experiments with commonly used photoswitchable fluorescent probes.

SMLM probe	Excitation Laser irradiance used for SMLM experiments	Reference
Alexa Fluor 488	1.2 kW/cm^2, 3 kW/cm^2	[4],[5]
ATTO 488	1.2 kW/cm^2	[4]
ATTO 520	3 kW/cm^2	[5]
Alexa Fluor 532	1.5 kW/cm^2	[5]
ATTO 532	10 kW/cm^2	[6]
Tetramethyl Rhodamine	~ 1 kW/cm^2	[7]
Cy3B	1.7 kW/cm^2, 2.2 kW/cm^2	[8],[4]
ATTO 565	1.5 kW/cm^2	[5]
Alexa Fluor 568	1.5 kW/cm^2	[5]
ATTO 590	4 kW/cm^2	[5]
ATTO 655	1.5 kW/cm^2	[9]
Alexa Fluor 647	0.8 kW/cm^2	[4]
Cy5	0.8 kW/cm^2	[4]
ATTO 680	0.8 kW/cm^2	[4]
ATTO 700	4 kW/cm^2	[5]
Cy7	1.3 kW/cm^2	[4]
Alexa Flour 750	1.3 kW/cm^2	[4]

Table B.2. Examples of the laser wavelengths and irradiances used for SMLM experiments with photoactivatable fluorescent probes.

Probe	Activation wavelength	Probe λ_{ex}	Probe λ_{em}	Activation laser irradiance	Excitation laser irradiance	Reference
Compound **3**	488 nm	498 nm	517 nm	0.16 kW/cm^2	NA	This study
NVOC caged si-Rhodamine	405 nm	637 nm	654 nm	1 W/cm^2	4 kW/cm^2	[10]
Rhodamine diazoketone	405 nm	558 nm	583 nm	0.1 W/cm^2	2 kW/cm^2	[11]
Caged Rh110	405 nm	473 nm	520 nm	5.5-23 W/cm^2	0.38 kW/cm^2	*[12]*
Nitroso-caged rhodamine	405 nm	532 nm	550 nm	0.1 W/cm^2	2 kW/cm^2	[13]
Rhodamine lactam	375 nm	532 nm	620 nm	50 W/cm^2	18 kW/cm^2	[14]
Coumarin oxazine	355 nm	532 nm	645 nm	10-100 W/cm^2	5 kW/cm^2	[15]

Data collection and analysis

Microscopy experiments were performed on a Nikon Eclipse TE2000U microscope (Melville, NY) equipped with an Argon ion laser (Uniphase, San Jose, CA). A schematic of the instrument is shown below. The laser irradiance was determined as previously reported.[16] An Andor iXon^{EM}+ DU-897 back illuminated electron-multiplying charge coupled device (EMCCD) was used to collect the filtered emitted light. A 30 ms acquisition time per frame and 10,000 - 50,000 frames were collected for each movie. SMLM movies were analyzed using ThunderSTORM plug-in for ImageJ.[17] Fitting point spread function model, integrated Gaussian by least square methods was used to achieve the sub-pixel localization of molecules. Merging was used to remove the localized molecules that appeared in sequential frames. This ensured that the same localized molecule did not contribute to the constructed SMLM image more than once. Diffracted limited images were constructed by summing all the frames into a single image using ImageJ.

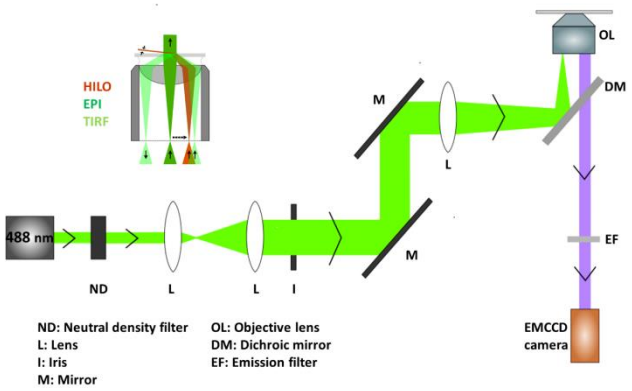

A schematic of the fluorescence microscope used for single molecule localization microscopy.

Uncertainty of the localized single molecules (s) is calculated using the equation:

$$\sigma = \sqrt{\left(\frac{s^2}{N}\right) + \left(\frac{a^2/12}{N}\right) + \left(\frac{8\pi s^4 b^2}{a^2 N^2}\right)}$$

where s is the standard deviation of the point spread function, N is the number of photons detected, a is the pixel size, and b is the standard deviation of the image background[18]. For our experimental conditions, the expected localization prevision is between 14-22 nm.

Cell sample preparation

HeLa cells (ATCC® CCL-2™, Manassas, VA) were cultured in Dulbecco's Modified Eagle Medium (DMEM, Invitrogen, Carlsbad, CA) supplemented with 10% fetal bovine serum, 12.5 mM streptomycin, and 36.5 mM penicillin (Fisher Scientific, Pittsburgh, PA). Cultures were maintained at 37 °C in a humidified 5% CO_2 incubator (Thermo Scientific, Waltham, MA). HeLa cells were sub-cultured using 0.25% (w/v) trypsin-EDTA (Life Technologies, Carlsbad, CA) solution every two days. Cells were seeded at 20,000 cells per well onto polylysine coated, 8-well chambered cover glass (Nunc™ Lab-Tek™ II, Thermo Scientific) a day before the microscopy experiment.

Live cell labeling

On the day of the microscopy experiment, the growth medium was replaced with 1 μM compound **3** and 25 μM verapamil hydrochloride (Sigma Aldrich, St. Louis, MO) in DMEM medium and incubated for 1 hour at 37 °C in a humidified 5% CO_2 incubator. Cells were rinsed with the imaging medium (pH = 7.4, 155 mM NaCl, 5 mM KCl, 2 mM $CaCl_2$, 1 mM $MgCl_2$, 2 mM NaH_2PO_4, 10 mM HEPES and 10 mM Glucose) several times prior to the microscopy experiment.

Glutaraldehyde fixation of cells and labeling

Growth medium was removed, and the cells were incubated in BRB-80 buffer (pH 6.8, 80 mM K-PIPES, 1 mM $MgCl_2$; 1 mM EGTA) containing 0.5% Triton X-100 for 1 min. Then cells were incubated for 10 min with BRB buffer containing 0.5% glutaraldehyde (Sigma Aldrich). Solution was replaced with a freshly prepared 0.1% sodium borohydride in PBS buffer and incubated for 5 min. This step was repeated twice to quench the unreacted glutaraldehyde. Then rinsed well with PBS and blocked with 1% BSA in PBS for 30 min. Samples were incubated for 1-2 h with 1 μM compound **3** in PBS. The cells were washed several times with PBS and imaged in PBS buffer.

Ethyleneglycol-bis-succinimidyl-succinate (EGS) fixation of cells and labeling

Growth medium of the cells was replaced with 0.5% Triton X-100 in BRB-80 buffer and incubated for 1 min. Then 2 mM ethyleneglycol-bis-succinimidyl-succinate (EGS) (Thermo Scientific) in BRB-80 buffer (freshly prepared from 250 mM EGS in DMSO) was added into the cells by replacing the previous solution and incubated for 10 min. The solution was removed and rinsed with PBS. Then, the samples were incubated with 1 μM compound **3** in PBS for 1h. The cells were rinsed several times with PBS and imaged in PBS buffer.

In vitro assembled microtubule preparation

A 2 mM stock of compound **3** was prepared in DMSO and 5 μL of this stock was added to 0.5 mL of BRB-80 buffer. This solution was added to a vial of 500 μg lyophilized microtubules (mt002, Cytoskeleton, Denver, CO). The solution was mixed gently and incubated for 15 minutes at room temperature. An 8-well chambered cover glass was sonicated for 10 minutes in 1 M potassium hydroxide (KOH) solution, then rinsed several times with Milli-Q water and air

dried overnight. The microtubule solution (50 µL) was added into the well and incubated for 15 minutes. The solution was removed and the immobilized microtubules on the cover glass were fixed with 0.5% glutaraldehyde in BRB-80 buffer for 10 minutes. The fixation solution was removed and a freshly prepared 0.1% sodium borohydride in PBS was added into the well and incubated for 5 minutes. The well was rinsed with PBS and imaged in PBS buffer.

Single molecule sample preparation

A 8-well chambered cover glass was cleaned by sonicating for 10 minutes in 1 M potassium hydroxide (KOH) solution, then several times rinsing with Milli-Q water followed by air drying for overnight. Compound **3** was dissolved in spectrophotometric grade ethanol (Fisher Scientific) and diluted to obtain a final concentration of ~ 0.1 µM. This solution (100 µL) was added into the well and after 10 minutes, the well was rinsed several times with PBS and imaged in PBS medium.

Additional Figures

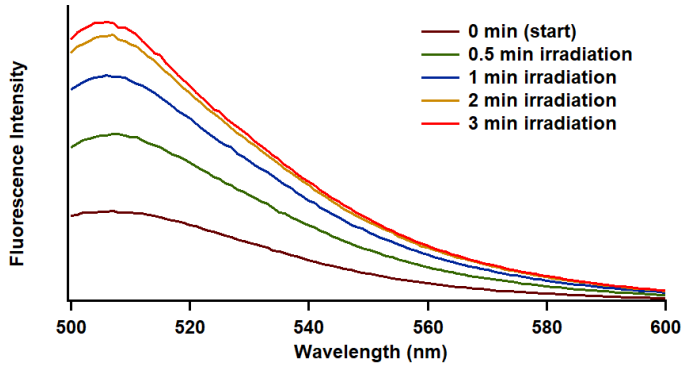

Figure B.3. Fluorescence increase of compound **1 (5 µM)** in PBS buffer in a quartz cuvette. The cuvette was irradiated with a polychromatic halogen lamp and the emission spectra were collected after the time periods indicated in the figure.

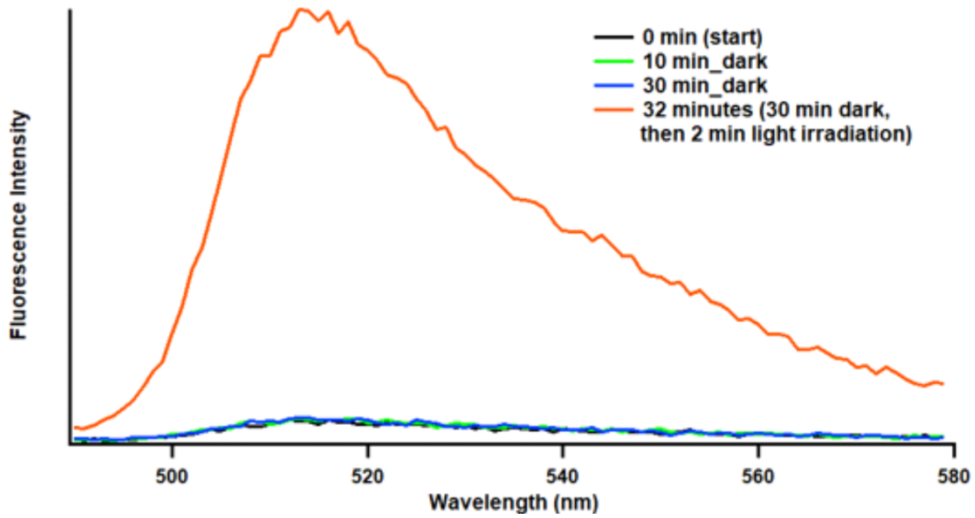

Figure B.4. Fluorescence spectra collected by dissolving 5 μM compound **3** in PBS buffer in a quartz cuvette. The cuvette was kept in dark and the time measuring was started at 0 min. Emission spectra were collected after 10 min and 30 min. After keeping the cuvette in the dark for 30 minutes, it was irradiated for 2 minutes with a polychromatic halogen lamp and the emission spectrum was collected.

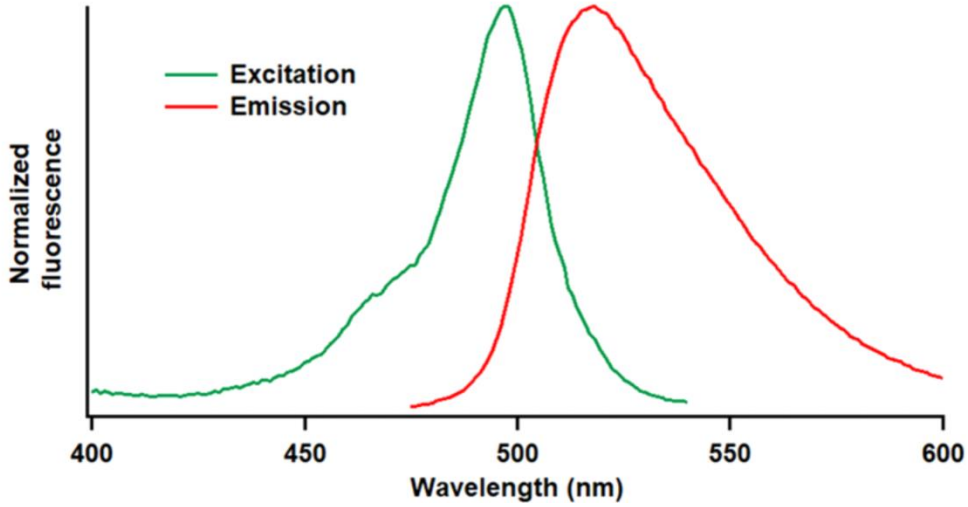

Figure B.5. Excitation and emission spectra of Compound **3** after irradiation for 30 minutes with a polychromatic halogen lamp. The excitation spectrum was collected using a fixed 550-nm emission wavelength, and the emission spectrum was collected using a fixed 450-nm excitation wavelength.

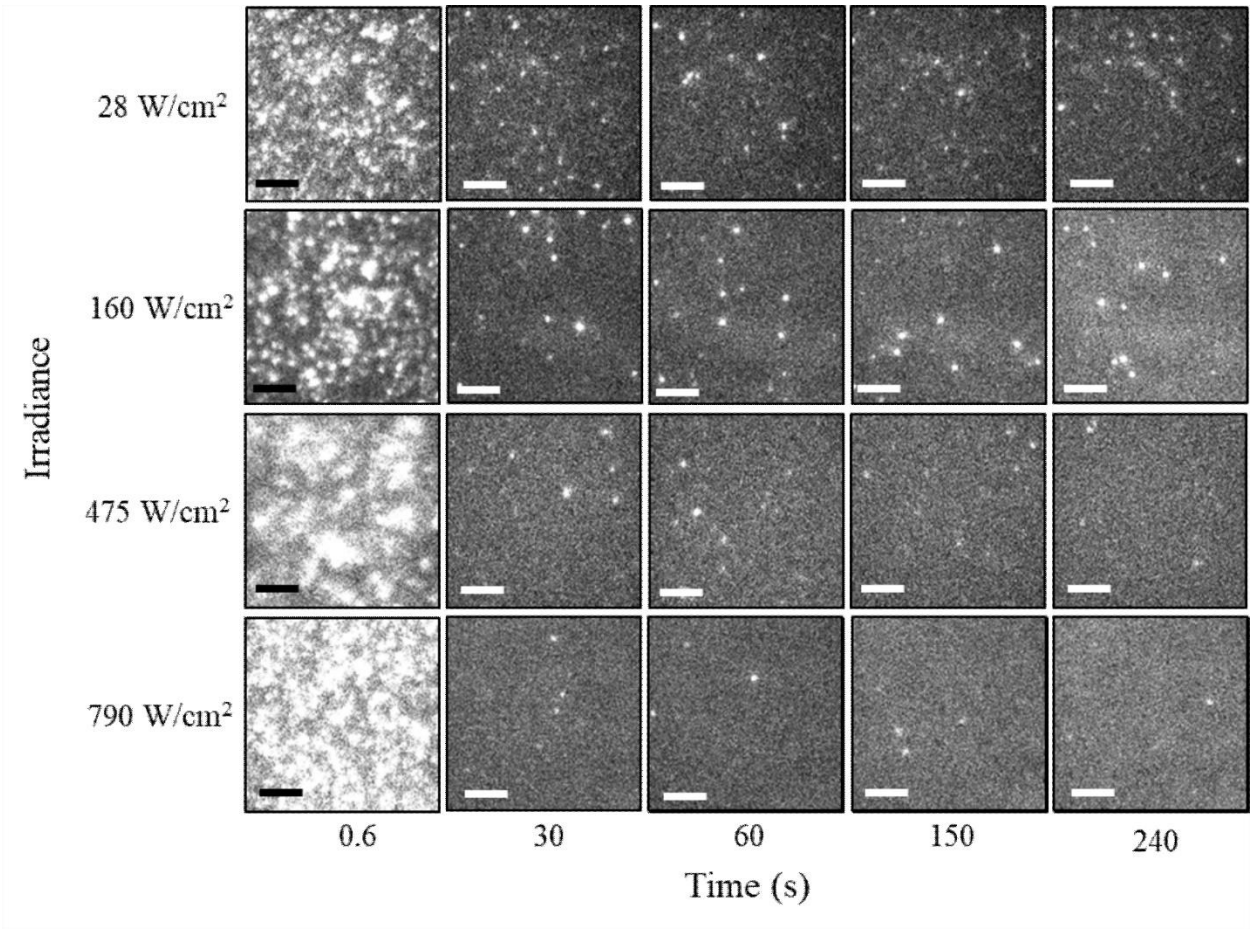

Figure B.6. Selected frames from movies collected at 28, 160, 475, and 790 W/cm^2 laser irradiances. Compound **3** was adsorbed on a cover glass and imaged in PBS buffer. The fluorescence signal is a result of the photoactivation of Compound **3**. Time 0.6 s shows the photoactivation of numerous molecules with the amount increasing with laser irradiance. At later times (after 3 s), the photoactivation events are sparse enough for accurate localization. All images are shown using the same intensity scale. Scale bar is 3 μm.

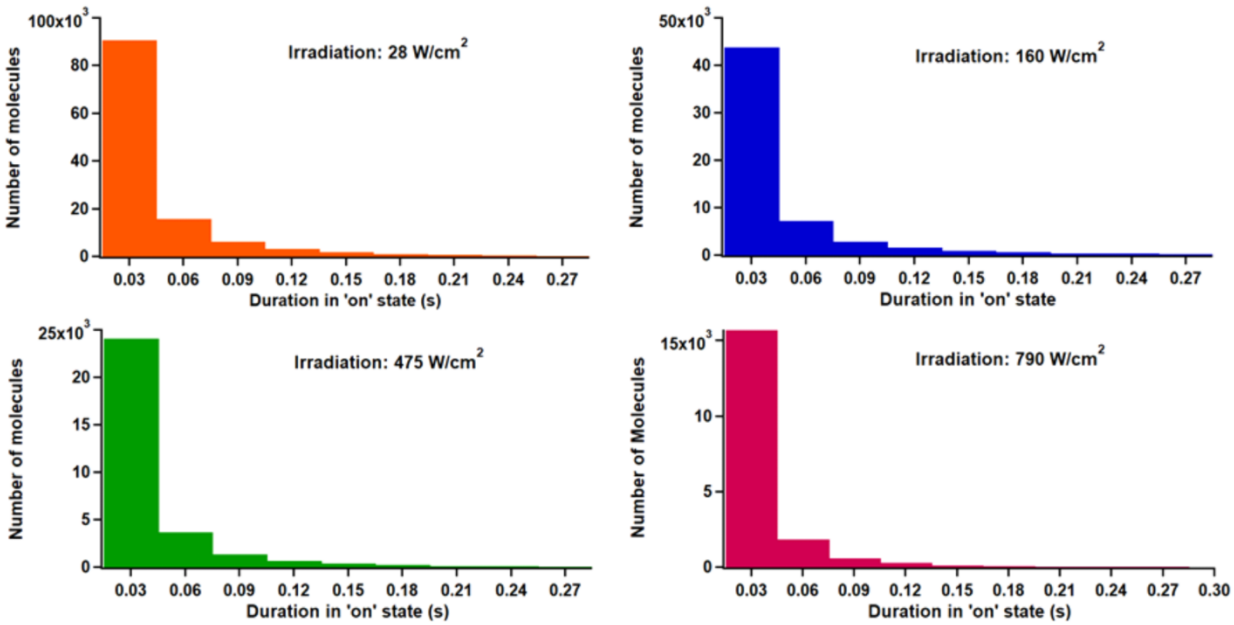

Figure B.7. Histograms of the time photoactivated compound **3** was in the 'on' state for each laser irradiance. Each frame in the movie was captured using a 0.03 s acquisition time (i.e., most molecules were in the 'on' state for only one frame).

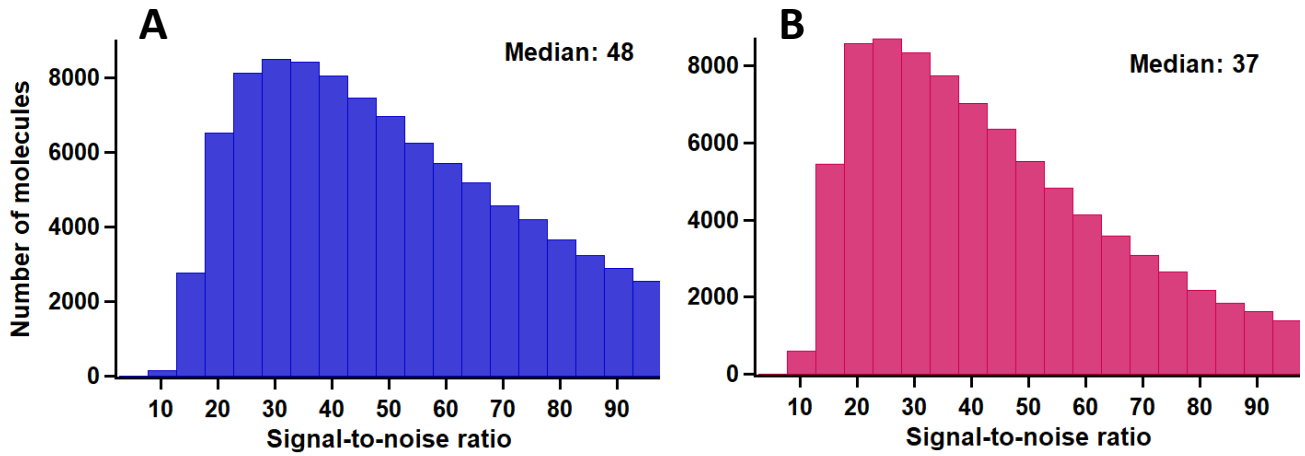

Figure B.8. Histograms of signal-to-noise ratio of compound **3** (A) adsorbed on a cover glass and (B) bound to microtubules in HeLa cells and imaged using a 488-nm laser line. The median values of the distributions are (A) 48 and (B) 37.

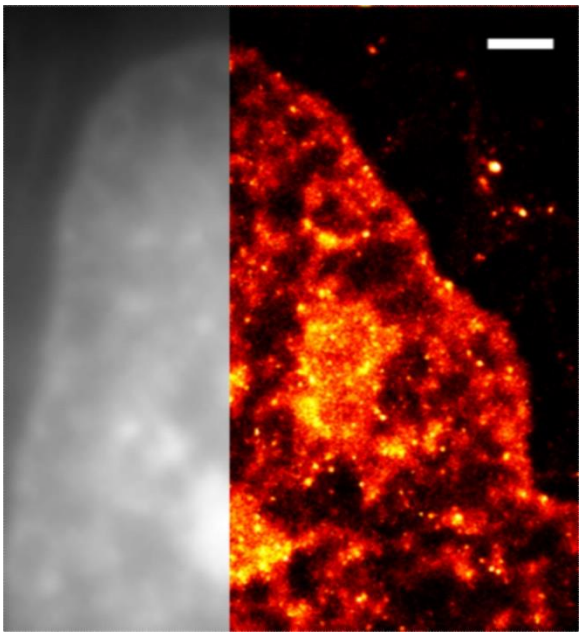

Figure B.9. SMLM image of the nuclear area of a glutaraldehyde fixed HeLa cell labeled with compound **3** (color scale). The gray scale image is the diffraction-limited image generated by summing all the images in the movie without localizing the fluorophores. PBS buffer was used as the imaging medium. Scale bar is 1 μm.

References

1. S. B. Choi, J.; Kim, Y., *Chemical Science* **2014**, *5*, 751-755.

2. R. Guy, Z. Scott, R. Sloboda, K. Nicolaou, *Chem Biol* **1996**, *3*, 1021-1031.

3. A. B. More, S. Mula, S. Thakare, N. Sekar, A. K. Ray, S. Chattopadhyay, *J Org Chem* **2014**, *79*, 10981-10987.

4. G. T. Dempsey, J. C. Vaughan, K. H. Chen, M. Bates, X. Zhuang, *Nat Methods* **2011**, *8*, 1027-1036.

5. M. Heilemann, S. van de Linde, A. Mukherjee, M. Sauer, *Angew Chem Int Ed Engl* **2009**, *48*, 6903-6908.

6. J. Folling, M. Bossi, H. Bock, R. Medda, C. A. Wurm, B. Hein, S. Jakobs, C. Eggeling, S. W. Hell, *Nat Methods* **2008**, *5*, 943-945.

7. T. Klein, A. Loschberger, S. Proppert, S. Wolter, S. van de Linde, M. Sauer, *Nat Methods* **2011**, *8*, 7-9.

8. M. Lehmann, G. Lichtner, H. Klenz, J. Schmoranzer, *J Biophotonics* **2016**, *9*, 161-170.

9. S. A. Jones, S. H. Shim, J. He, X. Zhuang, *Nat Methods* **2011**, *8*, 499-508.

10. J. B. Grimm, T. Klein, B. G. Kopek, G. Shtengel, H. F. Hess, M. Sauer, L. D. Lavis, *Angew Chem Int Ed Engl* **2016**, *55*, 1723-1727.

11. B. Roubinet, M. Bischoff, S. Nizamov, S. Yan, C. Geisler, S. Stoldt, G. Y. Mitronova, V. N. Belov, M. L. Bossi, S. W. Hell, *J Org Chem* **2018**, *83*, 6466-6476.

12. D. Pan, Z. Hu, F. Qiu, Z. L. Huang, Y. Ma, Y. Wang, L. Qin, Z. Zhang, S. Zeng, Y. H. Zhang, *Nat Commun* **2014**, *5*, 5573.

13. H. He, Z. Ye, Y. Zheng, X. Xu, C. Guo, Y. Xiao, W. Yang, X. Qian, Y. Yang, *Chem Commun (Camb)* **2018**, *54*, 2842-2845.

14. J. Folling, V. Belov, R. Kunetsky, R. Medda, A. Schonle, A. Egner, C. Eggeling, M. Bossi, S. W. Hell, *Angew Chem Int Ed Engl* **2007**, *46*, 6266-6270.

15. E. Deniz, M. Tomasulo, J. Cusido, I. Yildiz, M. Petriella, M. L. Bossi, S. Sortino, F. M. Raymo, *J Phys Chem C* **2012**, *116*, 6058-6068.

16. S. van de Linde, A. Loschberger, T. Klein, M. Heidbreder, S. Wolter, M. Heilemann, M. Sauer, *Nat Protoc* **2011**, *6*, 991-1009.

17. M. Ovesny, P. Krizek, J. Borkovec, Z. Svindrych, G. M. Hagen, *Bioinformatics* **2014**, *30*, 2389-2390.

18. R. E. Thompson, D. R. Larson, W. W. Webb, *Biophys J* **2002**, *82*, 2775-2783.

APPENDIX C. SUPPORTING INFORMATION FOR CHAPTER 3

Qualitative photorelease of alcohols followed by ^{1}H NMR

Samples for NMR qualitative release studies were prepared by dissolving 1-10 mg of sample in 1 mL 50:50 deuterated methanol with either deuterated chloroform or deuterated DMSO. NMR solutions were then irradiated with a 500W white halogen lamp and spectra were taken at varying time intervals. Solvent peaks were removed and spectra were zoomed in to show the relevant peaks. Presence of release product was confirmed by spiking with known standards.

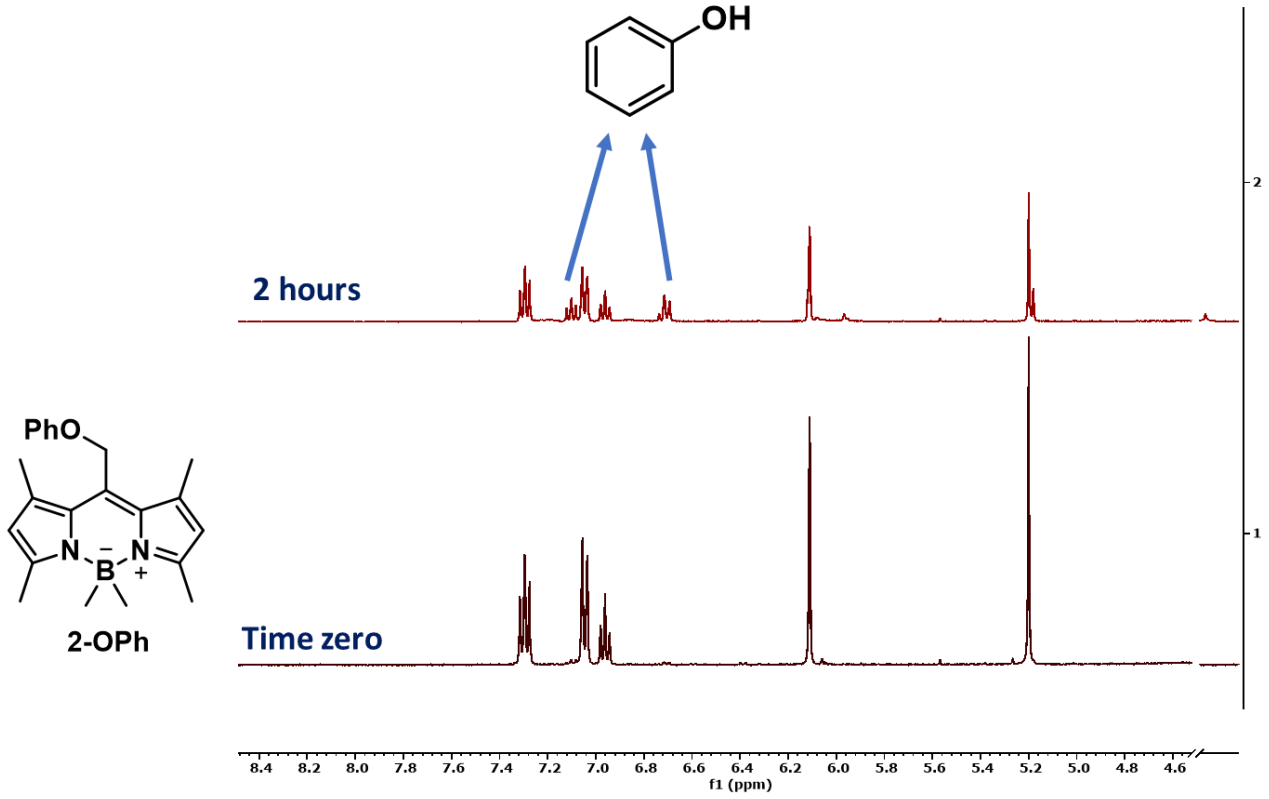

Figure C.1. Photorelease of phenol from **2-OPh**

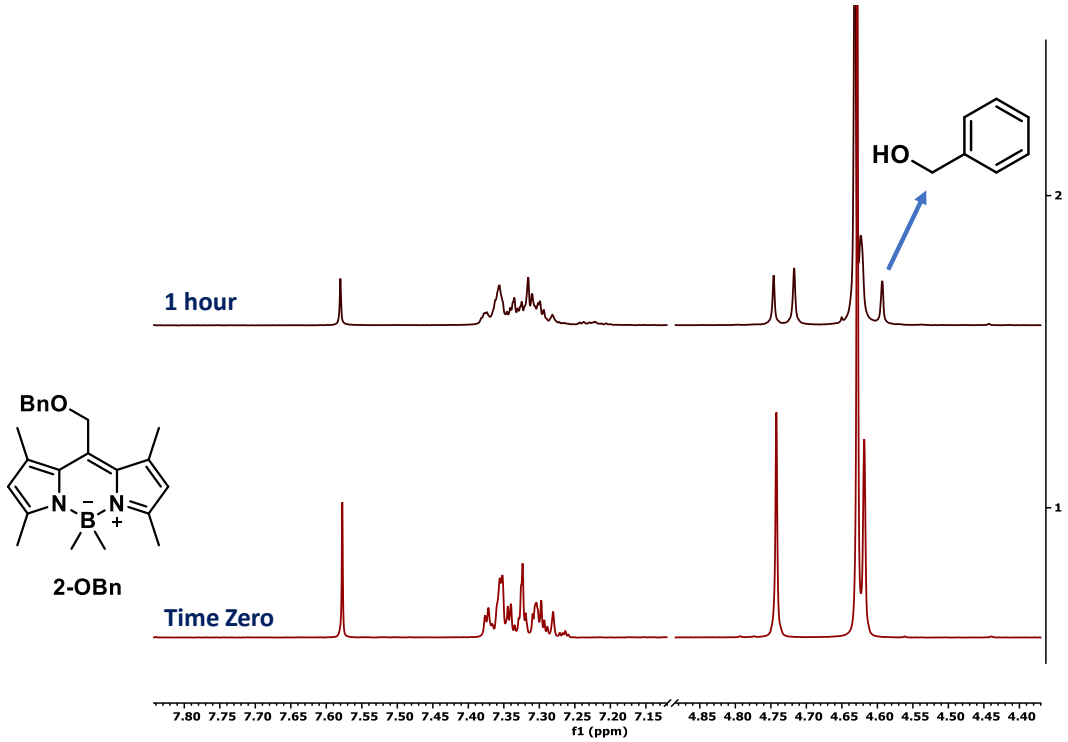

Figure C.2. Photorelease of benzyl alcohol from **2-OBn**

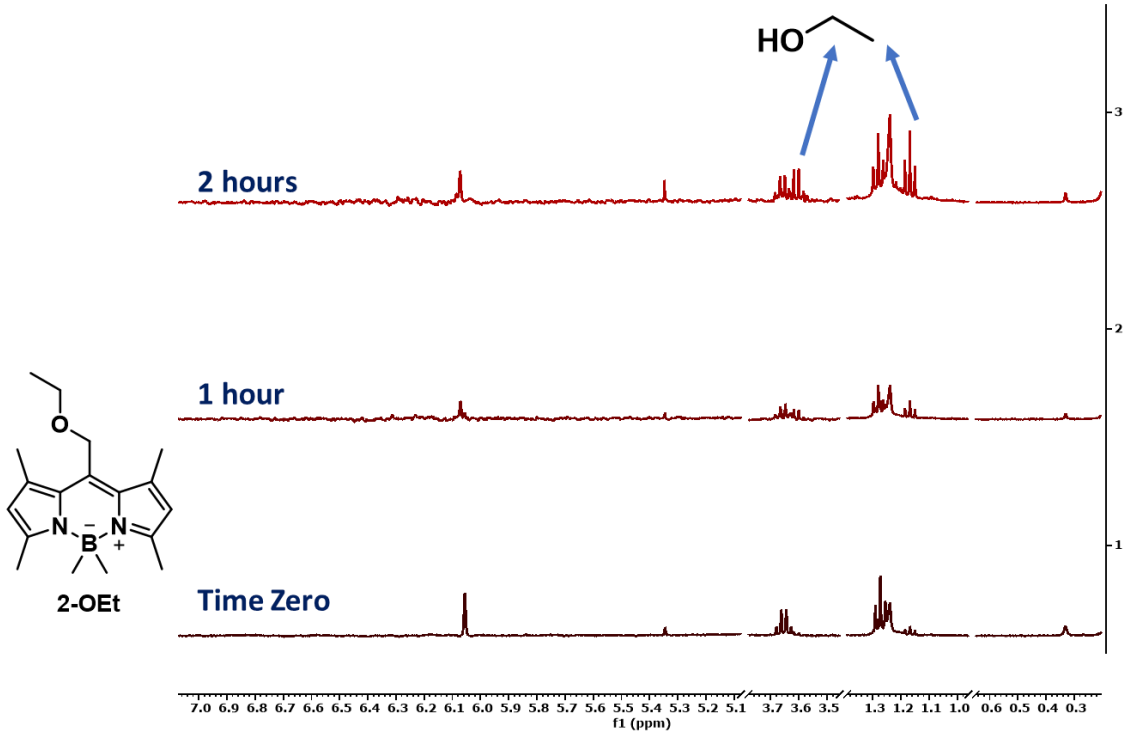

Figure C.3. Photorelease of ethanol from **2-OEt**

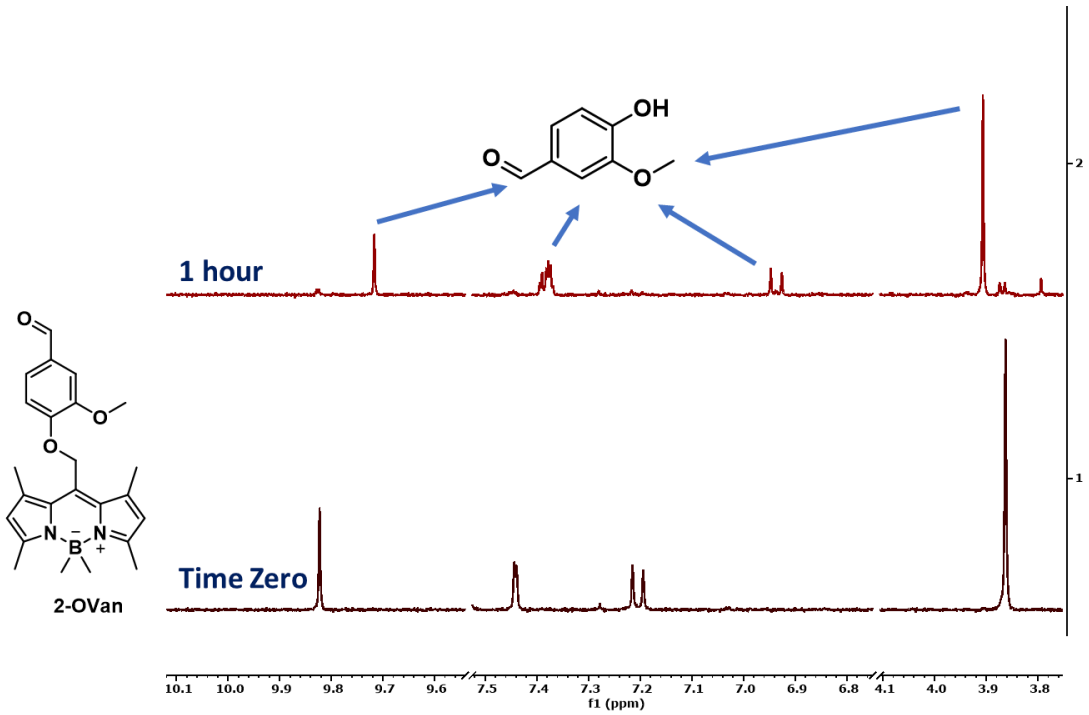

Figure C.4. Photorelease of vanillin from **2-OVan**

A photorelease curiosity: formation of benzaldehyde only with laser irradiation

When solutions for quantum yield studies were prepared in 50:50 deuterated dimethylsulfoxide and methanol, benzaldehyde appeared in the NMR spectra after irradiation with the 532 nm Nd:YAG laser. This effect had not been previously observed in samples irradiated with white light or green LED. At this time, the mechanism for this oxidation is unknown. It is also unclear why this benzaldehyde product is only observed with laser irradiation but not lamp or LED irradiation, and only in certain solvent systems.

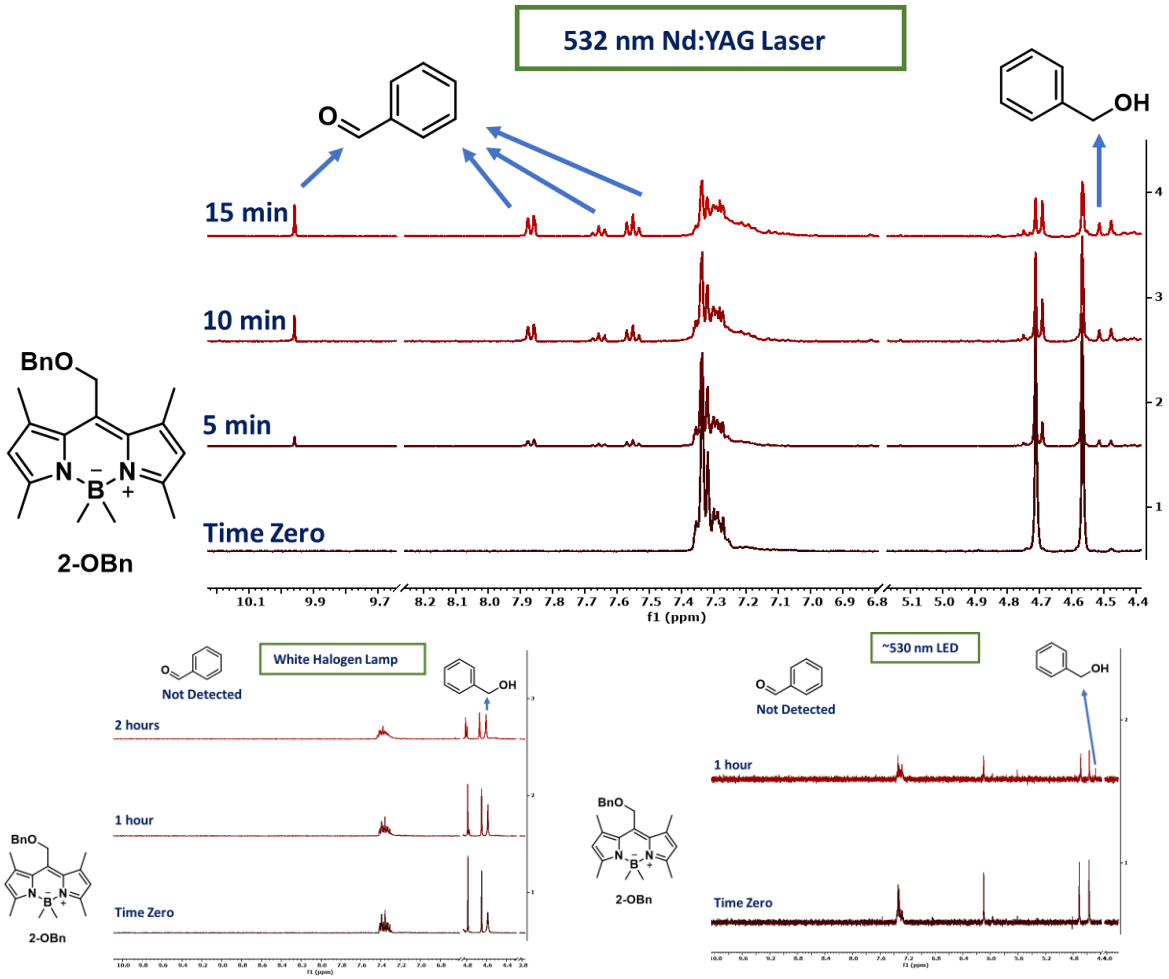

Figure C.5. Photorelease of benzyaldehyde in conjunction with benzyl alcohol upon irradiation with a 532 nm Nd:YAG laser (top). Photorelease of benzyl alcohol with no detection of benzaldehyde with irradiation of **2-OBn** with a white halogen lamp or a 530 nm LED (bottom left and right, respectively)

Ratios of benzaldehyde:benzyl Alcohol upon irradiation of compound 4

1 mM solutions of compound **4** were prepared in the following deuterated solvents. Solutions were transferred to cuvettes and irradiated with the Nd:Yag 532 nm laser for 5 minutes or with the lower intensity light sources for 2 h. In all cases the conversion was less than 10% except for the case of the mixture of chloroform and methanol, which went to completion within 5 minutes of irradiation with no benzaldehyde observed.

Table C.1 Ratios of benzaldehyde to benzyl alcohol upon irradiation of **2-OBn** with a 532 nm Nd:YAG laser in different solvent systems

Solvent and Light	Ratio of benzaldehyde: benzyl alcohol
Laser DMSO:MeOH	2:1
Laser ACN:MeOH	4:1
Laser CDCl3:MeOH	0:1

Quantum yields were determined in a methanol:chloroform mixture because of the absence of benzaldehyde. More studies need to be done to determine the mechanism for the formation of benzaldehyde.

Photodegradation of Iodinated Compounds Upon Irradiation

The photodegradation of the samples for quantum yield studies were determined based on the DMS internal standard. While **3-OPh** has a lower quantum yield of photorelease, it photodegrades faster than **2-OPh**. This suggests that the iodines on the photocage contribute to nonproductive photoreactions.

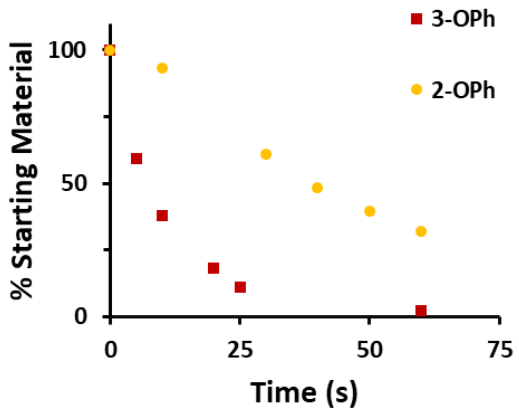

Figure C.6. Photodecomposition of **3-OPh** and **2-OPh** indicating that even though the quantum yield of release is higher for **2-OPh**, **3-OPh** is undergoing photodecomposition at a faster rate

Cell Studies

Preparation of cells for microscopy experiments. The photoactivation of **2-Cou** was studied in the

human cervical cancer HeLa cell line. HeLa cells were maintained in a water jacketed CO_2 incubator at 37 ^oC with DMEM medium supplemented with 10 % fetal bovine serum, 12.5 mM streptomycin, and 36.5 mM penicillin. Cells were sub-cultured on custom-made glass-bottom dishes and incubated a day before performing the microscopy experiments. On the day of the microscopy studies, the growth medium was replaced with 25 µM **2-Cou** (or 7-hydroxy coumarin) in serum-free DMEM medium and incubated at 37 ^oC for 15 minutes. Cells were then rinsed three times with HEPES imaging buffer (pH=7.2, 155 mM NaCl, 5 mM KCl, 2 mM $CaCl_2$, 1 mM $MgCl_2$, 2 mM NaH_2PO_4, 10 mM HEPES and 10 mM Glucose) and imaged in the imaging buffer.

Microscopy studies. Fluorescence imaging experiments were performed on a Nikon Eclipse TE2000U microscope (Melville, NY) operating in wide-field, epi-fluorescence mode and equipped with a 100×Apo, 1.49-numerical-aperture oil-immersion objective. Samples were illuminated with a mercury lamp (X-cite 120 PC, EXFO Photonic Solutions Inc, Canada) and the fluorescence images were collected using a PhotonMAX 512 EMCCD camera (Princeton Insruments, NJ). Images were further analyzed with ImageJ program (National Institute of Health). **2-Cou** or 7-hydroxy coumarin treated cells were irradiated using a 365 ± 18 nm filter and the emission was collected with a 450 ± 50 nm filter (Omaga Optical, VT). A series of fluorescence images were collected with 100 ms acquisition time per image. To demonstrate the green light photoactivation of **2-Cou**, the cells were irradiated with 510 ± 10 nm light. Images were collected every 10 seconds using 365 ± 18 nm excitation and 450 ± 50 nm emission filters with 100 ms image acquisition time (images taken after green light irradiation below).

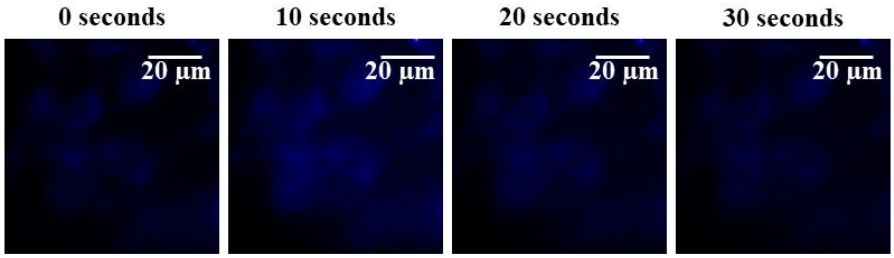

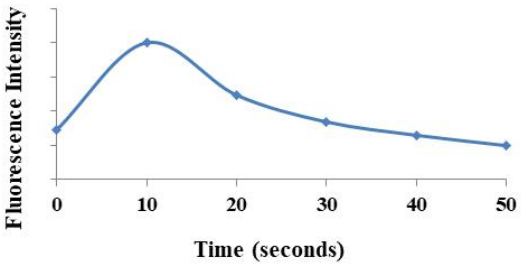

Figure C.7. Change in fluorescence of HeLa cells incubated with **2-OCou** at 450 nm (collected with short 365 nm excitation) after periods of irradiation with 510 nm light

Cytotoxicity study. Cytotoxicity of **2-Cou** in Hela cells were determined using Trypan blue exclusion assay. Hela cells were treated with 25 µM **2-Cou** in DMEM medium for 15 minutes. Cells were trypsinized and equal volumes of cell suspension and 0.4 % Trypan blue dye were incubated at room temperature for 2 minutes. Cells that excluded the dye were considered to be viable cells. The viable cell percentage was measured using a hemacytometer and an optical microscope. No significant decrease in cell viability was observed for the **2-Cou** treated cells (92 ± 2 %) compared to the control cells that were not treated with **2-Cou** (94 ± 5 %).

Percent yields of phenol and benzyl alcohol Release

2 mM solutions of the BODIPY ethers dissolved in 1 mL of 1:1 CD_3OD:$CDCl_3$ with dimethyl sulfone as an internal standard were irradiated in glass NMR tubes with a 500 W halogen lamp using a 500 mL beaker of water between the sample to filter out IR and with fans blowing on the sample and the lamp to prevent overheating. NMRs were taken over time and the percent release of the alcohols were calculated based on the relative integration with dimethyl sulfone.

When the B-methylated derivatives were irradiated, there was fast release at first (28% in the first hour) after which the rate of release dropped off. At the same time, the methyls on the boron disappeared and the remaining BODIPY peaks shifted (example of "b" shown below). Previously we have seen that the methyls on the boron can be exchanged for solvent with decent efficiency.[1] We believe that this is happening in this case and resulting in a slower secondary release pathway. Importantly, release is still occurring (albeit slowly) after **2-OBn** has been completely consumed.

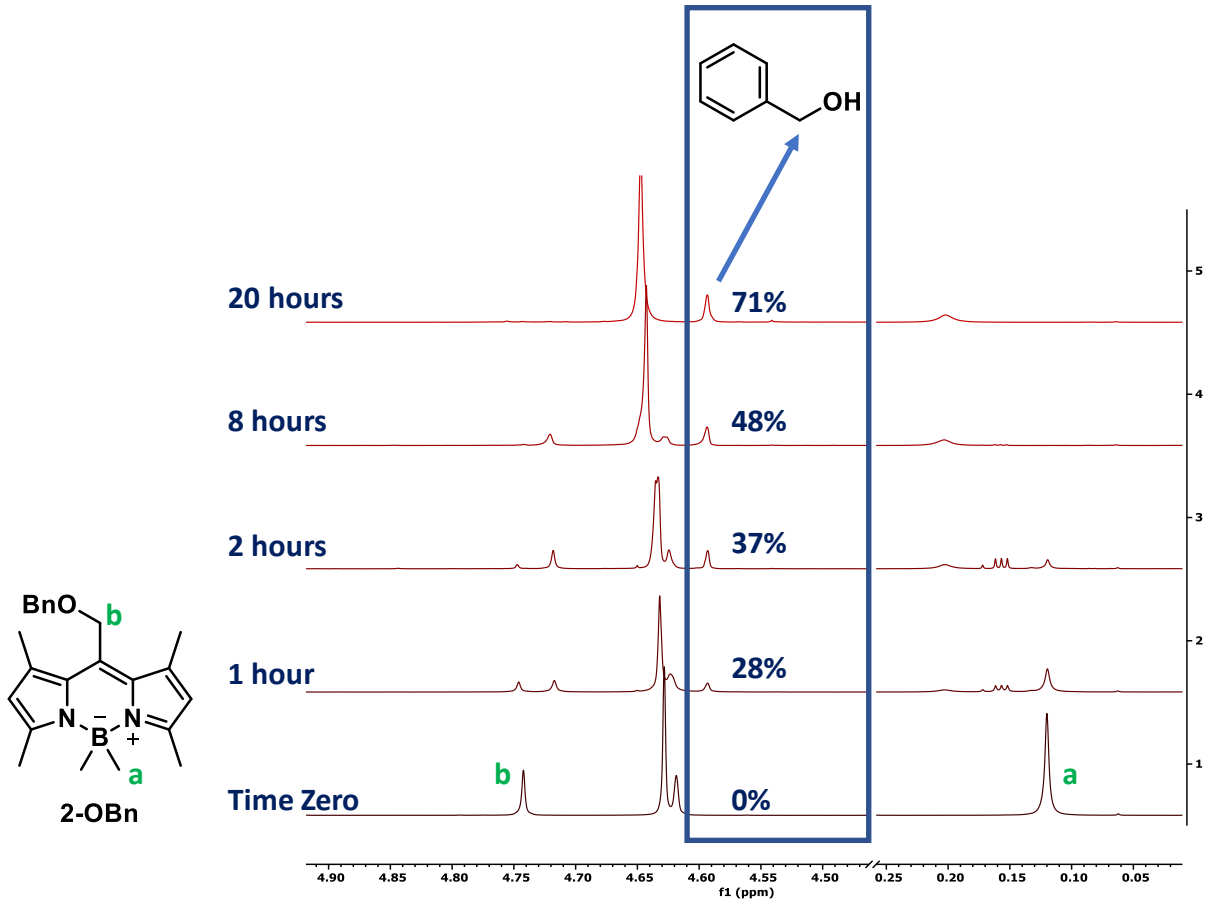

Figure C.8. [1]HNMR before and after intervals of irradiation of **2-OBn** with a 500 W halogen lamp. Percents shown are percent release of benzyl alcohol over time. Peak a and b correspond to the methyls on the boron and the methylene of the BODIPY ether, respectively. Both decrease over time. A new peak near the methylene peak grows in, which may correspond to the compound where the methyls on the boron have been substituted with solvent.

Characterization of New Compounds

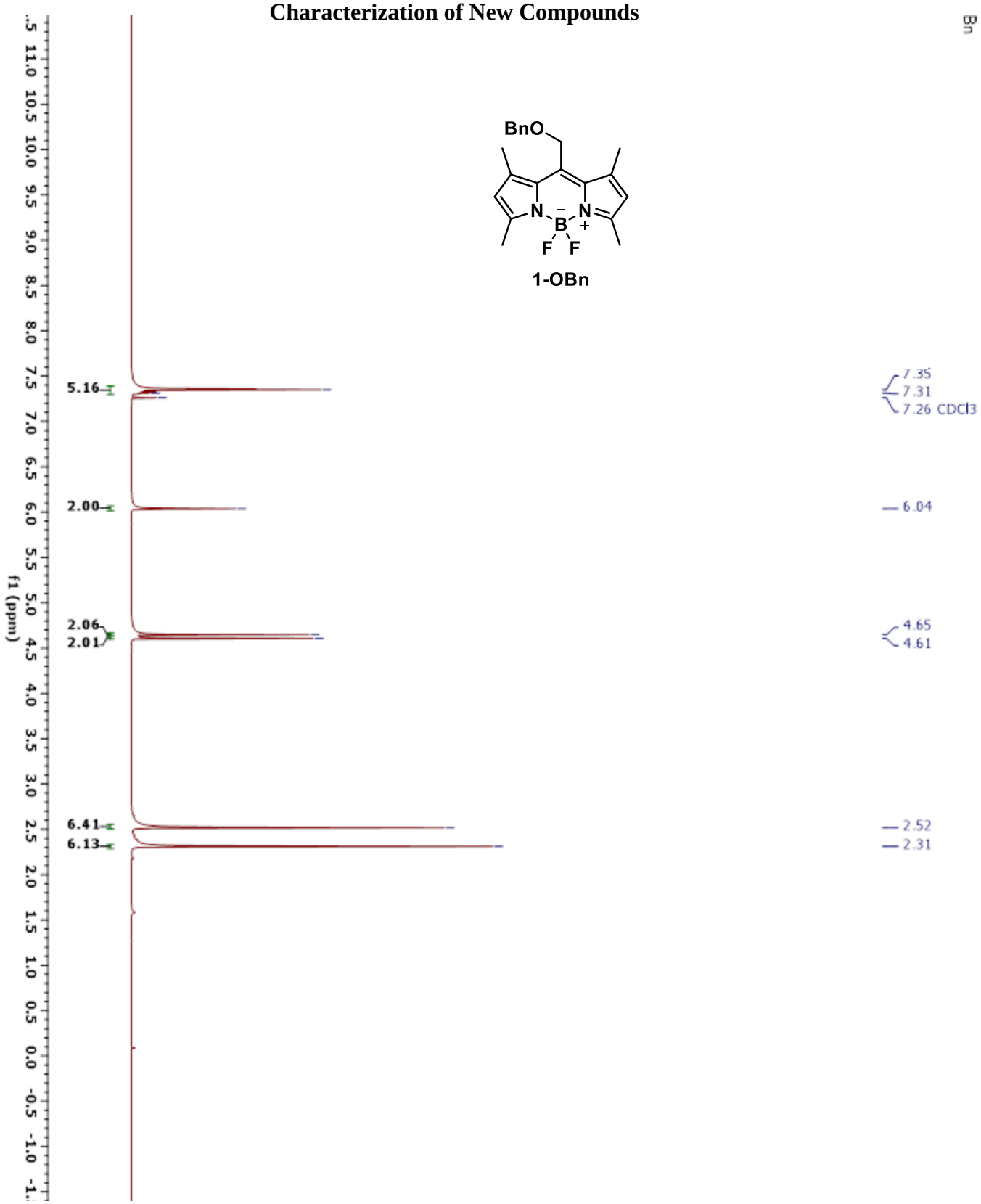

^{13}C NMR (400 MHz, $CDCl_3$)

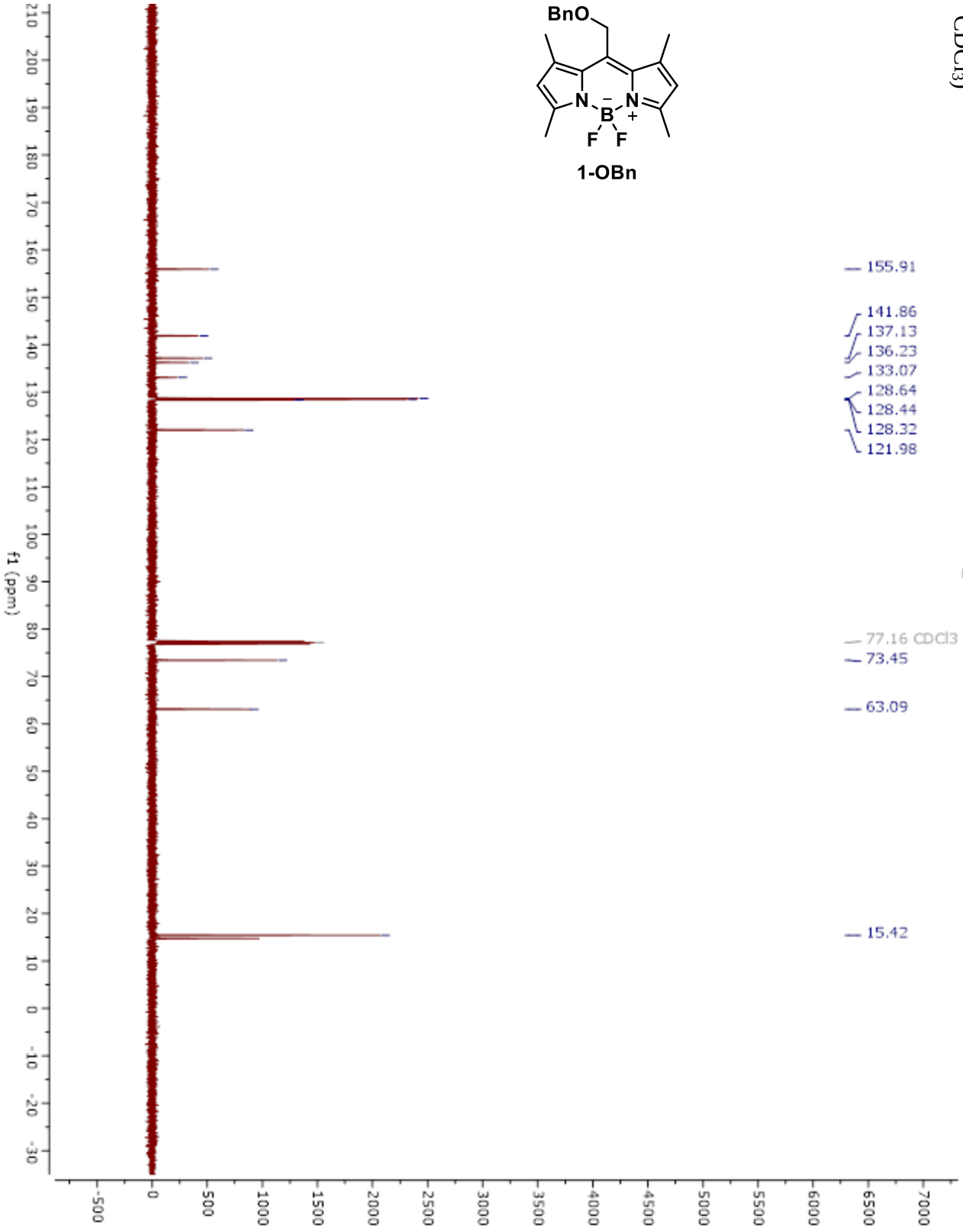

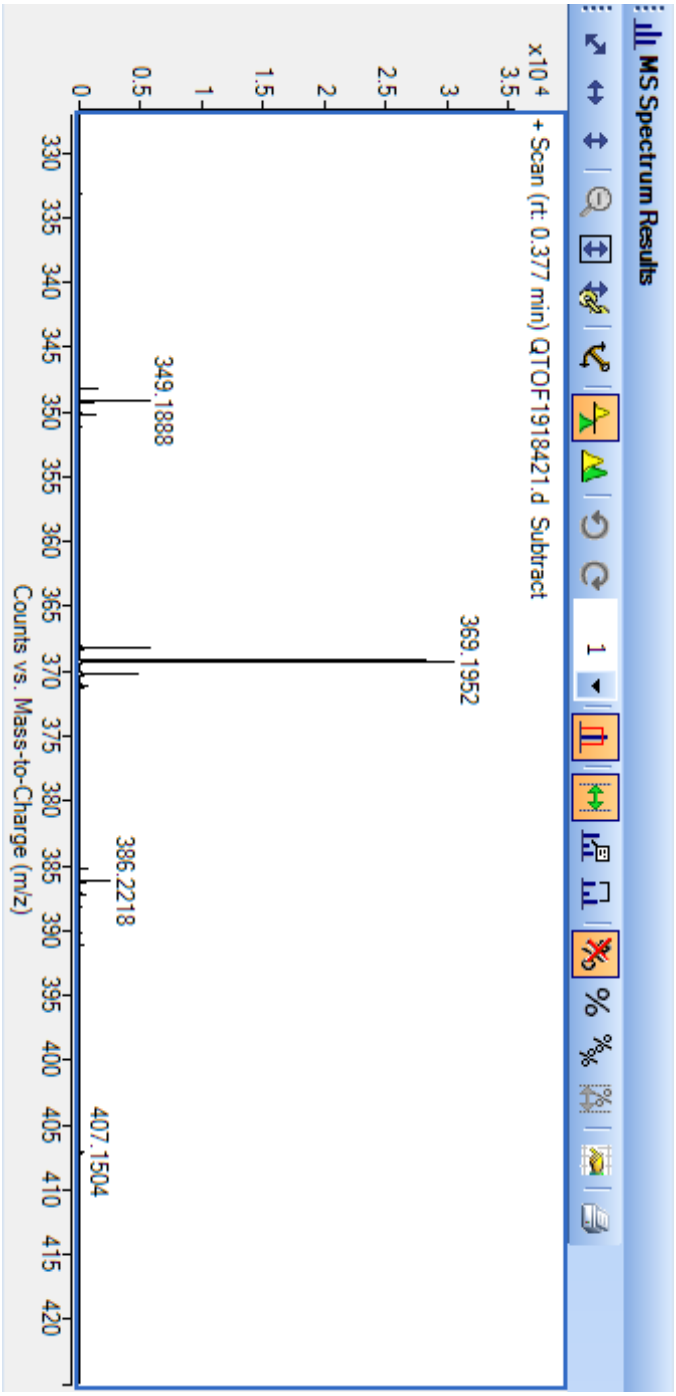

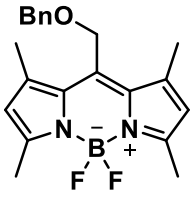

1-OBn

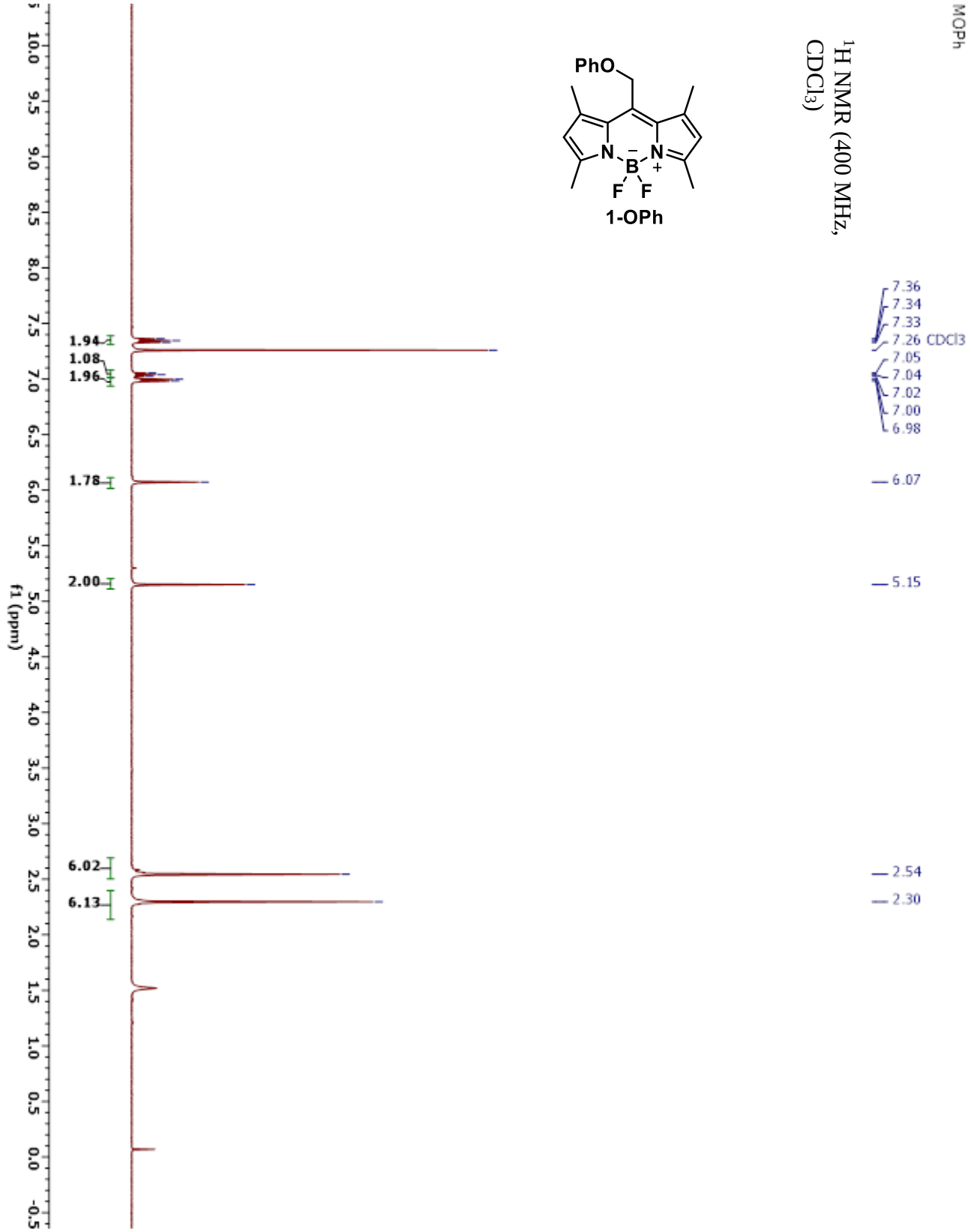

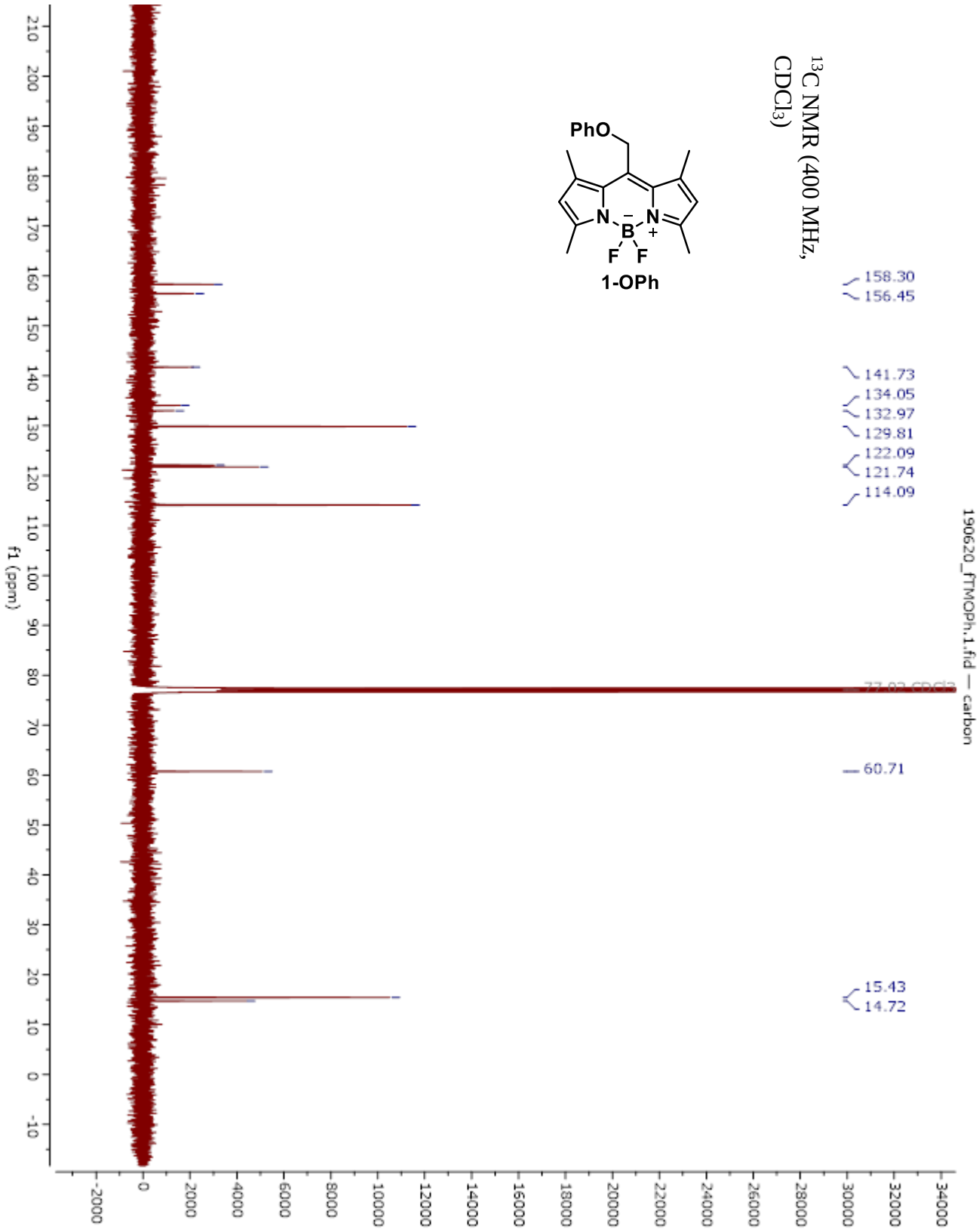

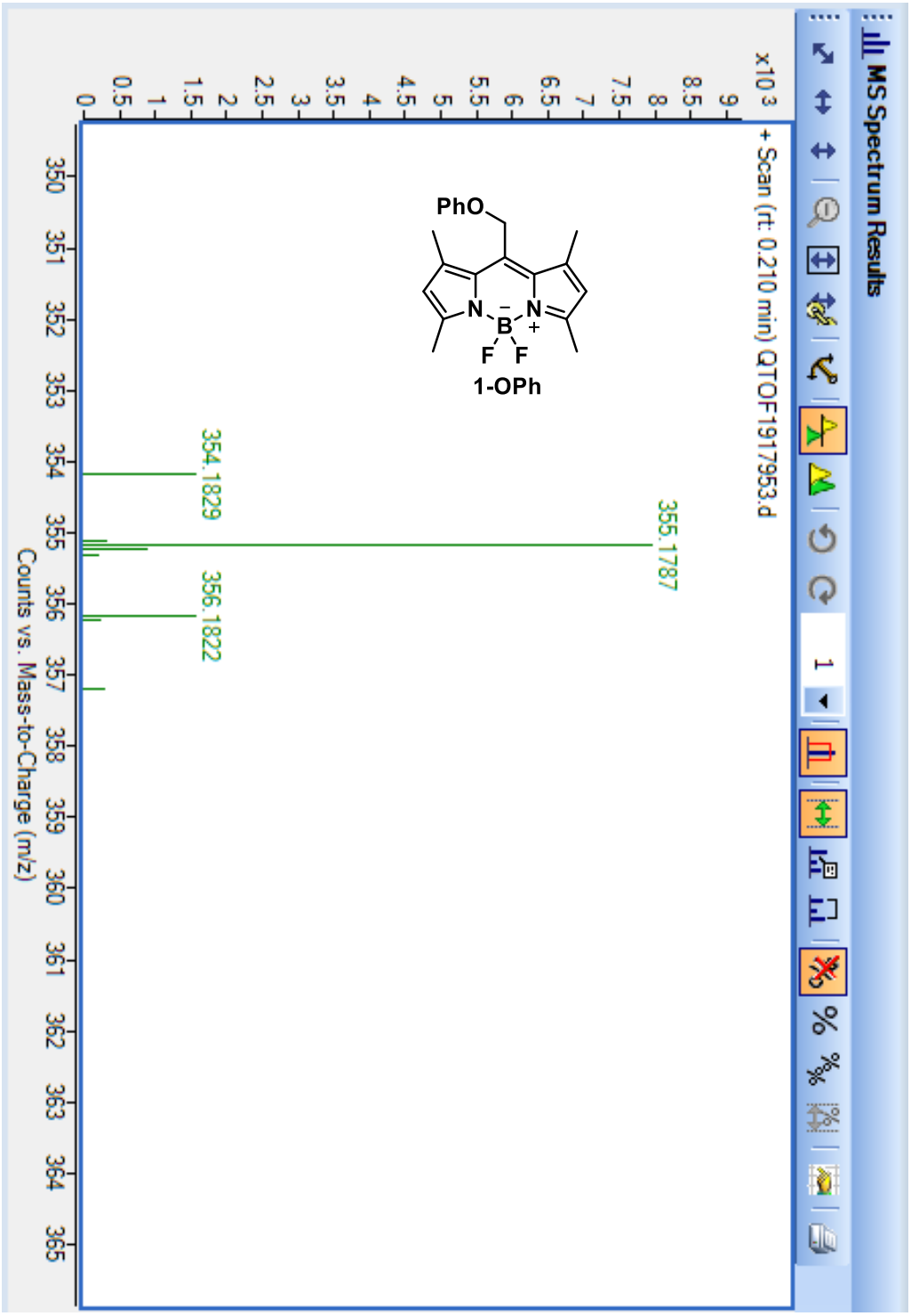

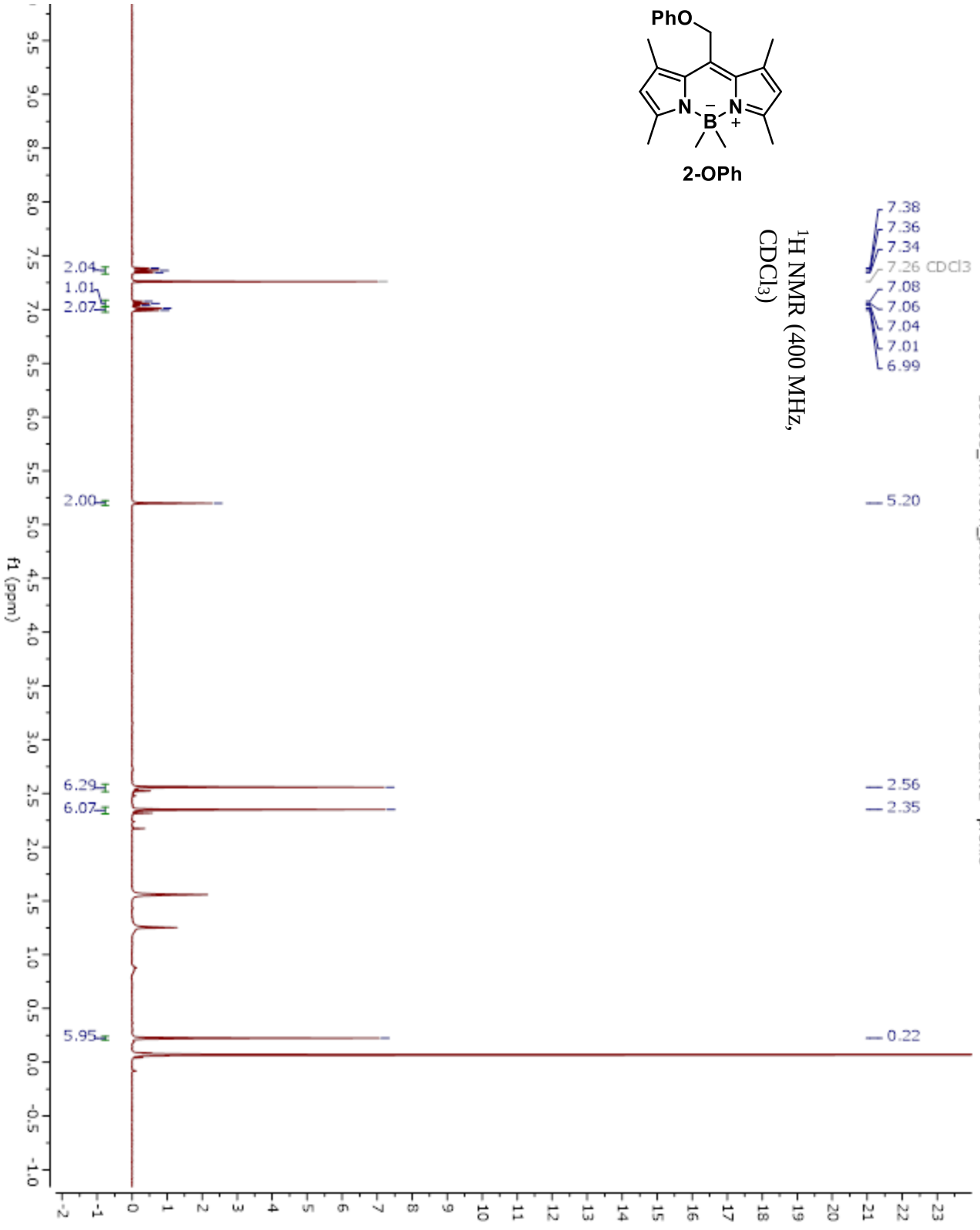

^{13}C NMR (400 MHz, $CDCl_3$)

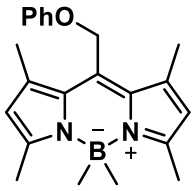

2-OPh

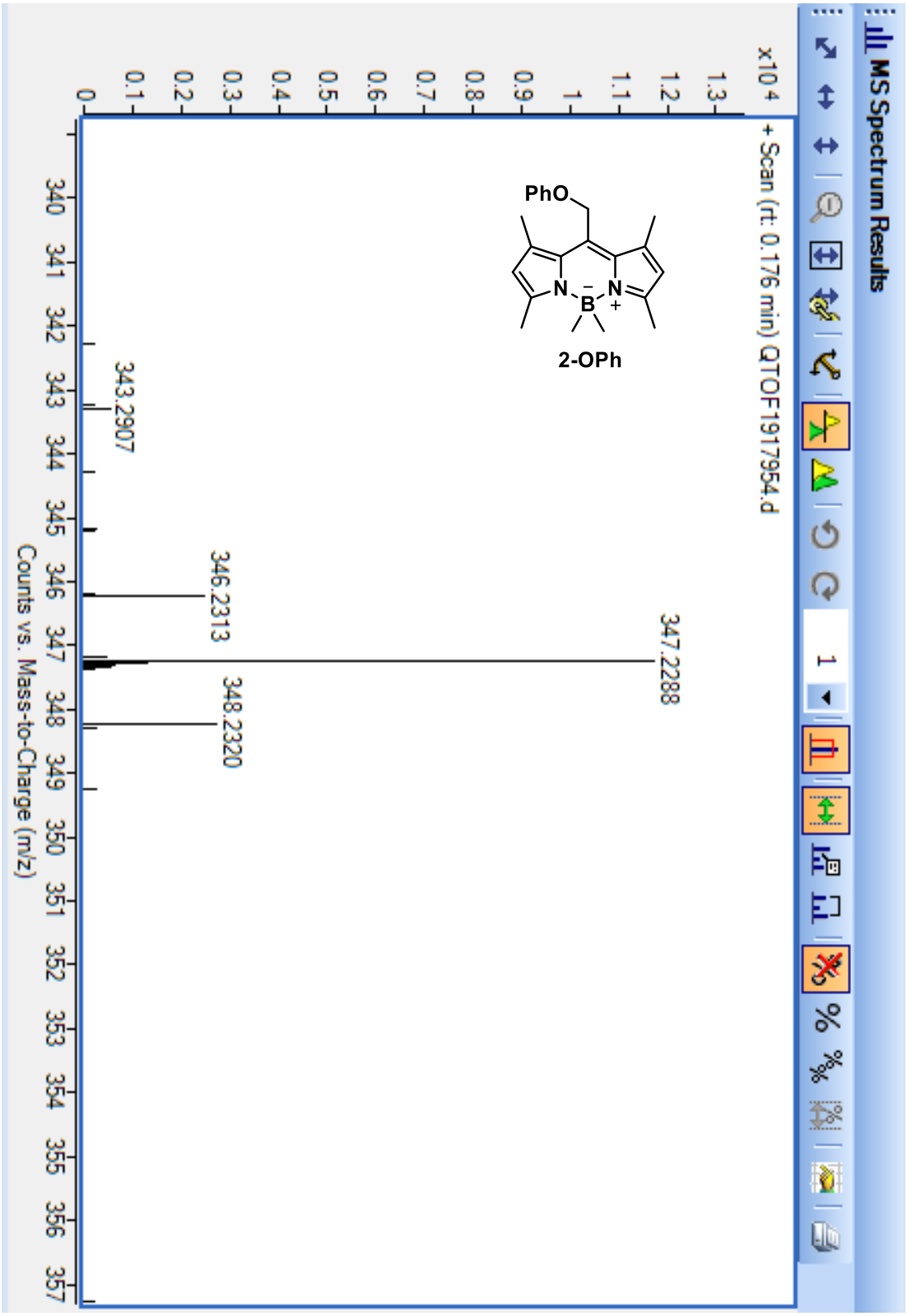

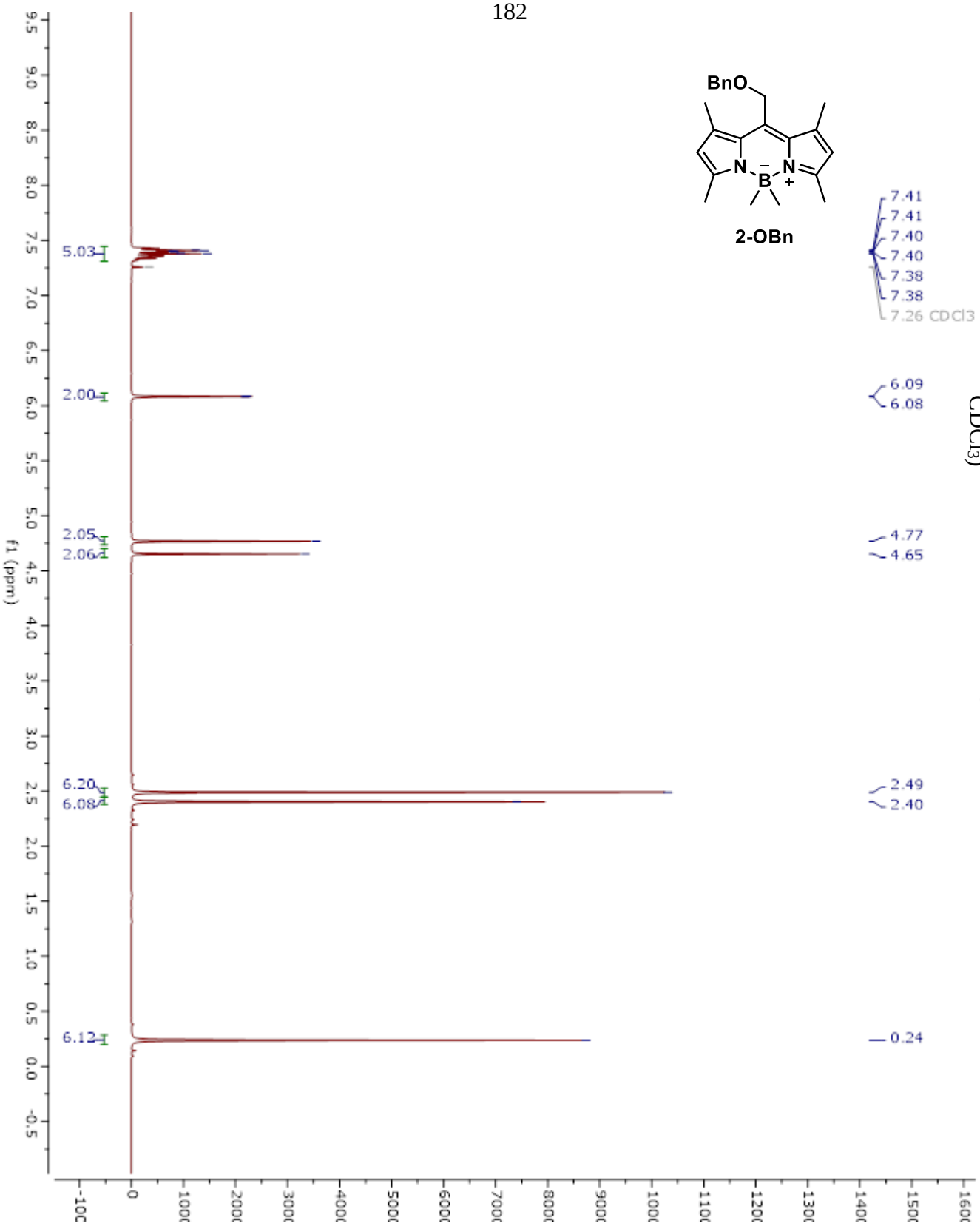

^{1}H NMR (400 MHz, $CDCl_3$)

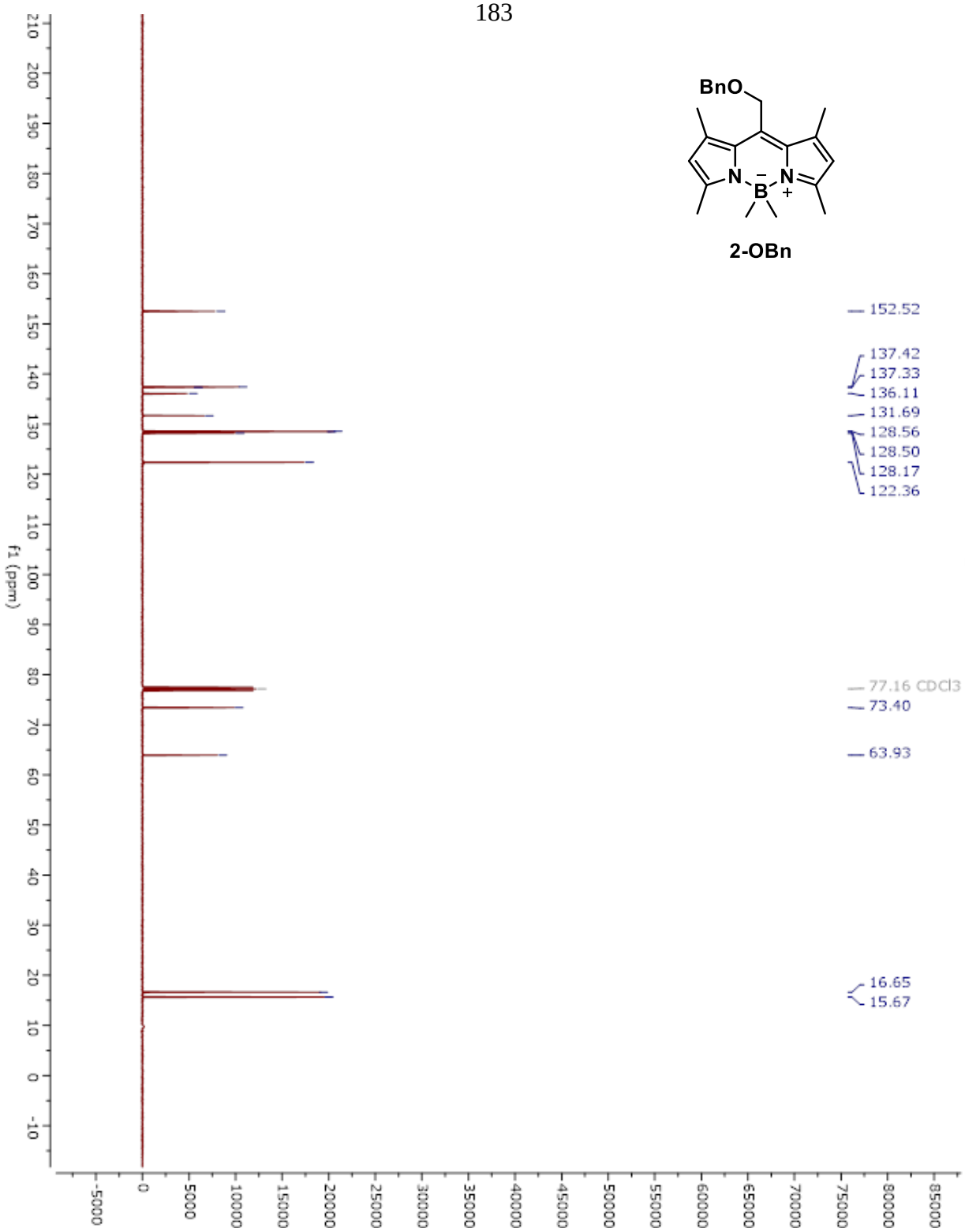

^{13}C NMR (400 MHz, $CDCl_3$)

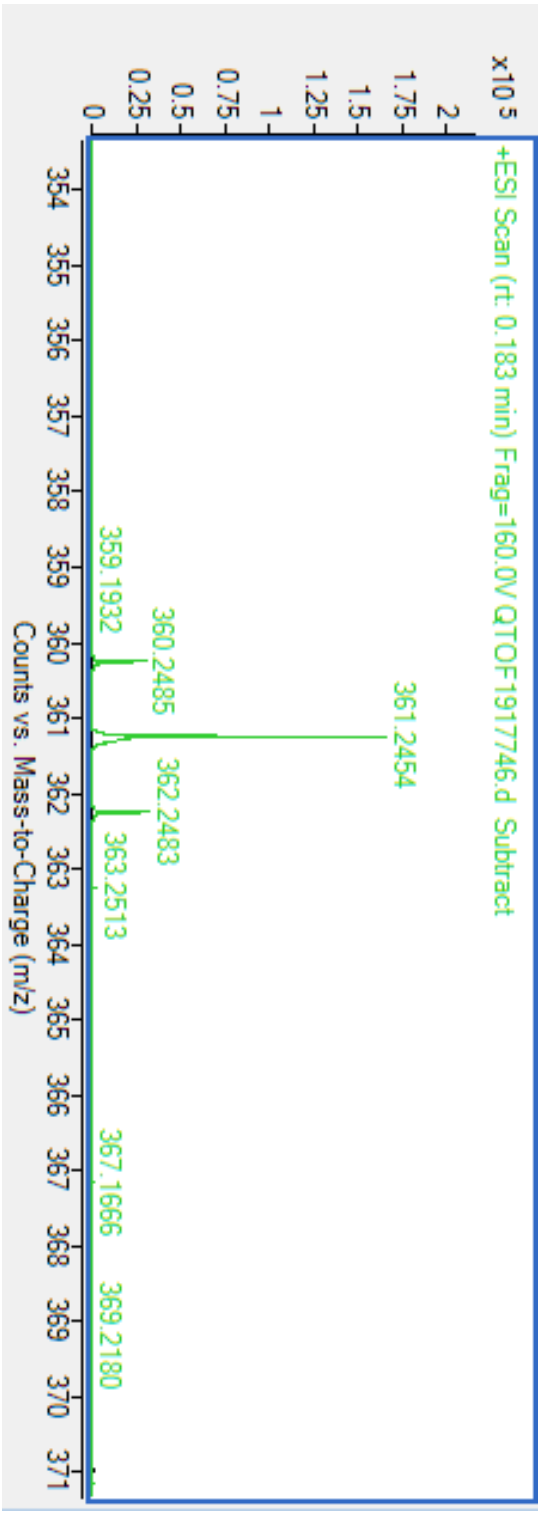

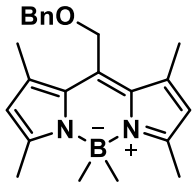

2-OBn

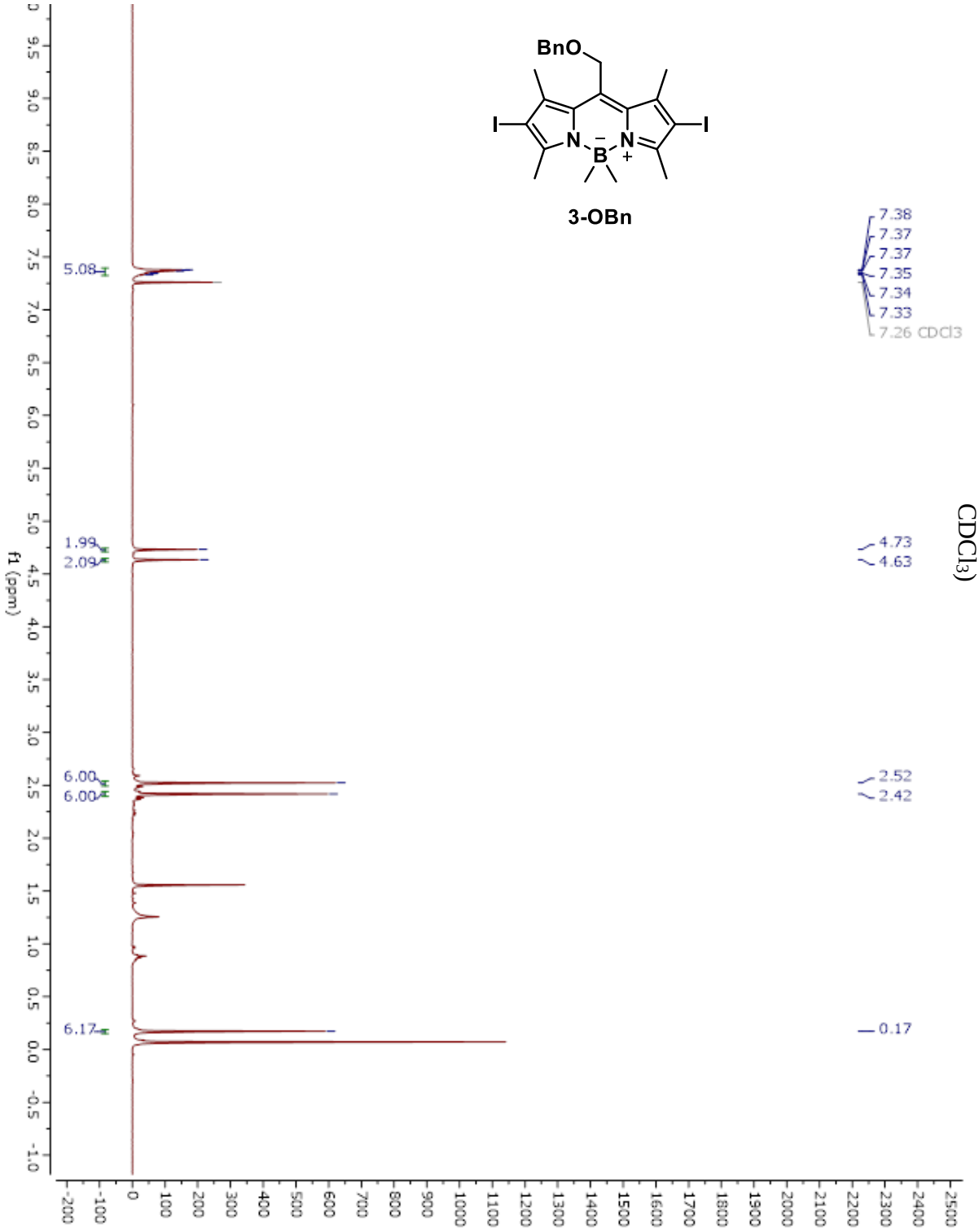

^{1}H NMR (400 MHz, $CDCl_3$)

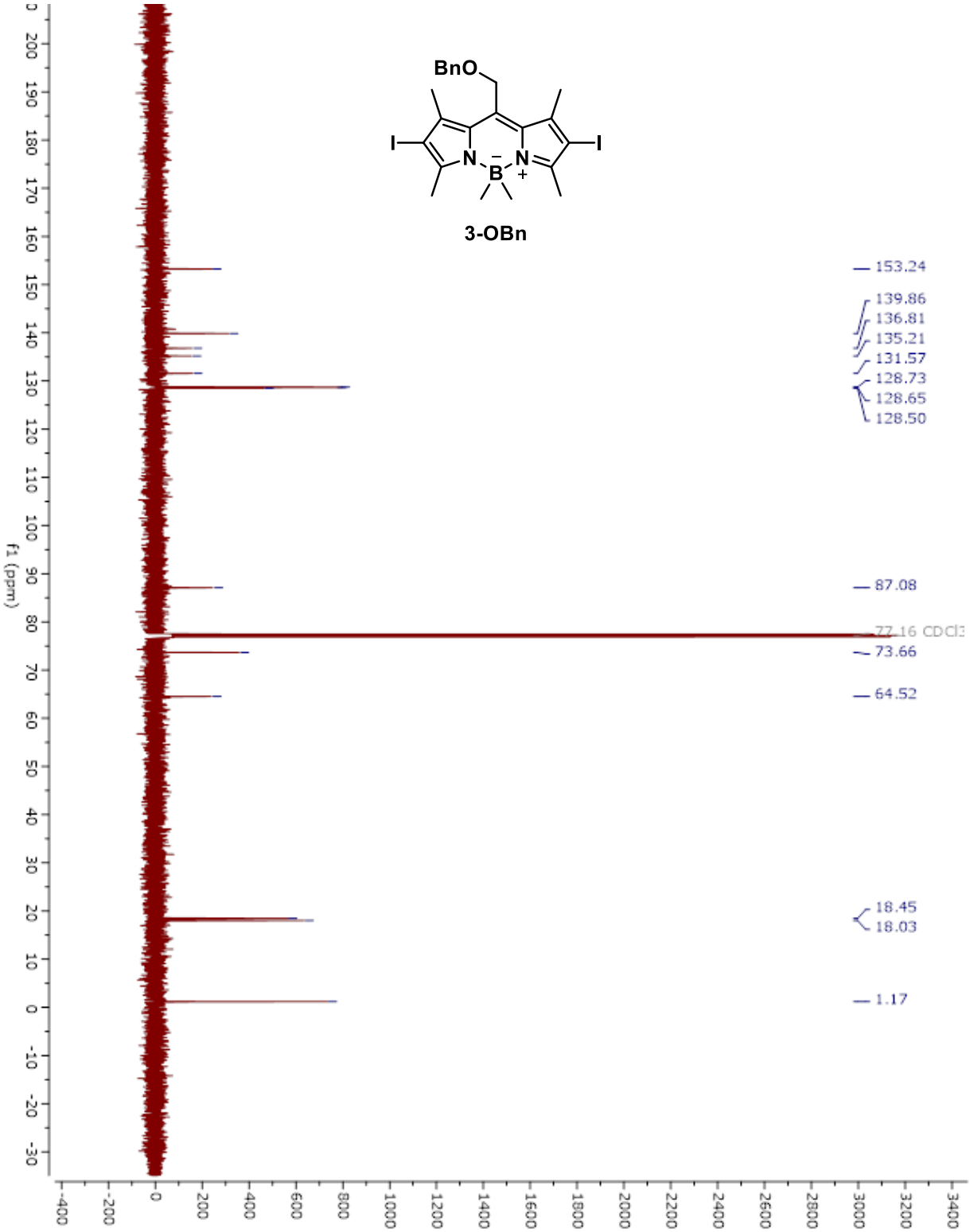

^{13}C NMR (400 MHz, $CDCl_3$)

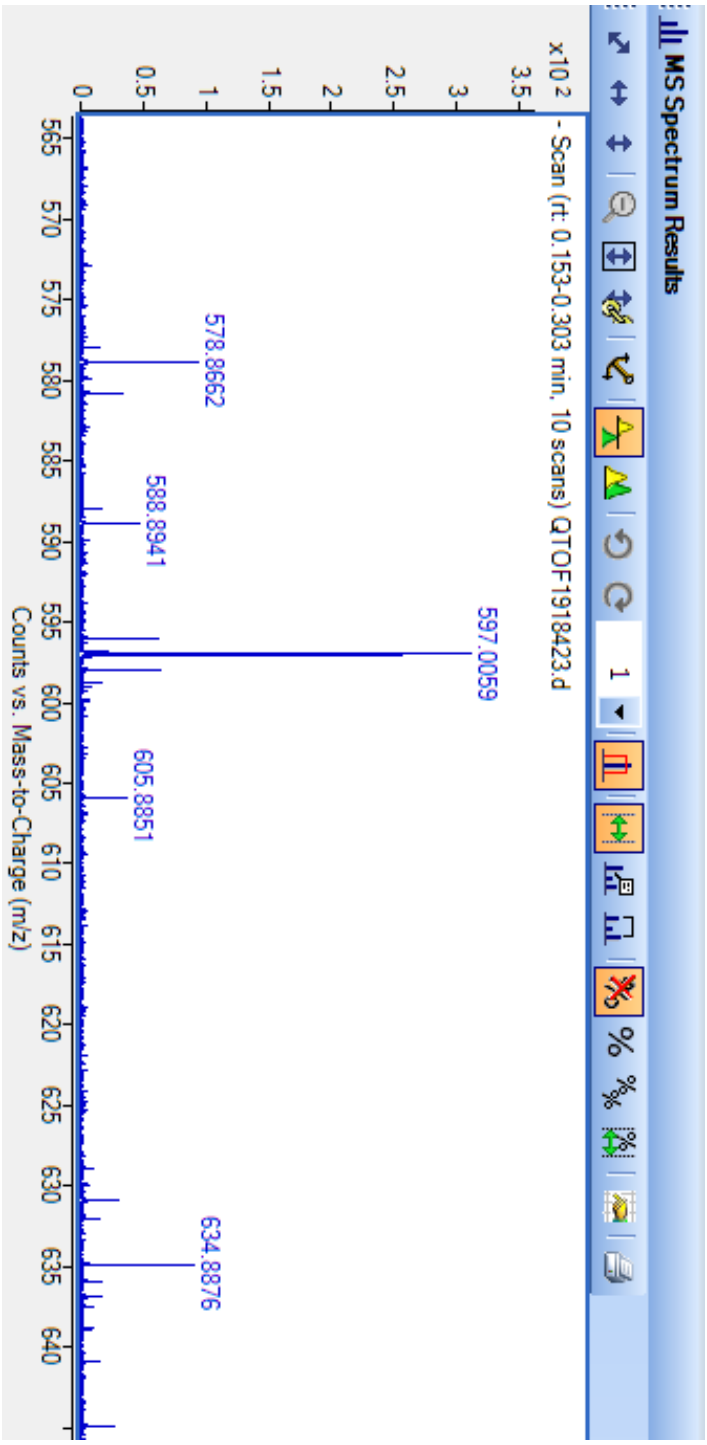

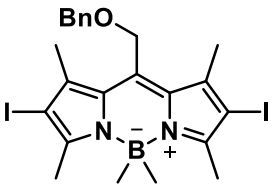

3-OBn

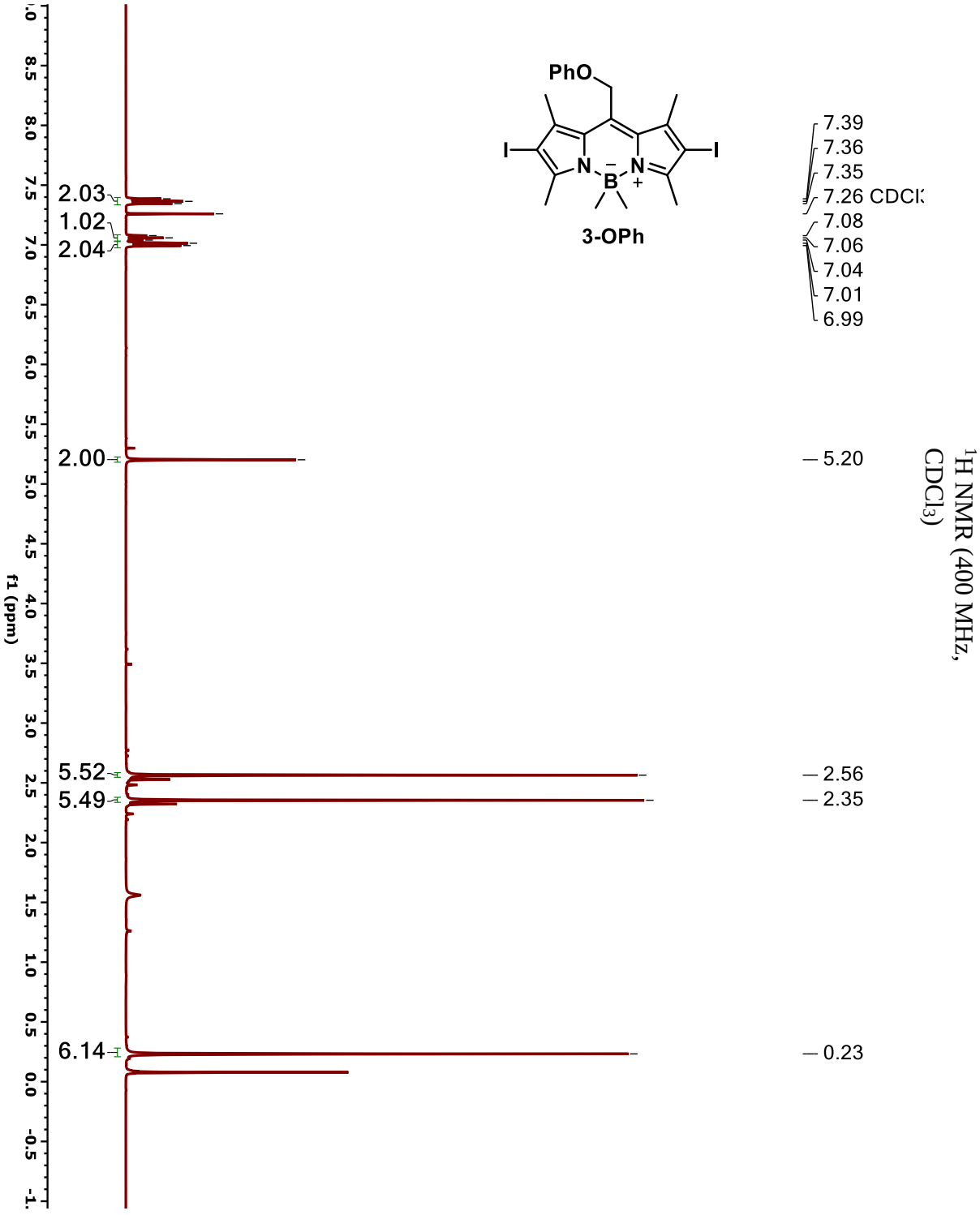

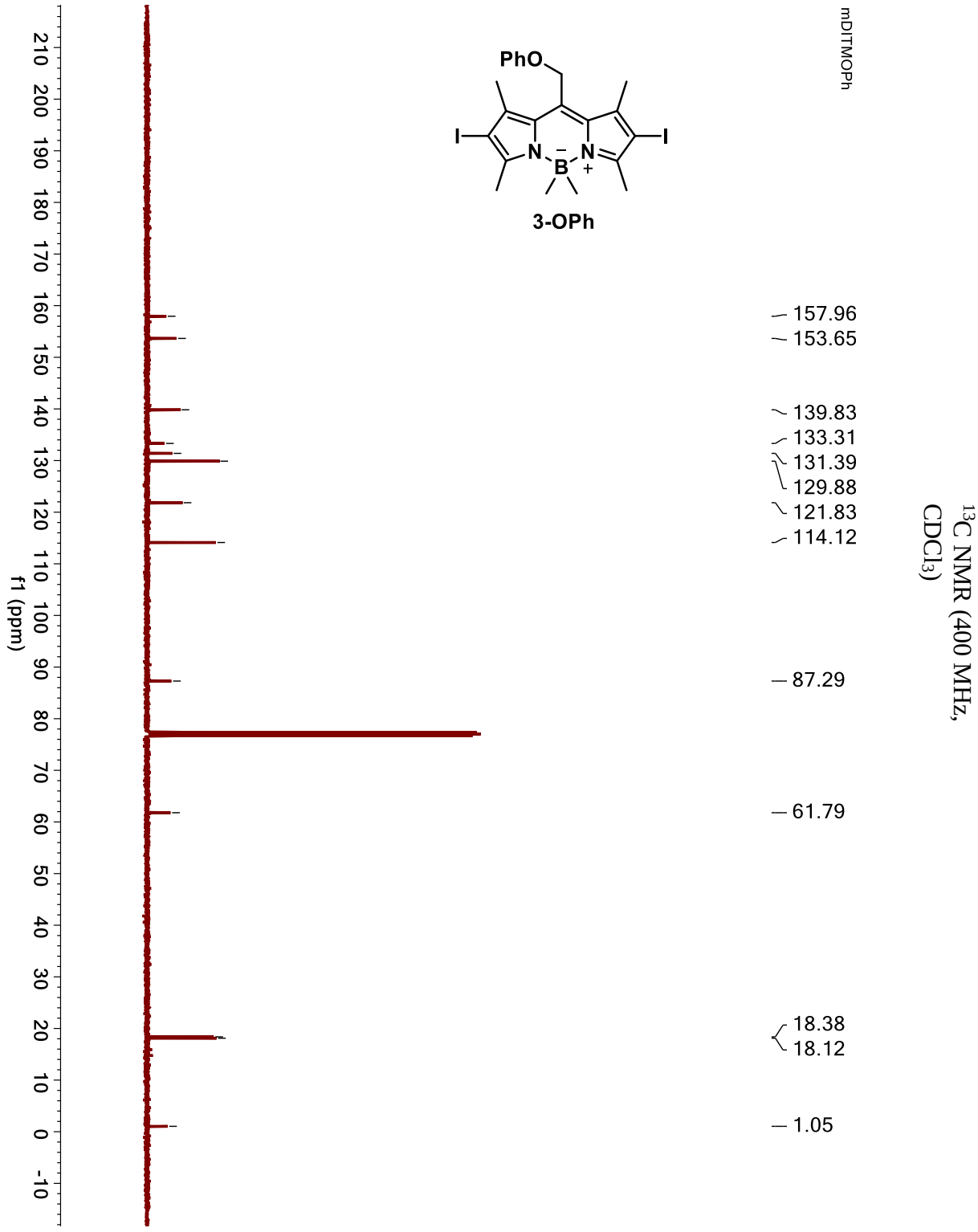

^{13}C NMR (400 MHz, $CDCl_3$)

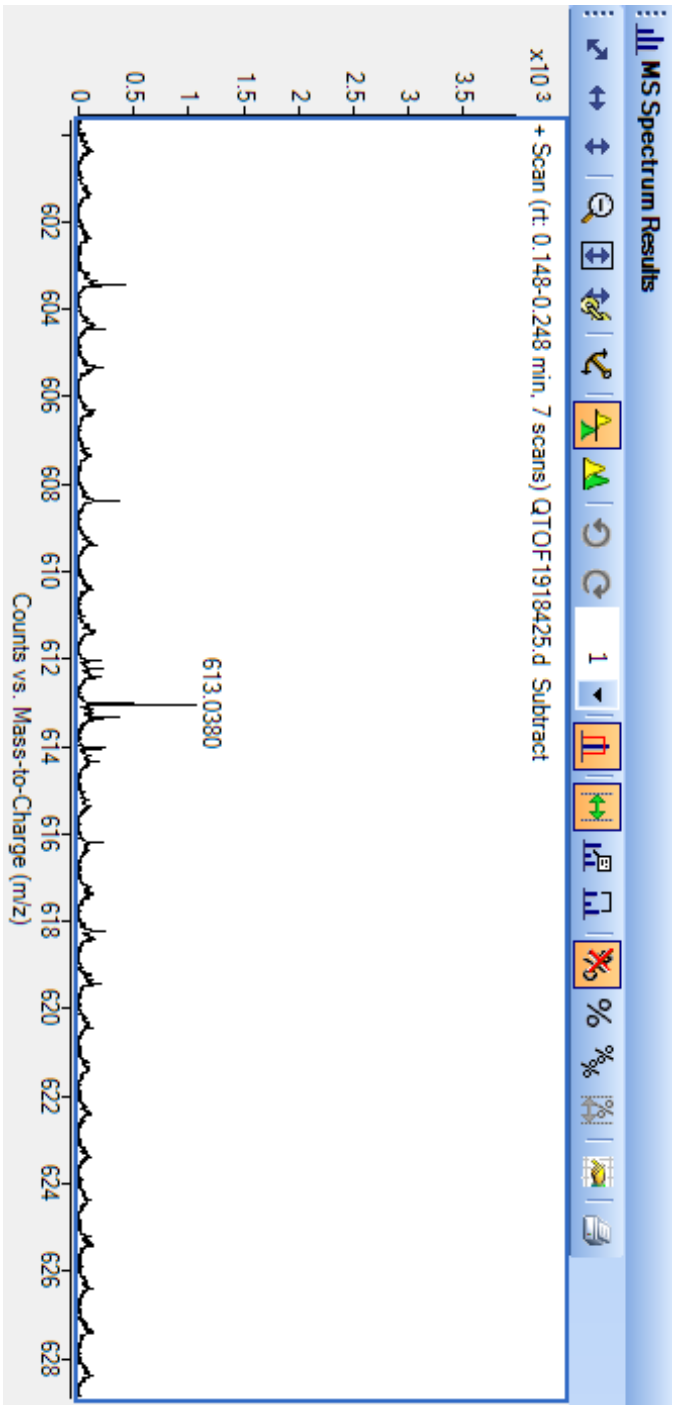

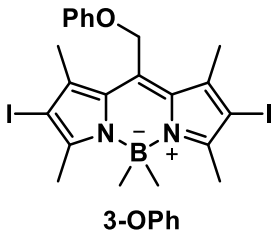

3-OPh

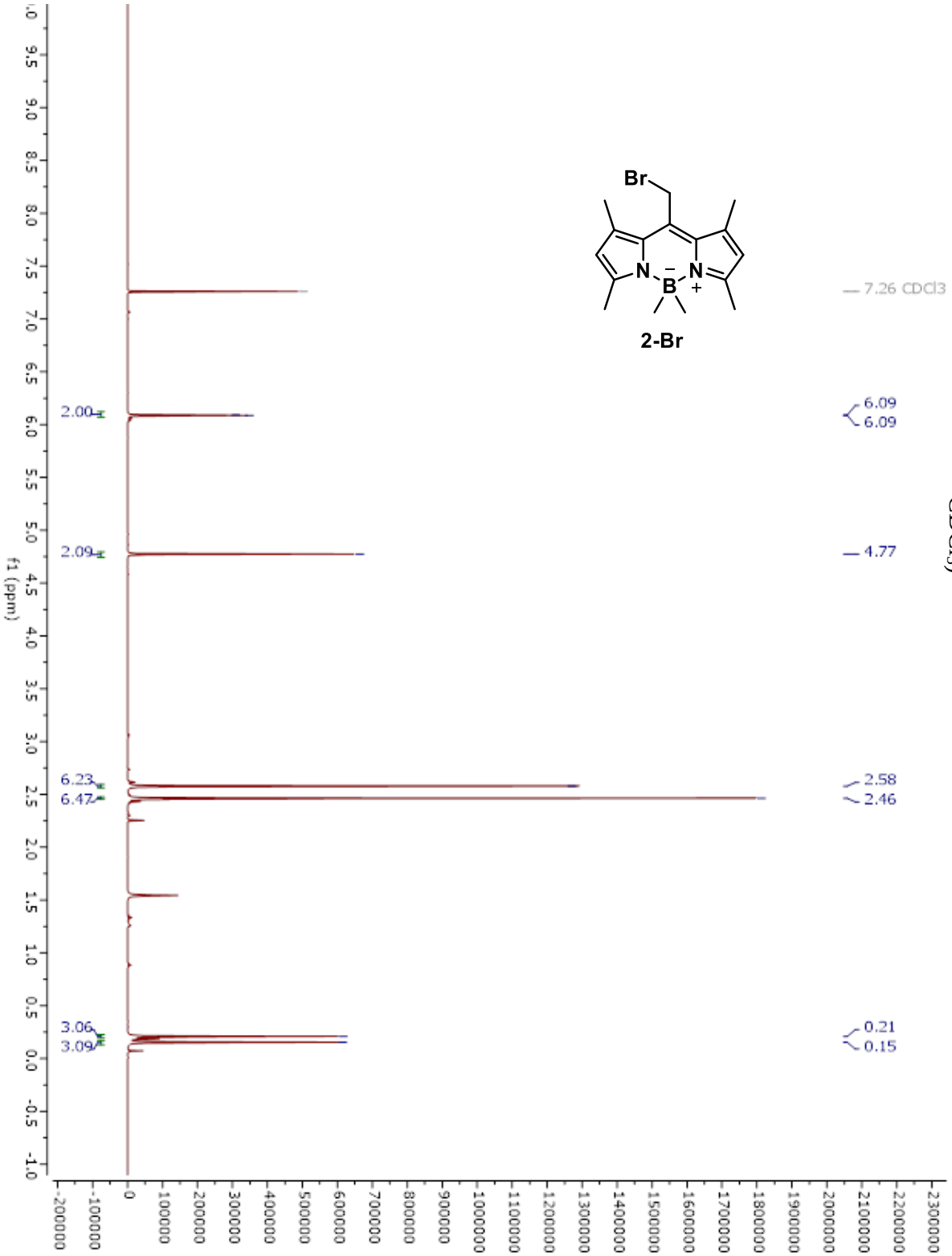

^{1}H NMR (400 MHz, $CDCl_3$)

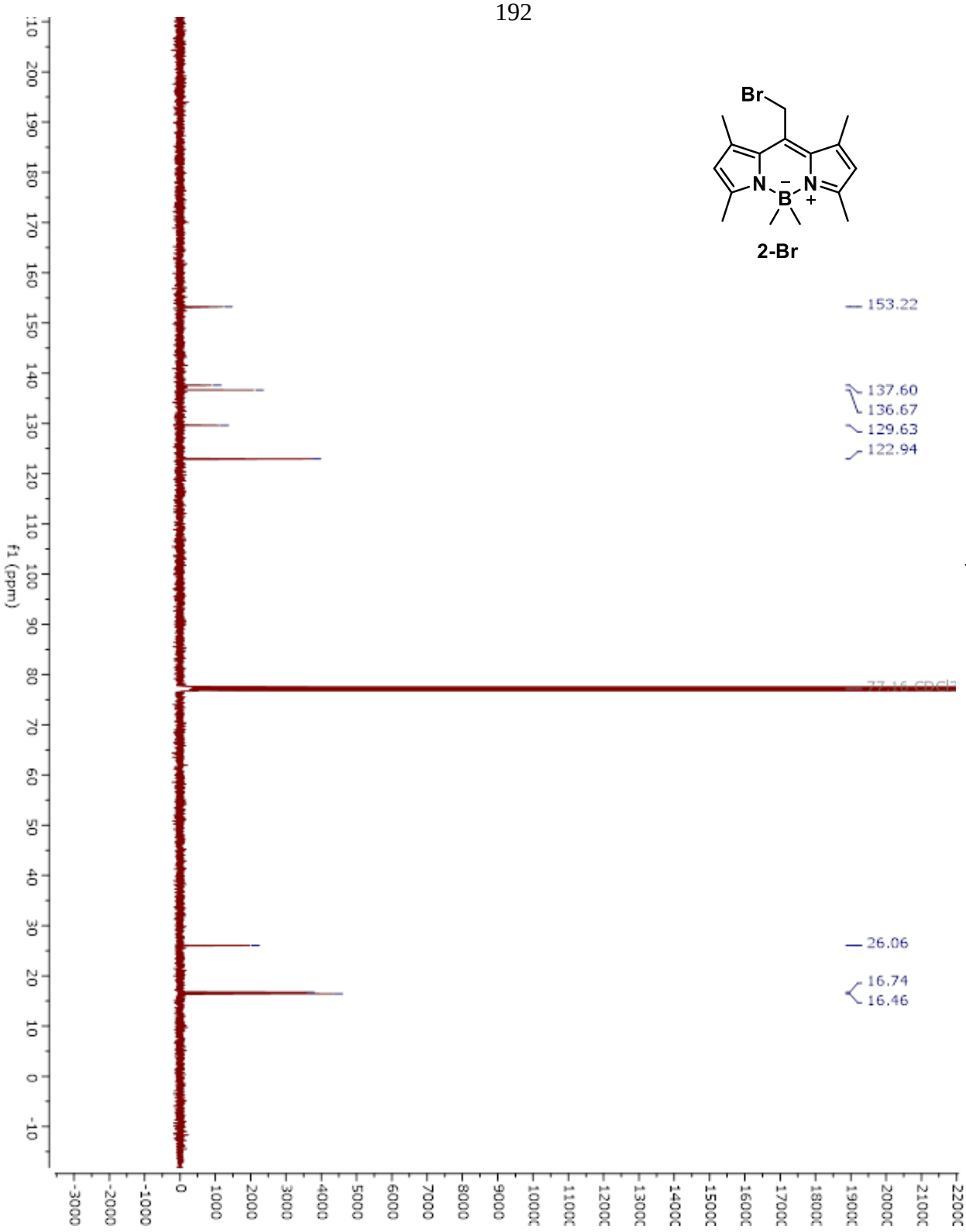

^{13}C NMR (400 MHz, $CDCl_3$)

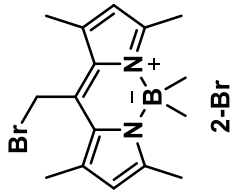

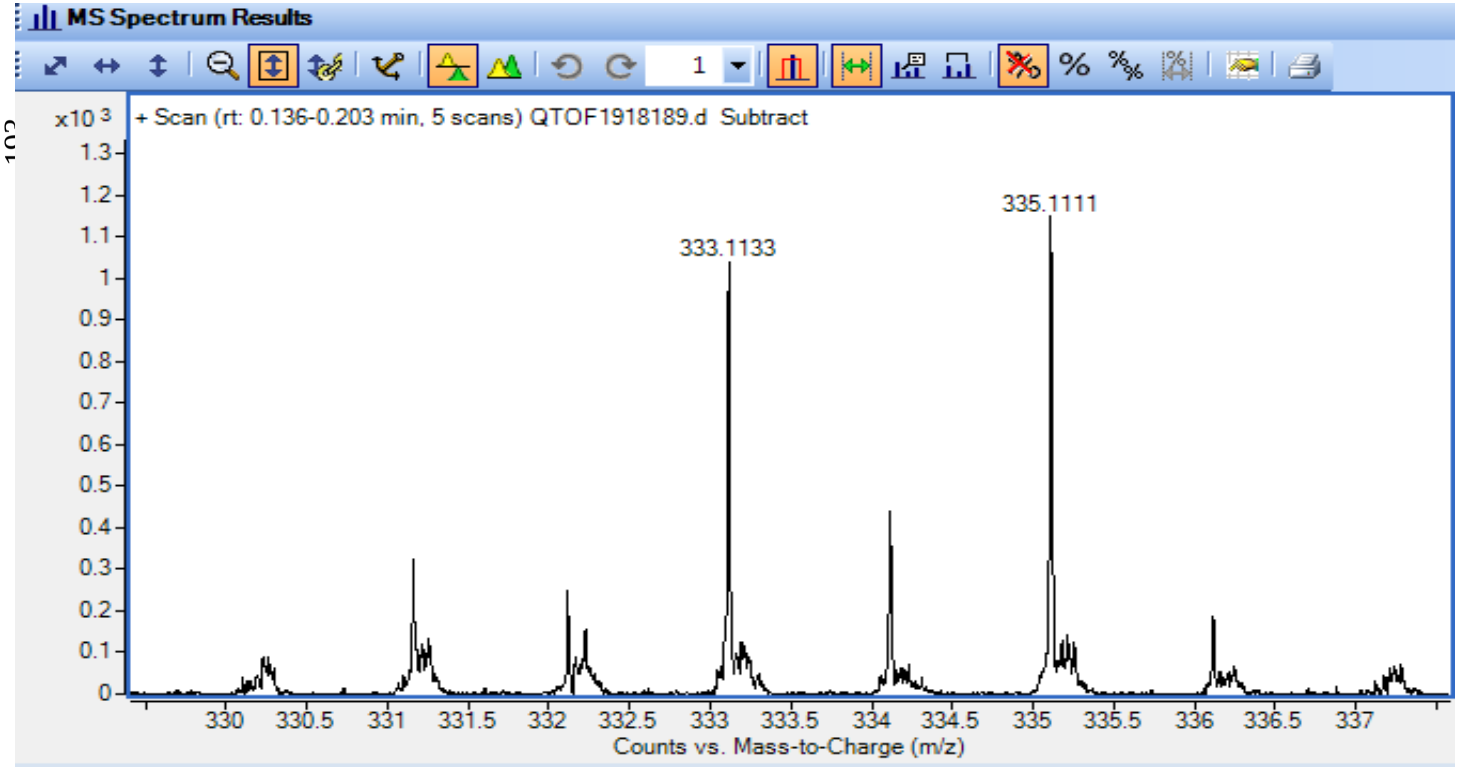

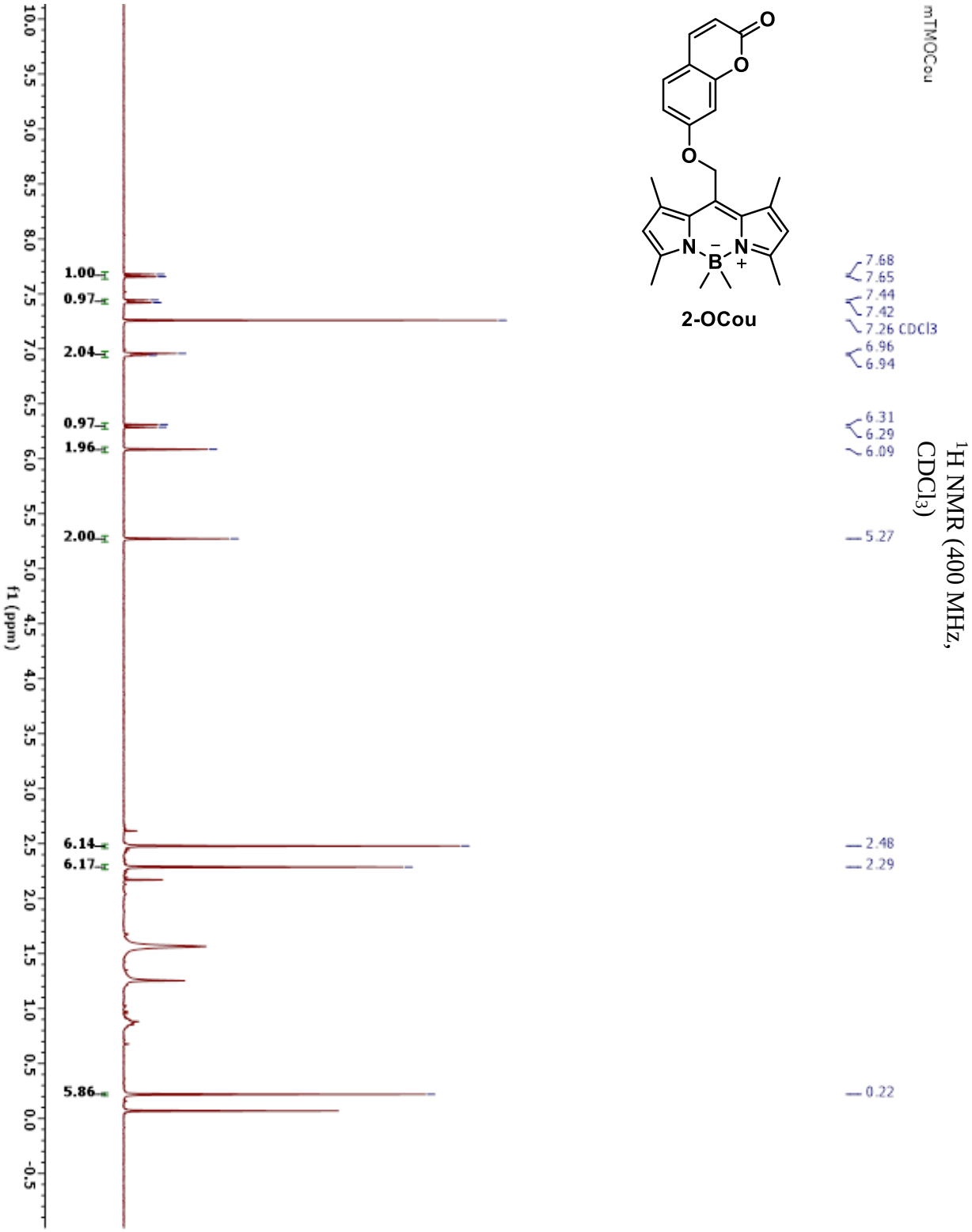

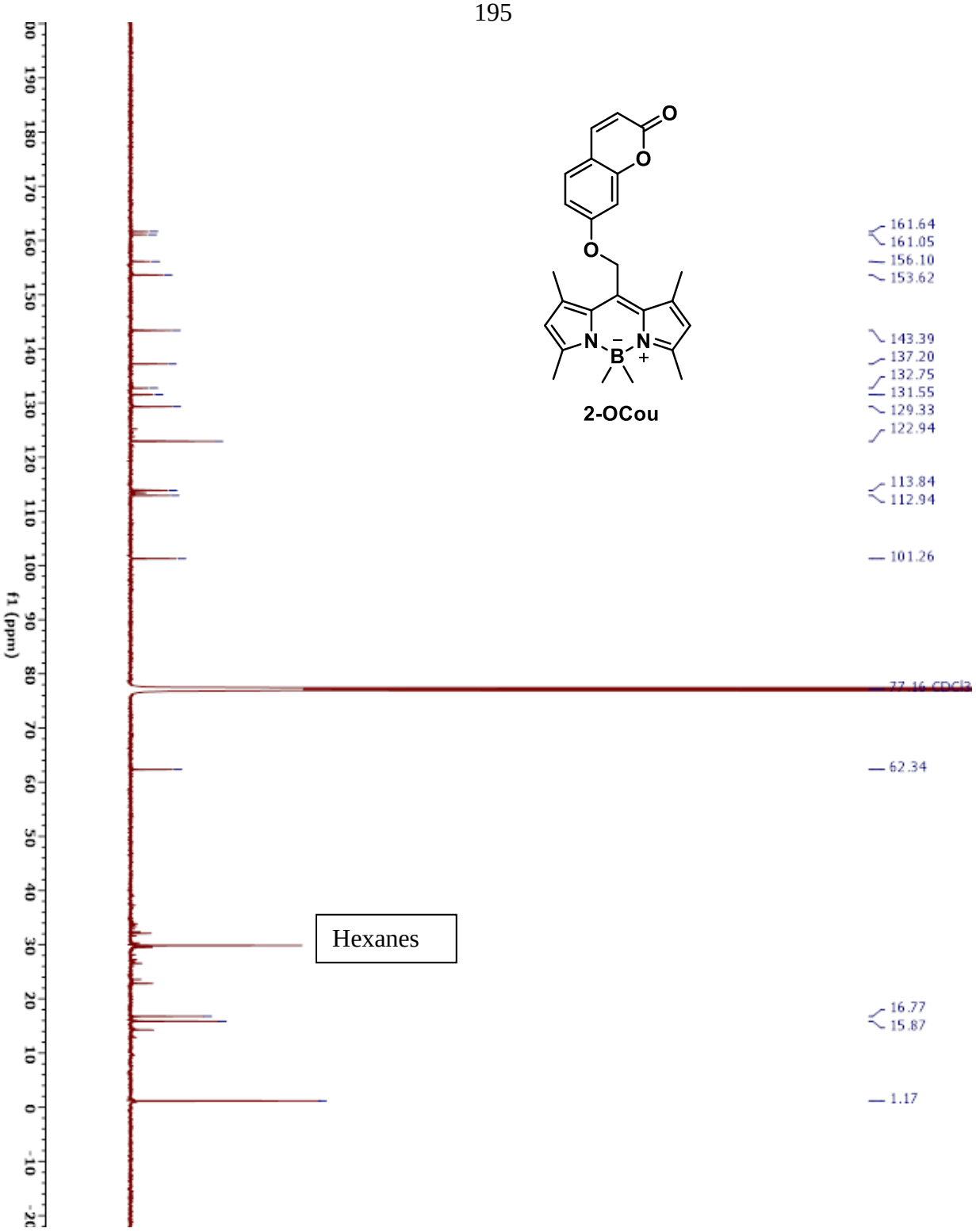

^{13}C NMR (600 MHz, $CDCl_3$)

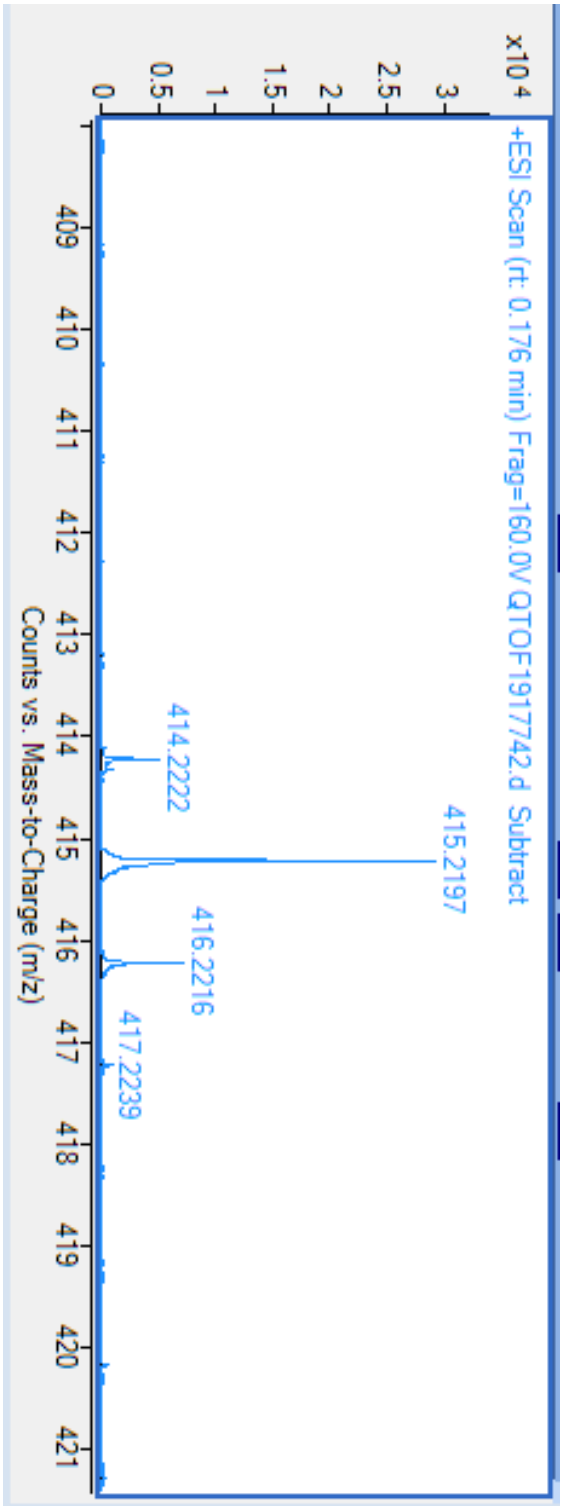

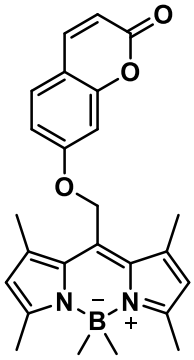

2-OCou

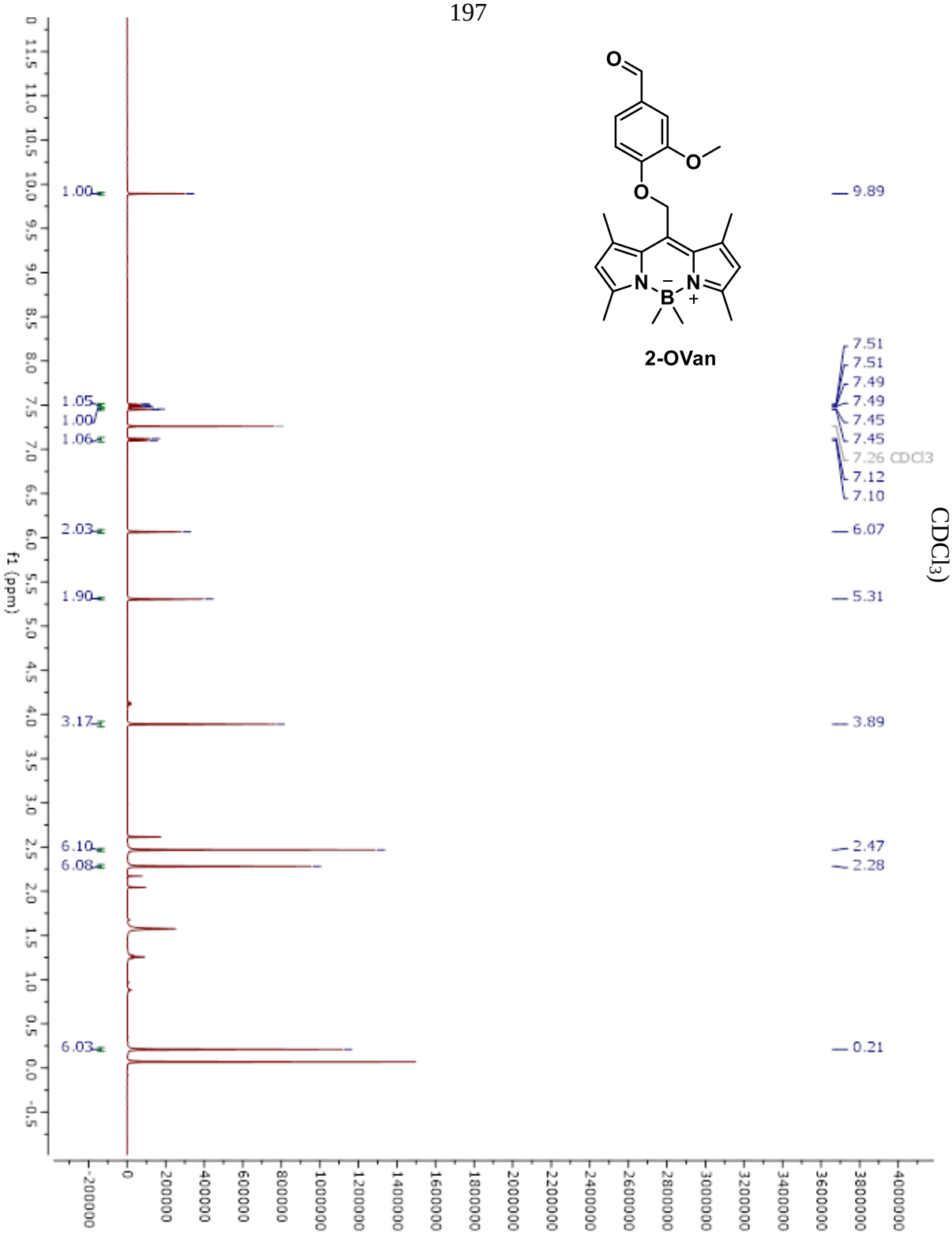

^{1}H NMR (400 MHz, $CDCl_3$)

f

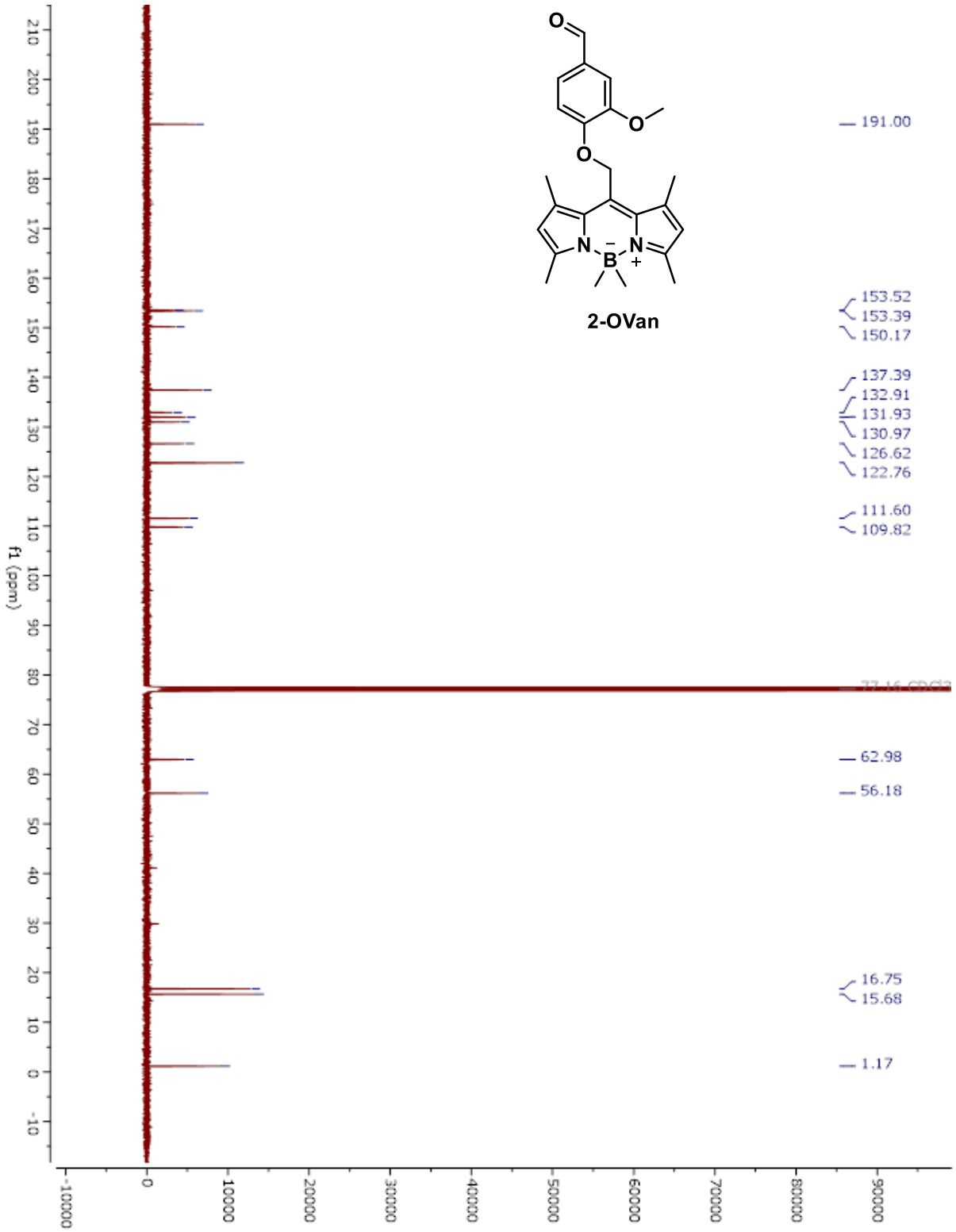

^{13}C NMR (400 MHz, $CDCl_3$)

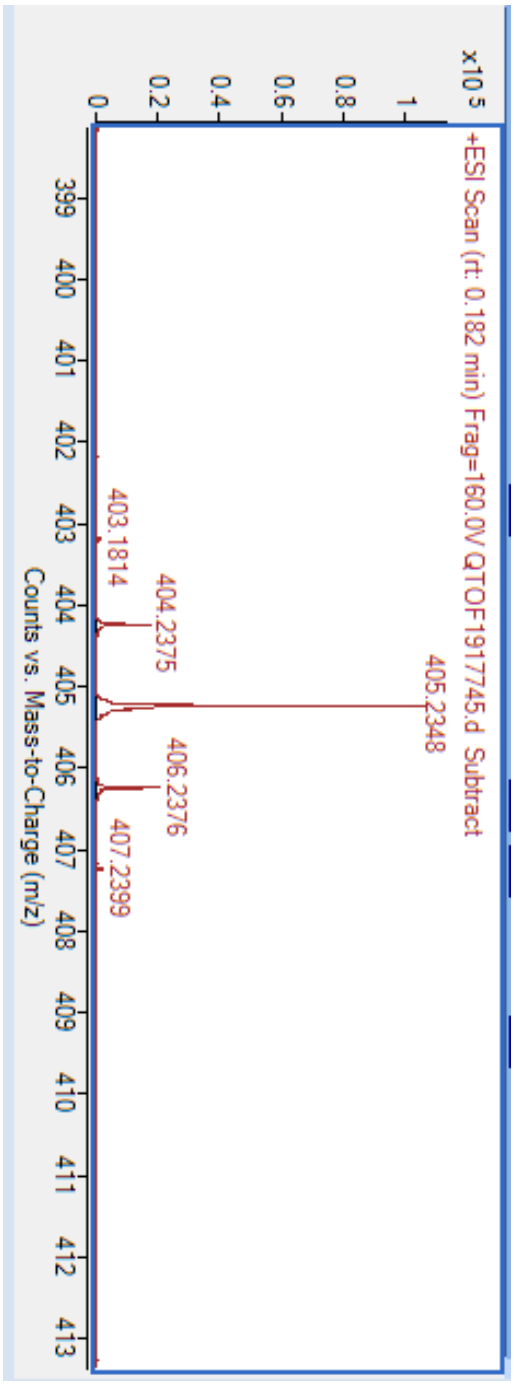

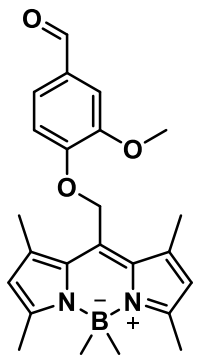

2-OVan

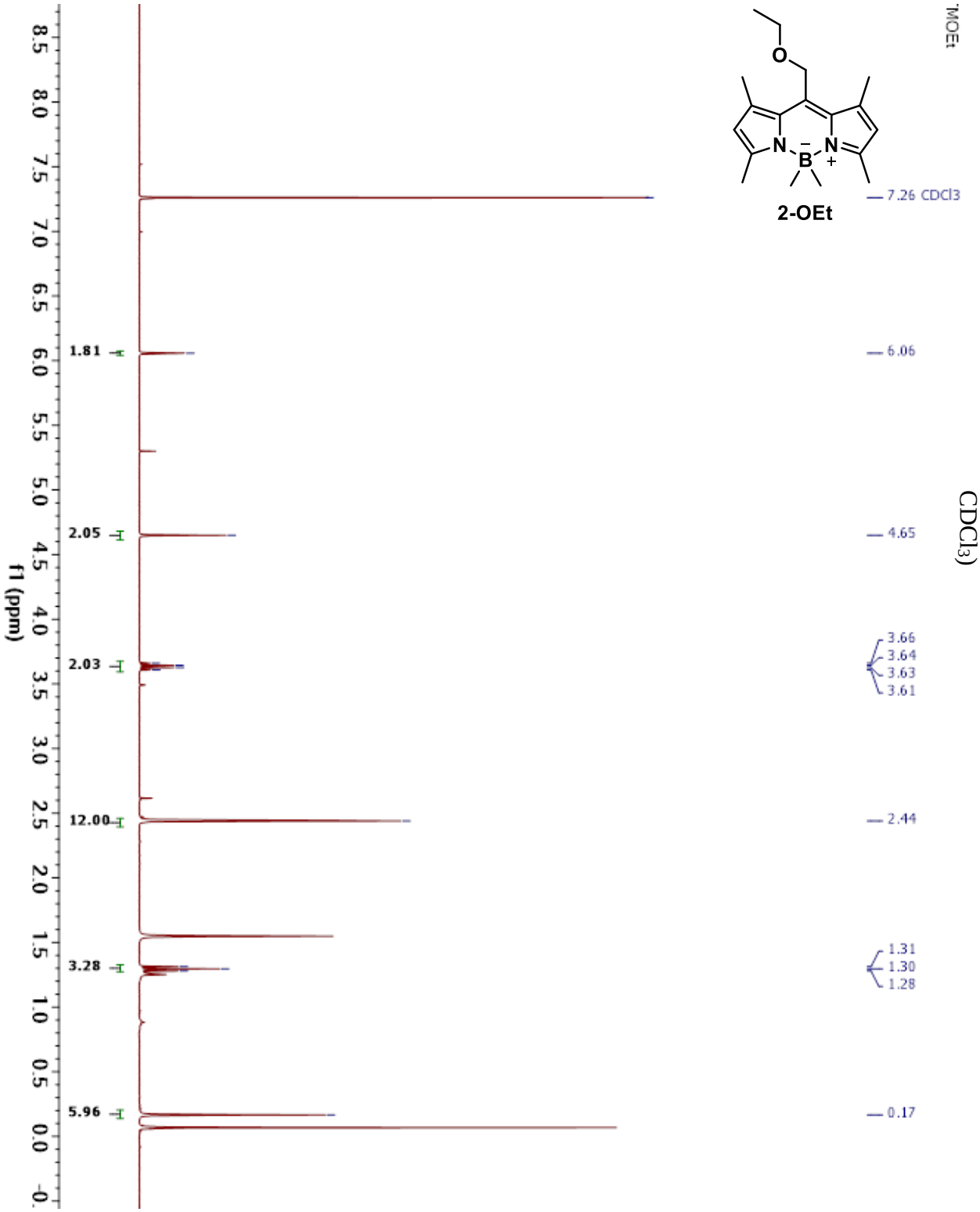

^{1}H NMR (400 MHz, $CDCl_3$)

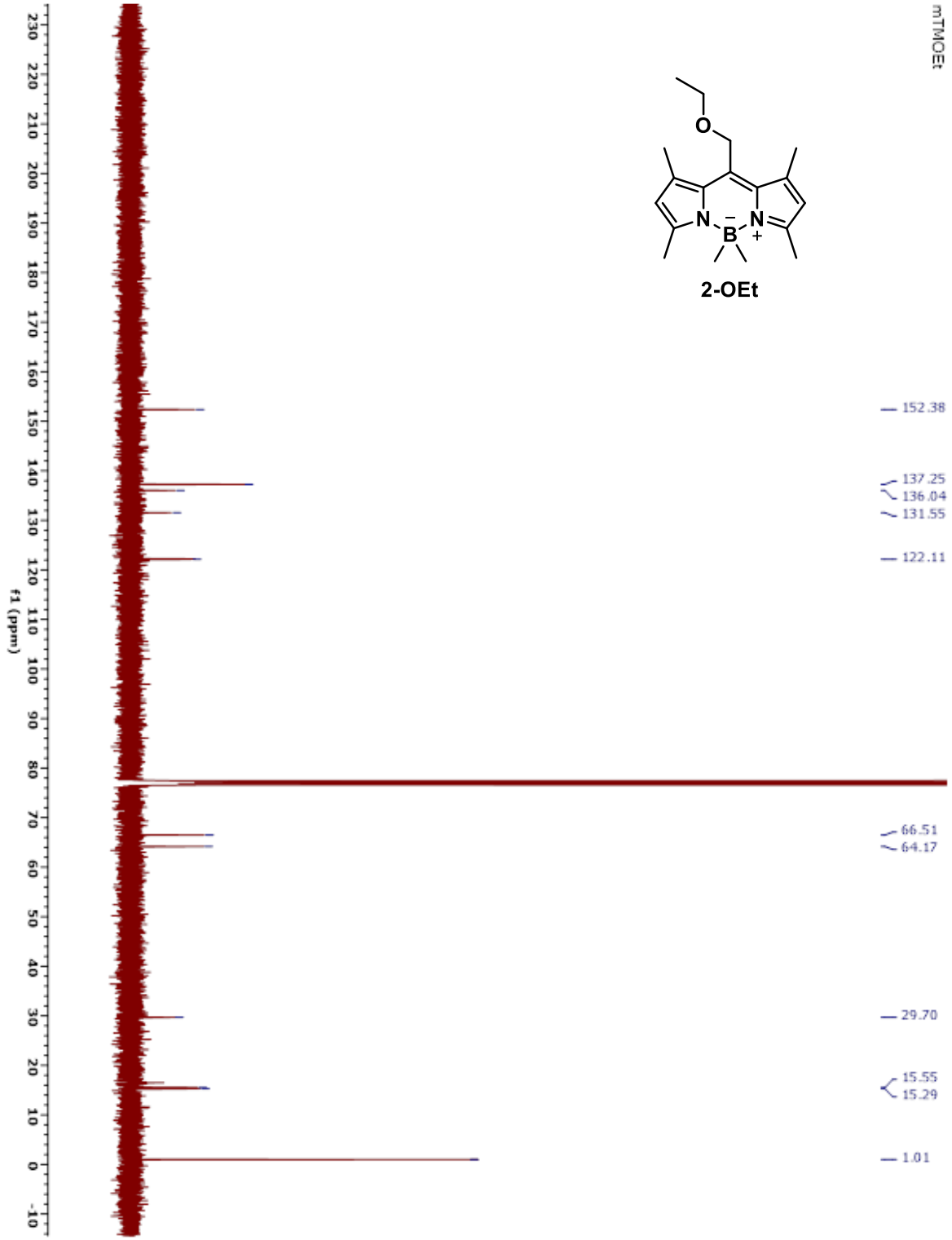

^{13}C NMR (400 MHz, $CDCl_3$)

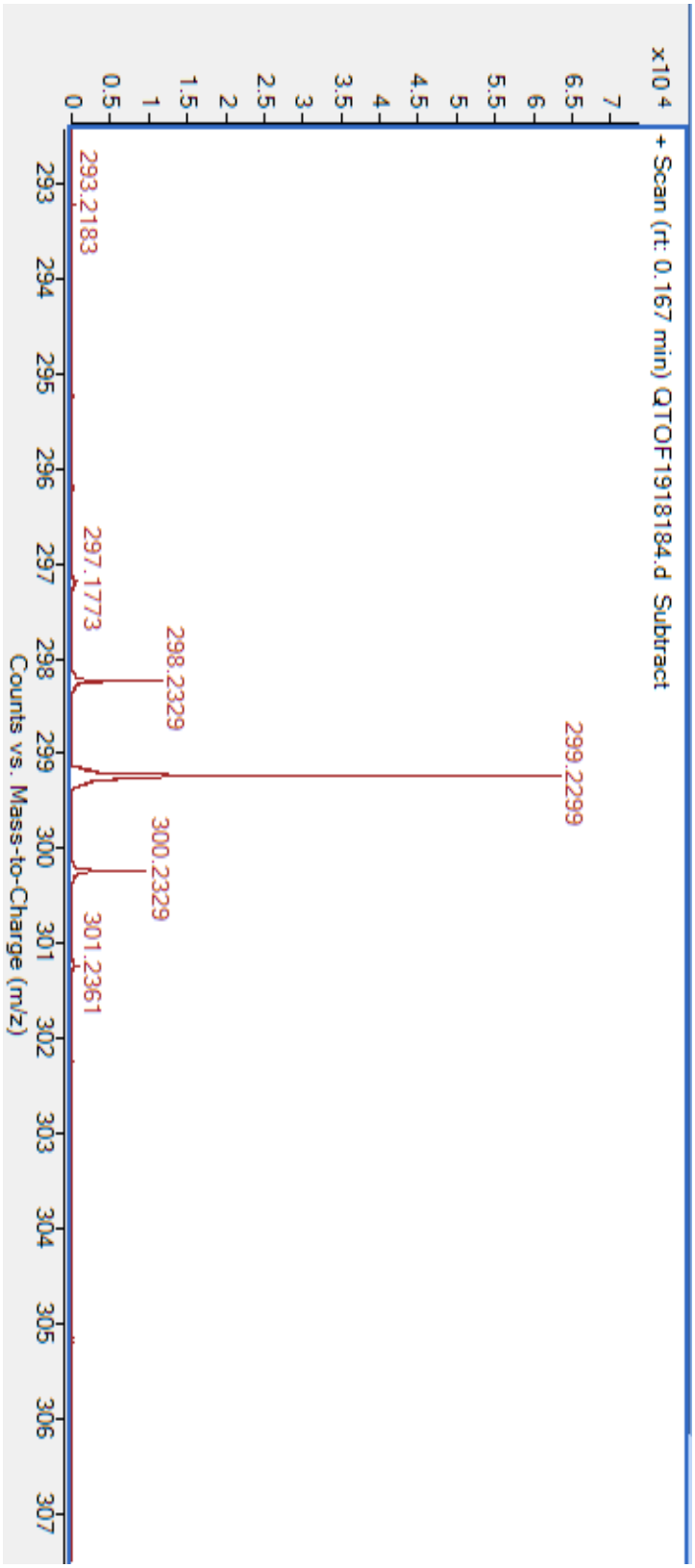

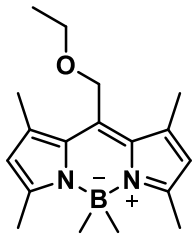

2-OEt

References

1. Wijesooriya, C. S.; Peterson, J. A.; Shrestha, P.; Gehrmann, E. J.; Winter, A. H.; Smith, E. A., A Photoactivatable BODIPY Probe for Localization-Based Super-Resolution Cellular Imaging. *Angewandte Chemie International Edition* **2018,** *57* (39), 12685-12689.

APPENDIX D. SUPPORTING INFORMATION FOR CHAPTER 4

Synthesis Scheme

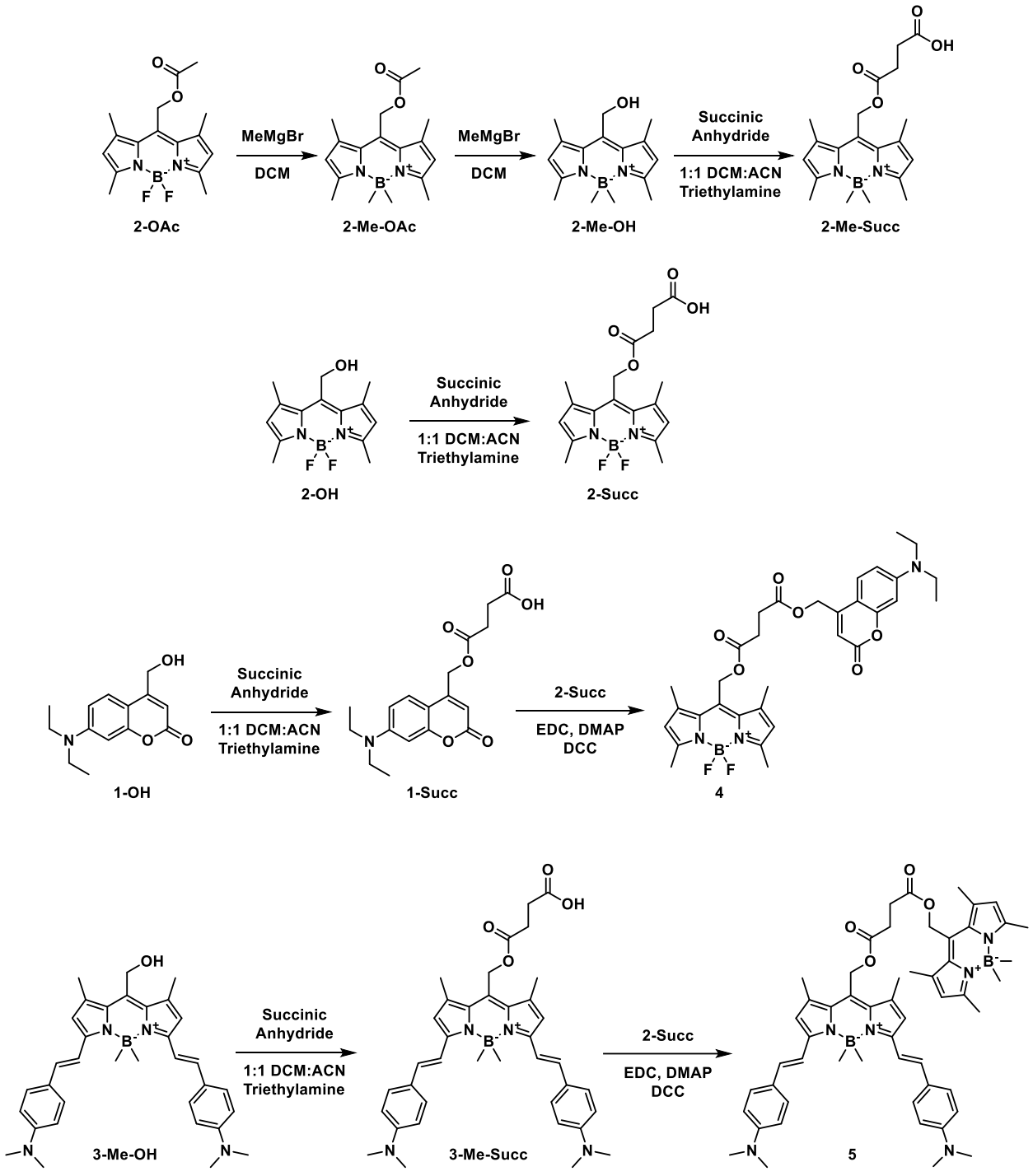

Figure D.0.1. Synthesis scheme of compounds used in this study

Experimental

Reagents were purchased and used as received unless otherwise specified. Solvents when necessary were dried over activated molecular sieves for 3 days before use. **1-OH**,[1] **2-OAc**,[2] **2-OH**,[3] **2-Me-OH**,[4] **3-OAc**,[5] and **3-Me-OH**[5] were synthesized as previously reported.[3, 5]

Light Sources

A Nd:YAG 532 nm laser was used for green irradiation and a Rayonet equipped with 350 nm lamps was used. For all other studies a Luzchem LED Illuminator with a mounted cuvette holder and stir bar was used, with LEDi-RGB (green-466-538 nm, red-602-660 nm) or LEDi-HUV (uv-356-389 nm) equipped.

General reaction with succinic anhydride

BODIPY alcohols (1 eq) were dissolved in 5 mL 1:1 dichloromethane: acetonitrile to which was added 5 equivalents succinic anhydride and excess triethyl amine. The mixture was stirred for 30 minutes or until the alcohol was consumed. 10 mL dichloromethane and 20 mL saturated ammonium chloride were added. The organic layer was washed 3 times with water, once with brine, and dried over sodium sulfate. The solvent was removed under vacuum and the crude mixture was purified by silica gel column chromatography with the eluents listed below.

1-Succ. **1-OH** (100 mg, 0.404 mmol, 1 eq) was dissolved in 10 mL acetonitrile to which was added (200 mg, 2.0 mmol, 5 eq) of succinic anhydride.. Triethylamine (1 mL, excess) was then added. The solution was stirred at room temperature overnight after which 10 mL of dichloromethane and 20 mL saturated ammonium chloride were added. The organic layer was

separated and washed three times with water, once with brine, and dried over sodium sulfate. The solvent was removed under vacuum and the crude mixture was purified with silica gel column chromatography using 50:50 hexanes:acetone as the eluent to give 92 mg of pure product (66% yield). ^{1}HNMR (400 MHz, DMSO-D_6) δ 7.46 (1H, d, *J* = 8.8), 6.69 (1H, dd, *J* = 8.8, 2.8), 6.54 (1H, d, *J* = 2.8), 6.01 (1H, s), 5.29 (2H, s), 3.43 (4H, q, *J* = 6.8), 2.67 (2H, m), 2.55 (2H, m), 1.12 (6H, t, *J* = 6.8). ^{13}CNMR (400 MHz, DMSO-D_6) δ 173.95, 172.31, 161.10, 156.23, 151.02, 150.92, 125.93, 109.22, 105.69, 105.47, 97.28, 61.74, 44.46, 29.13, 12.77. HRMS (ESI/QTOF) m/z: $[M-H]^-$ Calculated for $C_{18}H_{21}NO_6$ 346.1296; Found 346.1310

2-Succ. **2-OH** (50 mg, 0.180mmol, 1 eq) was dissolved in 5 mL dichloromethane to which was added succinic anhydride (100 mg, 0.1 mmol, 5.6 eq) dissolved in 5 mL acetonitrile. Triethylamine (1 mL, excess) was then added and the mixture was stirred for 30 minutes at room temperature. 10 mL of dichloromethane and 20 mL of saturated ammonium chloride were added and the organic layer was then washed three times with water, and once with brine. It was then dried over sodium sulfate and the solvent was removed under vacuum. The crude mixture was purifiedsilica gel column chromatography using acetonitrile as the eluent to give 31 mg of pure **2-Succ** (46% yield). ^{1}HNMR (400 MHz, $CDCl_3$) δ 6.08 (2H, s), 5.33 (2H, s), 2.70 (4H, m), 2.53 (6H, s), 2.35 (6H, s).^{13}CNMR (400 MHz, $CDCl_3$) δ 173.23, 171.97, 155.61, 141.89, 134.00, 131.77, 122.12, 57.47, 28.55, 28.29, 14.86, 14.09. HRMS (ESI/QTOF) m/z: $[M-H]^-$ Calculated for $C_{18}H_{21}BF_2N_2O_4$ 376.1526; Found 376.1529

2-Me-Succ. **2-Me-OH** (25 mg, 0.093 mmol, 1 eq) was dissolved in 5 mL acetonitrile to which was addedsuccinic anhydride (46 mg, 0.46 mmol, 5 eq).Trithylamine (1 mL, excess) was then added. The solution was stirred at room temperature overnight after which 10 mL dichloromethane and 20 mL saturated sodium chloride was added. The organic layer was washed

three times with water, once with brine, dried over sodium sulfate, and the solvent was removed under vacuum. The crude solid was purified with silica gel column chromatography using a 80:20 to 20:80 hexanes: acetone gradient as the eluent to give 22 mg of pure **2-Me-OH** (65% yield). ^{1}HNMR (400 MHz, $CDCl_3$) δ 6.08 (2H, s), 5.38 (2H, s), 2.71 (4H, m), 2.46 (6H, s), 2.34 (6H, s), 0.19 (6H, s). ^{13}CNMR (400 MHz, $CDCl_3$) δ 177.49, 172.09, 153.30, 137.15, 132.96, 131.24, 122.78, 59.13, 28.72, 28.59, 16.60, 15.80. HRMS (ESI/QTOF) m/z: $[M-H]^-$ Calculated for $C_{20}H_{27}BN_2O_4$ 369.1991; Found 369.2021

3-Me-Succ. 3-Me-OH (25 mg, 0.047 mmol, 1 eq) was reacted with 5 equivalents(24 mg, 0.24 mmol) of succinic anhydride. The compounds were dissolved in 5ml acetonitrile. Excess amount of triethylamine was then added. The solution was then stirred at room temperature overnight. The mixture was purified with silica gel column chromatography using 50:50 hexanes: acetone with 1% acetic acid as the eluent to give 10 mg of product (33.7% yield). ^{1}HNMR (400 MHz, $CDCl_3$) δ 7.47 (4H, d, *J*=8), 7.45 (2H, d, *J*=16), 7.10 (2H, d, *J*=16), 6.76 (4H, d, *J*=8), 6.74 (2H, s), 5.44 (2H, s), 3.05 (12H, s), 2.76 (4H, m), 2.43 (6H, s), 0.48 (6H, s). ^{13}CNMR (400 MHz, $CDCl_3$) δ 175.96, 172.36, 151.07, 150.78, 136.13, 133.62, 133.34, 128.70, 128.59, 125.75, 118.75, 117.21, 112.50, 59.56, 40.50, 29.42, 28.93, 28.69, 16.18. HRMS (ESI/QTOF) m/z: $[M-H]^-$ Calculated for $C_{38}H_{45}BN_4O_4$ 631.3461; Found 631.3576

2-Me-OAC. To a solution of **2-OAc** (100 mg, 0.312 mmol, 1 eq) stirring at room temperature in 5 mL dry dichloromethane was added 1 eq of methylmagnesium bromide (1 M solution in THF, mmol). The mixture was stirred for 1 h, when the reaction was complete by TLC. 10 mL of saturated ammonium chloride was added, followed by 20 mL of additional dichloromethane. The organic layer was separated and washed 2 times with saturated ammonium chloride and once with brine. It was dried over sodium sulfate and the solvent was removed under vacuum. The

crude product was purified with silica gel column chromatography using 80:20 dichloromethane: hexanes as the eluent to give 68 mg of **2-OAc** (69.7% yield). ^{1}HNMR (400 MHz, $CDCl_3$) δ 6.09 (2H, s), 5.34 (2H, s), 2.74 (6H, s), 2.36 (6H, s), 2.14 (3H, s), 0.20 (6H, s). ^{13}CNMR (400 MHz, $CDCl_3$) δ 170.82, 153.23, 137.08, 133.35, 131.21, 122.75, 58.79, 20.70, 16.60, 15.91. HRMS (ESI/QTOF) m/z: $[M+H]^+$ Calculated for $C_{18}H_{25}BN_2O_2$ 312.2118; Found 312.2094

4. To a solution of **1-Succ** (25 mg, 0.07 mmol , 1 eq) dissolved in 10 mL dry DCM was added EDC (11 mg, 0.07 mmol, 1 eq), DMAP (1 mg, 0.007 mmol, 0.1 eq), and **2-OH** (20 mg, 0.07 mmol, 1 eq). The mixture was stirred overnight after which it was washed 5 times with water and dried with sodium sulfate. The solvent was removed under vacuum and the crude mixture was purified with silica gel chromatography using 50:50 hexanes: dichloromethane to give 21 mg of **4** (49% yield). ^{1}HNMR (400 MHz, $CDCl_3$) δ 7.23 (1 H, d, J = 9.2), 6.56 (1H, dd, J = 9.2, 2.4), 6.50 (1H, d, J = 2.4), 6.08 (1H, s), 6.07 (2H, s), 3.40 (4H, q, J = 7.2), 2.76 (4H, m), 2.50 (6H, s), 2.35 (6H, s), 1.20 (6H, t, J = 7.2). ^{13}CNMR (400 MHz, $CDCl_3$) δ 171.59, 171.38, 161.76, 156.70, 156.25, 150.66, 149.00, 141.53, 132.87, 132.59, 124.35, 122.36, 108.63, 106.42, 105.90, 97.83, 61.69, 58.12, 44.74, 28.86, 28.80, 15.61, 14.65, 12.41, 1.00. HRMS (ESI/QTOF) m/z: $[M-H]^-$ Calculated for $C_{32}H_{36}BF_2N_3O_6$ 606.2592; Found 606.2701

5. To a solution of **2-Me-Succ** (35 mg, 0.094 mmol, 2 eq) dissolved in dry dichloromethane under nitrogen atmosphere. Solutions of *N*,*N*'-dicyclohexylcarbodiimide (47 mg, 0.23 mmol, 2.4 eq), 4-dimethylaminopyridine (1.5 mg, 0.01 mmol, 0.1 eq), and **3-Me-OH** (25 mg, 0.047 mmol, 1 eq) dissolved in 1 mL dry dichloromethane were sequentially. The solution was then stirred at room temperature overnight after which it was transferred to the freezer to precipitate out dicylohexylurea. After 2 h the mixture was filtered and the solvent was removed under vacuum. The crude product was purified with silica gel chromatography using 70:30 hexanes:ethyl acetate

to give 25 mg of **5** (61%yield). ^{1}HNMR (400 MHz, $CDCl_3$) δ 7.45 (4H, d, *J*=8), 7.28 (4H, d, *J*=12), 6.91 (2H, s), 6.79 (4H, d, *J*=4), 6.19 (2H, s), 5.31 (2H, s), 5.29 (2H, s), 2.99 (12H, s), 2.74 (4H, s), 2.41 (6H, s), 2.34 (6H, s), 2.28 (6H, s), 0.36 (6H, s), 0.12 (6H, s). ^{13}CNMR (400 MHz, $CDCl_3$) δ 171.94, 152.66, 150.70, 150.25, 137.34, 136.13, 134.18, 133.60, 132.56, 130.63, 128.20, 124.44, 122.69, 118.73, 115.35, 113.30, 112.29, 58.37, 54.47, 28.95, 23.10, 22.03, 16.15, 15.43, 15.22, 13.88. HRMS (ESI/QTOF) m/z: $[M-H]^-$ Calculated for $C_{54}H_{66}B_2N_6O_4$ 883.5259; Found 883.5283

Selective Release Studies of mixtures

Mixtures were prepared by dissolving equimolar amounts of the compounds in 50:50 DMSO: Methanol. 3-4 milliliters of the solutions were transferred to quartz cuvettes equipped with a stir bar and irradiated with the above lights. At determined time intervals, 20 microliters of the samples were transferred to mass spec vials fitted with 100 microliter inserts. Samples were run with a LC/UV/QTOF to separate and identify the peaks. The percent of starting material reacted was determined by calculating the percent disappearance of the LC/UV peaks. Percent conversion was determined by the appearance of LC/UV peaks of products based on calibration curves of known concentrations. Solutions of compounds 4 and 5 were purged for 30 minutes with argon before irradiation to simplify product mixtures. Mass spec was used to confirm the identity of the peaks on LC.

LC/UV/QTOF Methods

LC/UV/MS analysis was conducted using the Agilent 6540 QTOF mass spectrometer. All LC separations were achieved using the Agilent C18-XDB (4.6 x 50 mm, 7 micron particle size) column and a 1 microliter injection with a flow rate of 0.7 mL/min. Mobile phases were prepared from HPLC grade solvents with 0.1% formic acid and 10% methanol added to avoid polymerization of the acetonitrile and growth in the water. The UV trace was measured at 370 nm and the mass spec was run in negative ionization mode using ESI as the ionization source.

Gradient 1: Used for irradiation of compound 5

Time (min)	**% Acetonitrile**	**% Water**
0	40	60
4	80	20
20	99	1
25	100	0
30	100	0

*7 minute post-run time

Gradient 2: Used for mixtures of 2-Me-Succ and 3-Me-Succ as well as the mixture of 1-Succ, 2-Me-Succ, and 3-Me-Succ

Time (min)	**% Acetonitrile**	**% Water**
0	40	60

4	80	20
20	99	1
25	100	0

*5 minute post-run time

Gradient 3: Used for irradiation of compound 4 and mixtures of 1-Succ and 2-Succ

Time (min)	**% Acetonitrile**	**% Water**
0	30	60
4	50	20
7	100	1
11	100	0

*7 minute post-run time

Gradient 4: Used for mixtures of 2-Me-OAc and 3-OAc

Time (min)	**% Acetonitrile**	**% Water**
0	80	20
4	85	15
15	99	1

*5 minute post-run time

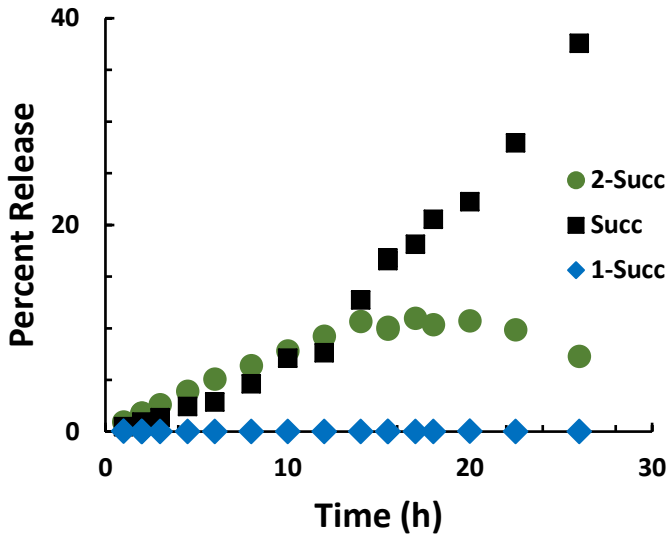

Figure D.0.2. Growth of Succinic Acid during irradiation of compound **4**

A 0.03 mM solution of compound 4 dissolved in 50:50 DMSO:MeOH was irradiated in a quartz 4-sided cuvette with a rayonett photoreactor equipped with 350 nm bulbs. 2-Succ never reached more than 10% release and began to decrease over longer irradiation times. Succinic acid grew in steadily during the entire irradiation. In addition, the irradiation time was much longer than irradiation of 1-Succ alone, which is fully reacted in less than 1 h at the same concentration with the identical setup.

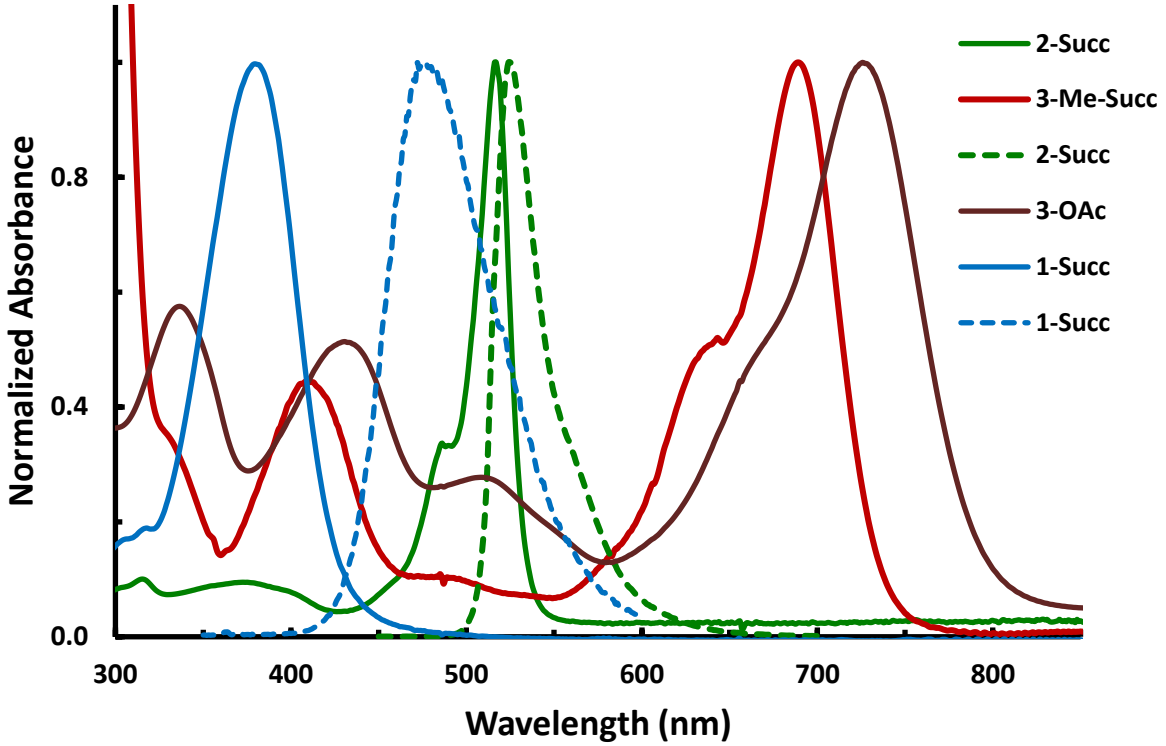

Figure D.0.3. Absorbance (solid lines) and emission (dotted lines) spectra of **1-Succ** and **2-Succ** as well as absorbance spectra of **3-OAc** and **3-Me-Succ**

The emission of **1-Succ** has good overlap with the absorbance of **2-Succ**, indicating that they are a good FRET pair. This energy may be interfering with the selectivity when the two chromophores are close in proximity (i.e. the linked compound **4**). However, the emission of **2-Succ** does not have good overlap with the absorbance of **3-Succ** or **3-Me-Succ**, indicating that there is likely a different sort of energy transfer occurring interfering with selectivity of these two compounds.

Table D.0.1. Quantum efficiency data for similar substrates

Compound	$\varepsilon*10^4$	Φ (%)	$\varepsilon\Phi$
1-Glutamate[1]	1.4	11	1540
2-OAc[4]	7.1	0.14	99
2-Succ[4]	6.9	5.5	3800
3-Me-Succ[5]	7.8	0.11	86
3-OAc[5]	6.5	0.0041	2.7

*The compounds in this study are assumed to have similar quantum efficiencies to those listed below

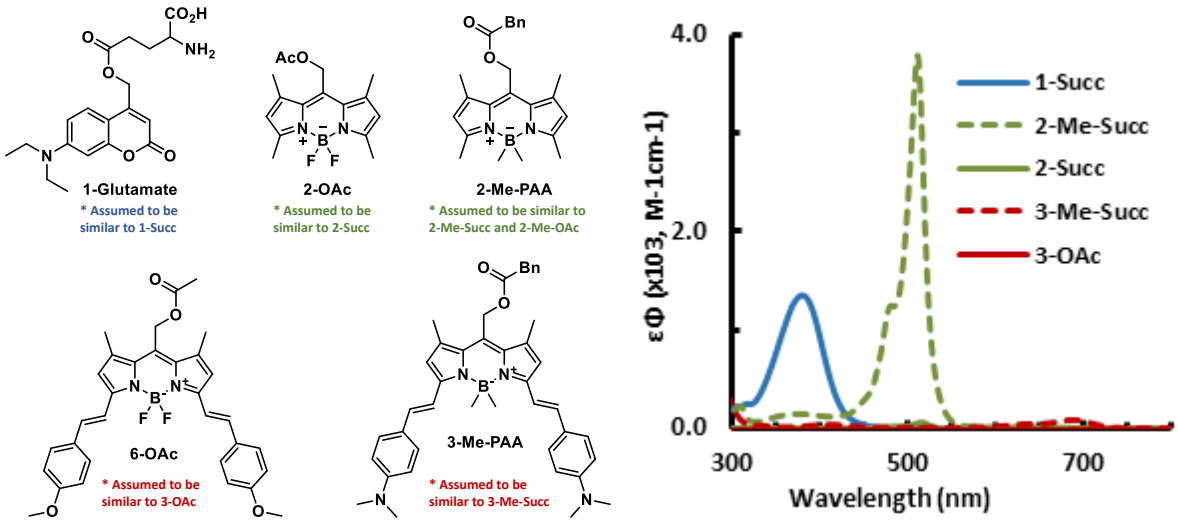

Figure D.0.4. Similar compounds to those addressed in this study that have known quantum efficiency data (left). Quantum efficiency of the compounds in this study assuming similar quantum efficiencies to similar compounds as described above (right).

Spectra of New Organic Compounds

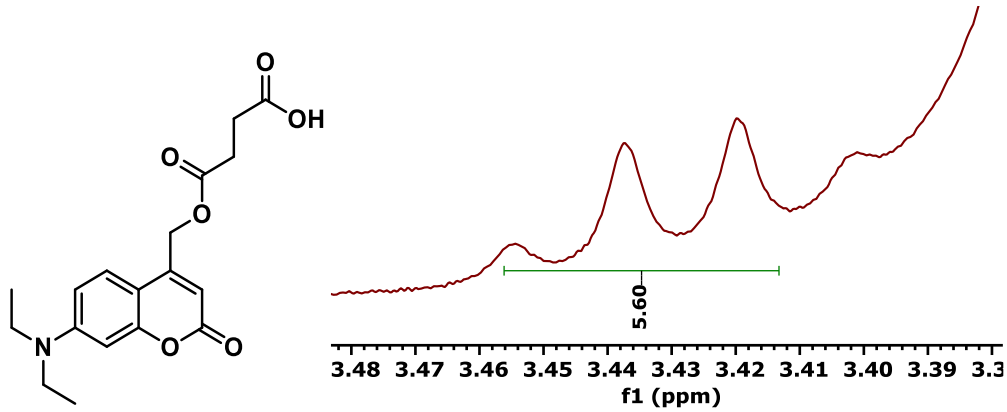

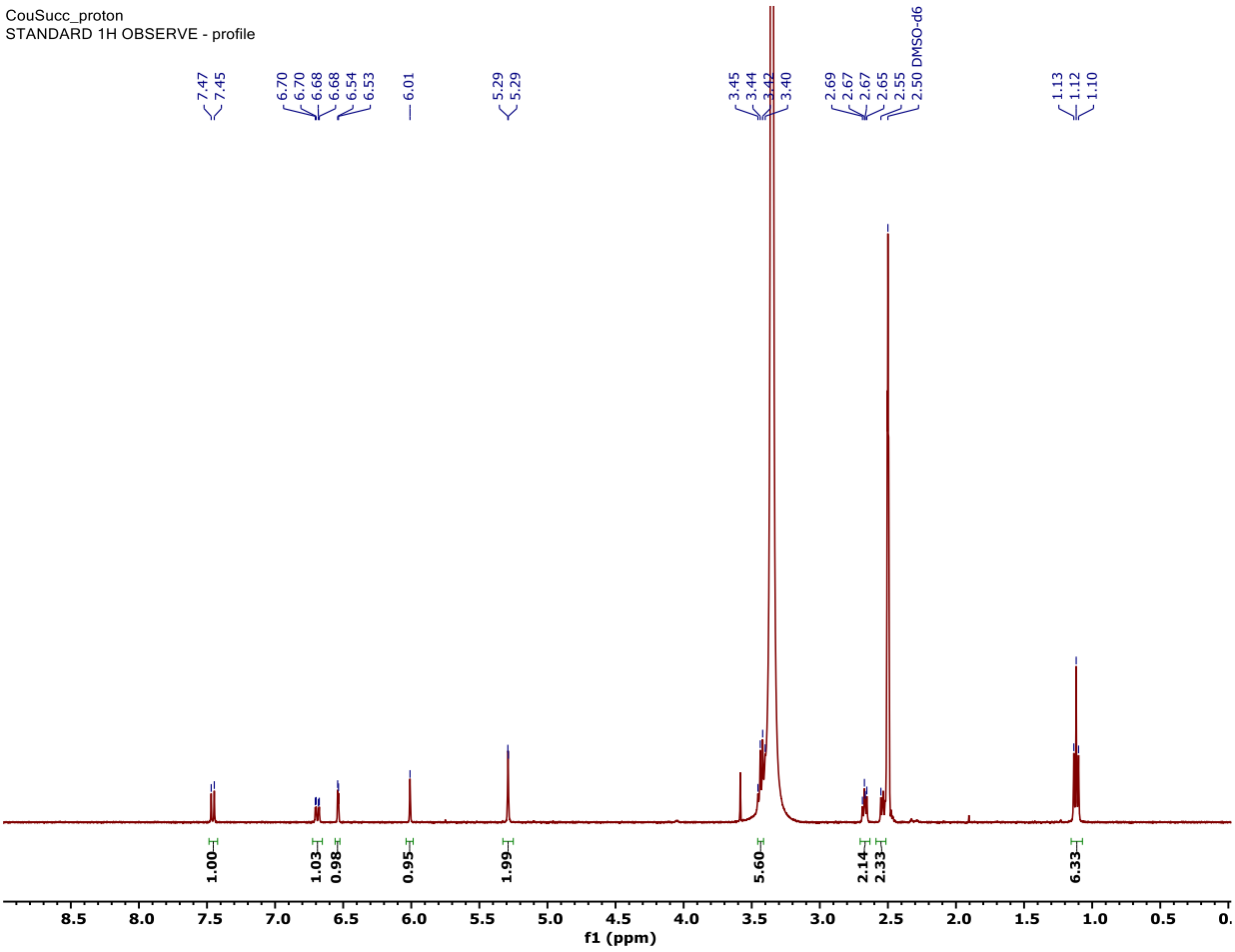

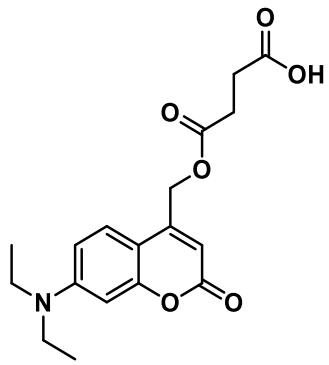

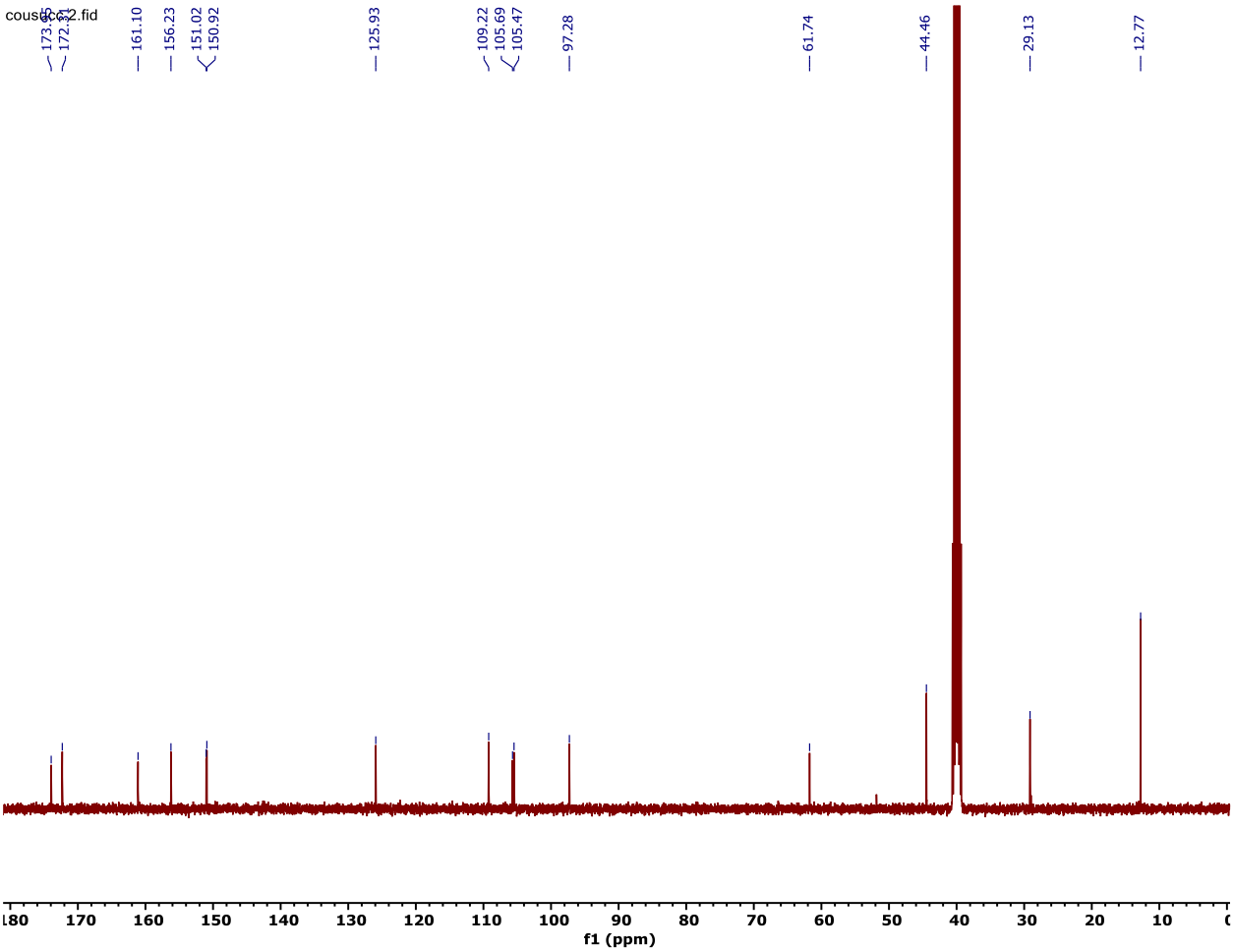

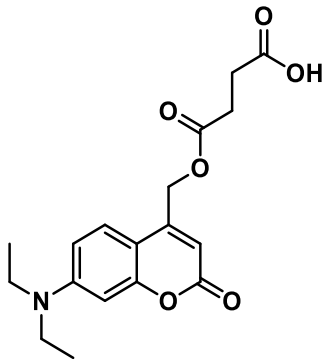

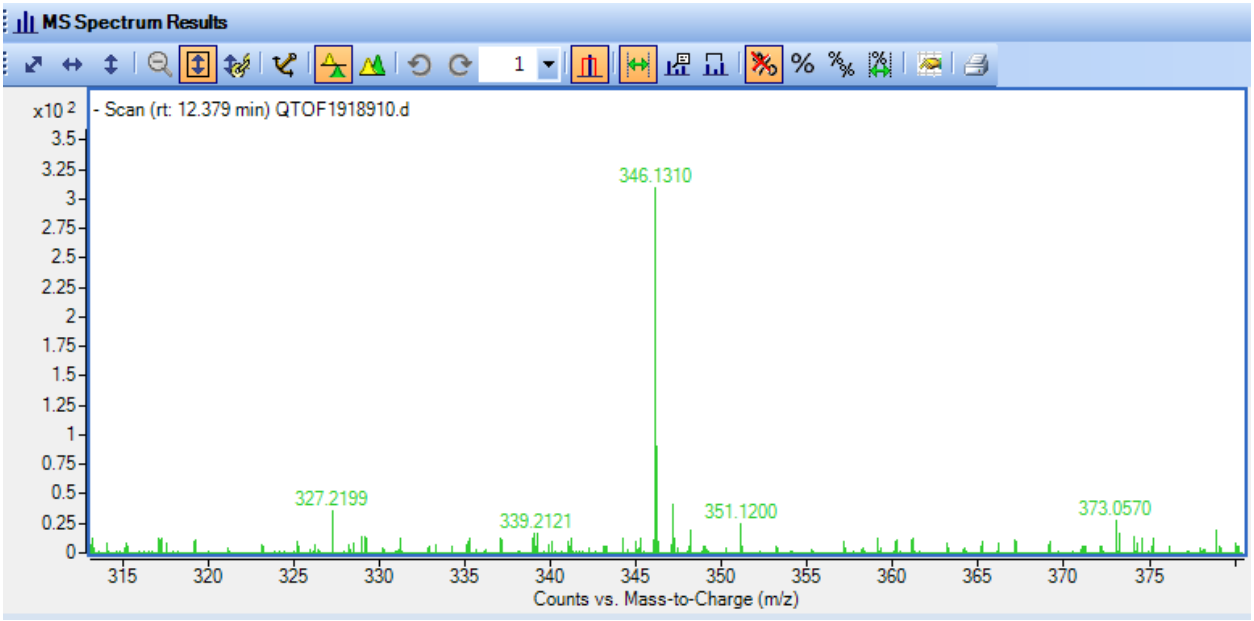

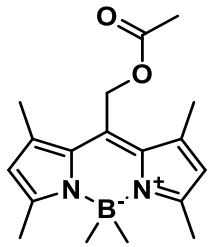

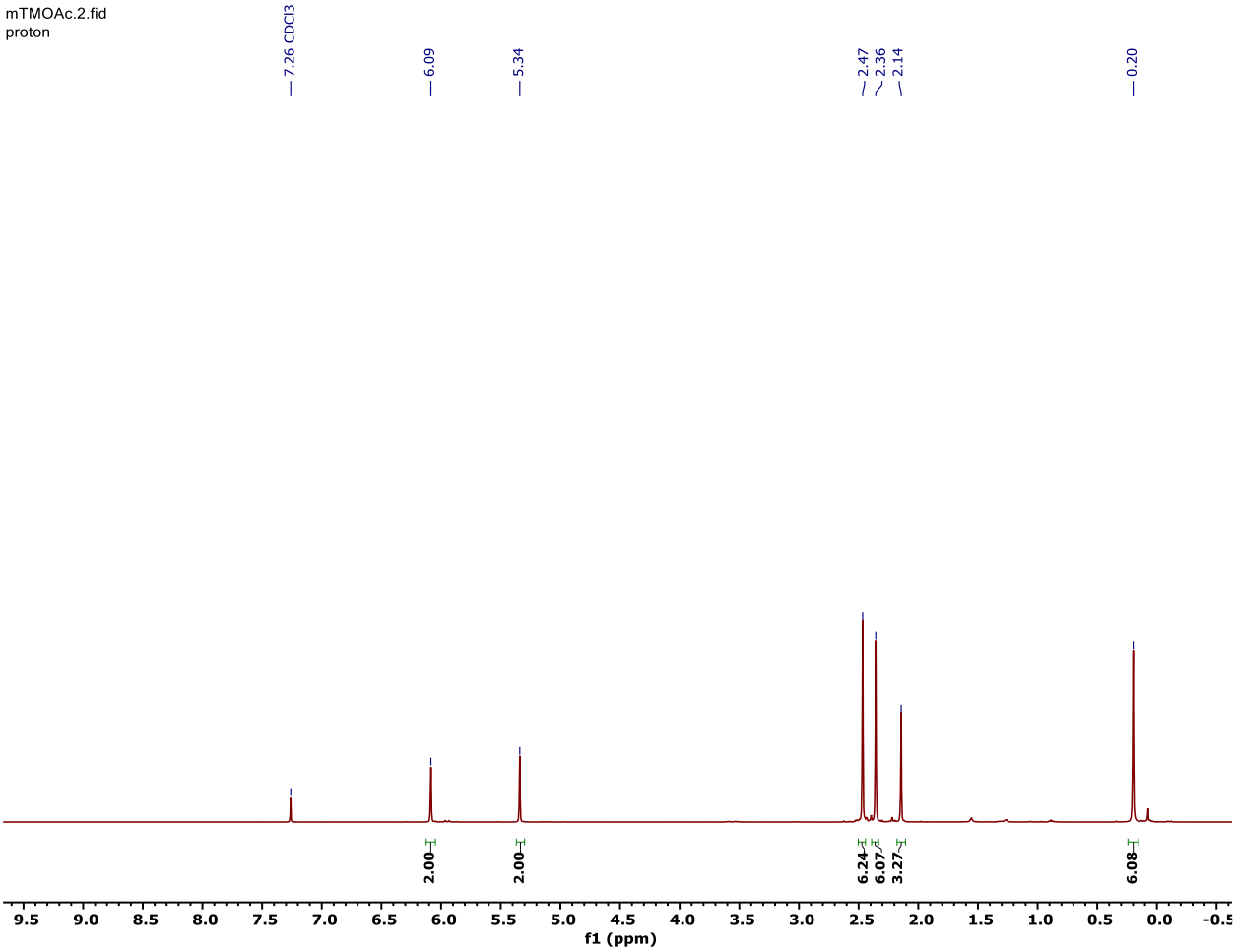

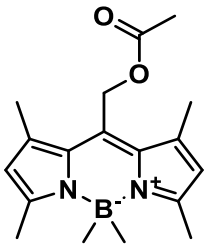

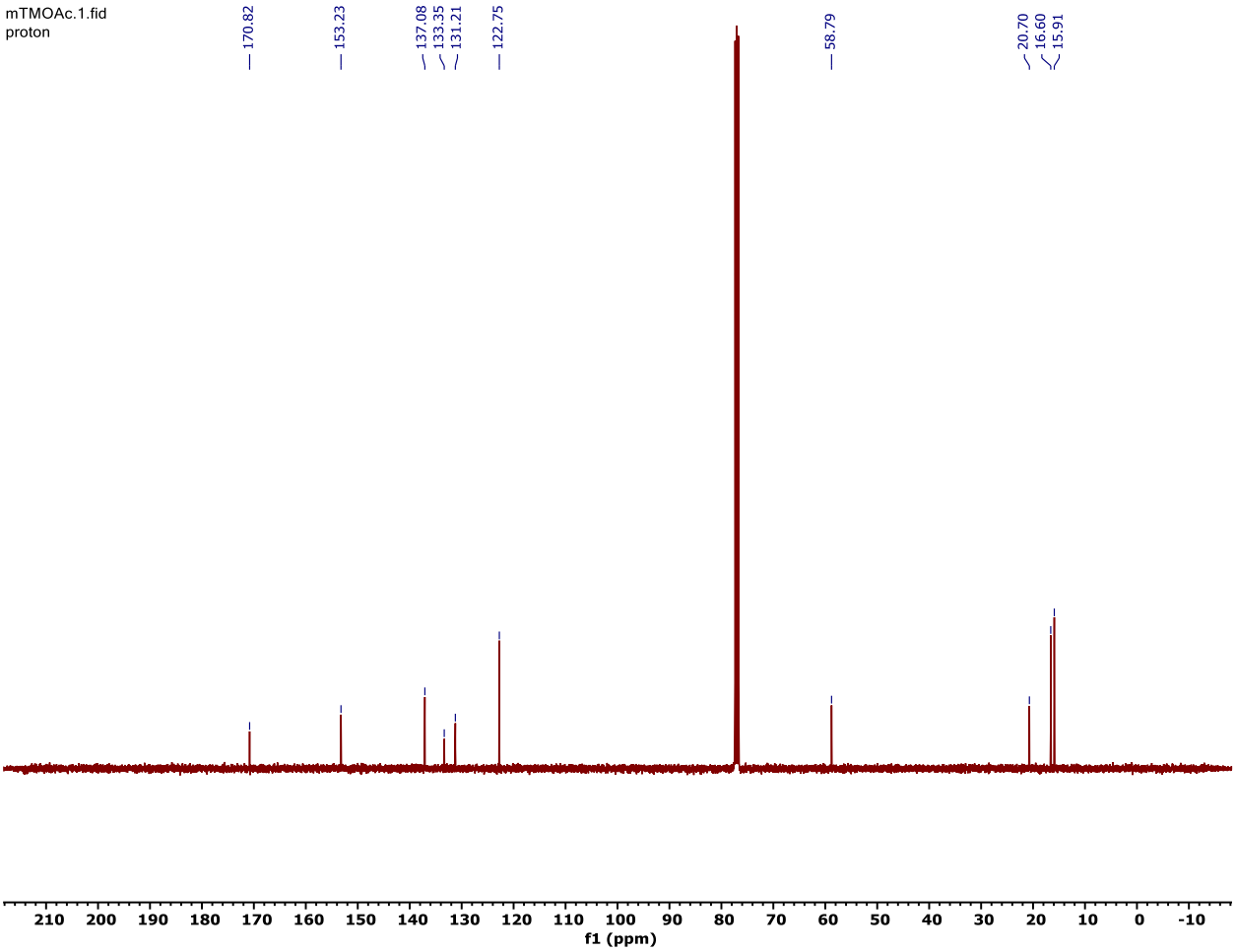

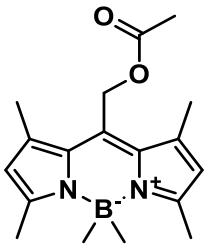

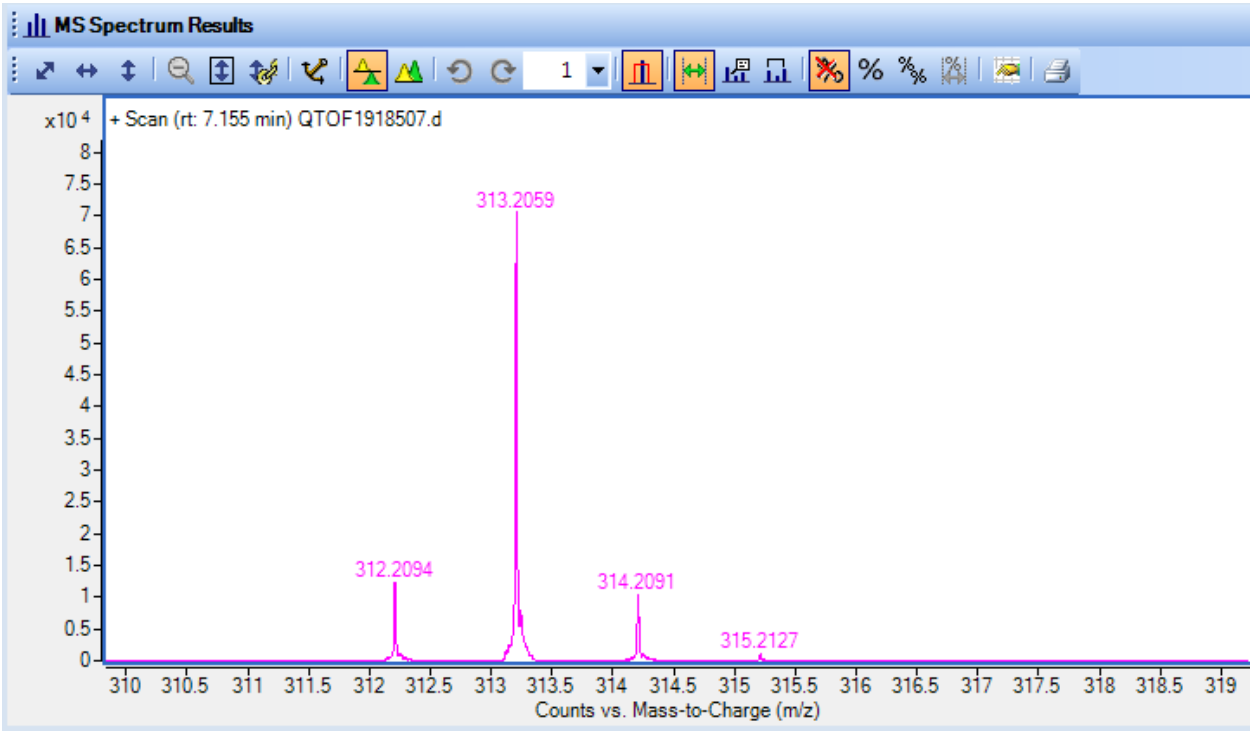

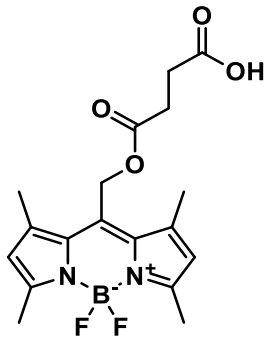

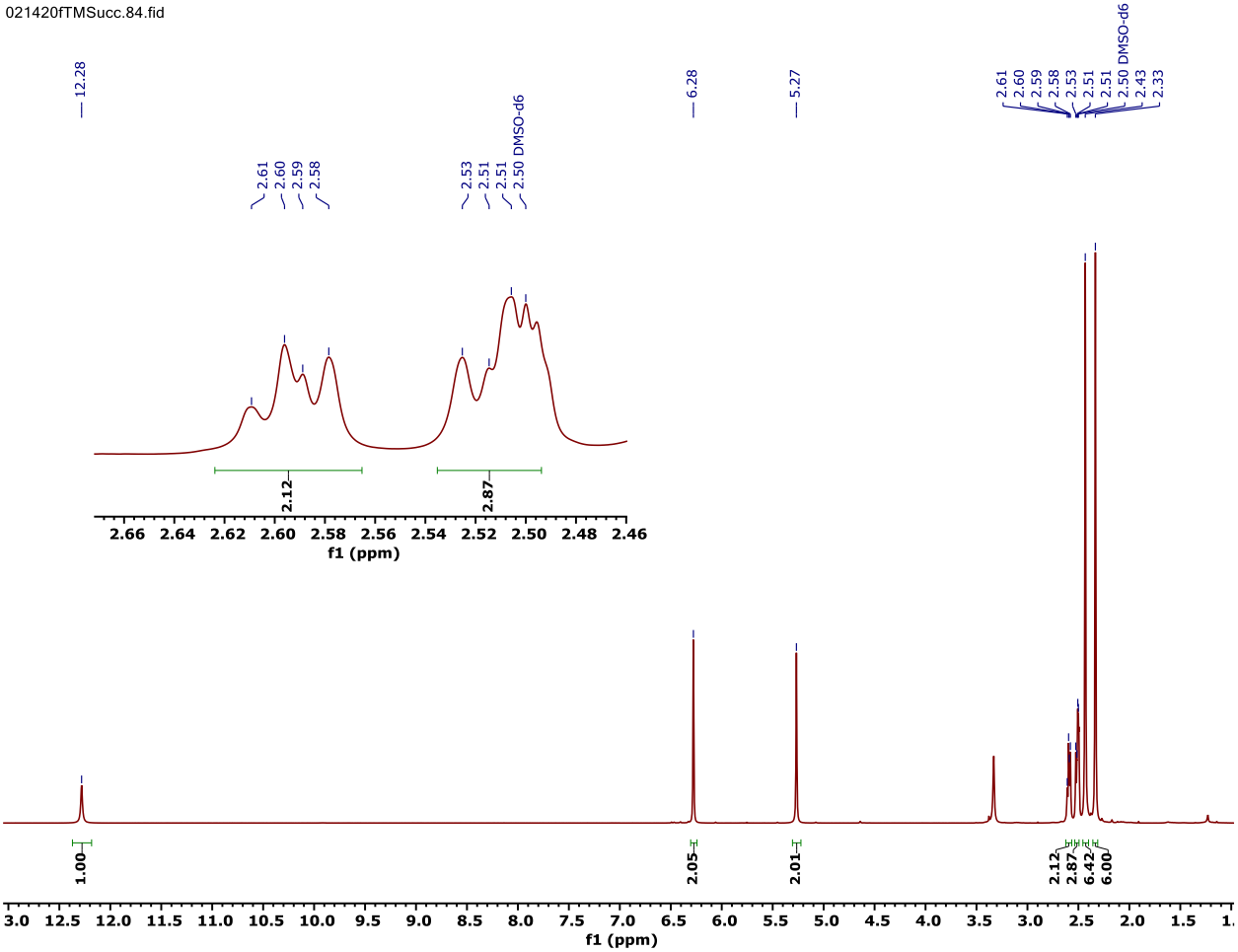

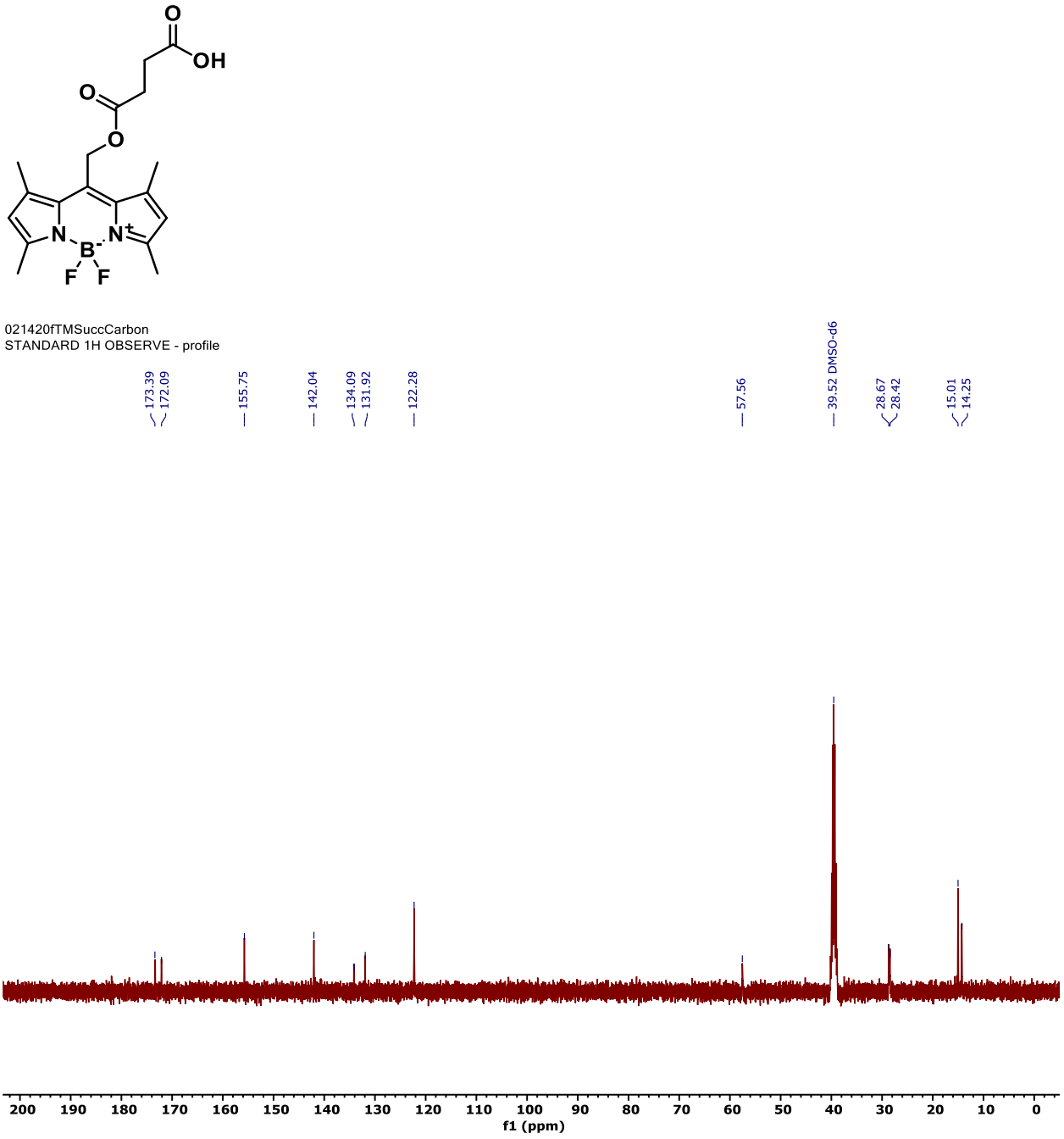

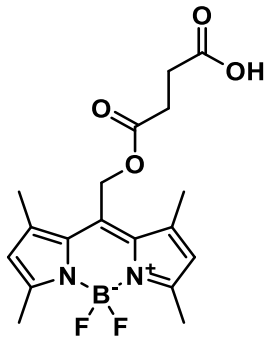

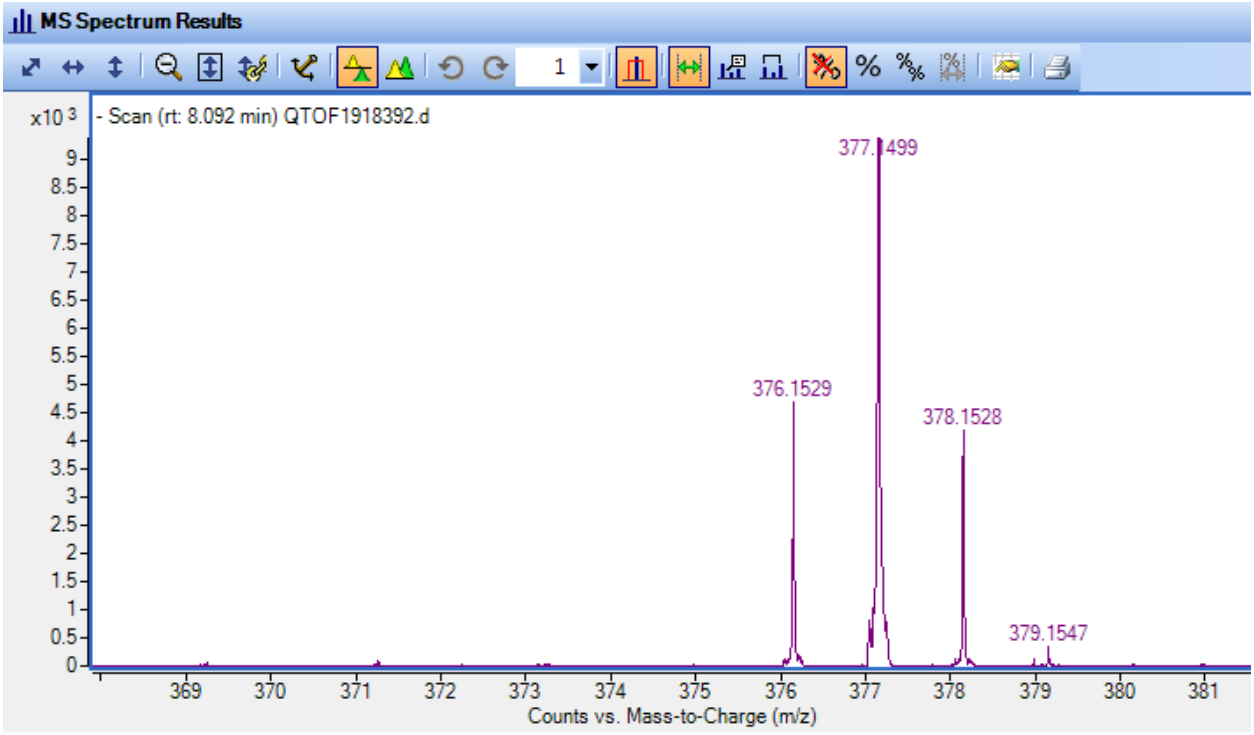

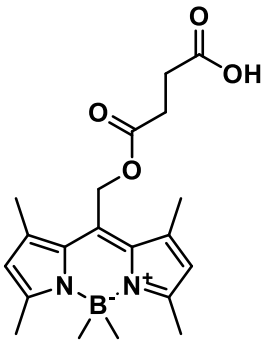

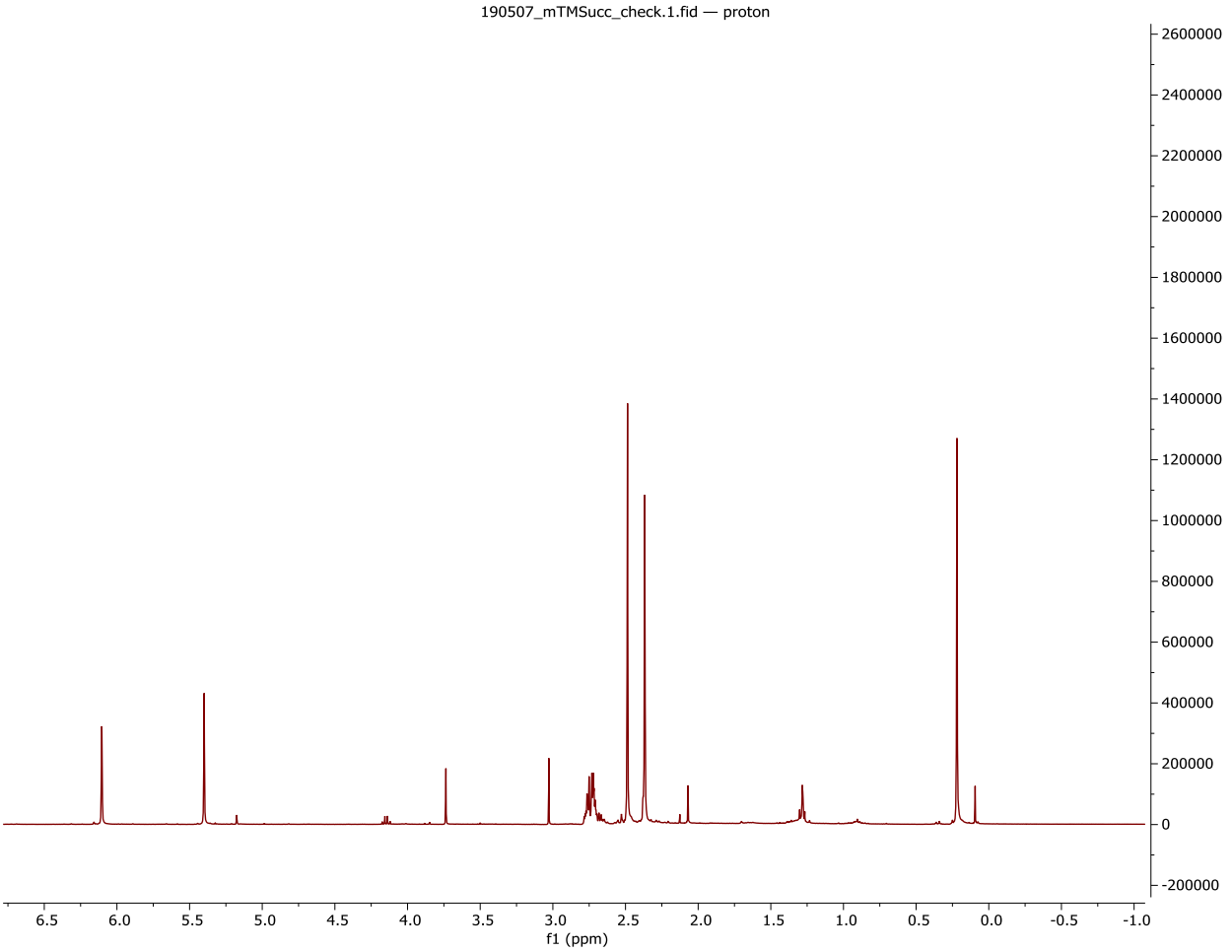

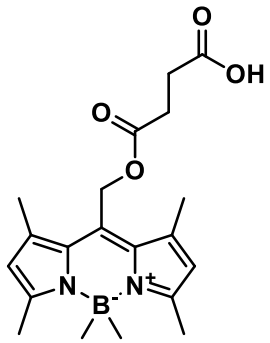

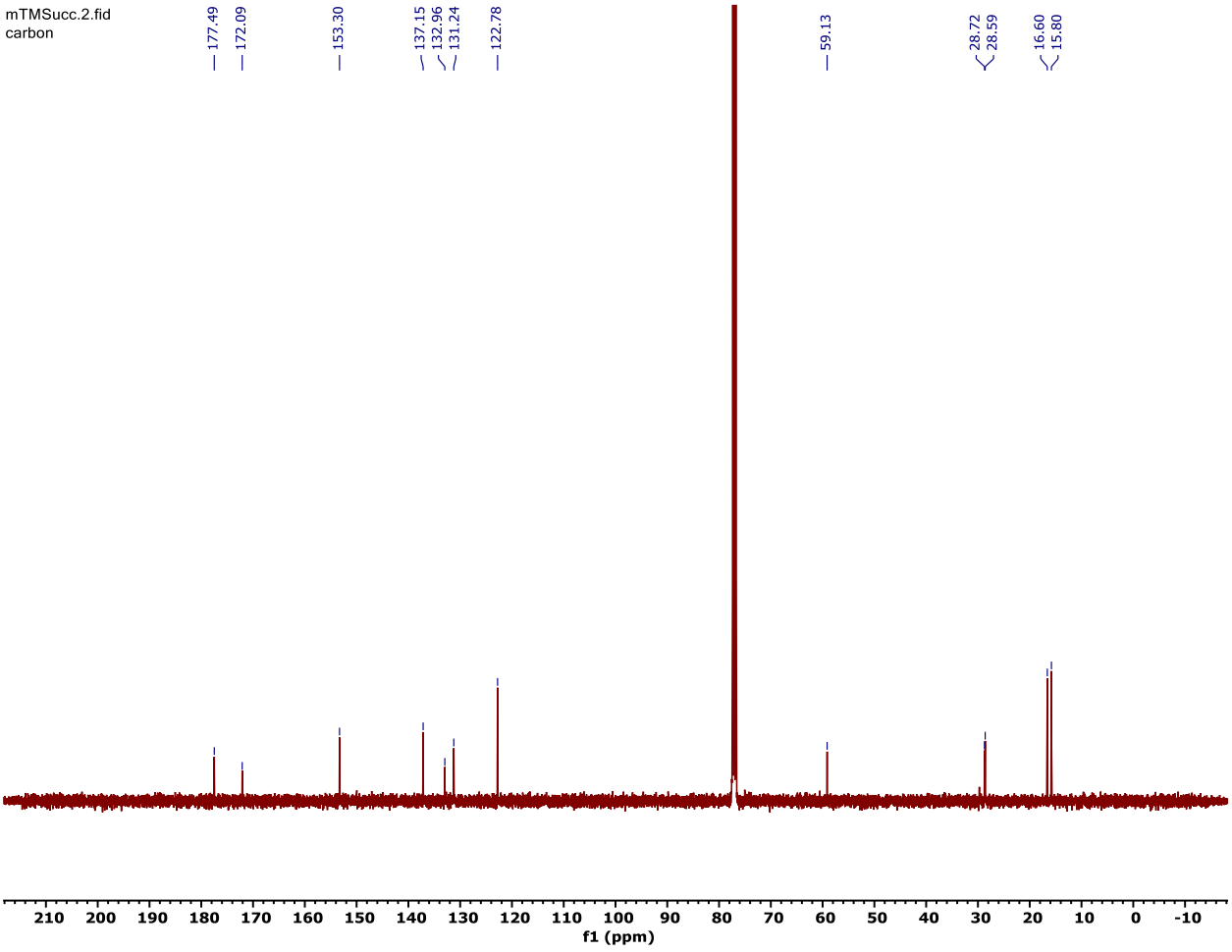

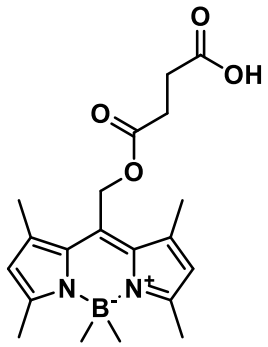

Chemical Formula: $C_{20}H_{27}BN_2O_4$
Molecular Weight: 370.26

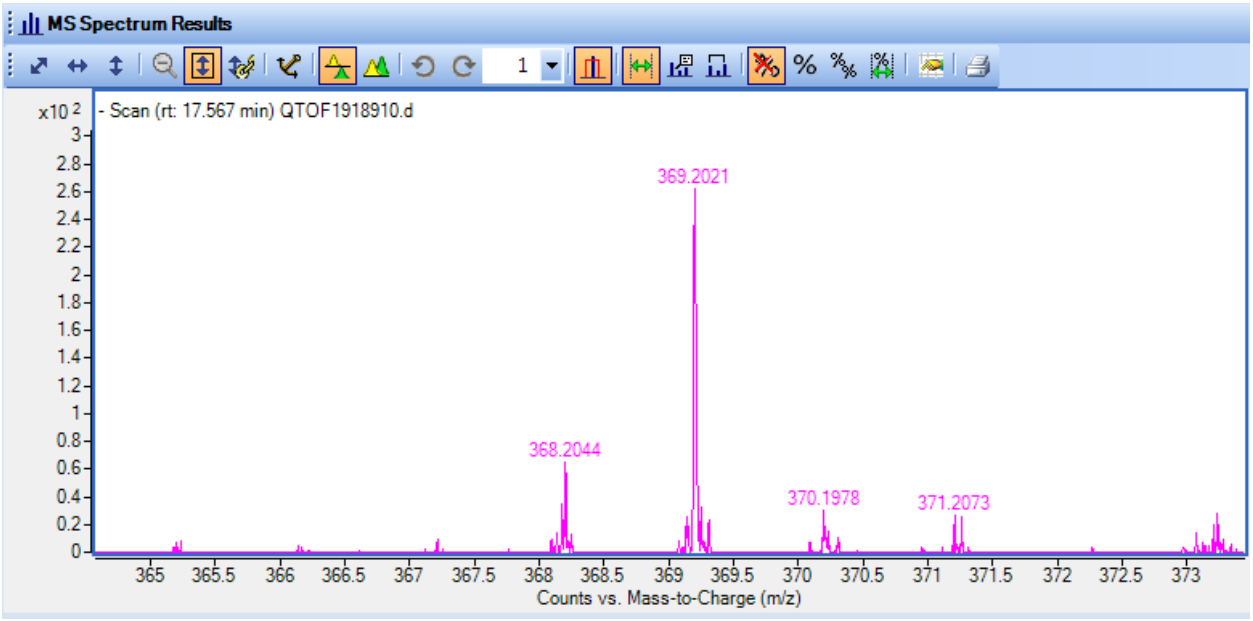

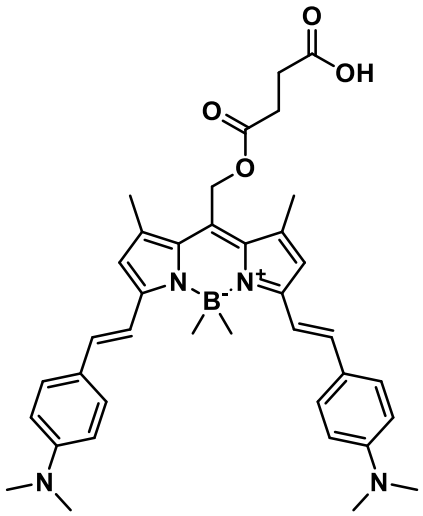

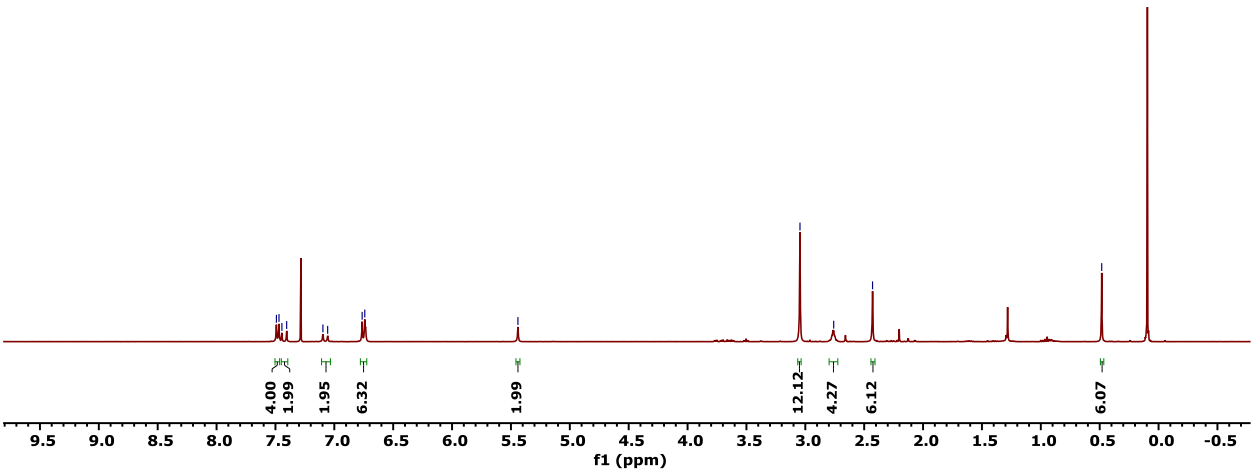

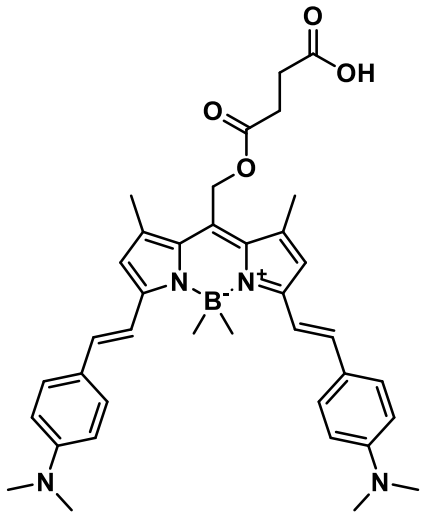

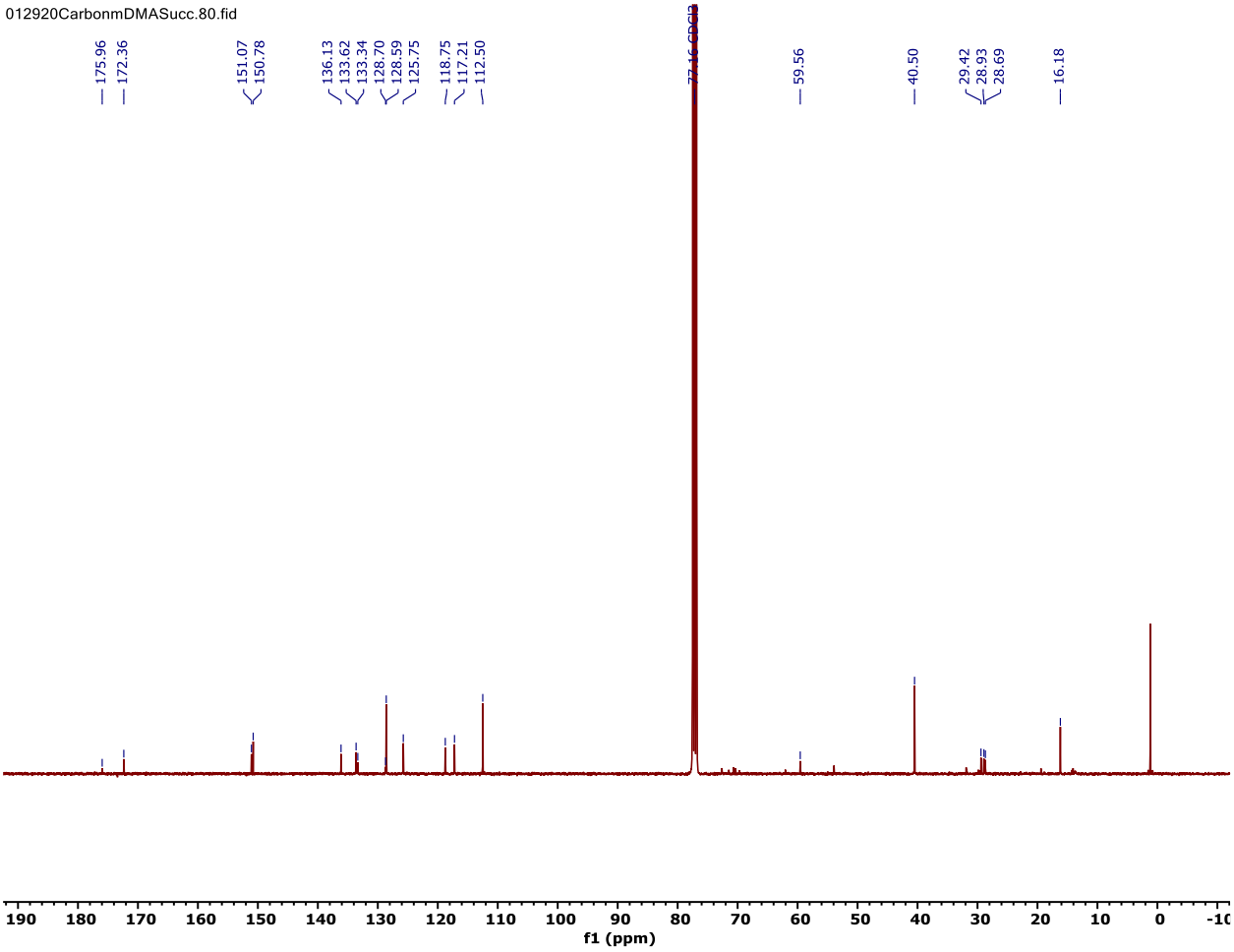

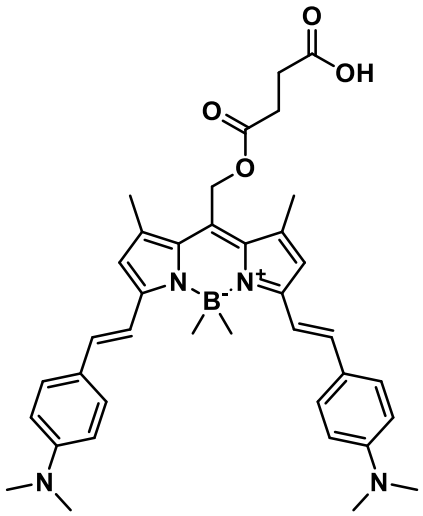

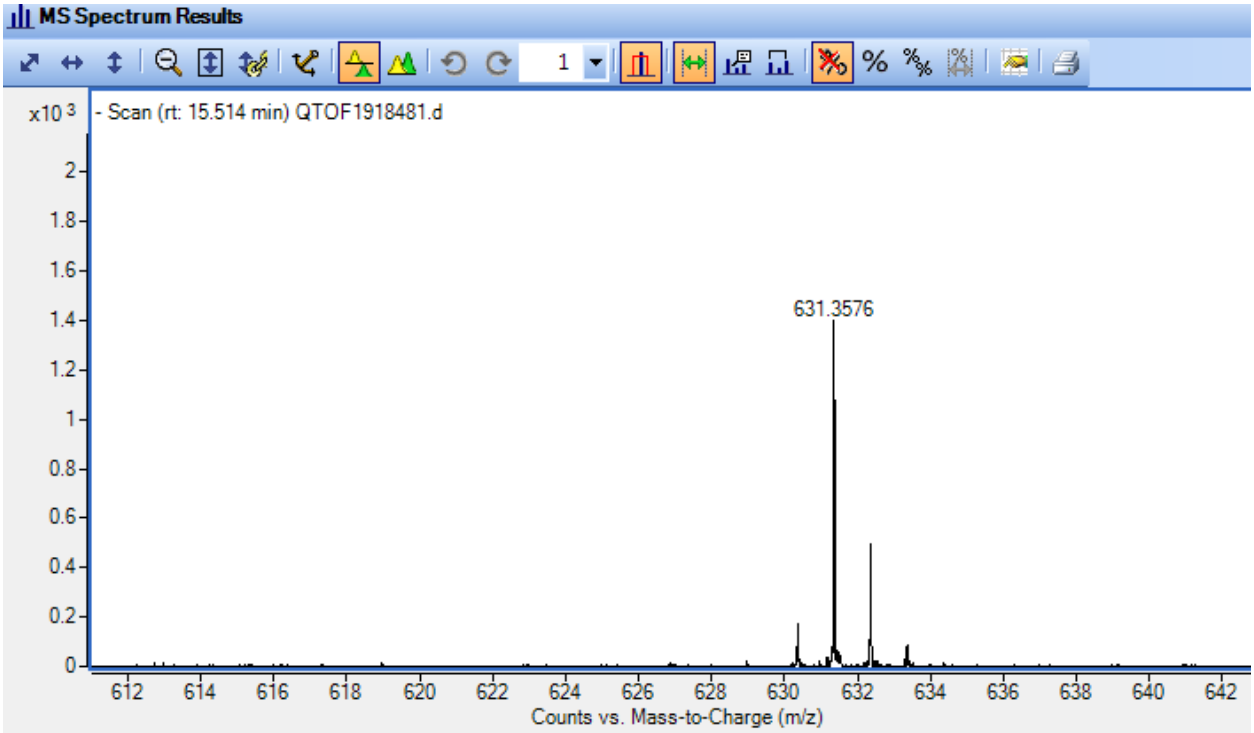

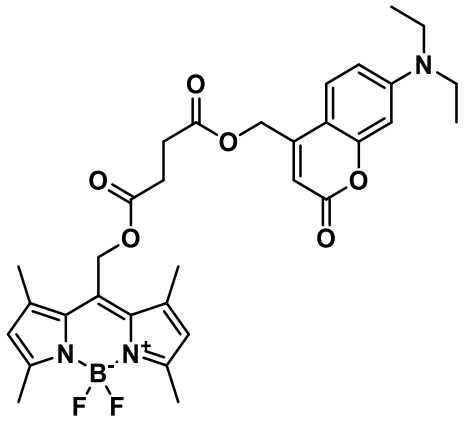

looksrealpure
STANDARD 1H OBSERVE - profile

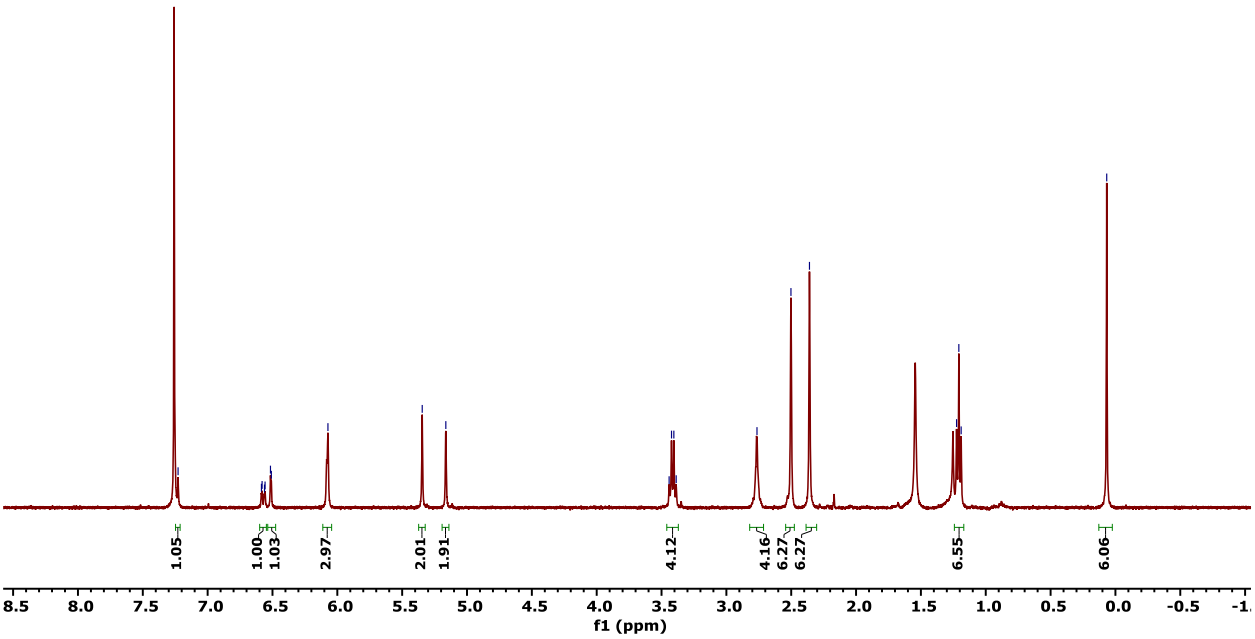

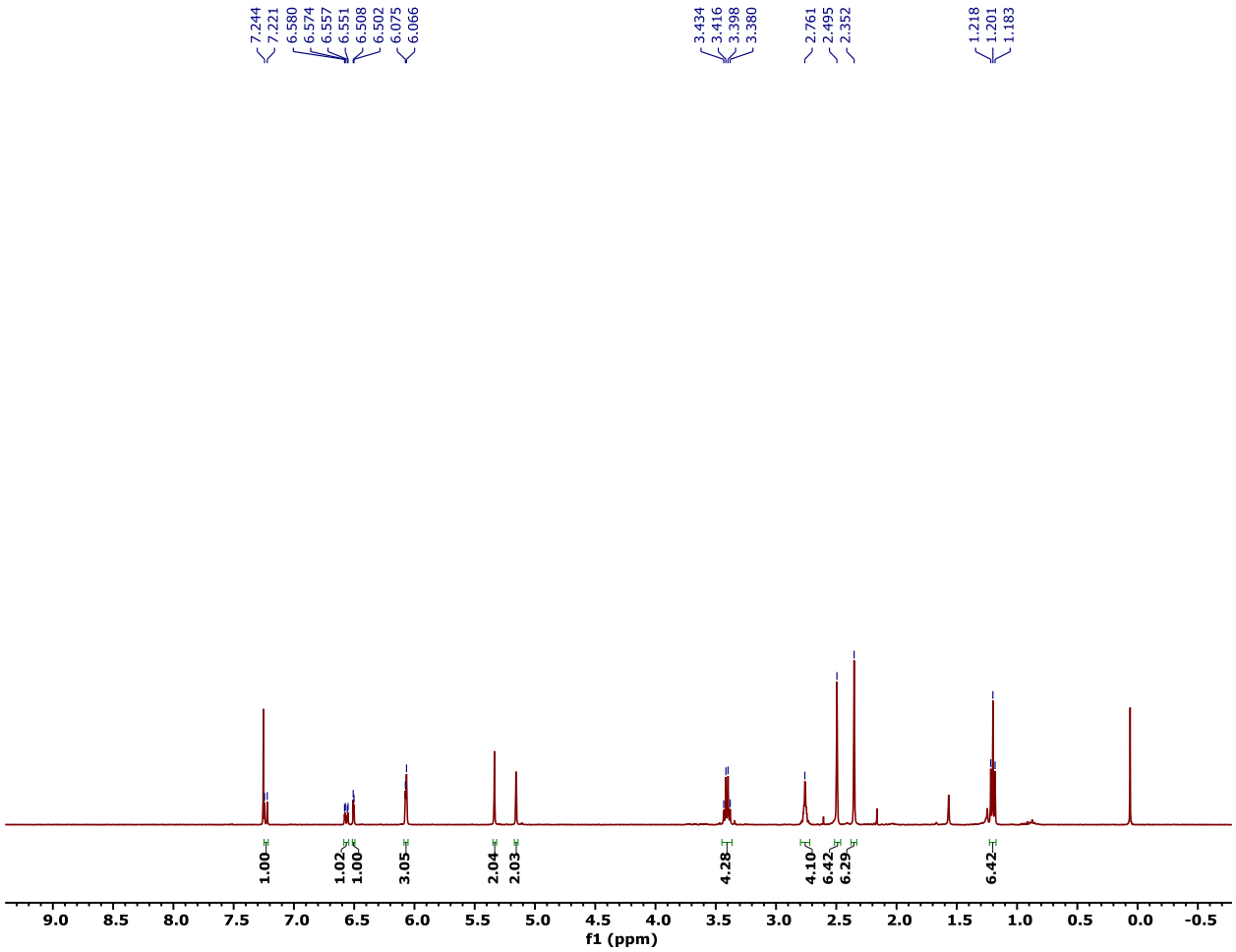

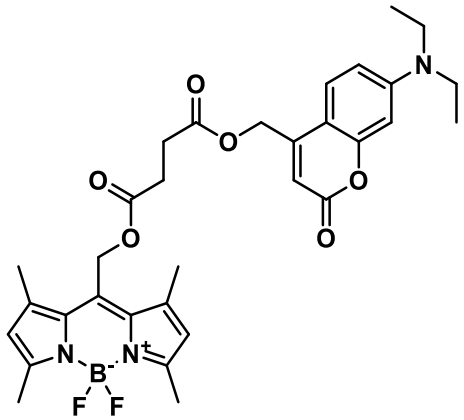

TMSuccCou_pureenough2_carbon
STANDARD 1H OBSERVE pcarbe

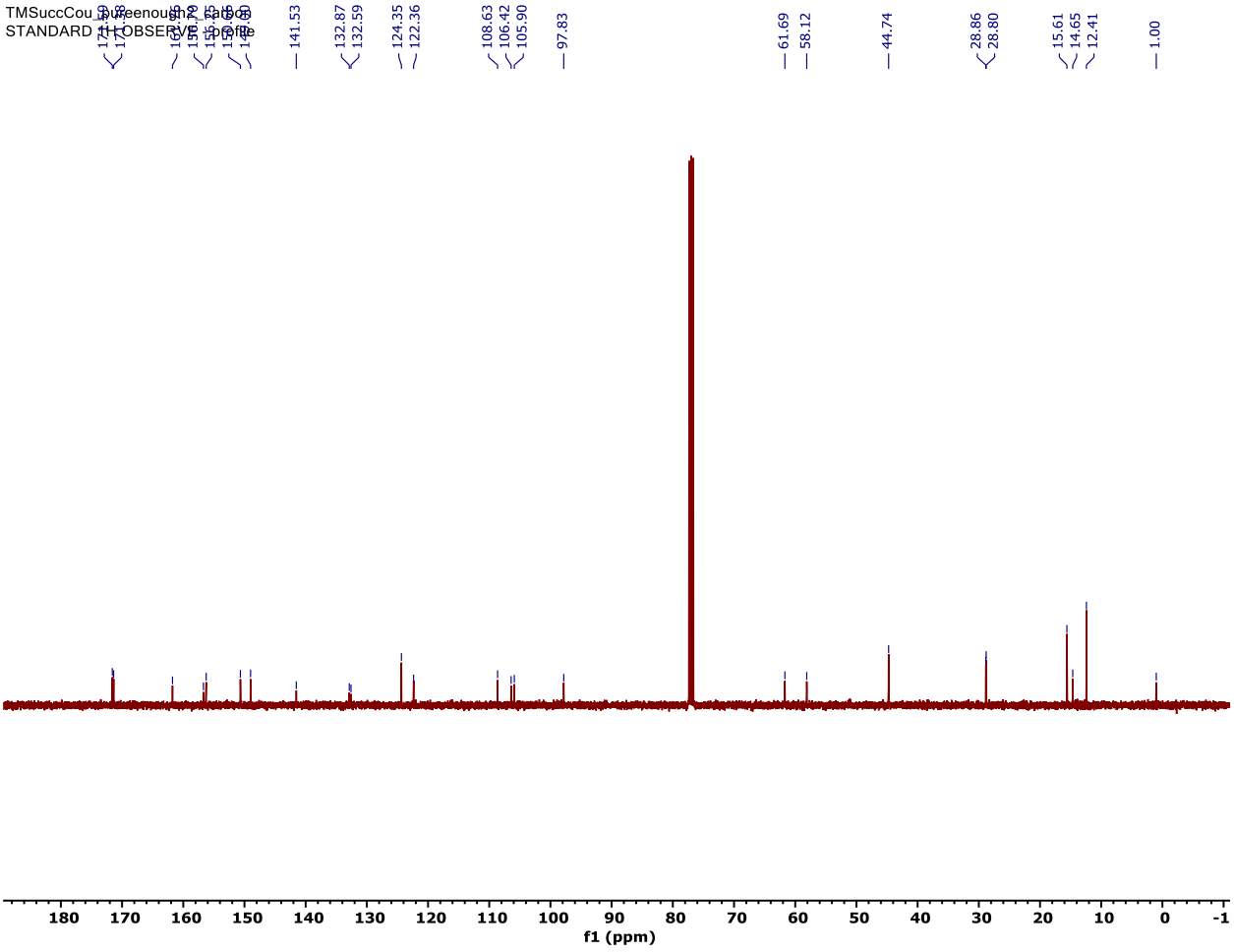

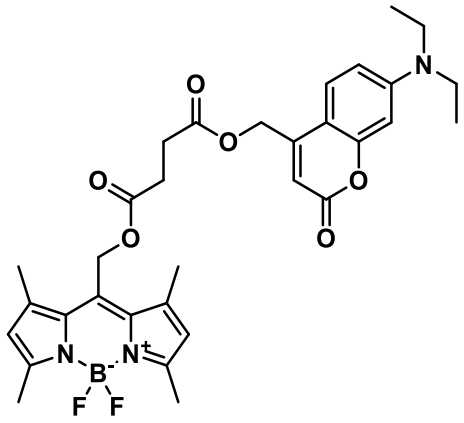

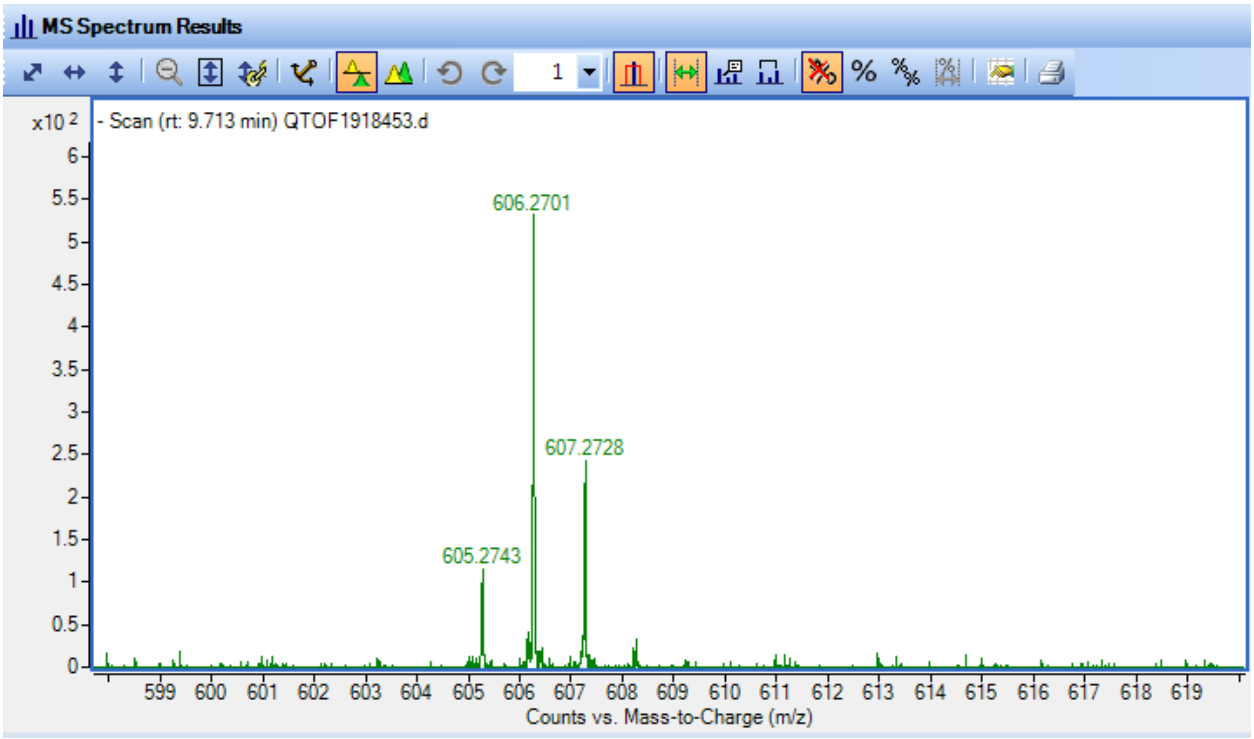

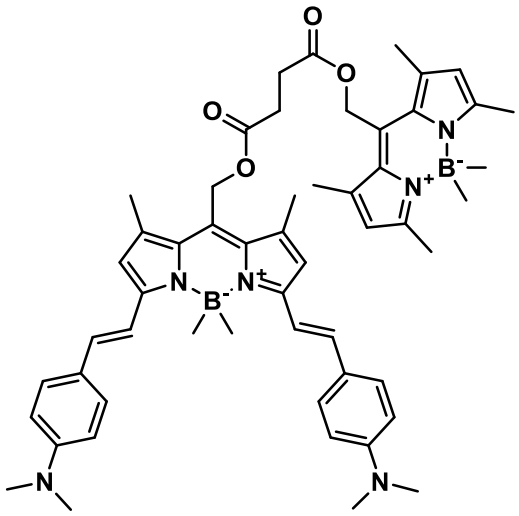

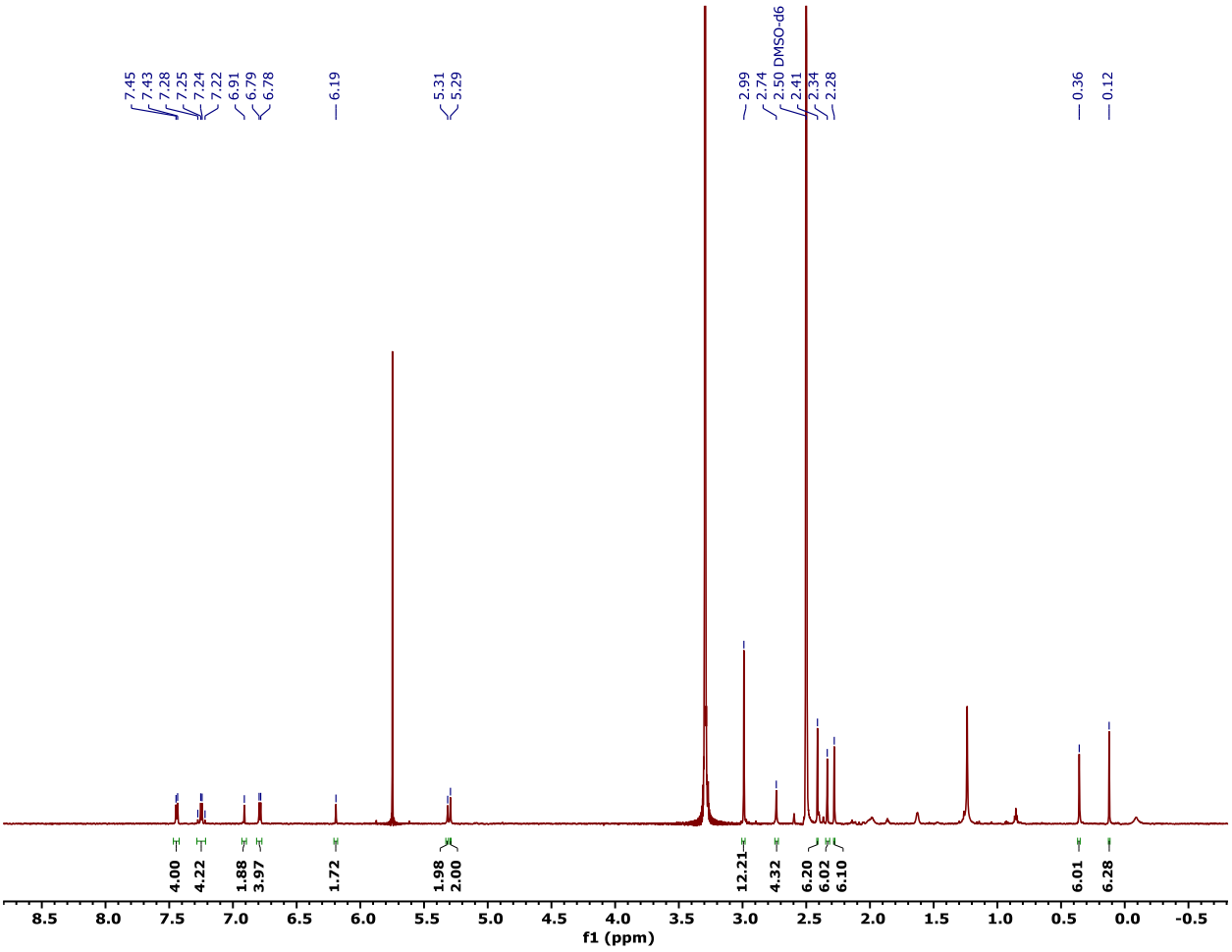

*DCM, Water, Hexanes are solvent impurities

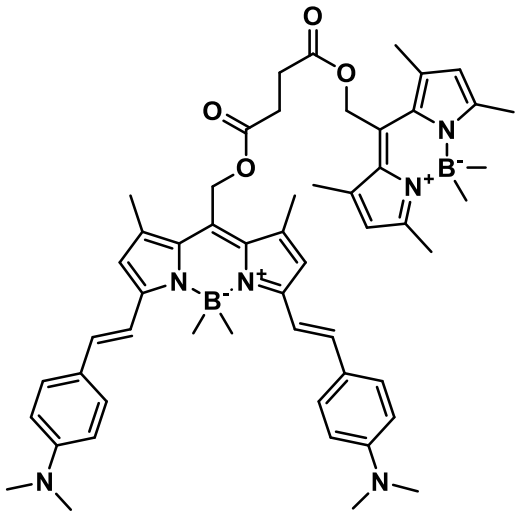

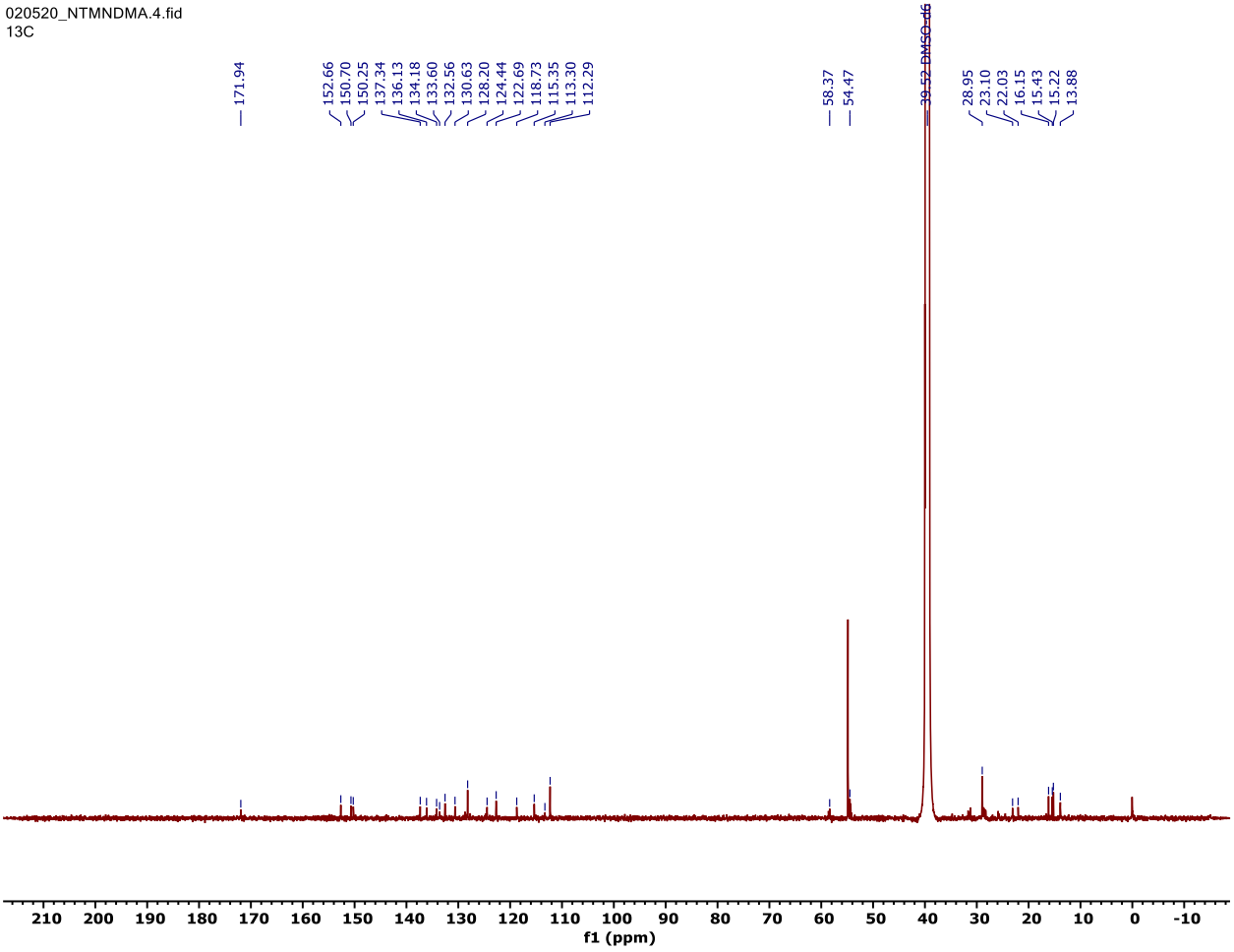

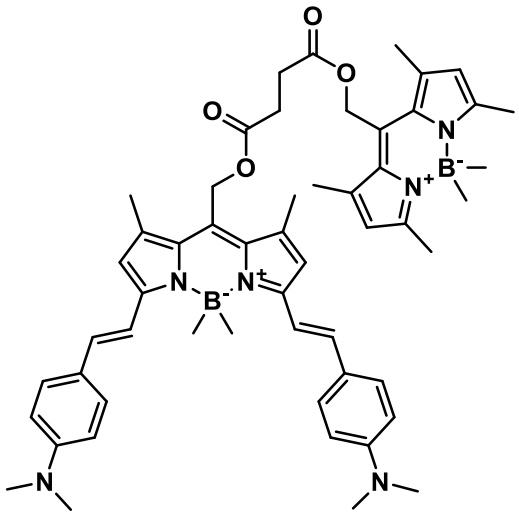

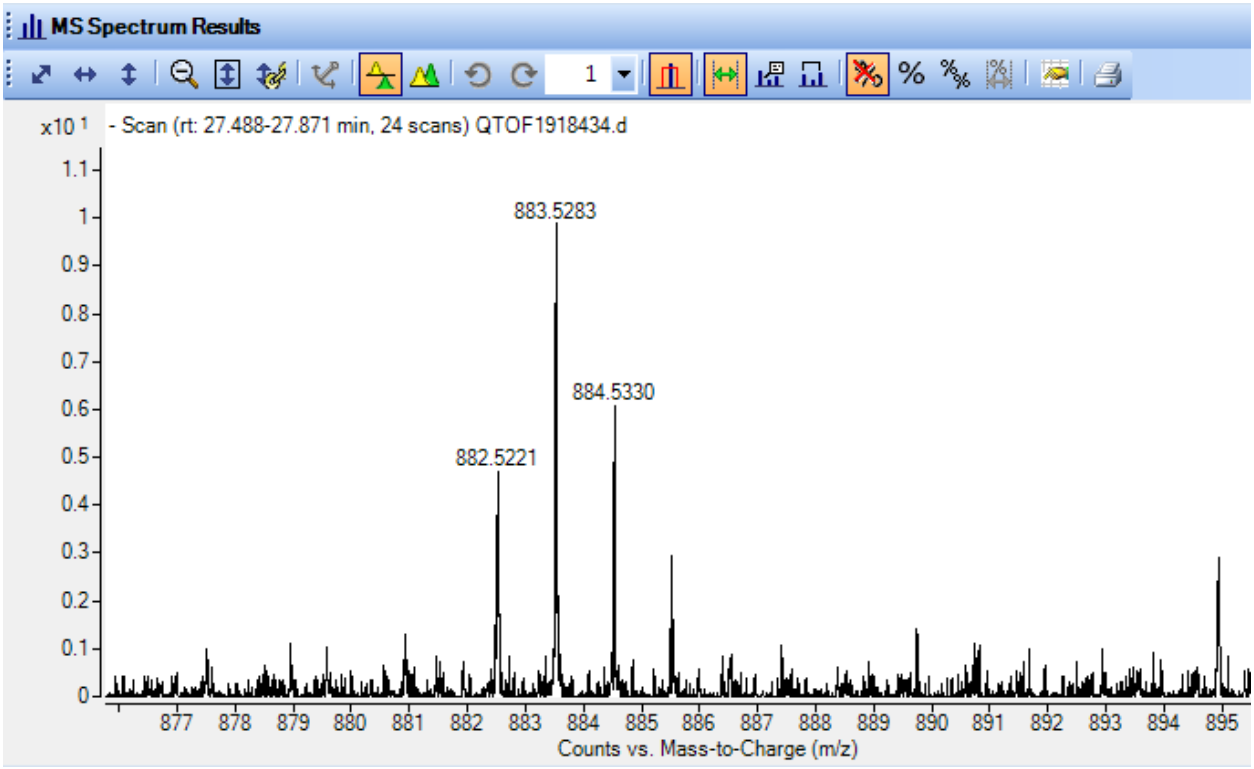

References

1. Shembekar, V. R.; Chen, Y.; Carpenter, B. K.; Hess, G. P., A Protecting Group for Carboxylic Acids That Can Be Photolyzed by Visible Light. *Biochemistry* 2005, *44* (19), 7107-7114.

2. Krumova, K.; Cosa, G., Bodipy Dyes with Tunable Redox Potentials and Functional Groups for Further Tethering: Preparation, Electrochemical, and Spectroscopic Characterization. *Journal of the American Chemical Society* 2010, *132* (49), 17560-17569.

3. Goswami, P.; Syed, A.; Beck, C. L.; Albright, T. R.; Mahoney, K. M.; Unash, R.; Smith, E. A.; Winter, A. H., BODIPY-Derived Photoremovable Protecting Groups Unmasked with Green Light. *J. Am. Chem. Soc* 2015, *137*, 3783-3786.

4. Slanina, T.; Shrestha, P.; Palao, E.; Kand, D.; Peterson, J. A.; Dutton, A. S.; Rubinstein, N.; Weinstain, R.; Winter, A. H.; Klán, P., In Search of the Perfect Photocage: Structure–Reactivity Relationships in meso-Methyl BODIPY Photoremovable Protecting Groups. *Journal of the American Chemical Society* 2017, *139* (42), 15168-15175.

5. Peterson, J. A.; Wijesooriya, C.; Gehrmann, E. J.; Mahoney, K. M.; Goswami, P. P.; Albright, T. R.; Syed, A.; Dutton, A. S.; Smith, E. A.; Winter, A. H., Family of BODIPY Photocages Cleaved by Single Photons of Visible/Near-Infrared Light. Journal of the American Chemical Society, 2018; Vol. 140, pp 7343-7346.